

# Table of Contents

|   |           |
|---|-----------|
| <b>Table of Contents</b> .....  | <b>1</b>  |
| <b>Acknowledgements</b> .....   | <b>4</b>  |
| <b>Declaration</b> .....  | <b>5</b>  |
| <b>Abbreviations</b> .....  | <b>6</b>  |
| <b>Chapter 1: Thesis Introduction</b> .....                                   | <b>10</b> |
| Introduction: The “Gap in the Knowledge” .....                                | 11        |
| Thesis Purpose .....  | 12        |
| Thesis Significance .....   | 12        |
| Thesis Primary Research Questions .....                                       | 12        |
| Thesis Research Design .....  | 13        |
| Thesis Assumptions and Scope.....   | 14        |
| Thesis Assumptions .....  | 14        |
| Thesis Scope.....   | 15        |
| Summary.....  | 16        |
| <b>Chapter 2: Thesis Background</b> .....                                     | <b>17</b> |
| Inhibition of Cyclooxygenase .....  | 18        |
| Cyclooxygenase and Prostanoid Synthesis .....                                 | 18        |
| Prostanoid Signalling and Inflammation .....                                  | 20        |
| Pharmacological Inhibition of Cyclooxygenase.....                             | 23        |
| Non-Steroidal Anti-Inflammatory Drugs and Adverse Cardiovascular Events ..... | 29        |
| Metabolomic Signatures.....   | 41        |
| The Metabolomic Signature of Heart Failure .....                              | 41        |
| The Metabolomic Signature of Coxib use .....                                  | 54        |
| <b>Chapter 3: Thesis Materials and Methods</b> .....                          | <b>57</b> |
| In Vivo Experiments .....   | 58        |
| Animal Husbandry .....  | 58        |
| Metabolomic Protocols .....   | 60        |
| Quantitative reverse transcription polymerase chain reaction (RT-qPCR) .....  | 67        |
| In Vitro Experiments .....  | 70        |
| C2C12 Murine Skeletal Muscle Cells .....                                      | 70        |
| Primary Murine Cardiomyocytes .....   | 71        |
| Metabolomic Protocols .....   | 73        |
| Statistical Analysis .....  | 74        |
| Univariate Analysis .....   | 74        |
| Multivariate Analysis.....  | 76        |
| <b>Chapter 4: Hypotheses Generation</b> .....                                 | <b>78</b> |
| Chapter Introduction.....   | 79        |

|   |            |
|---|------------|
| Chapter Background .....                                | 80         |
| Metabolomics for Hypothesis Generation .....            | 80         |
| Targeted and Untargeted Metabolomics .....              | 81         |
| Selection of Metabolomic Techniques.....                | 81         |
| Chapter Methods.....                                    | 86         |
| Chapter Results .....                                   | 87         |
| Heart.....  | 87         |
| Skeletal Muscle .....                                   | 94         |
| Kidney.....   | 97         |
| Liver.....  | 101        |
| Plasma.....   | 103        |
| Chapter Discussion .....                                | 105        |
| Carnitine Metabolism.....                               | 106        |
| Lipid Metabolism.....                                   | 108        |
| Chapter Conclusions and Future Directions .....         | 109        |
| <b>Chapter 5: Coxibs and Carnitine Metabolism .....</b> | <b>112</b> |
| Chapter Introduction.....                               | 113        |
| Chapter Background .....                                | 115        |
| The Cardiac Carnitine Shuttle .....                     | 115        |
| Systemic Carnitine Handling .....                       | 118        |
| Carnitines and Heart Failure .....                      | 123        |
| Chapter Methods.....                                    | 124        |
| Chapter Results .....                                   | 126        |
| Cardiac Carnitines.....                                 | 126        |
| The Cardiac Carnitine Shuttle .....                     | 130        |
| Renal Excretion of Carnitines.....                      | 132        |
| Microbiome-Mediated Carnitine Bioavailability .....     | 133        |
| Hepatic Carnitine Synthesis .....                       | 134        |
| Hepatic Total-Fatty Acids .....                         | 135        |
| Addendum: Dietary Carnitines .....                      | 138        |
| Chapter Discussion .....                                | 140        |
| Cardiac Carnitines.....                                 | 140        |
| The Cardiac Carnitine Shuttle .....                     | 142        |
| Renal Excretion of Carnitines.....                      | 142        |
| Microbiome-Mediated Carnitine Bioavailability .....     | 142        |
| Hepatic Carnitine Synthesis .....                       | 143        |
| Hepatic Total-Fatty Acids .....                         | 144        |
| Addendum: Dietary Carnitines .....                      | 145        |

|  |            |
|--|------------|
| Chapter Conclusions and Future Directions .....  | 147        |
| <b>Chapter 6: Development of an In Vitro Carnitine Shuttle Activity Assay .....</b>      | <b>149</b> |
| Chapter Introduction.....  | 150        |
| Chapter Background .....   | 152        |
| Limitations of Current <i>In Vitro</i> Carnitine Shuttle Activity Assays .....           | 153        |
| Theoretical Basis for an improved <i>In Vitro</i> Carnitine Shuttle Activity Assay ..... | 155        |
| Chapter Methods.....   | 157        |
| Chapter Results .....  | 158        |
| C2C12 Skeletal Muscle Cells .....  | 158        |
| Primary Murine Cardiomyocytes .....  | 160        |
| Chapter Discussion .....   | 162        |
| C2C12 Skeletal Muscle Cells .....  | 162        |
| Primary Murine Cardiomyocytes .....  | 163        |
| Chapter Conclusions and Future Directions .....  | 167        |
| <b>Chapter 7: Asymmetric Dimethylarginine and COX-2 Inhibition.....</b>                  | <b>169</b> |
| Chapter Introduction.....  | 170        |
| Chapter Background .....   | 172        |
| Methylarginines .....  | 172        |
| Global COX-2 <sup>-/-</sup> Mouse Models.....  | 178        |
| Chapter Methods.....   | 181        |
| Chapter Results .....  | 182        |
| IPNG COX-2 <sup>-/-</sup> Mouse Cardiac Metabolism.....                                  | 182        |
| IPNG COX-2 <sup>-/-</sup> Mouse Methylarginine Metabolism.....                           | 188        |
| Chapter Discussion .....   | 194        |
| IPNG COX-2 <sup>-/-</sup> Mouse Cardiac Metabolism.....                                  | 194        |
| IPNG COX-2 <sup>-/-</sup> Mouse Methylarginine Metabolism.....                           | 196        |
| Chapter Conclusions and Future Directions .....  | 199        |
| <b>Chapter 8: Thesis Conclusions .....</b>   | <b>201</b> |
| Thesis Themes.....   | 202        |
| Thesis Limitations and Future Directions .....   | 204        |
| Thesis Concluding Remarks .....  | 205        |
| <b>References .....</b>  | <b>207</b> |

# ***Acknowledgements***

I would like to acknowledge and thank my supervisor, Jules Griffin, whose mentorship has been invaluable and who has guided me in the design of this work, the interpretation of the results and the editing of this thesis.

Cecilia Castro has helped me with sample analysis and results interpretation and has also been a great friend throughout this process. James West has been a huge help in all things involving liquid chromatography-mass spectrometry and several of the experimental protocols used in this work are of his design. Many thanks to them both.

I would also like to thank the other members of The Griffin Group, in particular Tom Ashmore, who assisted me with the C2C12 murine skeletal muscle cell experiments, and Steve Murfitt. Thanks also to my collaborators in The Garrett FitzGerald Lab, especially Garrett FitzGerald and Emanuela Ricciotti, without whom this work would not have been possible and who made me feel very welcome in the four months I spent at the University of Pennsylvania. I would also like to acknowledge The Prosser Lab at the University of Pennsylvania, who performed the primary murine cardiomyocyte isolation.

My parents Tim and Rhiannon, sisters Sarah and Rachel, and girlfriend Georgia Hacke have been incredibly supportive and at various times helped guide my thinking and proof my work.

Finally, I would like to thank the MB/PhD programme at the University of Cambridge, School of Clinical Medicine and the British Heart Foundation Centre of Research Excellence Cambridge, who provided me with the opportunity and financial support necessary to undertake and complete this work.

## ***Declaration***

This dissertation is the result of my own work and includes nothing which is the outcome of work done in collaboration except as declared in the Preface and specified in the text. It is not substantially the same as any that I have submitted, or, is being concurrently submitted for a degree or diploma or other qualification at the University of Cambridge or any other University or similar institution except as declared in the Preface and specified in the text. I further state that no substantial part of my dissertation has already been submitted, or, is being concurrently submitted for any such degree, diploma or other qualification at the University of Cambridge or any other University or similar institution except as declared in the Preface and specified in the text. It does not exceed the prescribed word limit for the relevant Degree Committee.

# Abbreviations

|   |                         |
|---|-------------------------|
| One-Dimensional   | (1D)                    |
| Asymmetric Dimethylarginine   | (ADMA)                  |
| Alpha-Ketoglutarate   | (AKG)                   |
| Adenosine Monophosphate-Activated Protein Kinase                      | (AMPK)                  |
| Angiotensin II  | (Ang II)                |
| Analysis of Variance  | (ANOVA)                 |
| Adenomatous Polyp Prevention On Vioxx                                 | (APPROVe)               |
| Antithrombotic Trialist's   | (ATT)                   |
| Butyrobetaine Dioxygenase   | (BBD)                   |
| Branch-Chain Amino Acid   | (BCAA)                  |
| Blood Pressure  | (BP)                    |
| Bovine Serum Albumin  | (BSA)                   |
| 4-Trimethylammoniobutanoate   | (Butyrobetaine)         |
| Carnitine-Acylcarnitine Translocase                                   | (CACT)                  |
| Cyclic Adenosine Monophosphate  | (cAMP)                  |
| Cationic Amino Acid Transporter                                       | (CAT)                   |
| Cardiac Failure   | (CF)                    |
| Cyclic Guanosine Monophosphate  | (cGMP)                  |
| Congestive Heart Failure  | (CHF)                   |
| Confidence Interval   | (CI)                    |
| Cell Isolation Buffer   | (CIB)                   |
| COX-Inhibiting Nitric Oxide donator                                   | (CINOD)                 |
| Chronic Kidney Disease  | (CKD)                   |
| Celecoxib Long-term Arthritis Safety Study                            | (CLASS)                 |
| Cardiac Myocyte Medium  | (CMM)                   |
| Coxib and traditional Non-Steroidal Anti-Inflammatory Drug Trialists' | (CNT)                   |
| Coenzyme A  | (CoA)                   |
| Correlation Spectroscopy  | (COSY)                  |
| Cyclooxygenase  | (COX)                   |
| Cyclooxygenase-2 Knock-Out  | (COX-2 <sup>-/-</sup> ) |
| Cyclooxygenase-2 Wild-Type  | (COX-2 <sup>+/+</sup> ) |
| Cytosolic Prostaglandin-E Synthase                                    | (cPGES)                 |
| Carr-Purcell-Meiboom Gill   | (CPMG)                  |
| Carnitine Palmitoyltransferase 1                                      | (CPT1)                  |
| Carnitine Palmitoyltransferase 1 Isoform B                            | (CPT1B)                 |
| Carnitine Palmitoyltransferase 2                                      | (CPT2)                  |
| Carnitine O-Acetyltransferase   | (CRAT)                  |
| C-Reactive Protein  | (CRP)                   |
| Carnitine Shuttle Activity  | (CSA)                   |
| Cycle Threshold   | (C <sub>T</sub> )       |
| Cardiovascular  | (CV)                    |
| Analysis of Variance of Cross-Validated Residuals                     | (CV-ANOVA)              |
| Cytochrome p450   | (Cyp450)                |

|   |                          |
|---|--------------------------|
| Cytosine  | (Cyt)                    |
| Dilated Cardiomyopathy  | (DCM)                    |
| Dimethylarginine Dimethylaminohydrolase 1                             | (DDAH1)                  |
| Dulbecco's Modified Eagle's Medium                                    | (DMEM)                   |
| Dimethyl Sulfoxide  | (DMSO)                   |
| Prostaglandin-D <sub>2</sub> Receptor                                 | (DP)                     |
| 4,4-dimethyl-4-silapentane-1-sulfonic acid                            | (DSS)                    |
| Ejection Fraction   | (EF)                     |
| (ethylene glycol-bis(β-aminoethyl ether)-N,N,N',N'-tetraacetic acid   | (EGTA)                   |
| Electron Ionisation   | (EI)                     |
| Electromagnetic   | (EM)                     |
| Encyclopaedia of Deoxyribonucleic Acid Elements                       | (ENCODE)                 |
| Prostaglandin-E <sub>2</sub> Receptor                                 | (EP)                     |
| Oestrogen Receptor  | (ER)                     |
| Embryonic Stem Cell   | (ESC)                    |
| Electrospray Ionisation   | (ESI)                    |
| Fatty Acid  | (FA)                     |
| Fatty Acid Methyl Ester   | (FAME)                   |
| Foetal Bovine Serum   | (FBS)                    |
| Flavin Monooxygenase  | (FMO)                    |
| Prostaglandin-F <sub>2α</sub> Receptor                                | (FP)                     |
| Gas Chromatography  | (GC)                     |
| Gas Chromatography Mass Spectrometry                                  | (GC-MS)                  |
| Gastrointestinal  | (GI)                     |
| Guanine Nucleotide-Binding Protein-Coupled Receptor                   | (GPCR)                   |
| Guanine Nucleotide-Binding Protein                                    | (G-protein)              |
| Oxidised Glutathione  | (GSSG)                   |
| Hydroxyeicosatetraenoic Acid  | (HETE)                   |
| Heart Failure   | (HF)                     |
| Heart Failure with Preserved Ejection Fraction                        | (HFpEF)                  |
| Heart Failure with Reduced Ejection Fraction                          | (HFrEF)                  |
| Histidine   | (His)                    |
| Haematopoietic-type Prostaglandin-D synthase                          | (H-PGDS)                 |
| High Performance Liquid Chromatography                                | (HPLC)                   |
| Hazard Ratio  | (HR)                     |
| Heteronuclear Single Quantum Coherence                                | (HSQC)                   |
| 3-Hydroxy-Trimethyl-Lysine Aldolase                                   | (HTMLA)                  |
| Inducible Post-Natal Global Cyclooxygenase-2 Knock-Out Mouse          | (iCOX-2 <sup>-/-</sup> ) |
| Inducible Post-Natal Global Cyclooxygenase-2 Littermate-Control Mouse | (iCOX-2 <sup>+/+</sup> ) |
| Interleukin-1 Beta  | (IL-1β)                  |
| Prostacyclin Receptor   | (IP)                     |
| Inducible Post-Natal Global   | (IPNG)                   |
| Knock-Out   | (KO)                     |
| Liquid Chromatography   | (LC)                     |
| Liquid Chromatography-Mass Spectrometry/Mass Spectrometry             | (LC-MS/MS)               |

|  |                      |
|--|----------------------|
| Lactate Dehydrogenase  | (LDH)                |
| Monomethyl-L-Arginine  | (L-NMMA)             |
| Lipoxygenase   | (LOX)                |
| Lipocalin-type Prostaglandin-D synthase                          | (L-PGDS)             |
| Leukotriene B <sub>4</sub>                                       | (LTB <sub>4</sub> )  |
| Left Ventricular Systolic Dysfunction                            | (LVSD)               |
| Methylcytosine   | (MeCyt)              |
| Methylhistidine  | (MeHis)              |
| Methionine   | (Met)                |
| Methionine Sulfoxide   | (MetSO)              |
| Myocardial Infarction  | (MI)                 |
| Microsomal Prostaglandin-E Synthase                              | (mPGES)              |
| Multiple Reaction Monitoring                                     | (MRM)                |
| Mass Spectrometry  | (MS)                 |
| Oxidised Nicotinamide Adenine Dinucleotide                       | (NAD <sup>+</sup> )  |
| Reduced Nicotinamide Adenine Dinucleotide                        | (NADH <sup>+</sup> ) |
| Nuclear Factor-Kappa B   | (NF-κB)              |
| National Institutes of Health                                    | (NIH)                |
| Nuclear Magnetic Resonance                                       | (NMR)                |
| Nitric Oxide   | (NO)                 |
| Nuclear Overhauser Effect Spectroscopy                           | (NOESY)              |
| Nitric Oxide Synthase  | (NOS)                |
| Non-Steroidal Anti-Inflammatory Drug                             | (NSAID)              |
| New York Heart Association                                       | (NYHA)               |
| Osteoarthritis   | (OA)                 |
| Organic Cation Transporter 2                                     | (OCTN2)              |
| Principal Components Analysis                                    | (PCA)                |
| Primary Carnitine Deficiency                                     | (PCD)                |
| Phosphodiesterase Type 5   | (PDE5)               |
| Prostaglandin  | (PG)                 |
| Peroxisome Proliferator-Activated Receptor Gamma Coactivator 1-α | (PGC1α)              |
| Prostaglandin-D <sub>2</sub>                                     | (PGD <sub>2</sub> )  |
| Prostaglandin-E <sub>2</sub>                                     | (PGE <sub>2</sub> )  |
| Prostaglandin E <sub>2</sub> Metabolite                          | (PGEM)               |
| Prostaglandin-F <sub>2α</sub>                                    | (PGF <sub>2α</sub> ) |
| Prostaglandin-F Synthase   | (PGFS)               |
| Prostaglandin-G <sub>2</sub>                                     | (PGG <sub>2</sub> )  |
| Prostaglandin-H <sub>2</sub>                                     | (PGH <sub>2</sub> )  |
| Prostacyclin   | (PGI <sub>2</sub> )  |
| Prostacyclin Synthase  | (PGIS)               |
| Protein Kinase G   | (PKG)                |
| Phospholipase A <sub>2</sub>                                     | (PLA <sub>2</sub> )  |
| Pyridoxal Phosphate  | (PLP)                |
| Partial Least Squares Discriminate Analysis                      | (PLS-DA)             |
| Primary Murine Cardiomyocyte                                     | (PMC)                |
| Peroxisome Proliferator-Activated Receptor-Alpha                 | (PPAR-α)             |

|  |                     |
|--|---------------------|
| Proton Pump Inhibitors                                       | (PPI)               |
| Peroxisome Proliferator Response Element                     | (PPRE)              |
| Protein Arginine Methyltransferase                           | (PRMT)              |
| Proline  | (Pro)               |
| Hydroxyproline   | (ProOH)             |
| Polyunsaturated-Fatty Acid                                   | (PUFA)              |
| Rheumatoid Arthritis   | (RA)                |
| Randomised Controlled Trial                                  | (RCT)               |
| Radiofrequency   | (RF)                |
| Relative Risk  | (RR)                |
| Quantitative Reverse Transcription Polymerase Chain Reaction | (RT-qPCR)           |
| S-Adenosylhomocysteine                                       | (SAH)               |
| S-Adenosylmethionine   | (SAM)               |
| Symmetric Dimethylarginine                                   | (SDMA)              |
| Soluble Guanylyl Cyclase                                     | (sGC)               |
| Smooth-Muscle Cell   | (SMC)               |
| Total Area   | (TA)                |
| Transverse Aortic Constriction                               | (TAC)               |
| Trimethylamine   | (TMA)               |
| 4-Trimethylaminobutanal Dehydrogenase                        | (TMABADH)           |
| Trimethylamine-N-Oxide                                       | (TMAO)              |
| Trimethyl-Lysine   | (TML)               |
| Trimethyl-Lysine Deoxygenase                                 | (TMLD)              |
| Traditional Non-Steroidal Anti-Inflammatory Drug             | (tNSAID)            |
| Thromboxane-A <sub>2</sub> Receptor                          | (TP)                |
| Sodium-3-(tri-methylsilyl)-2,2,3,3-tetradeuteriopropionate   | (TSP)               |
| Thromboxane-A <sub>2</sub>                                   | (TxA <sub>2</sub> ) |
| Thromboxane-A Synthase                                       | (TXS)               |
| Tyrosine   | (Tyr)               |
| Hydroxytyrosine  | (TyrOH)             |
| Ultra-High Performance Liquid Chromatography                 | (UHPLC)             |
| Ultra Performance Liquid Chromatography                      | (UPLC)              |
| Vioxx Gastrointestinal Outcomes Research                     | (VIGOR)             |
| Variable Importance in Projection                            | (VIP)               |
| Wild-Type  | (WT)                |
| 4-(2-hydroxyethyl)-1-piperazineethanesulfonic acid           | (HEPES)             |

# ***Chapter 1: Thesis Introduction***

## *Introduction: The “Gap in the Knowledge”*

Cyclooxygenase-2 (COX-2) selective inhibitors, also known as “coxibs,” are a subclass of the non-steroidal anti-inflammatory drugs (NSAIDs). Like traditional NSAIDs, the coxibs are widely used to treat inflammation and pain. However, their use has been associated with a higher risk of adverse cardiovascular (CV) events. These include both thrombotic events, mainly myocardial infarction (MI) and stroke, and non-thrombotic events, of which heart failure (HF) is the most common [1]. Estimates suggest that one such coxib, rofecoxib, may have caused 88,000 to 140,000 excess serious CV events in the USA, before its market withdrawal in 2004 [2]. However a number of other coxibs are still available.

Several competing theories have been proposed to explain the thrombotic CV risk [3, 4], however the mechanisms which underlie the non-thrombotic CV risk are still to be established. One possibility is that the non-thrombotic CV risk merely reflects the mechanisms responsible for the thrombotic CV risk [5, 6]. However, this is likely to be a gross oversimplification, as the clinical evidence suggests that the non-thrombotic CV risk not only represents a greater adverse event signal than the thrombotic CV risk, but also presents earlier [1].

Metabolomic analyses, which have provided significant insights into the pathogenesis of various forms of HF, have been little used to explore this problem.

Therefore, the metabolic changes associated with coxib use, and how these relate to the mechanisms underlying the coxib-associated non-thrombotic CV risk are largely unknown.

## *Thesis Purpose*

This work will attempt to address the gap in the knowledge, namely the metabolic changes associated with coxib use and how these relate to the mechanisms underlying the coxib-associated non-thrombotic CV risk. To achieve this, mouse models of coxib use will be employed. Metabolites will be measured in tissues and biofluids and the findings related to what is already known about non-thrombotic CV disease, specifically HF. Pharmacological/genetic inhibition of COX-2, study length, inflammatory status and CV risk-factors will be varied, which will enable the gap in the knowledge to be explored from several angles.

## *Thesis Significance*

This work will contribute to the body of knowledge, in the fields of coxib-induced HF and cyclooxygenase biology, by providing detailed metabolomic insight into the effects of coxib treatment and genetic COX-2 deletion, in the mouse. It will examine both general metabolic perturbations and perturbations in selected pathways, identified on the basis of their involvement in the pathogenesis of other forms of HF, resulting from inhibition of COX-2 activity. Ultimately it will provide insight into the mechanisms underlying the off-target cardiac effects associated with coxib use.

This work will establish a basis for further exploration of the mechanisms underlying coxib-induced HF. It will enable the intelligent selection of pathways for further analysis and has the potential to accelerate the identification of molecular targets, which could then be exploited, to reduce the risk of coxib-induced HF.

## *Thesis Primary Research Questions*

This thesis will be framed by three primary research questions and two sub-questions:

**What are the metabolomic consequences of coxib treatment, in the mouse?**

**Do celecoxib and rofecoxib cause similar metabolic changes?**

**Are perturbations in pathways, as opposed to isolated metabolites, evident?**

**Is there an evidence-base linking these pathways to HF?**

**What are the underlying mechanisms, driving these pathway differences?**

These research questions will direct the study design and influence the selection of study hypotheses at each stage.

## *Thesis Research Design*

This thesis will examine metabolic changes, related to the inhibition of COX-2 activity, in the mouse. The work will be divided into two phases. The first phase will employ nuclear magnetic resonance (NMR) spectroscopy and mass spectrometry (MS), in a screening-capacity, to identify metabolic pathways affected by coxib treatment. The effects of two coxibs, celecoxib and rofecoxib, on metabolite concentrations in various tissues and bio-fluids will be explored. Candidate pathways will be selected, on the basis of the biological plausibility of their involvement in coxib-induced HF, as determined by their degree of perturbation and the strength of published evidence linking them to other forms of HF. Hypotheses will be generated, based on these results. In the second phase, these hypotheses will be tested using targeted metabolomic techniques and supplementary techniques, such as quantitative reverse transcription polymerase chain reaction (RT-qPCR). The results of this testing will guide further exploration of the problem, which will be achieved by varying the experimental protocol in terms of inflammatory status, study length, presence of CV risk-factors, and genetic COX-2 knock-out.

# *Thesis Assumptions and Scope*

## **Thesis Assumptions**

This thesis makes a number of key assumptions.

Firstly, it is assumed that coxib treatment will alter the metabolome in the mouse and that these alterations will, at least in part, reflect the changes responsible for the HF risk with which they are associated. This is a reasonable assumption as previous animal models of coxib treatment have reported metabolomic alterations and other forms of HF are associated with metabolic remodelling [4, 7-10].

Secondly, this work assumes that coxib-induced HF is likely to involve similar metabolic remodelling to that detected in other forms of HF. Cardiac metabolism is tightly regulated and provisioned by a number of major metabolic pathways, particularly fatty acid (FA) oxidation, to meet the high energy demand of the heart [11-13]. Metabolic remodelling is a feature common to many forms of HF [14-18]. Therefore, it is reasonable to assume that the progression of coxib-induced HF will follow a pattern of energetic dysregulation similar to that seen in other forms of HF, such as impaired FA oxidation.

Thirdly, this work assumes that the metabolomic analyses employed will be both broad and deep enough to capture these changes. The techniques used in these experiments were selected to provide such coverage. Moreover, MS, NMR spectroscopy and RT-qPCR have been used previously, to provide insight into metabolic alterations affecting the heart [19, 20].

Finally, like other animal studies, this work assumes that the findings in the mouse will be both relevant and generalisable to the human. The mouse has been used

extensively to provide insight into cardiac and systemic metabolism. Recently, the mouse Encyclopaedia of DNA Elements (ENCODE) consortium published data supporting the utility of the mouse, as a model of human metabolism and the immune and stress responses [21-23].

## **Thesis Scope**

To ensure that the research aims of this study are met, a series of delimitations will be applied, to focus this work and define its scope.

Firstly, whilst other techniques will be used in a supplementary capacity, to provide additional insight, metabolomic analyses will form the foundation of this work. This decision is based on both relevance to the 'gap in the knowledge' and practical considerations, such as time-frame, cost, access to instrumentation and expertise. Naturally, this dictates that this thesis will not incorporate measures of cardiac function. This will not detract from the thesis purpose, to address the gap in the knowledge, nor its desired significance, to establish a basis for further exploration of the mechanisms underlying coxib-induced HF.

To address the 'gap in the knowledge,' this work will focus on exploring the HF risk associated with coxib used. Therefore, background related to the mechanisms, clinical picture and metabolomic fingerprints of coxib-induced thrombotic events will not be discussed in detail. Moreover, only metabolomic findings that offer a possible explanation for the HF risk will be pursued.

This work will focus on two specific coxibs, celecoxib and rofecoxib. This selection ensures insight into the metabolomic consequences of treatment with a coxib withdrawn from the market, rofecoxib, and one still available despite evidence associating it with a higher risk of HF, celecoxib [6, 24]. This de-limitation

simultaneously allows the question of a possible class-wide effect to be addressed, whilst also ensuring that the project scope is in-line with its timely completion.

The mouse is the only *in vivo* model organism that will be used in this work. This is justified by the time, risk and cost advantages related to the use of a single non-human model system, as well as advantages regarding the simplification of study design, approval, implementation, analysis and inter-study comparison.

## *Summary*

A metabolomic approach will be employed, to identify metabolic perturbations associated with coxib use in the mouse. These changes will be explored, and candidate pathways selected for follow-up analysis, in an attempt to provide insight into the mechanisms underlying the risk of HF associated with coxib use. The coxibs and their association with HF, as well as the current body of knowledge regarding the metabolic changes observed with coxib use and in HF, are reviewed in Chapter 2. This provides the theoretical frame-work for, and biological plausibility of, the primary research questions of this thesis.

## ***Chapter 2: Thesis Background***

## *Inhibition of Cyclooxygenase*

Use of cyclooxygenase inhibitors, in clinical practice, is associated with adverse thrombotic and non-thrombotic cardiovascular events. Some have better safety profiles than others and some exhibit variability in the risk of thrombotic compared to non-thrombotic events. The mechanisms underlying the thrombotic events have been extensively discussed, but little consensus has been reached regarding the cause of the non-thrombotic events. The cyclooxygenase inhibitors, their mode of action, CV risk profile and putative mechanisms for this risk are reviewed below.

### **Cyclooxygenase and Prostanoid Synthesis**

Cyclooxygenase (COX) is a membrane bound enzyme which, amongst other functions, catalyses the committed step in the production of prostanoids (prostaglandins, prostacyclin and thromboxanes). In humans, two functional isoforms of COX have been described: COX-1 and COX-2.

#### *Cyclooxygenase-1*

COX-1 is constitutively expressed, at low levels, by most cells and is primarily localised to the endoplasmic reticulum [25]. It functions as the principal source of homeostatic prostanoids [26] and is widely distributed. COX-1 mRNA transcripts and protein are found in a variety of organs, for example the intestines, liver, kidney, heart, spleen and brain, from highest to lowest mRNA level [27].

#### *Cyclooxygenase-2*

COX-2 is localised to both the endoplasmic reticulum and the nuclear envelope [25] and its expression is dramatically increased in response to inflammatory stimuli, such as cytokines [26] and mitogens [28]. COX-2 is the major source of inflammatory

prostanoids. However, it would be a misleading over-simplification to describe COX-1 as the constitutive house-keeping isoform and COX-2 as the inducible inflammatory isoform. Indeed, COX-1 can contribute to the production of prostanoids during inflammation and COX-2 to homeostatic prostanoid production [26]. Under basal conditions, COX-2 mRNA transcripts and protein are found in organs such as the kidney, brain, spleen, liver, heart and intestine, from highest to lowest mRNA level [27], as well as the reproductive tract [29] and thymus [30]. In the kidney, COX-2 is differentially expressed and regulated in the cortex and medulla [31]. Constitutive expression of COX-2, in the kidney, is independent of microbial infection and is not associated with inflammatory signalling through nuclear factor-kappa B (NF- $\kappa$ B) [30], emphasising its homeostatic role in this organ.

### *Cyclooxygenase Structure and Function*

Structurally, COX exists as a homodimer, with each monomer possessing both a cyclooxygenase and peroxidase active site [32]. COX-1 and COX-2 share 60 % amino acid sequence identity and possess three-dimensional structures which closely resemble one-another [33]. Both possess a long narrow hydrophobic channel which ends in a hairpin, although the COX-2 channel is about 20 % larger [34, 35]. COX catalyses the two-step formation of prostaglandin (PG) endoperoxide  $H_2$ , the common precursor to all prostanoids [36], from 20-carbon polyunsaturated FAs, via the oxidative cyclization of their central 5 carbons [37]. The prostanoids derived from the 20-carbon polyunsaturated ( $\omega$ -6) FA - arachidonic, are the most biologically active in inflammation. In the first enzymatic step the cyclooxygenase active site catalyses the oxygenation of arachidonic acid to form the hydroperoxy endoperoxide, prostaglandin- $G_2$  ( $PGG_2$ ), intermediate. In the second step the peroxidase active site

catalyses the reduction of PGG<sub>2</sub>, to form the hydroxyl endoperoxide, prostaglandin-H<sub>2</sub> (PGH<sub>2</sub>), product [38, 39].

### *Cyclooxygenase Coupled Terminal Synthases*

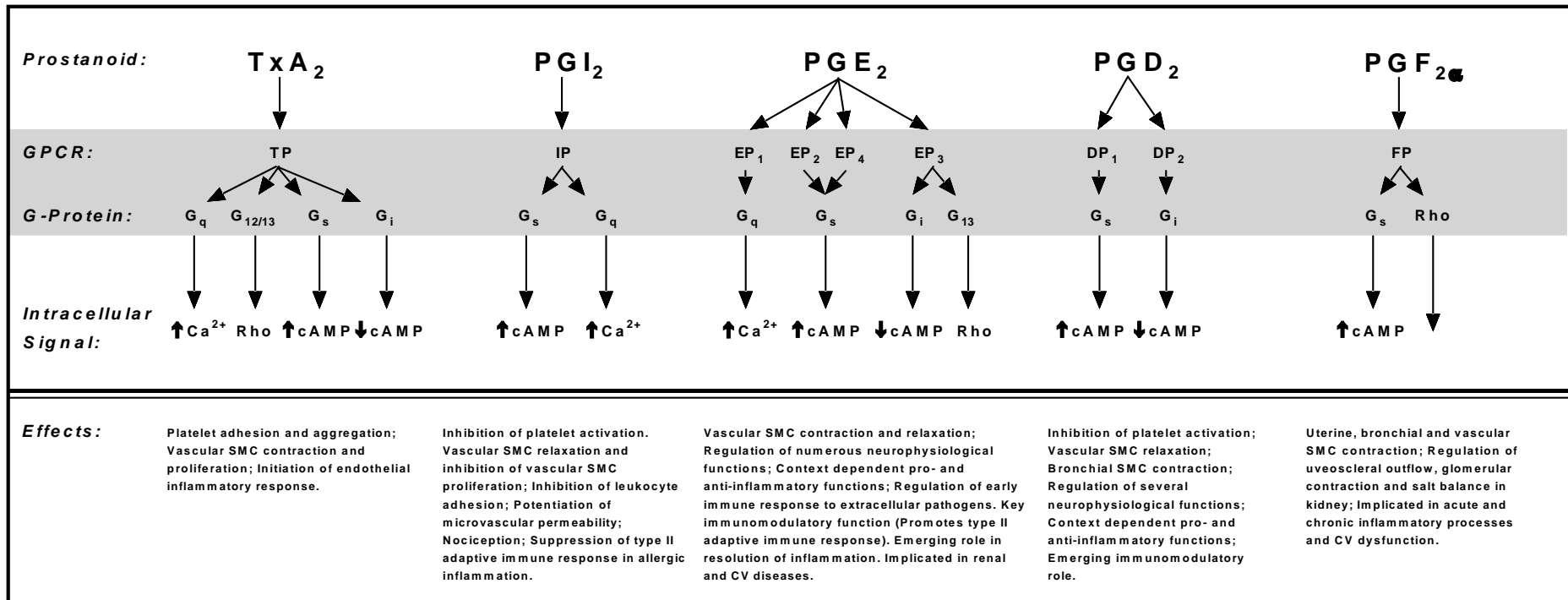
PGH<sub>2</sub> is transformed, by specific isomerases and synthases, into one of an array of different prostanoids. The five principal bioactive prostanoids are: thromboxane-A<sub>2</sub> (TxA<sub>2</sub>) - synthesised by thromboxane-A synthase (TXS); prostacyclin (PGI<sub>2</sub>) - synthesised by PGI synthase (PGIS); prostaglandin-E<sub>2</sub> (PGE<sub>2</sub>) - synthesised by cytosolic and microsomal PGE synthases (cPGES and mPGES), which preferentially couple to COX-1 and COX-2, respectively [26, 40]; prostaglandin-D<sub>2</sub> (PGD<sub>2</sub>) - synthesised by haematopoietic- and lipocalin-type PGD synthases (H-PGDS and L-PGDS) and prostaglandin-F<sub>2α</sub> (PGF<sub>2α</sub>) - synthesised by PGF synthase (PGFS). The two COX isoforms exhibit different preferential coupling to these enzymes: COX-1 with TXS, PGFS and cPGES; COX-2 with PGIS and mPGES, which are often co-induced in response to inflammatory stimuli [26, 40]. Therefore, basal COX-1 and COX-2 activity, as well as the inducible component of COX-2 activity and the specific coupling and activity of the downstream enzymatic machinery, determines the profile of prostanoids synthesised. For a particular cell type, one or two prostanoids will usually predominate [26]. Vascular endothelial cells, for example, primarily synthesise PGI<sub>2</sub>, whereas platelets typically synthesise TxA<sub>2</sub>. Macrophages synthesise TxA<sub>2</sub>, with PGE<sub>2</sub> produced at lower levels. However, on activation, COX-2 is induced and PGE<sub>2</sub> synthesis exceeds that of TxA<sub>2</sub> [41].

### **Prostanoid Signalling and Inflammation**

Prostanoids are a subclass of eicosanoids, derived from the oxidation of 20-carbon FAs. They serve as autocrine and paracrine mediators and possess diverse roles in

homeostasis, as well as the initiation, propagation and resolution of inflammation [26, 42-50] (*Figure 1*).

**Figure 1.**



*Prostanoid Signalling. The five principle bioactive prostanoids can be grouped into three sub-classes: Thromboxanes (of which TxA<sub>2</sub> is a member), prostacyclins (of which PGI<sub>2</sub> is a member) and prostaglandins (of which PGE<sub>2</sub>, PGD<sub>2</sub> and PGF<sub>2α</sub> are members). They exert their effect through five sub-types of seven transmembrane GPCRs, named according to the prostanoid that they are most sensitive to. Through these GPCRs, the prostanoids have diverse homeostatic and inflammatory functions. Abbreviations: thromboxane-A<sub>2</sub> (TxA<sub>2</sub>); Prostacyclin (PGI<sub>2</sub>); Prostaglandin-E<sub>2</sub> (PGE<sub>2</sub>); Prostaglandin-D<sub>2</sub> (PGD<sub>2</sub>); Prostaglandin-F<sub>2α</sub> (PGF<sub>2α</sub>); Thromboxane-A<sub>2</sub> receptor (TP); Prostacyclin receptor (IP); Prostaglandin-E<sub>2</sub> receptor (EP); Prostaglandin-D<sub>2</sub> receptor (DP); Prostaglandin-F<sub>2α</sub> receptor (FP); Cyclic adenosine monophosphate (cAMP); Guanine nucleotide-binding protein (G-protein); Guanine nucleotide-binding protein-coupled receptor (GPCR); Smooth-muscle cell (SMC); Cardiovascular (CV). Adapted from Boor et al. [51] and Alfranca et al. [52].*

Taken together, the homeostatic roles of the different prostanoids influence almost every major organ system and their inflammatory and immune regulatory functions are equally diverse. It is, perhaps, then unsurprising that pharmacological inhibition of their production has profound consequences, some of which may be desirable and others unwanted or unanticipated.

## **Pharmacological Inhibition of Cyclooxygenase**

For thousands of years nutraceutical preparations were used, without mechanistic insight, to treat inflammation and pain [53]. Then in 1971 John Vane identified the COX inhibitory action of the pharmaceutical preparation of aspirin [54]. Subsequently, several of the natural remedies for pain were shown to inhibit COX [55, 56]. Other pharmaceutical preparations, which we now know as the NSAIDs, exploit this enzyme system and represent one of the most widely used drug class.

### *Salicylates and Aspirin*

In its crudest form, use of the active ingredient in aspirin, salicylic acid, to treat inflammation and pain dates back almost 2500 years to a time when the Greek physician Hippocrates would prescribe an extract from willow bark [57]. Aspirin itself, acetylsalicylic acid, has been produced by Bayer since 1899 and is more palatable than underived salicylic acid [58]. Unlike other NSAIDs, aspirin irreversibly and covalently modifies COX. It first binds rapidly and reversibly through weak ionic interactions, which allow it to orientate in the active site, then it irreversibly transacetylates serine-530 or serine-516 of COX-1 and COX-2, respectively [25, 59]. This results in the irreversible total inhibition of COX-1 oxygenase activity and prostanoid synthesis. Acetylation of COX-2 serine-516 also abolishes PGG<sub>2</sub> and prostanoid synthesis. However, because the COX-2 active site is larger, arachidonic

acid can still gain access. This drives synthesis of 15- and 11-hydroxyeicosatetraenoic acid (HETE) via the rarely occurring lipoxygenase reaction [60]. Aspirin is more than three times as active against COX-1 compared to COX-2, in whole blood [61]. This selectivity and cell-type specific rates of COX turnover are responsible for the antiplatelet effects of low-dose (75 mg/day) aspirin administration, which remains the gold standard in the prophylaxis of arterial thrombosis [62, 63]. The ratio of TxA<sub>2</sub> (which is synthesised by platelet COX-1 and is pro-thrombotic) to PGI<sub>2</sub> (which is synthesised by endothelial COX-2 and is anti-thrombotic) is a key regulator of platelet aggregation. Aspirin inhibits platelet COX-1 irreversibly and because platelets are anuclear and, unlike endothelial cells, can't re-synthesise COX, low-dose aspirin administration tips the haemostatic balance in favour of PGI<sub>2</sub> and the anti-thrombotic state. However, in the context of acute myocardial infarction (MI) and ischaemic stroke, the anti-thrombotic state predisposes patients to bleed and aspirin use is associated with an elevated risk of haemorrhagic stroke [64]. Aspirin administration is also associated with gastrointestinal (GI) toxicity, including potentially life-threatening peptic ulcer formation and bleeding [65]. These effects are thought to be mediated by the inhibition of PGE<sub>2</sub> and PGI<sub>2</sub> synthesis, which protect the GI mucosa by forming a cytoprotective layer and promoting, acid-neutralising, bicarbonate ion synthesis [66]. Even very low-dose (10 mg/day) aspirin has been shown to reduce prostaglandin concentrations in the gastric mucosa and induce gastroduodenal injury [67].

### *Traditional Non-Steroidal Anti-Inflammatory Drugs*

Following on from the success of aspirin, in 1969 the Boots Company launched ibuprofen. This was the first of many non-aspirin NSAIDs. Traditional non-steroidal anti-inflammatory drugs (tNSAIDs) may be classified on the basis of either their chemical structure or their binding characteristics, but all competitively and reversibly

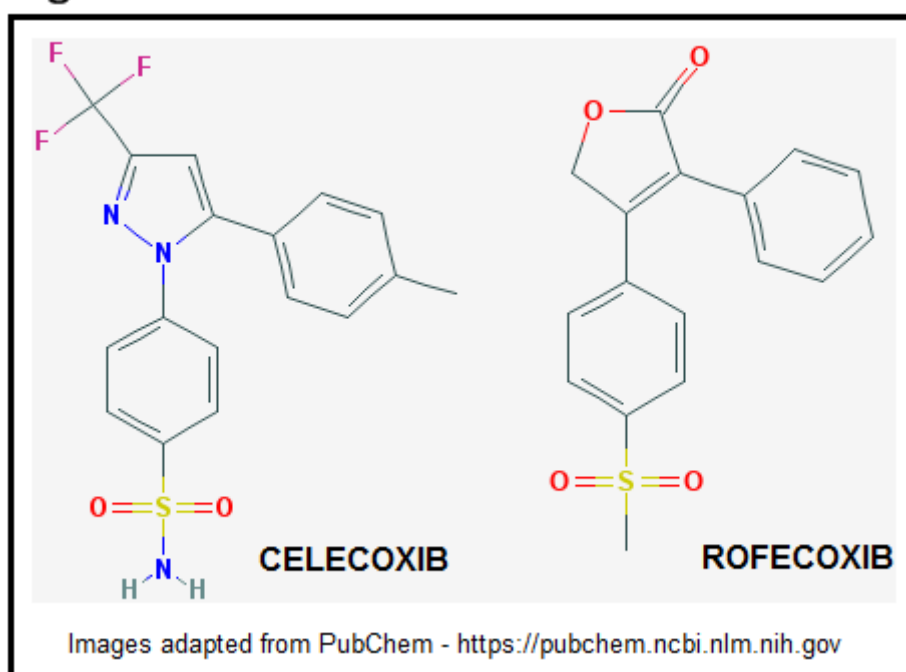
inhibit COX-1 and COX-2 to variable degrees [34]. Broadly speaking, tNSAIDs fall into one of three chemical classes: carboxylic acids, enolic acids and anilides (e.g. acetaminophen). The carboxylic acids are further sub-classified: propionates (e.g. ibuprofen and naproxen), acetic acids (e.g. indomethacin and diclofenac) and anthranilates (e.g. mefenamic acid); as are the enolic acids: oxicams (e.g. piroxicam) and pyrazolones (e.g. phenylbutazone) [68]. Traditional NSAIDs may also be considered in terms of their binding characteristics. Some, such as ibuprofen, piroxicam and mefenamic acid, exhibit rapid competitive reversible binding. Others, such as diclofenac and indomethacin, exhibit rapid low-affinity reversible binding, followed by time-dependent, higher-affinity, slowly-reversible binding [25]. Traditional NSAIDs exhibit compound specific relative activity against COX-1 and COX-2. Of those that are more active against COX-1, some have a greater whole blood COX-1:COX-2 inhibitory ratio than aspirin (3.14). These include flurbiprofen (10.27), ketoprofen (8.16) and fenoprofen (5.14). Others have a lower COX-1:COX-2 inhibitory ratio, such as naproxen (1.79), indomethacin (1.78) and ibuprofen (1.69). Some tNSAIDs are more active against COX-2. These include piroxicam (0.79), mefenamic acid (0.08) and diclofenac (0.05) [61]. Traditional NSAIDs are associated with a range of adverse events. They elevate the risk of major and minor GI events (as per aspirin), sodium and fluid retention, renal insufficiency and adverse CV outcomes including hypertension, oedema, MI, exacerbations of HF and perhaps HF itself [34].

### *Coxibs: Cyclooxygenase-2 selective Non-Steroidal Anti-Inflammatory Drugs*

Before it was known that tNSAIDs increase CV risk, the main drawback to their use was considered the adverse GI outcomes, caused by COX-1 inhibition, with which they were associated. Major events, such as GI bleeds, were a pressing concern and

minor events, such as nausea and dyspepsia made taking tNSAIDs less tolerable for the patient. Selective COX-2 inhibitors were therefore developed in an attempt to circumvent these side-effects. Chemically these 'coxibs' are divided into the diaryl-substituted cycles, which possess a tricyclic ring and a sulfone (e.g. rofecoxib and etoricoxib) or sulphonamide (e.g. celecoxib and valdecoxib) moiety, and the phenyl acetic acid derivatives (e.g. lumiracoxib) [69, 70].

**Figure 2.**



Coxibs exploit amino acid substitutions at positions 434 (isoleucine for valine), 513 (histidine for arginine) and 523 (isoleucine for valine) in COX-1 versus COX-2, respectively [35]. This allows access to a polar hydrophilic side-pocket, in COX-2, with which a chemical group of the coxib, for example the phenylmethylsulfone group of rofecoxib or the phenylsulfonamide group of celecoxib, is able to interact [35, 71, 72]. This side pocket is inaccessible in COX-1. This engenders the coxibs with their COX-2 selectivity. The COX-1:COX-2 inhibitory ratio is 0.05 for rofecoxib and 0.11 for celecoxib and, like tNSAIDs, COX inhibition is competitive and reversible [61]. The first

coxibs; rofecoxib, celecoxib and valdecoxib; were licenced for use in 1999 [24]. Several, small, randomised controlled trials (RCTs) were conducted in patients with arthritis and concluded that the coxibs possessed equal efficacy and a lower incidence of endoscopically detected gastroduodenal ulceration, when compared to tNSAIDs [73]. Three studies examined the cumulative incidence of gastroduodenal ulceration in patients, with osteoarthritis (OA) and/or rheumatoid arthritis (RA), taking 200 mg celecoxib twice a day. Two of these studies compared celecoxib and 500 mg naproxen taken twice a day over 12 weeks. The other one compared celecoxib and 75 mg diclofenac twice a day over 24 weeks. The 12 week studies reported a significantly lower ( $P < 0.001$ , in both) incidence of gastroduodenal ulceration in the celecoxib (4 % & 9 %) treated groups compared to the naproxen (26 % & 41 %) treated groups. The 24 week study reported a significantly lower ( $P < 0.001$ ) incidence of gastroduodenal ulceration in the celecoxib (4 %) treated group compared to the diclofenac (16 %) treated group [74-76]. Two 24 week studies compared the cumulative incidence of gastroduodenal ulceration in OA patients taking 25 mg or 50 mg rofecoxib once a day with those taking 800 mg ibuprofen three times a day. Both studies reported a significantly lower ( $P < 0.001$ , in all) incidence of gastroduodenal ulceration in the 25 mg (9.6 % & 9.9 %) and the 50 mg (12.4 % & 14.7 %) rofecoxib treated groups compared to the ibuprofen (45.8 % & 46.8 %) treated groups [77, 78]. Two 12 week studies compared the cumulative incidence of gastroduodenal ulceration in OA patients taking either 5 mg, 10 mg or 20 mg of valdecoxib once a day with those taking either 500 mg naproxen twice a day, 800 mg ibuprofen three times a day or 75 mg diclofenac twice a day. The first study reported a significantly lower ( $P < 0.05$ , in both) incidence of gastroduodenal ulceration in the 5 mg (3 %) and 10 mg (3 %), but not 20 mg (5 %), valdecoxib treated group compared to the naproxen (10 %) treated

group, whilst the second study reported a significantly lower ( $P < 0.05$ , in all) incidence in the 10 mg (5 %) and 20 mg (4 %) valdecoxib treated group compared to the ibuprofen (16 %) and diclofenac (17 %) treated groups [79, 80]. Subsequently, these findings were validated in larger clinical trials [73, 81]. The Celecoxib Long-term Arthritis Safety Study (CLASS) examined the incidence of adverse gastroduodenal events in 8059 patients, with OA or RA, taking 400 mg celecoxib twice a day or a tNSAID (800 mg ibuprofen three times a day or 75 mg diclofenac twice a day) over a 6-month period. The study reported a significantly lower ( $P < 0.05$ ) annualised incidence of symptomatic gastroduodenal ulcers and their complications, with celecoxib (2.08 %) compared to the tNSAIDs (3.54 %). Moreover, when the study population was sub-divided into those taking low-dose aspirin and those not, it was evident that low-dose aspirin use confounds this effect [82]. The Vioxx Gastrointestinal Outcomes Research (VIGOR) study explored the cumulative incidence of adverse gastroduodenal events in 8076 patients with glucocorticoid treated RA, taking 50 mg rofecoxib once a day or 500 mg naproxen twice a day, over a median 9-month follow-up in both groups. Occurrence of confirmed predefined adverse gastroduodenal events were measured: gastric and duodenal ulcers, bleeding, perforations and obstructions. Events were further categorised as complicated and non-complicated. The incidence of total confirmed gastroduodenal events was significantly lower ( $P < 0.001$ ) in the rofecoxib (1.4 %) treated group compared to the naproxen (3 %) treated group, as was the incidence of confirmed complicated events (0.4 % and 0.9 %, respectively;  $P = 0.005$ ). Startlingly, a significantly greater ( $P < 0.005$ ) incidence of acute MI was observed in the rofecoxib (0.4 %) treated group compared to the naproxen (0.1 %) treated group. The authors attributed this to the coronary protective effect of naproxen [75]. However, this conclusion was scrutinised and subsequent

studies demonstrated that the coronary-protection, conferred by naproxen, is insufficient to account for the difference in MI incidence of the two drugs [83-85]. A CV safety warning was added to rofecoxib in April 2002. These findings raised serious safety concerns and precipitated a significant scientific effort to evaluate and characterise the CV safety of the COX-2 inhibitors.

## **Non-Steroidal Anti-Inflammatory Drugs and Adverse Cardiovascular Events**

If the results of the VIGOR study sparked scientific interest in the CV safety of the coxibs, the Adenomatous Polyp PRevention On Vioxx (APPROVe) study set that interest alight. The APPROVe study was designed to determine whether rofecoxib once a day could be used as a prophylactic for colorectal polyps. 2586 patients, with a history of colorectal adenomas, were randomised to 25 mg rofecoxib once a day or placebo groups. Whilst the study was scheduled to last three years, it was terminated two months early, on the advice of the safety-monitoring board [1]. The investigators reported a higher cumulative incidence/incidence rate of adjudicated major adverse thrombotic events (fatal/non-fatal MI and ischaemic stroke, unstable angina, transient ischaemic attack, mortality due to cardiac cause, peripheral arterial/venous thrombosis and pulmonary embolism) in the rofecoxib (3.6 %/1.50 per 100 patient years) treated group compared to placebo (2 %/0.78 per 100 patient years) group (Relative risk (RR) = 1.79, 95 % confidence interval (CI) 1.11-2.87/Hazard ratio (HR) = 1.92, 95 % CI 1.19-3.11). They concluded that this was primarily due to a higher incidence of MI and ischaemic stroke in the rofecoxib (MI = 1.63 %; Stroke = 0.85 %) treated group compared to the placebo (MI = 0.69 %; Stroke = 0.46 %) group (MI RR = 2.36, 95 % CI 1.08-5.12; Stroke RR = 1.85, 95 % CI 0.69-4.99) [1]. Post-hoc analysis indicated that the higher risk of adjudicated major adverse thrombotic events become

apparent after 18 months. Subgroup analysis demonstrated that the risk with rofecoxib compared to placebo was enhanced by a history of symptomatic atherosclerotic disease (RR = 9.59, 95 % CI 1.36-416) and diabetes (RR = 6.10, 95 % CI 1.36-56.1) [1]. The investigators also noted a significant ( $P < 0.01$ ) elevation in mean systolic blood pressure in the rofecoxib ( $3.4 \pm 0.4$  mm Hg) treated group compared to the placebo ( $-0.5 \pm 0.3$  mm Hg) group, evident after 4 weeks [1]. Intriguingly, the cumulative incidence/incidence rate of the congestive heart failure (CHF), pulmonary oedema and cardiac failure (CF) combined endpoint was also greater in the rofecoxib (1.3 %/0.6 per 100 patient years) treated group compared to the placebo (0.3 %/0.1 per 100 patient years) group (RR = 4.29, 95 % CI 1.45-12.71/HR = 4.61, 95 % CI 1.50-18.83) [1]. This represents a greater adverse CV event signal than that of the thrombotic events. Moreover, Kaplan-Meier estimates indicated that this difference in CHF, pulmonary oedema and CF was evident from around 5 months. This is considerably earlier than the time taken for the differences in thrombotic event rates to become evident. In September 2004, these and other findings, lead to the withdrawal of rofecoxib from the worldwide market [24]. Attention then turned to other members of this drug class and, in 2005, valdecoxib was withdrawn [86]. Lumiracoxib has also been withdrawn, but owing to its hepatotoxic rather than CV effects [87].

Over the last decade, hundreds of animal and clinical studies have compared the CV effects of different coxibs with each other, other tNSAIDs and placebo. However, the results they reported were often incongruent, in part owing to intra-study confounding factors, and weighing up the evidence has been challenging. Nevertheless, these studies served to raise important questions: Is the higher risk of adverse CV events, first seen with rofecoxib, a class-wide effect and does this apply to the elevated risk of adverse vascular events and HF? If so, are some NSAIDs safer than others? What

might underlie this heterogeneity? Recently, several large meta-analyses have provided some insight into the answers to these questions.

### *A Class Wide Effect? Evidence from Meta-Analyses*

The risk of adverse vascular events and HF in coxib users has been extensively evaluated. Kearney et al. published the first rigorous meta-analysis of the risk of adverse vascular events with coxib use compared to both placebo and tNSAIDs [88]. They reviewed published and unpublished tabular data from 138 randomised trials, totalling 145,373 individuals, of at least 4 weeks duration [88]. These included 121 studies which compared a coxib to placebo: They reported a significantly higher incidence of first major vascular events (non-fatal MI, non-fatal stroke and vascular death) in the coxib treated group compared to the placebo group (RR = 1.42, 95 % CI 1.13-1.78;  $P = 0.003$ ); This was largely due to a higher risk of MI (RR = 1.86, 95 % CI 1.33-2.59;  $P = 0.0003$ ); i. no significant differences in the risk of stroke or vascular death were observed; ii. there was no significant heterogeneity amongst the coxibs studied (rofecoxib, celecoxib, valdecoxib, etoricoxib and lumiracoxib), with respect to these findings, although the authors noted the limited power to identify such differences [88]. Subsequent meta-analyses have supported and extended these findings. The meta-analysis performed by the Coxib and traditional NSAID Trialists' (CNT) collaboration is the most extensive to date [89]. The authors reviewed published and unpublished individual participant data (or tabular data if individual participant data were unavailable) from 639 randomised trials, of at least 4 weeks duration. These included 184 studies, totalling 88,367 individuals, which compared a coxib to placebo and 35 studies, totalling 25,931 individuals, which compared a coxib with another coxib [89]. Compared to placebo, the authors reported a higher risk of major vascular events (non-fatal MI, non-fatal stroke and vascular death) in the coxib treated group (RR =

1.37, 95 % CI 1.14-1.66;  $P = 0.0009$ ) which they primarily attributed to an increase in major coronary events (non-fatal MI and coronary death) (RR = 1.76, 99 % CI 1.31-2.37;  $P = 0.0001$ ) [89]. The coxibs did not increase the risk of stroke. However, they did increase the risk of any cause of mortality (RR = 1.22, 95 % CI 1.04-1.44;  $P = 0.0139$ ) compared to placebo, largely due to an increase in vascular mortality (RR = 1.58, 99 % CI 1.00-2.49;  $P = 0.0103$ ) [89]. This meta-analysis concluded that rofecoxib (RR = 1.38, 95 % CI 1.07-1.80;  $P = 0.0137$ ) and celecoxib (RR = 1.36, 95 % CI 1.00-1.84;  $P = 0.05$ ) elevate the risk of major vascular events, to a similar extent, when compared to placebo. However, they noted that lower doses of celecoxib were associated with a lower risk of adverse vascular events ( $P$  for trend = 0.0117). Although little placebo controlled data is available for etoricoxib and lumiracoxib, they are also thought to possess a similar vascular risk, based on inference from studies comparing coxibs to tNSAIDs [89]. The CNT collaboration also reported that coxibs increase the risk of hospitalisations due to HF, compared to placebo (RR = 2.28, 95 % CI 1.62-3.20;  $P < 0.0001$ ) and, as in the APPROVe study, this relative risk represents the greatest adverse CV event signal [89]. However, there may be a distinction between risk of HF development and exacerbation, with coxib use. Ungprasert et al. performed a recent meta-analysis of 7 observational studies, totalling 7,543,805 individuals, and examined the development of HF in patients taking tNSAIDs and coxibs compared to non-users. Sub-group analysis, of data from 2 studies, showed no significant elevation in relative risk for the development of HF in patients taking coxibs (RR = 1.03, 95 % CI 0.92-1.16) [5]. The same group also performed a second meta-analysis of 6 observational studies, totalling 161,472 individuals, explored the exacerbation of existing HF in patients taking tNSAIDs and coxibs compared to non-users. Sub-group analysis of data from 4 studies

demonstrated a significant elevation in relative risk for the exacerbation of HF in patients taking celecoxib (RR = 1.34, 95 % CI 0.98-1.85) and rofecoxib (RR = 2.04, 95 % CI 1.68-2.48). While the authors didn't directly compare celecoxib and rofecoxib, they noted that rofecoxib exhibited a significantly greater risk when compared to tNSAIDs ( $P = 0.02$ ), whilst celecoxib did not [6].

In summary, current evidence suggests that coxibs increase the risk of major vascular events, in particular MI, and mortality due to vascular causes and that this risk is similar among the coxibs [88, 89]. Evidence also indicates that coxibs increase the risk of HF hospitalisations, which may be largely due to exacerbations of HF rather than its development, such that HF represents the greatest coxib adverse CV event signal. Moreover, the risk of HF exacerbation may be worse with rofecoxib than celecoxib [5, 6, 89].

Evidence from meta-analyses also supports the assertion that some tNSAIDs elevate the risk of major adverse vascular events and HF. Kearney et al. examined the risk of major vascular events with tNSAIDs compared to placebo by combining data from direct and indirect (via a common coxib) comparisons [88]. They reported a significantly higher risk of major vascular events with diclofenac (RR = 1.63, 99 % CI 1.12-2.37) a non-significantly higher risk with ibuprofen (RR = 1.51, 99 % CI 0.96-2.37) and a non-significantly lower risk with naproxen (RR = 0.92, 99 % CI 0.67-1.26) compared to placebo [88]. In addition, the authors compared tNSAIDs with coxibs. They found incidence rates of major vascular events to be similar when comparing all tNSAIDs combined and non-naproxen tNSAIDs with coxibs. However, in sub-group analyses they noted a significantly greater risk with coxibs compared to naproxen (RR = 1.57, 95 % CI 1.21-2.03;  $P = 0.0006$ ). They also reported a greater risk of MI with coxibs compared to all tNSAID combined (RR = 1.53, 95 % CI 1.19-1.97;  $P = 0.0009$ )

and naproxen (RR = 2.04, 95 % CI 1.41-2.96;  $P = 0.0002$ ), but not non-naproxen tNSAIDs (RR = 1.20, 95 % CI 0.85-1.68;  $P = 0.3$ ) [88]. These results suggested that, like the coxibs, high dose regimens of diclofenac is associated with a higher risk of major adverse vascular events, whilst naproxen is not. In addition, naproxen, may be also be associated with a lower risk of MI. The CNT meta-analysis supported and extended these findings. Of the 639 trials they reviewed, 158 studies, including 38,081 individuals, compared tNSAIDs to placebo. The data from these direct comparisons was combined with data from indirect (via a common coxib) comparisons [89]. The authors reported that diclofenac increased the risk of major adverse vascular events (RR = 1.41, 95 % CI 1.12-1.78;  $P = 0.0036$ ), which they attributed primarily to a higher risk of major coronary events (RR = 1.70, 95 % CI 1.19-2.41;  $P = 0.0032$ ), and mortality due to vascular causes (RR = 1.65, 99 % CI 0.95-2.85;  $P = 0.0187$ ) compared to placebo. Ibuprofen didn't significantly increase the risk of major vascular events, or mortality due to vascular causes, but did significantly increase the risk of major coronary events (RR = 2.22, 99 % CI 1.10-4.48;  $P = 0.0253$ ) compared to placebo. Naproxen was neither associated with a higher risk of major vascular or coronary events, nor mortality due to vascular causes, compared to placebo [89]. The CNT collaboration also reviewed 474 studies, totalling 229,296 individuals, which compared NSAID regimens, of which 113 studies compared a coxib to a tNSAID and 335 studies compared two tNSAID regimens [89]. Unlike the other tNSAIDs, naproxen was not associated with a higher vascular and coronary risk (heterogeneity,  $P = 0.04$ ). Whilst the authors did not report whether the comparisons between the coxibs and the individual tNSAIDs achieved statistical significance, they were estimated based on a mathematical method outlined by Altman et al [90]. Of the tNSAIDs, the coxibs were associated with a higher risk of serious vascular events (RR = 1.49, 95 % CI 1.16-

1.92;  $P = 0.0020$ ), coronary events (RR = 2.11, 95 % CI 1.44-3.09;  $P = 0.0001$ ) and death due to vascular causes (RR = 1.53, 99 % CI 0.89-2.62;  $P = 0.0426$ ), only when compared to naproxen [89]. The CNT collaboration also reported that diclofenac (RR = 1.85, 95 % CI 1.17-2.94;  $P = 0.0088$ ), ibuprofen (RR = 2.49, 95 % CI 1.19-5.20;  $P = 0.0155$ ) and naproxen (RR = 1.87, 95 % CI 1.10-3.16;  $P = 0.0197$ ) all increase the risk of hospitalisation due to HF, compared to placebo. The HF risk was similar for all NSAIDs in this analysis; however the coxibs were presented as a combined group [89]. More recent meta-analyses provide greater granularity with respect to the comparative risk of HF between coxibs and NSAIDs and differences related to the development versus exacerbation of HF. Ungprasert et al. reported that, in pooled data from 5 observational studies, tNSAIDs increased the risk of developing HF compared to placebo (RR = 1.35, 95 % CI 1.15-1.57). As discussed, this effect was not seen with the coxibs [5]. The second meta-analysis, from the same group, explored the exacerbation of HF in NSAID users. They reported that tNSAIDs significantly increase the risk of HF exacerbation compared to placebo (RR = 1.39, 95 % CI 1.20-1.62). Moreover, they noted that, whilst the elevation in risk of HF exacerbation with tNSAIDs was comparable to celecoxib, it was significantly lower compared to rofecoxib ( $P = 0.02$ ) [6]. In summary, current evidence suggests that high dose regimens of diclofenac, and perhaps ibuprofen to a lesser extent, are associated with a higher risk of major adverse vascular events and mortality due to vascular causes, compared to placebo. The increase in major vascular events is primarily due to a higher incidence of coronary events such as MI. These outcomes are analogous to those seen with the coxibs. On the other hand, naproxen is not associated with a higher risk of these vascular outcomes and may actually reduce the risk of MI [88, 89]. Traditional NSAIDs appear to increase the risk of HF development, exacerbation and hospitalisation. They

present a greater risk of HF development, but a similar risk of hospitalisation, when compared to the coxibs. The tNSAIDs are also associated with a similar risk of HF exacerbation compared to celecoxib, but a lower risk compared to rofecoxib [5, 6, 89].

Unlike the coxibs and tNSAIDs, comprehensive meta-analyses support a role for low-dose aspirin in the primary and secondary prevention of major adverse vascular, especially thrombotic, events [91]. The Antithrombotic Trialist's (ATT) collaboration have twice undertaken meta-analyses comparing the occurrence of major vascular events (MI, stroke and vascular death) in patients taking long-term low-dose aspirin with controls [92, 93]. Their most recent analysis examined aspirin use in 6 primary prevention studies, totalling 95,000 low-average risk individuals. In the context of primary prevention they reported a lower risk of composite major vascular events (RR = 0.88, 95 % CI 0.82-0.94;  $P = 0.0001$ ) as well as non-fatal MI (RR = 0.77, 95 % CI 0.69-0.86;  $P < 0.0001$ ) and ischaemic stroke (RR = 0.86, 95 % CI 0.74-1.00;  $P = 0.05$ ) in patients taking aspirin compared to controls. They also examined aspirin use in 16 secondary prevention studies, totalling 17,000 high-average risk individuals. In the context of secondary prevention they reported a lower risk of composite major vascular events (RR = 0.81, 95 % CI 0.75-0.87;  $P < 0.0001$ ) as well as non-fatal MI (RR = 0.69, 95 % CI 0.60-0.80;  $P < 0.0001$ ) and ischaemic stroke (RR = 0.78, 95 % CI 0.61-0.99;  $P = 0.04$ ) in patients taking aspirin compared to controls [93]. Higher daily doses, up to 1500 mg, of aspirin also prevent adverse thrombotic CV events [91]. The evidence of the effect that aspirin has on HF risk is less conclusive. To date, HF risk in aspirin users has not been compared to placebo in any meta-analyses, although it has been compared to other treatments. Meta-analyses, comparing low-dose aspirin with warfarin in HF patients, have reported no significant differences in the incidence of HF hospitalisations [94, 95]. A recent retrospective cohort study reported that low-dose

aspirin use was associated with a lower risk of mortality in HF patients (HR = 0.58, 95 % CI 0.46-0.74) and a 30 % lower risk of HF hospitalisations in adjusted multivariable analysis, compared to non-aspirin use (HR = 0.70, 95 % CI 0.54-0.90). This effect was not seen with higher doses, 150 mg and 300 mg, of aspirin [96]. However, Cleland et al. suggest that it is implausible that low-dose aspirin has such a large effect on HF mortality and rightly criticise the study on the basis of a lack of randomisation [97]. A couple of older prospective studies have reported that higher doses, 162 mg and 300 mg, of aspirin once a day may be associated with a higher risk of hospital admissions due to HF, compared to either no-treatment or warfarin [98, 99]. In summary, whilst both low- and high-dose aspirin appear to protect against adverse thrombotic CV events, higher doses may be implicated in exacerbations of HF [91].

### *Are some Non-Steroidal Anti-Inflammatory Drugs Safer than Others? What might Underlie this Heterogeneity?*

As evidenced by the meta-analyses reviewed above, it is important to make the distinction between the risk of vascular events and the risk of HF, when considering the CV safety of the NSAIDs.

In the context of adverse vascular events, aspirin is protective, especially at lower doses [91]. Naproxen has a near-neutral risk. Of the other compounds reviewed, ibuprofen has the next lowest risk. Rofecoxib and Diclofenac possess the highest risks [89]. Higher doses of celecoxib are attributed with a risk similar to rofecoxib; however lower doses, which are often used in the community, are of lower risk [89, 100]. As discussed, aspirin is likely to derive its protective vascular effects from shifting the TxA<sub>2</sub>:PGI<sub>2</sub> ratio in favour of anti-thrombotic, PGI<sub>2</sub> [64]. In a similar vein, Fitzgerald et al. hypothesise that perturbation of the TxA<sub>2</sub>:PGI<sub>2</sub> ratio may underlie the elevated risk of adverse vascular events seen with the coxibs [3]. Briefly, coxibs exhibit greater

activity against COX-2 than COX-1. They therefore inhibit the synthesis of endothelial COX-2 derived PGI<sub>2</sub> to a greater extent than the synthesis of platelet COX-1 derived TxA<sub>2</sub>. This elevates the relative level of prothrombotic TxA<sub>2</sub> in the vasculature, predisposing to atherothrombotic vascular events, such as MI [3]. The compound specific risk is primarily thought to relate to the absolute COX-2 inhibitory activity. This is because the relationship between COX-1 inhibition and platelet activation *in vivo* is non-linear and a wide range of COX-1 inhibition, seen with therapeutic doses of different NSAIDs, leads to a similar level of platelet activation [91]. Garcia Rodriguez et al. noted that therapeutic doses of NSAIDs that inhibit more than 90 % of COX-2 activity (e.g. rofecoxib and diclofenac) are associated with a significantly greater risk of MI (RR = 1.60, 95 % CI 1.41-1.81) than those that inhibit less than 90 % of COX-2 activity (e.g. ibuprofen and lower dose celecoxib) (RR = 1.18, 95 % CI 1.02-1.38) [101]. This is consistent with the greater risk of adverse vascular events seen with rofecoxib and diclofenac and the lower risk seen with ibuprofen and community dose celecoxib. At higher doses, celecoxib would be expected to exhibit a greater vascular risk, owing to greater COX-2 inhibition, and that is indeed what is observed [89, 100]. The near-neutral risk of adverse vascular events with naproxen is often attributed to a mitigating, aspirin-like, anti-platelet effect [91].

Ahmetaj-Shala et al. contend the Fitzgerald hypothesis and present their own explanation [4]. They suggest that the endogenous nitric oxide synthase (NOS) inhibitors, asymmetric dimethylarginine (ADMA) and monomethyl-L-arginine (L-NMMA) serve as a mechanistic link between COX-2 inhibition in the kidney and the adverse vascular events associated with these drugs [4]. Briefly, COX-2 inhibition in the kidney enhances the synthesis of methylarginines and reduces their degradation, perhaps through inhibition of PGI<sub>2</sub> synthesis. This results in a net increase in plasma

ADMA and L-NMMA, which inhibit endothelial NOS and reduce nitric oxide (NO) production. Given the roles of NO, as a vasodilator and anti-platelet, this inhibition enhances the risk of the adverse vascular events, as seen with the NSAIDs [4]. In summary, the hierarchy of vascular risk with the different NSAIDs is now fairly well established, but the underlying mechanism is still disputed. Whilst the Fitzgerald hypothesis represents the favoured explanation of this risk, the mechanism proffered by Ahmetaj-Shala et al. seems biologically plausible. Further studies, exploring the role of ADMA and L-NMMA in NSAID vascular risk, are therefore warranted to interrogate the validity of this new hypothesis.

Stratifying the NSAIDs, according to the risk of HF with which they are associated, is challenging, not least because a range of outcome measures are used in describing HF risk (development, exacerbation, hospital admission and mortality). Low dose aspirin may provide some protection against mortality and hospital admission, due to the exacerbation of HF, although the jury is still out [96, 97]. However, at higher, anti-inflammatory, doses it seems likely that aspirin elevates the HF risk, much like the tNSAIDs [91]. Both coxibs and tNSAIDs elevate the risk of HF hospital admissions to a similar extent, but only tNSAIDs appear to elevate the risk of a first occurrence of HF. Rofecoxib is associated with a significantly greater risk of exacerbations of pre-existing HF, compared to other NSAIDs [5, 6, 89]. The prevailing explanation, of the elevation in HF risk seen with higher doses of NSAIDs, places inhibition of COX-2 in the kidney and systemic vasculature front and centre [91]. In the systemic vasculature, inhibition of endothelial COX-2 reduces PGI<sub>2</sub> synthesis, as described. In addition to its anti-thrombotic function, PGI<sub>2</sub> is a potent vasodilator. Consequently, inhibition of PGI<sub>2</sub> synthesis leads to vasoconstriction which may cause hypertension and lead to the exacerbation of HF [5, 6]. In the kidney, inhibition of cortex and

juxtaglomerular COX-2 reduces PGE<sub>2</sub> and PGI<sub>2</sub> synthesis. These prostaglandins play an important role in the maintenance of renal blood flow and glomerular filtration rate. In addition they inhibit Na<sup>+</sup> reabsorption, at the loop of Henle and cortical collecting tubules, and H<sub>2</sub>O reabsorption, at the collecting tubules leading to volume overload and exacerbation of HF [5, 6]. Rofecoxib causes greater Na<sup>+</sup> and H<sub>2</sub>O retention than celecoxib or tNSAIDs, which may go some way to explaining the greater risk of HF exacerbation associated with its use [102]. In addition, low-dose aspirin doesn't affect renal function, which may contribute to its apparent ability to reduce the risk of HF [91]. However, this mechanism does little to explain the similarity of HF hospitalisation risk amongst NSAIDs and the tNSAID specific risk of HF development. Another suggested explanation is that the risk of HF may reflect the risk of MI seen with some NSAIDs. MI is an established risk factor for HF. Extending those hypotheses that present mechanisms for the elevated risk of MI, to include the MI-HF relationship, may therefore explain some of the elevated risk of HF seen with NSAIDs. This may help explain the greater risk of HF exacerbation with rofecoxib, which has the greatest vascular risk, and the protective effect of low-dose aspirin, which also protects against adverse vascular events [5, 6]. However, once again, this fails to explain the similarity of HF hospitalisation risk amongst NSAIDs and the tNSAID specific risk of HF development. Moreover, it fails to address the discrepancy that naproxen appears to protect against, or carries neutral risk for, vascular events, but exhibits a similar risk of HF, compared to the other tNSAIDs. Research, using animal models, has provided further insight into this intra-NSAID variability [69, 103-107]. In summary, whilst proposed class-wide type mechanisms provide a fair account of the general higher risk of HF with NSAIDs, some of the more nuanced aspects of this risk are left unexplained. In addition, compound specific effects have been identified.

## *Metabolomic Signatures*

Metabolomics is the study of small-molecule metabolites produced by cellular processes [108]. Specific cellular processes leave behind a specific set of metabolites. Characterisation of the different metabolites and their concentrations provides us with information about the cellular processes that occurred in a system [109]. In practice, metabolite concentrations are most commonly measured with high resolution MS and NMR spectroscopy. The background, advantages and disadvantages of these techniques are discussed in Chapter 4. The use of metabolomic techniques in cardiac research has been extensively reviewed [19, 20]. The metabolite information these techniques provide serves as a sort-of biochemical “signature,” [110]. Changes in this signature can be tracked, allowing us to follow the metabolic repercussions of alterations to the system, such as caused by disease-states and pharmacological intervention.

### **The Metabolomic Signature of Heart Failure**

In the last decade, metabolomic analyses have described the metabolic remodelling that occurs during HF and provided mechanistic insight into its pathogenesis.

#### *An Overview of Heart Failure*

It is estimated that, globally, between 23 and 26 million people are living with HF [111]. HF is a phenotypically heterogeneous syndrome, characterised by the inability of the heart to pump sufficient blood to meet tissue oxygen demand [112, 113]. It is associated with cardiac remodelling, changes in gene expression, which drives structural, functional and metabolic derangements that contribute to the pathogenesis of HF [14, 15]. Functionally, HF can be divided into two syndromes, on the basis of the presence and absence of left ventricular systolic dysfunction (LVSD). HF with LVSD

exhibits a reduced ejection fraction, whilst in HF without LVSD, the ejection fraction is preserved [112]. Accordingly the two, equally common, syndromes are termed heart failure with reduced ejection fraction (HFrEF) and heart failure with preserved ejection fraction (HFpEF), and they are diagnosed in cases of HF with an EF  $\leq 40\%$  and  $\geq 50\%$ , respectively [112, 114]. The clinical utility of this distinction is still debated. Some believe that these two phenotypes are merely overlapping extremes in a HF spectrum, and cite clinical evidence demonstrating a unimodal EF distribution in support [115, 116]. Others argue that HFrEF and HFpEF should be considered as two separate phenotypes and counter with clinical evidence demonstrating a bimodal EF distribution [117-120]. Whilst it is true that HFrEF and HFpEF share a similar clinical expression, including signs and symptoms, their pathogeneses probably differ [117]. This is supported by evidence from clinical trials, assessing a range of pharmacological interventions for HF, which demonstrate an improvement in the risk of HF mortality and hospitalisations in HFrEF, but not HFpEF patients [117]. Moreover, HFrEF and HFpEF are associated with distinct types of structural remodelling. Typically, concentric hypertrophy, where sarcomeres assemble in parallel, is found in HFrEF hearts and eccentric hypertrophy, where sarcomeres assemble in series, is found in HFpEF hearts [117, 121]. These structural and functional observations belie the paucity of evidence related to mechanistic differences in the metabolic remodelling seen with the two syndromes. Instead, hypotheses that suggest a metabolic basis of HF rarely attempt to disentangle HFrEF from HFpEF.

The heart is one of the most metabolically active organs. It rapidly hydrolyses ATP ( $0.5 \mu\text{mol/g wet weight/s}$ ) and, if un-replenished, would exhaust its ATP pool ( $5 \mu\text{mol/g wet weight}$ ) within seconds [12, 14]. At normal oxygen concentrations, over 95 % of the cardiac ATP pool is derived from mitochondrial oxidative phosphorylation [12]. The

healthy heart is a metabolic omnivore, allowing it to maintain a steady supply of ATP in the face of variations in fuel supply and oxygen availability. It preferentially oxidises FAs, which provide 50-70 % of its ATP demand, with the remaining proportion accounted for by glucose, lactate, ketone and amino acid metabolism [11-13]. It is hypothesized that imbalances in cardiac energy metabolism, leading to metabolic inflexibility and fuel starvation, may be causative in HF and could underlie the remodelling observed [10, 122]. As HF develops, lower cardiac FA oxidation is reported and in animal studies a progressive down-regulation of genes involved in the delivery and oxidation of FAs is detected [14]. A relative increase in cardiac glycolysis, uncoupled from oxidative phosphorylation, is thought to be a compensatory effect [11, 14]. However, whilst the relative contribution of glycolysis to the cardiac ATP pool is higher, recent evidence suggests that its absolute rate may actually be lower, further compounding cardiac energy depletion [10]. The net effect is to reduce the availability of ATP for those cellular processes, such as actin-myosin interaction and ion pump activity, which govern cardiomyocyte contraction [12]. As HF develops, metabolic remodelling perturbs normal cellular functions. This remodelling and its consequences leave a metabolomic signature.

### *Metabolite Changes in Human and Animal Models of Heart Failure*

Over the last 10 years, a number of human studies have attempted to provide insight into the metabolic changes associated with HF. These studies have primarily profiled metabolite changes in the blood, most relying on a single sample from each individual. The disadvantage of this approach is that the results serve as a snap-shot of the exchange of metabolites between multiple organs and the circulation [14, 123-129]. Another approach that has been used, to provide a greater level of insight, is paired

blood sampling. In this approach, blood is collected from a peripheral arterial site and the coronary sinus, simultaneously. Transmyocardial metabolite extractions can be calculated by subtracting metabolite concentrations in the peripheral arterial blood from those in the coronary sinus blood [130]. A limited number of studies have directly measured metabolites in patients with HF, from cardiac biopsies, typically in a cardiac-transplant setting [13]. The fact so few studies have done so reflects the technical and ethical difficulties associated with biopsying the human heart. Moreover, HFpEF and HFrEF diagnoses are rarely distinguished in human studies and the 'typical' HF patient has multiple co-morbidities and takes several different medications. However, a variety of animal models have been used in the study of HF, to circumvent the confounding factors present in human studies [14, 16, 17, 131-137]. Species and model specific differences are likely to contribute to variability in the metabolomic signature of HF inferred from these models. The metabolite changes, identified below, are those best supported by evidence from both human and animal studies.

Work by Bedi et al. supports the view that FA oxidation is impaired in HF. They performed metabolomic analysis of transmural left ventricular heart tissue, from patients with end-stage HF and noted lower myocardial concentrations of long-chain acyl-carnitines [13]. L-carnitine shuttles activated long-chain FAs across the inner mitochondrial membrane to the mitochondrial matrix, where they are oxidised [138]. The authors therefore concluded that their findings reflect lower myocardial uptake of FAs [13]. This is supported by Turer et al., who used paired-blood sampling to calculate that, following ischaemia-reperfusion, patients with LVSD are less able to extract free FAs from the blood, compared to controls [130]. A number of human studies have noted higher concentrations of long-chain acylcarnitine species in the blood. This is also thought to reflect lower cardiac FA uptake and oxidation. Ahmad et

al. noted significantly higher concentrations of C16, C18:1 and C18:2 long chain acylcarnitines in blood from patients with end-stage HF as compared to milder HF. Moreover, elevations in these species were lower, in blood from end-stage HF patients, following circulatory support [14]. These findings are supported by those of Cheng et al. who demonstrated that C18:1 and C18:2 carnitines are elevated in HF. Interestingly, they also found elevations in C4 and C4-OH carnitines [127]. Differences in the concentrations of carnitines in the blood have also been identified between HFrEF and HFpEF patients. Zordoky et al. reported higher concentrations of L-carnitine and acylcarnitines in HFpEF compared to control patients and higher concentrations of medium and long chain acylcarnitines compared to HFrEF patients [128]. Animal studies support and extend the view that HF is associated with alterations in FA metabolism, as well as highlighting the heterogeneity of HF. Shibayama et al. used a canine, tachypacing-induced, model of HF. They examined the differences between HF with synchronous and dyssynchronous ventricular contraction. They noted significantly lower myocardial L-carnitine and FA concentrations in dyssynchronous HF compared to either synchronous HF or controls [132]. Differences in FA metabolism are also seen in small animal models of HF. Yang et al. and Qiu et al used the coronary artery ligation, MI induced-HF rat model. They inferred alterations in FA biosynthesis and elongation from urinary metabolites and noted higher concentrations of long-chain FAs in the blood, respectively [131, 135]. Omori et al. fed Dahl-salt sensitive rats a high salt diet, to model HFpEF. They noted lower plasma and left ventricular L-carnitine and higher urinary L-carnitine excretion [16]. Sansbury et al. examined myocardial tissue derived from male mice with pressure overload induced HF, brought about by transverse aortic constriction (TAC). They reported lower levels of multiple myocardial free FA and acyl-carnitine species [17].

These findings are consistent with those in human studies. On the other hand, Lai et al. noted higher concentrations of myocardial long-chain acyl-carnitine species and lower L-carnitine in mice with HF [133]. These differences may reflect differences in the mouse model used. While both studies employed TAC, Lai et al. augmented this with a small apical MI, and as Sansbury et al. noted, mice with MI exhibit differences in their myocardial metabolomic profiles, including acyl-carnitines, when compared to those with TAC [17, 133]. This raises the possibility that a previous MI could be an important factor in driving the heterogeneity seen in human HF. In addition Lai et al. used female mice, whereas Sansbury et al. used male mice, perhaps suggesting that gender might play a role [17, 133]. In summary, both human and animal studies support the view that HF is associated with lower FA oxidation, reflected by higher plasma concentrations of FAs and long-chain acyl-carnitines and lower myocardial concentrations.

Turer et al. noted that, following ischaemia-reperfusion, the hearts of patients with LVSD release more lactate into the circulation than those of control patients [130]. In addition, Wang et al. reported that patients with HF exhibited lower blood glucose concentrations and higher blood lactate concentrations, compared to controls, reflecting increased glycolysis uncoupled from the oxidation of lactate/pyruvate [129]. This evidence supports the metabolic-switch hypothesis. On the other hand, Tenori et al. reported lower concentrations of lactate in patients with stable HF compared to controls. They conclude that this result may be viewed with speculation [126]. However, whilst this finding is apparently incongruent with the rest of the evidence from human studies, it is not without support from animal models. Animal studies have provided further insight into the effect HF has on glycolysis. De Souza et al. observe higher concentrations of myocardial glucose in ventricular tachypaced induced-HF

dogs and Lai et al. noted higher concentrations of myocardial lactate in mice with HF [133, 137]. These results support the hypothesis that there is an increase in glycolysis uncoupled from oxidative phosphorylation in HF. However, Qiu et al. observed lower blood glucose and lactate in a coronary artery ligation, MI induced-HF rat model, suggesting higher levels of myocardial glycolysis, without the uncoupling from oxidative metabolism seen in the other studies, supporting the human data of Tenori et al. [126, 135]. Shibayama et al. reported lower concentrations of myocardial glycolytic intermediates and lactate in the myocardium of ventricular tachypaced induced-HF dogs, but no differences in glucose. In addition, they noted higher expression of the glycolytic enzymes. They concluded that this suggests a mismatch in substrate supply and demand [132]. In support of this, Maekawa et al. also noted lower concentrations of myocardial glycolytic intermediates in J2N-k cardiomyopathy induced-HF hamsters [136]. Taken together these results suggest that HF promotes myocardial demand for glucose, perhaps in an attempt to derive a greater relative energy supply from glycolysis in the presence of lower FA oxidation.

The TCA cycle occupies a central position in energy metabolism. It is therefore unsurprising that a disease such as HF, which has profound effects on glucose and FA metabolism, also affects the concentrations of TCA cycle intermediates. Bedi et al. observed higher myocardial concentrations of acetyl-CoA, which delivers carbon atoms to the TCA cycle, and lower concentrations of the TCA intermediates succinyl-CoA, succinate and fumarate in patients with end-stage HF. They concluded that this represents reduced flux through the TCA cycle, resulting in an accumulation of acetyl-CoA [13]. Other human studies have also reported that HF affects the concentrations of TCA intermediates in the blood. Du et al. noted higher succinate concentrations and Dunn et al. noted higher alpha-ketoglutarate concentrations in the blood of patients

with HF. They reasoned that these findings reflect reduced flux through the TCA cycle, leading to an intra-cellular accumulation of intermediates, which spill-over into the blood [123, 124]. Deficiency in succinate dehydrogenase, the enzyme responsible for catalysing the conversion of succinate to fumarate, has been reported to cause HF [123, 139]. Du et al. suggest that a reduction in its activity may contribute to the metabolic derangements seen in HF, including reduced flux through the TCA cycle [123]. In support of this, in addition to higher concentrations of succinate, succinate dehydrogenase knock-out (KO) cells exhibit lower concentrations of citrate, which Tenori et al. noted in the blood from patients with HF [126, 140]. However, although the findings of Bedi et al. and Du and Dunn et al. were both interpreted as lower flux through the TCA cycle in HF, their respective reasonings seem to be at odds. Bedi et al. proposed that lower concentrations of myocardial TCA cycle intermediates reflect reduced flux through the cycle [13]. Du and Dunn et al. suggested that the higher concentrations of blood TCA intermediates they saw was due to over-flow from an elevated myocardial TCA intermediate pool and also reflective of less TCA flux [123, 124]. As it seems unlikely that both a smaller and larger myocardial TCA intermediate pool is reflective of reduced flux, it follows that one interpretation is wrong. One possible explanation could be that these apparent differences reflect the heterogeneity of HF. In support of this, blood citrate concentrations were found to be the same in HFrEF patients and controls, but higher in those patients with HFpEF [128].

Further insight has been gained from animal studies, which largely support the findings of Bedi et al. and report lower myocardial TCA intermediates. Lai et al. noted lower concentrations of the TCA intermediates fumarate, malate and alpha-ketoglutarate and higher concentrations of succinate, whilst Sansbury et al. observed lower concentrations of myocardial malate, in mice with HF [17, 133]. In addition, Makeawa

et al. found that concentrations of myocardial TCA intermediates were generally lower in hamsters with HF compared to non-HF controls [136]. In contrast to the lower blood citrate concentrations, noted by Tenori et al., in patients with HF, Qiu et al. observed higher blood citrate concentrations in rats with HF [126, 135]. When data from both human and animal studies are considered together, the balance of evidence suggests that lower concentrations of myocardial TCA cycle intermediates are seen during HF, probably reflecting reduced TCA flux.

When the TCA cycle is starved of substrate, certain anaplerotic pathways introduce intermediates into the cycle in an attempt to maintain flux. Evidence suggests that the concentrations of certain anaplerotic substrates, and potentially their contribution to energy production, may vary according to HF stage. For example, Bedi et al. reported lower propionyl-CoA concentrations in the myocardium of patients with late stage HF [13]. On the other-hand Deidda et al. noted higher concentrations of methylmalonate in the blood of patients with mild/moderate HF, not found in those without HF or with late stage HF [125]. Higher concentrations of methylmalonate have also been observed in the urine of patients with HF [141, 142]. Hence, these anaplerotic substrates may play a context dependent role in maintaining energy status in HF [125].

The increased oxidation of ketone bodies has recently been implicated as a metabolic adaptation to HF. Ketone bodies are primarily synthesised in the liver. When they are released into the blood, they can be taken up by other tissues, including the heart, and converted into acetyl-CoA. Bedi et al. noted lower blood and higher myocardial  $\beta$ -hydroxybutyrate concentrations in HF patients compared to controls. They reasoned that these findings represented an increased extraction of  $\beta$ -hydroxybutyrate, from the blood, by the heart. This, they suggested, reflected a greater reliance on the metabolism of ketone bodies, as an energy substrate, in HF and is consistent with the

picture of an energy depleted heart utilising less preferred substrates [13]. On the other hand, paired-blood sampling by Turer et al. demonstrated lower uptake of ketone bodies, following ischaemia-reperfusion, in patients with LVSD compared to controls. These differences may be explained by the presence of ischaemia-reperfusion as a confounding factor in the work by Turer et al. [130]. Du et al. noted elevated concentrations of acetone and  $\beta$ -hydroxybutyrate in the blood, supporting previous findings by Lommi et al. [123, 143]. Higher concentrations of acetone have also been noted in the urine of patients with HF [141]. Du et al. suggested that the higher concentrations of blood ketone bodies they observed were likely to increase the rate of cardiac ketone body metabolism. They based this conclusion on the observation that the rate of cardiac ketone body metabolism has been found to depend on their concentration in the blood [144]. Both Du and Bedi et al. suggest that ketone body metabolism is upregulated in HF; however, their metabolite data appears to be conflicting. Du et al. present data showing higher concentrations of blood ketone bodies, whilst Bedi et al. present data showing lower blood and higher myocardial concentrations of ketone bodies. Resolving these differences is particularly difficult as Bedi et al. present additional gene expression data in support of their argument whilst Du et al. cite metabolite flux data in support of theirs [13, 123, 144]. These differences may reflect the heterogeneity of HF and differences in blood ketone body concentrations have also been identified between HFrEF and HFpEF patients. Zordoky et al. reported higher concentrations of acetoacetate and  $\beta$ -hydroxybutyrate in patients with HFpEF compared to HFrEF [128]. Whilst the human blood ketone body metabolomic data does not present a consistent picture in terms of directionality of change, it serves to highlight ketone body metabolism as a pathway affected in the progression of HF.

The data from studies examining the effects of HF, on amino acid metabolism, presents a clouded picture. Some studies have reported higher concentrations of amino acids in the blood of people with HF, including alanine, glutamate, glycine, isoleucine, leucine, ornithine, phenylalanine, proline, tryptophan and tyrosine [125-127, 145]. Other studies have reported lower concentrations of amino acids in the blood of people with HF, including arginine, glutamate, glutamine, glycine, histidine, lysine, tyrosine and valine [126, 127, 145]. Some of these findings may appear contradictory. These differences could be explained by the heterogeneity of HF. In support of this, Zordoky et al. noted higher concentrations of alanine, asparagine, histidine and threonine, in patients with HFpEF compared to controls, not seen with HFrEF in their study populations [128]. Of course, other confounding factors, such as pharmacotherapy, are also likely to contribute. Animal studies do little to clarify amino acid changes in HF. In canine studies of HF, elevations in myocardial cysteine and alanine have been observed [132, 137]. In rat models of HF higher concentrations of myocardial arginine, glutamine, glycine, histidine, phenylalanine, tryptophan, and valine and lower concentrations of alanine, valine and serine have been variably reported [134, 135]. Higher concentrations of urinary lysine, ornithine, serine, threonine, tryptophan, tyrosine and valine have also been observed [131]. In murine models of HF, Lai et al. observed higher blood concentrations of the branch-chain amino acids (BCAAs) leucine and isoleucine [133]. Sansbury et al. noted higher concentrations of myocardial BCAAs (leucine, isoleucine and valine) as well as other amino acids: asparagine, aspartate, beta-alanine, lysine, ornithine, prolylhydroxyproline, serine and threonine [17]. Whilst animal models and human studies present a varied picture of amino acid concentrations in HF, it is fair to conclude that HF does perturb their metabolism. This could be due to changes in

cardiac substrate selection (especially BCAAs) or as part of osmoregulation [146]. In support of this, changes in other organic osmolytes have been observed in human and animal studies of HF, including higher levels of creatine, myo-inositol, betaine, and glycerophosphocholine [17, 128, 132].

Several human studies have also noted lower concentrations in the blood of structural lipids, for instance phosphatidylcholines and sphingomyelins, and messenger lipids, including lyso-phosphatidylcholines, as well as their break-down products, phosphocholine and choline, in patients with HF [127-129, 147]. These findings are supported by the work performed by Sansbury et al. In their mouse model of pressure-overload induced-HF, they noted lower myocardial concentrations of several lysolipid and sphingolipid species [17]. This may lead to dysregulated signalling in the heart, via alterations in messenger lipids and arachidonic acid. Arachidonic acid, the substrate of COX, lipoxygenase (LOX) and cytochrome p450 (Cyp450), is cleaved from membrane lipids by phospholipase A<sub>2</sub> (PLA<sub>2</sub>). Alterations in membrane lipid homeostasis therefore has the potential to affect the signalling products of these pathways, which govern inflammation, vascular tone, ion channel function and viability in the heart [148]. These alterations in lipid signalling may contribute to the pathogenesis of HF [149]. The differences observed in the structural lipids could represent alterations in lipid degradation, or membrane turnover and fluidity, reflecting cardiac remodelling seen in HF [17].

Myo-inositol which, in addition to its role as an organic osmolyte, is an important signalling component of the plasma membrane, has been shown to be elevated in the blood of patients with HF [125, 146]. In addition Sansbury et al. demonstrated a lower concentration of myocardial myo-inositol in mice with HF compared to non-HF controls [17]. Myo-inositol plays an important role in regulating intracellular Ca<sup>2+</sup>

concentrations, which are dysregulated in late-stage HF. It has therefore been proposed that the observed changes in myo-inositol may either reflect a compensatory mechanism in HF or part of its progression [125].

Higher concentrations of creatine and its break-down product creatinine have also been noted in the blood of patients with HF [126-129]. In addition to its role as an organic osmolyte, creatine, in the form creatine phosphate, acts as a phosphate donor to ADP, enabling the rapid regeneration of ATP in muscle [146, 150]. Muscle creatine is non-enzymatically converted to creatinine at a fairly constant rate. Given its consistent production and the fact it is freely filtered by the kidney it serves as a useful marker of kidney function [151]. The higher concentrations of creatinine may reflect higher blood creatine, or the impaired kidney function which often goes hand-in-hand with HF. Canine and mouse models of HF demonstrate lower myocardial creatine and phosphocreatine concentrations [17, 132]. It is thought that transient changes in the activity of creatine kinase system, as HF progresses, may underlie these differences [132].

An elevation in the polyamines, spermine and spermidine, in the blood of patients with HF has also been observed. Polyamine synthesis and NO synthesis are thought to be inter-regulated. Cheng et al. suggests that, in the context of lower blood concentrations of arginine, a NO precursor, and higher concentrations of ornithine, a polyamine precursor, the results may reflect lower NO and higher polyamine synthesis [127]. This could be linked to the endogenous NOS inhibitor ADMA, which reduces NO production. It is found in elevated concentrations in the blood of HF patients compared to controls and correlates with worsening HF [152, 153]. Another possible explanation for the elevation in blood polyamines is that they may reflect cardiac remodelling [154]. Both possible explanations are supported by data presented by Sansbury et al.

demonstrating higher myocardial concentrations of putrescine, spermidine, the endogenous NOS inhibitor ADMA and prolylhydroxyproline, a breakdown product of collagen, in a mouse model of HF [17].

In conclusion, human data and that from animal studies paint a picture of HF as a disease of profoundly perturbed energy metabolism. On balance, the metabolomic data support the hypothesis that FA metabolism is downregulated and glycolysis is upregulated. As one might anticipate, due to the interrelation of metabolic pathways, these changes have far-reaching metabolic consequences. These consequences may manifest as changes in TCA cycle intermediates, amino acids and ketones, as well as a number of other metabolites. However, perhaps owing to the heterogeneity of HF and inter-model and species differences, the precise metabolic changes in human and animal studies are difficult to dissect.

## **The Metabolomic Signature of Coxib use**

As coxibs inhibit COX, two studies focussed on the products of arachidonic acid metabolism. These include changes in COX derived products and those products that may be enhanced through substrate diversion, as a result of COX inhibition. Liu et al. profiled changes in plasma arachidonic acid and linoleic acid derived oxylipins, in mice treated with rofecoxib, via drinking water, for 3 months [7]. Oxylipins are oxidised metabolites of the polyunsaturated FAs. They can be synthesised by COX, LOX, Cyp450 and other enzyme systems. Eicosanoids, such as prostanoids and leukotrienes, are a sub-class of oxylipin [155]. Liu et al. noted a 120-fold higher plasma concentrations of 20-HETE, in the rofecoxib treated mice compared with controls, which they attributed to a reduction in its COX-mediated degradation [7]. The authors also demonstrated that 20-HETE reduces mouse tail-bleeding time, indicative of

greater platelet aggregation. They suggested this could relate to the adverse CV side-effects seen with this drug [7]. Attur et al. measured changes in COX and LOX products, in human OA cartilage explants incubated with celecoxib or indomethacin for 24-120 hours [156]. They noted lower concentrations of PGE<sub>2</sub>, PGF<sub>1α</sub>, PGF<sub>2α</sub>, TXB<sub>2</sub>, and PGD<sub>2</sub> in the celecoxib treated group, as anticipated. However, they also saw increases in leukotriene B<sub>4</sub> (LTB<sub>4</sub>), the end-product of the 5-LOX pathway, which they suggested was a result of arachidonic acid diversion [156].

Other studies have explored changes in some of the key metabolic energy pathways. Um et al. profiled urinary metabolite changes in rats, treated with a single high dose of orally administered celecoxib, indomethacin or ibuprofen, for the purpose of identifying biomarkers of NSAID induced GI damage [8]. The doses they used were 20 times greater than the typical daily dose. They reasoned that this was consistent with other GI safety studies that have used a 20 times greater dose of indomethacin as a positive control [8]. The authors noted lower urinary concentrations of citrate, alpha-ketoglutarate, acetate and hippurate, in celecoxib treated rats compared to controls [8].

In addition, some studies have explored changes in methylarginine concentrations. Ahmetaj-Shala et al. measured plasma concentrations of endogenous methylarginines in mice treated for 4 days with paracoxib, constitutive COX-2<sup>-/-</sup> mice and patients treated for 7 days with celecoxib or naproxen [4]. They noted significantly higher concentrations of ADMA and L-NMMA in mice treated with paracoxib and constitutive COX-2<sup>-/-</sup> mice. In addition, they reported slightly higher plasma concentrations of ADMA in patients treated with celecoxib and naproxen [4]. These findings, in the context of the higher ADMA concentrations seen in mouse models of HF and patients with HF, represent an interesting observation [17, 152, 153].

In summary, studies examining the metabolic implications of coxib use have highlighted unanticipated consequences of their COX inhibitory effect. This includes diversion of the COX substrate, arachidonic acid, to other pathways. In addition, studies have also noted higher concentrations of ADMA with COX inhibition. These effects have been posited as potential mechanisms underlying the adverse CV risk seen with coxibs. Finally, studies have also noted coxib-induced changes to metabolites that are part of pathways involved in regulating energy homeostasis, pathways which are profoundly affected in HF. It is therefore biologically plausible that coxibs, either through on-target or off-target effects, have metabolic implications that may induce or exacerbate HF. However, the metabolomic consequences of coxib use are not well characterised and large gaps in our knowledge remain.

## ***Chapter 3: Thesis Materials and Methods***

# *In Vivo Experiments*

## **Animal Husbandry**

Animal care and experimental procedures were carried out by Dr Emanuela Ricciotti, of the University of Pennsylvania. The studies were approved and performed in accordance with the ethical standards set by the Institutional Animal Care and Use Committee of the University of Pennsylvania and by the National Institutes of Health (NIH).

### *Studies 1 and 2:*

Male C57BL/B6 mice, aged 9-11 weeks, were housed for 3 weeks in a temperature-controlled environment with a 12 hour light:dark cycle and allowed *ad libitum* access to food and water. During this time they were fed either regular chow, a celecoxib-containing or a rofecoxib-containing diet. The bespoke diets containing celecoxib (650 ppm per kg diet) or rofecoxib (325 ppm per kg diet) were purchased from Teklad-Harlan. The celecoxib diet was customized to release 100 mg celecoxib/kg body weight per day, while the rofecoxib diet was customized to release 50 mg rofecoxib/kg body weight per day, thereby accounting for the differences in bioavailability of the two drugs in mice. These drug doses are equivalent to a low human dose. Urine was collected between 09:00 and 14:00, at the beginning of weeks 0 (baseline), 1 and 3 in Study 1 and at week 3 in Study 2, using metabolic cages. Food was removed during collection. At the end of Study 1, interleukin 1 beta (IL-1 $\beta$ ) was injected 4 hours before sacrifice. At the end of Study 2, IL-1 $\beta$  was not injected before sacrifice. The mice were sacrificed, at the end of the 3 weeks, using CO<sub>2</sub>. All mice were sacrificed between 15:00 and 17:00, to prevent diurnal variation, and were

approximately 12-14 weeks old. Tissues (skeletal muscle, heart, kidney, liver and aorta) and plasma were harvested and stored in liquid nitrogen to prevent degradation.

### *Studies 3 and 4:*

In Study 3 male and female, and in Study 4 only female, 9-11 weeks old C57BL/B6 mice were housed, for 8 weeks, as described in Studies 1 and 2. The next part of this protocol is based on a method modified from that outlined by Daugherty and Cassis [157]. In study 4, after 4 weeks, the mice had an osmotic mini-pump (Alzet, model 2004) surgically implanted under light anaesthesia (ketamine/xylazine): The skin was washed and shaved over the implantation site, located slightly posterior to the scapulae; a mid-scapular incision was made adjacent to the implantation site; a haemostat was inserted into the incision and used to blunt dissect a pocket for the pump; the pump was implanted subcutaneously, having already been aseptically filled with angiotensin II (Ang II) (Calbiochem) in saline solution, and the incision was closed with two stitches. For the next 4 weeks, the pump infused a high dose of Ang II at a constant rate of 1.5 mg/kg body weight per day. Osmotic mini-pumps were not surgically implanted in Study 3. Urine was collected at the beginning of week 3, as per Studies 1 and 2. The mice were sacrificed, at the end of the 8 weeks, as per Studies 1 and 2, at approximately 17-19 weeks old. Tissues (heart and kidney, which was dissected into cortex and medulla) and plasma were harvested and stored in liquid nitrogen to prevent degradation.

### *Studies 5 and 6:*

Male and female inducible post-natal global (IPNG) COX-2 KO (COX-2<sup>-/-</sup>) mice were generated using a Cre-Lox recombination strategy [158]. Briefly, DNA homologous recombination was used to generate floxed COX-2 mice, on a C57BL/B6 background,

by inserting LoxP sites at introns 5 and 8 of the COX-2 gene [159]. Floxed COX-2 mice were then crossed with Cre-Oestrogen receptor (ER) mice. The Cre-ER mouse expresses a fusion protein between Cre and a mutated form of the ER ligand binding domain. Cre activity is tamoxifen inducible in this mouse [160]. The resultant crosses exhibit tamoxifen inducible global COX-2 KO. Littermate floxed COX-2 mice were used as controls. In Study 5 only male, in Study 6 male and female, 8 weeks old IPNG COX-2<sup>-/-</sup> and floxed COX-2 littermate control mice were housed, for 8 weeks, in a temperature-controlled environment with a 12 hour light:dark cycle and allowed *ad libitum* access to food (regular chow) and water. At the start of the 8 weeks, the IPNG COX-2<sup>-/-</sup> mice and the floxed COX-2 littermate control mice received injections of intraperitoneal tamoxifen (100 mg/kg body weight per day, in corn oil) for 5 days. This induced global COX-2 deletion in the IPNG COX-2<sup>-/-</sup> mice but not the floxed COX-2 littermate control mice. Deletion was confirmed using qPCR of genomic DNA [158, 159]. In study 6, after 4 weeks, the mice had an Ang II infusing osmotic mini-pump implanted, as per Study 4. Osmotic mini-pumps were not surgically implanted in Study 5. Urine was collected at the beginning of week 3, as per Studies 1 and 2. The mice were sacrificed, at the end of the 8 weeks, as per Studies 1 and 2, at 16 weeks old. Tissues and plasma were harvested as per Studies 3 and 4.

## **Metabolomic Protocols**

### *Methanol/Chloroform/Water Metabolite Double Extraction*

This protocol is based on a method modified from that outlined by Le Belle et al. [161]. Either the entirety of each frozen plasma sample (~100-200  $\mu$ L), or 50 mg  $\pm$  10 % of each frozen tissue/diet sample were extracted. 600  $\mu$ L of methanol:chloroform 2:1 was added and the tissue lysed (4 min, at a frequency of 22 s<sup>-1</sup>). The samples were sonicated for 15 min. Following this, 200  $\mu$ L of chloroform and 200  $\mu$ L of water were

added. The samples were centrifuged (20 min at 15,000 rcf) causing the separation of the organic and aqueous layers from the protein pellet. To achieve a double extraction another 600  $\mu\text{L}$  of 2:1 methanol:chloroform was added to the pellet, the procedure repeated to this point and the fractions pooled. The organic fraction was left to dry in a fume hood overnight, whilst the aqueous fraction and pelleted material were dried using a speed-vac. For the plasma samples, the dried mass of pelleted material was measured, for normalisation. All samples were stored at  $-80\text{ }^{\circ}\text{C}$  for further analysis.

### *Nuclear Magnetic Resonance (NMR) Spectroscopy*

**Urine:** To 100  $\mu\text{L}$  of urine from each sample, 600  $\mu\text{L}$  of urine buffer ( $\text{D}_2\text{O}$  containing 0.2 mM sodium-3-(tri-methylsilyl)-2,2,3,3-tetradeuteriopropionate (TSP) (Cambridge Isotope Laboratories) as an internal standard, 40 mM  $\text{NaH}_2\text{PO}_4$ , 160 mM  $\text{Na}_2\text{HPO}_4$  and sodium azide) was added. The samples were centrifuged (10 min at 15,000 rcf) and the supernatant transferred to separate NMR spectroscopy tubes.

**Plasma:** To 110  $\mu\text{L}$  of intact plasma, 500  $\mu\text{L}$  of buffer ( $\text{D}_2\text{O}$  containing 0.12 mM 4,4-dimethyl-4-silapentane-1-sulfonic acid (DSS) (Cambridge Isotope Laboratories) as an internal standard and sodium azide) were added. The samples were transferred to separate NMR spectroscopy tubes.

**Tissue:** Each sample of the total dried aqueous tissue extract was dissolved in 600  $\mu\text{L}$  of  $\text{D}_2\text{O}$ , containing 0.05 mM TSP (Cambridge Isotope Laboratories) as an internal standard and sodium azide, and transferred to an NMR spectroscopy tube.

All the samples were analysed using an AVANCE II+ NMR spectrometer operating at 500.13 MHz for the  $^1\text{H}$  frequency (Bruker) using a 5 mm TXI probe. Spectra were collected at 300 K for urine and tissue, and 310 K for plasma. A solvent suppression pulse sequence, based on the first increment of a one-dimensional nuclear

Overhauser effect spectroscopy (NOESY) pulse sequence, designed to saturate the residual  $^1\text{H}$  water signal, was used to collect spectra from all urine, plasma and tissue samples (relaxation delay = 2 s,  $t_1$  increment = 3  $\mu\text{s}$ , mixing time = 150 ms, solvent presaturation applied during the relaxation time and the mixing time). One hundred and twenty-eight transients were collected into 16 K data points over a spectral width of 12 ppm. A Carr-Purcell-Meiboom Gill (CPMG) pulse sequence was run on the plasma. In addition,  $^1\text{H}$ - $^1\text{H}$  correlation spectroscopy (COSY), and sensitivity-enhanced heteronuclear ( $^1\text{H}$ - $^{13}\text{C}$ ) single quantum coherence (HSQC) spectroscopy were used for structure elucidation and metabolite identification.

### *Fatty Acid Methyl Ester (FAME) Derivatisation of the Organic Fraction, for Gas Chromatography Mass Spectrometry (GC-MS) Analysis*

This method is based on that outlined by Morrison et al. [162]. Following methanol/chloroform/water double extraction of the plasma and tissue samples, one-quarter of the organic fraction was derivatised for GC-MS analysis. 650  $\mu\text{L}$  of 1:1 methanol:chloroform was added, followed by 100  $\mu\text{L}$  of  $\text{D}_{25}$ -tridecanoic acid (200  $\mu\text{M}$  in chloroform) as an internal standard and 125  $\mu\text{L}$  of 10 %  $\text{BF}_3$ /Methanol (Sigma-Aldrich). The samples were incubated at 80  $^\circ\text{C}$  for 90 min, allowing a trans-esterification reaction to occur. 500  $\mu\text{L}$  of MiliQ water and 1 mL of hexane were added. Two layers formed, and the organic (upper) layer was separated. The dried, derivatised, organic fraction was reconstituted in 200  $\mu\text{L}$  of hexane and analysed by GC-MS.

### *GC-MS Analysis of Total FAMES*

The samples were analysed using a Trace GC Ultra coupled to a Trace DSQ II mass spectrometer (Thermo Scientific). The derivatised fatty acids were injected onto a

TR-FAME stationary phase column (Thermo Electron; 30 m × 0.25 mm ID × 0.25 μm; 70 % cyanopropyl polysilphenylene-siloxane) with a split ratio of 20. The injector temperature was 230 °C and the helium carrier gas flow rate was 1.2 mL/min. The column temperature was 60°C for 2 min, increased by 15 °C/min to 150 °C, and then increased at a rate of 4 °C /min to 230 °C (transfer line = 240 °C; ion source = 250 °C, EI = 70 eV). The detector was turned on after 240 s, and full-scan spectra were collected using 3 scans/s over a range of 50–650 *m/z*. Peaks were assigned using the Food Industry FAME Mix (Restek 6098) [163].

### *Butylating Method of Sample Preparation for Liquid Chromatography-Mass Spectrometry/Mass Spectrometry (LC-MS/MS) Carnitine Assay*

This group protocol was developed by Dr James A. West, MRC Human Nutrition Research, for the preparation of samples for the LC-MS/MS carnitine assay and involves the butylation of carnitine species [163]. For tissue and plasma samples, half of the organic and half of the aqueous extracts were recombined. The recombined samples were dried down and 100 μL of deuterated internal standard (C0D<sub>9</sub>, C2D<sub>3</sub>, C3D<sub>3</sub>, C4D<sub>3</sub>, C5D<sub>9</sub>, C8D<sub>3</sub>, C14D<sub>9</sub> and C16D<sub>3</sub>) in acetonitrile was added. The samples were dried down again, before 400 μL of 3M hydrogen chloride in 1-butanol was added, and the samples were sonicated for 10 min. Samples were then placed in a 60 °C water bath for 15 min, dried down again and reconstituted in 200 μL of acetonitrile:water 80:20 with 0.1 % formic acid (for all the tissues, excluding the aorta) and 100 μL of acetonitrile:water 80:20 with 0.1 % formic acid (for the plasma and aorta). Finally, samples were sonicated (10 min), centrifuged (5 min at 15,000 rcf) and the supernatant transferred to a glass vial for LC-MS/MS analysis.

## *Non-Butylating Method of Sample Preparation for LC-MS/MS Carnitine Assay*

This updated group protocol was developed by Dr James A. West, MRC HNR, for the preparation of samples for the LC-MS/MS carnitine assay and does not involve butylation of carnitine species, significantly reducing the sample preparation time. For tissue and plasma samples, half of the organic and half of the aqueous extracts were recombined and dried down. To the tissue samples 200 µL, to the plasma samples 100 µL and to the un-extracted urine samples 150 µL of deuterated internal standard (C0D<sub>9</sub>, C2D<sub>3</sub>, C3D<sub>3</sub>, C4D<sub>3</sub>, C5D<sub>9</sub>, C8D<sub>3</sub>, C14D<sub>9</sub> and C16D<sub>3</sub>) in acetonitrile:water 1:1 was added. Samples were vortex mixed, sonicated (10 min) and the supernatant was transferred to 1.2 µm 96-well Filter Plates (Corning) over PlateOne 96-well Microplates with V bottoms (Starlab) for collection. The samples were centrifuged (10 min at 2000 rcf) to filter, the filter plate discarded and the collection plate sealed.

## *LC-MS/MS Carnitine Assay*

This group protocol was developed by Dr James A. West, MRC HNR, for targeted analysis of carnitine species [163]. Chromatographic separations were performed using a T3 ultra-performance liquid chromatography (UPLC) column (Waters) kept at 30 °C on an Ultimate 3000 ultra-high performance liquid chromatography system (UHPLC) (Dionex), coupled with a TSQ Quantiva (Thermo Scientific) triple quadrupole mass spectrometer. The temperature of the autosampler was set to 7 °C. The mobile phase consisted of solvent A: 0.1 % formic acid in high performance liquid chromatography (HPLC) grade water (Sigma-Aldrich) and solvent B: 0.1 % formic acid in acetonitrile (Sigma-Aldrich). When eluting the column the following gradient was used: Initial conditions were 95 % A held for 1 min followed by a linear gradient with increase of B to 100 % at 6 min, held for 2 min, with re-equilibration for 2 min giving a

total run time of 10 min with a flow rate of 500  $\mu\text{L}/\text{min}$ . The needle wash consisted of 10 % aqueous acetonitrile and was set at 200  $\mu\text{L}$ , whilst the injection volume was 2  $\mu\text{L}$ . Samples were analysed by detecting the precursors of product ions with an  $m/z$  of 85 using a multiple reaction monitoring (MRM) approach. The ionisation mode used by the mass spectrometer was electro spray ionisation with a capillary voltage of 3.5kV for positive ion mode. Ion source gas flows and temperatures were established using the default values provided by the Quantiva tune page software for the desired flow rate. All compound-dependent parameters were established using the Quantiva automatic optimisation protocol infusion with standards of the relevant compounds.

### *LC-MS/MS Aqueous Metabolite Assay*

This group protocol was developed by Dr James A. West, MRC HNR, for targeted analysis of aqueous metabolites including oxidative stress biomarkers, TCA cycle intermediates, nucleotides and amino acids [164]. Half of the aqueous extract was dried down and reconstituted in 200  $\mu\text{L}$  of 10 mM ammonium acetate containing universally  $^{13}\text{C}$  and  $^{15}\text{N}$  labelled glutamic acid (Cambridge Isotope Laboratories) at a concentration of 20  $\mu\text{M}$ . Aortic extracts were reconstituted in 100  $\mu\text{L}$  of the solution described above. Chromatographic separations were performed using a C18 pentafluorophenyl UPLC column (Ace) kept at 30  $^{\circ}\text{C}$  on an Ultimate 3000 UHPLC (Dionex), coupled with a TSQ Quantiva (Thermo Scientific) triple quadrupole mass spectrometer. The temperature of the autosampler was set to 7  $^{\circ}\text{C}$ . The mobile phase consisted of solvent A: 0.1 % formic acid in HPLC grade water (Sigma-Aldrich) and solvent B: 0.1 % formic acid in acetonitrile (Sigma-Aldrich). When eluting the column, the following gradient was used: initial conditions were 100 % A held for 1.5 min followed by a linear gradient with increase of B to 100 % at 4.5 min with re-equilibration for 1.5 min giving a total run time of 6 min with a flow rate of 400  $\mu\text{L}/\text{min}$ . The needle

wash consisted of 10 % aqueous acetonitrile and was set at 200  $\mu$ L whilst the injection volume was 2  $\mu$ L. Samples were analysed using an MRM approach. The ionisation mode used by the mass spectrometer was electro spray ionisation with a capillary voltage of 3.5kV for positive ion mode and 2.5 kV for negative ion mode. Ion source gas flows and temperatures were established using the default values provided by the Quantiva tune page software for the desired flow rate. All compound dependent parameters were established using the Quantiva automatic optimisation protocol infusion with standards of the relevant compounds.

### *Processing of Metabolomic Data*

GC-MS and LC-MS/MS chromatograms were analysed using version 2.0 of Xcalibur (Thermo Scientific). For the GC-MS data, the peaks were integrated individually and the samples normalised to total area (TA), such that the sum of the peaks for each was 100. For the LC-MS/MS data, the peaks were integrated individually and normalised to internal standard. NMR spectra were processed using the one-dimensional NMR processor from ACD suite (ACD, Montreal, version 12). Free induction decays were Fourier transformed following multiplication by a line broadening of 1 Hz, and referenced to TSP or DSS at 0.0 ppm. Spectra were phased and baseline corrected manually. Each spectrum was integrated using 0.02 ppm integral regions between 0.5-4.5 ppm and 5.5-9.5 ppm. For the urine samples, the region between 5.5 ppm and 6 ppm was also excluded to avoid the urea peak. The spectral region for each sample was normalized to total area, such that the total sum of integrals for each sample was 1.

## Quantitative reverse transcription polymerase chain reaction (RT-qPCR)

RT-qPCR was used to determine relative mRNA levels of gene transcripts coding for selected proteins, in murine tissue (transcript (gene/protein)):

Heart: *Slc22a5* (*Slc22a5*/OCTN2), *Cpt1b* (*Cpt1b*/CPT1B), *Cpt2* (*Cpt2*/CPT2), *Cact* (*Cact*/CACT) and *Crat* (*Crat*/CRAT). Liver: *Ppara* (*Ppara*/PPAR- $\alpha$ ), *Bbox1* (*Bbox1*/BBD), *Aldh9a1* (*Aldh9a1*/TMABADH) and *Tmlhe* (*Tmlhe*/TMLD). House-keeping in heart and liver: *Actb* (*Actb*/ $\beta$ -Actin).

Gene expression levels were inferred from these results.

### *RNA Isolation from Tissue*

50 mg of frozen tissue was added to aliquots of QIAzol Reagent (Qiagen), containing a stainless steel bead. The tissue was lysed (2 x 3 min, at a frequency of 30 s<sup>-1</sup>) until homogenous. The homogenate was transferred and centrifuged (10 min at 15,000 rcf at 4 °C). The supernatant was transferred and left to stand at room temperature for 5 min, after which 200  $\mu$ L of chloroform was added. The mixture was then shaken vigorously for 15 s and left to stand at room temperature for 2 min. The sample was centrifuged (15 min at 15,000 rcf at 4 °C) and the upper, colourless, aqueous phase transferred to a new collection tube. An RNeasy Mini Kit (Qiagen) was then used as follows: 500  $\mu$ L of 70 % ethanol was added to the aqueous phase and the two mixed by pipetting. The sample was transferred into an Rneasy Mini Spin Column in a 2 mL collection tube and centrifuged (15 s at 10,000 rcf). The flow-through was discarded. 700  $\mu$ L of buffer RW1 was added to the column and it was centrifuged (15 s at 10,000 rcf). The flow-through was discarded. 500  $\mu$ L of buffer RPE was added to the column and it was centrifuged (15 s at 10,000 rcf). The flow-through was discarded. Another

500  $\mu\text{L}$  of buffer RPE was added to the column and it was centrifuged (2 min at 10,000 rcf). The column was placed in a new 2 mL collection tube and centrifuged (1 min at 15,000 rcf) to dry the column membrane and remove residual ethanol. The column was then placed in a 1.5 mL collection tube. 30  $\mu\text{L}$  of Rnase-free  $\text{H}_2\text{O}$  was added directly to the column membrane. The column was incubated at room temperature for 10 min, then centrifuged (2 min at 15,000 rcf) to elute the RNA.

### *Reverse Transcription*

The RNA concentration and absorption at 260 nm/280 nm and 260 nm/230 nm ratios of the eluted RNA samples were measured using a NanoDrop spectrophotometer (Thermo Scientific). If the 260/280 ratio was less than 1.8 or the 260/240 ratio less than 1.7 the sample was deemed contaminated (by DNA or protein, respectively) and the RNA was re-isolated from fresh tissue (as previously described). The eluted RNA samples were diluted, with Rnase-free  $\text{H}_2\text{O}$ , to exactly the same concentration (between 50 ng/ $\mu\text{L}$  and 62.5 ng/ $\mu\text{L}$ ). An RT<sup>2</sup> First Strand Kit (Qiagen) was then used and the following protocol followed: 8  $\mu\text{L}$  of diluted RNA was transferred to a 0.5 mL PCR tube and 2  $\mu\text{L}$  of GE (5X genomic DNA Elimination Buffer) added. The sample was placed in a PT-200 Peltier Thermal Cycler (MJ Research) and the following thermal protocol run, to digest genomic DNA: 5 min Incubation at 42 °C followed by 10 min at 4 °C. 10  $\mu\text{L}$  of First Strand Mix (containing 4  $\mu\text{L}$  of BC3 (5X Reverse Transcription Buffer 3), 3  $\mu\text{L}$  of Rnase-free  $\text{H}_2\text{O}$ , 2  $\mu\text{L}$  RE3 (RT Enzyme Mix 3) and 1  $\mu\text{L}$  of P2 (Primer and External Control Mix)) was added to the sample. The sample was placed in a PT-200 Peltier Thermal Cycler (MJ Research) and the following thermal protocol run, to synthesise complementary DNA: 15 min incubation at 42 °C followed by 5 min at 95 °C.

## *Quantitative Real Time PCR*

MicroAmp Fast Optical 96-well PCR reaction plates (Applied Biosystems) were prepared such that levels of the target gene and house-keeping gene were measured, in duplicate, for each sample. A 20  $\mu\text{L}$  reaction volume was used containing 20 ng of sample complementary DNA per PCR plate well. To this, a volume of Master Mix (containing 10  $\mu\text{L}$  of SYBR Green, 0.6  $\mu\text{L}$  of target gene or house-keeping gene primer, and a volume of Rnase-free  $\text{H}_2\text{O}$ , Qiagen) was added. The volume of Rnase-free  $\text{H}_2\text{O}$ , which serves to bring the total system volume up to 20  $\mu\text{L}$ , depends on the concentration, hence volume, of the 20 ng complementary DNA added. The PCR Plates were sealed using MicroAmp Optical Adhesive Film (Applied Biosystems), centrifuged (pulsed to 4,000 rcf) to remove trapped air and run on a StepOnePlus Real-Time PCR System (Applied Biosystems) according to the following thermal protocol: 10 min Incubation at 95  $^{\circ}\text{C}$  followed by 40 cycles of elongation and cooling, where the temperature cycled between 95  $^{\circ}\text{C}$  for 15 s and 60  $^{\circ}\text{C}$  for 1 min. In addition, primers underwent melt curve analysis, to ensure each possessed only 1 melt point temperature. Following thermal cycling, the cycle threshold ( $C_T$ ) for each well was recorded.

## *Processing of RT-qPCR Data*

The house-keeping gene  $C_T$  duplicate mean was subtracted from the target gene  $C_T$  duplicate mean, for each sample, giving the  $\Delta C_T$ . The relative concentration of target mRNA was calculated, for each sample, using the formula:

$$[mRNA]_{rel} = \frac{1}{2^{\Delta C_T}}$$

The relative [mRNA], of each sample, was normalised to the mean control relative [mRNA], to give the relative target mRNA level, thus giving rise to the  $\Delta\Delta C_T$  method.

# *In Vitro Experiments*

## **C2C12 Murine Skeletal Muscle Cells**

### *C2C12 Culture*

C2C12 cell culture was performed according to a modified group protocol [165]. C2C12 cells (Sigma-Aldrich) were cultured in 1 mL of growth medium (Dulbecco's Modified Eagle's Medium (DMEM; 4.5 g/L glucose, L-glutamine, NaHCO<sub>3</sub> and pyridoxine-HCl) supplemented with 10 % fetal bovine serum (FBS; Sigma-Aldrich) and 1X penicillin/streptomycin (100 U/mL and 100 g/mL, respectively; Sigma-Aldrich)) in 12-well collagen pre-coated tissue culture plates (Millipore) at 37 °C and 5 % CO<sub>2</sub>. Growth medium was changed each day. When cells reached confluence, they were swapped to differentiation medium (DMEM supplemented with 2 % horse serum (Sigma-Aldrich) and 1X penicillin/streptomycin) for 6 days. Differentiation medium was changed each day.

### *C2C12 Stable Isotope Labelling Assay*

After 6 days of differentiation, the differentiation medium was replaced with differentiation medium supplemented with 0.2 mM L-carnitine (Trimethyl-D<sub>9</sub>, 98 %; Cambridge Isotope Laboratories). The C2C12 mouse skeletal muscle cells were then incubated for 1 hour at 37 °C and 5 % CO<sub>2</sub>, whilst the stable isotope labelling assay was performed: 50 µL aliquots of media were taken, from each well at time 0, 1, 5, 10, 15, 30 and 60 min.

## Primary Murine Cardiomyocytes

### *Primary Murine Cardiomyocyte Cell Isolation*

Primary murine cardiomyocyte isolation [166], was performed by Dr Ben Prosser of the University of Pennsylvania. This experimental procedure was approved and performed in accordance with the ethical standards set by the Institutional Animal Care and Use Committee at the University of Pennsylvania and the NIH. Adult (> 8 weeks old) male C57BL/B6 mice were heparinised. After 15 min they were anaesthetised with isoflurane. Thoracotomies were performed to remove the hearts and lungs, which were placed in cold, pH 7.4, cell isolation buffer (CIB; containing: 130 mM NaCl, 25 mM 4-(2-hydroxyethyl)-1-piperazineethanesulfonic acid (HEPES), 22 mM dextrose, 5.4 mM KCl, 1 mM lactic acid, 0.5 mM MgCl<sub>2</sub>\*6H<sub>2</sub>O, 0.33 mM NaH<sub>2</sub>PO<sub>4</sub>\*H<sub>2</sub>O) supplemented with insulin (100 µU/mL) and (ethylene glycol-bis(β-aminoethyl ether)-N,N,N',N'-tetraacetic acid (EGTA) (0.4 mM EGTA + 0.1 mM HEPES, pH 7.4). The lungs and the fat surrounding the hearts and aortas were removed and the aortas cut before their bifurcations. The aortas were cannulated and the hearts suspended from Langendorff perfusion apparatus. The hearts were perfused with CIB supplemented with insulin and EGTA, as described. The left atria were removed and the septa manipulated, through the mitral valves, to improve perfusion. Once the run-throughs became clear in colour, the hearts were perfused with CIB supplemented with insulin (100 µU/mL), collagenase II (0.66 mg/mL; Worthington), protease XIV (0.033 mg/mL; Sigma-Aldrich), trypsin (0.033 mg/mL; Sigma-Aldrich) and 0.3 mM CaCl<sub>2</sub>. The hearts were perfused for 6-7 min, or until they became pale and swollen, indicating an appropriate level of digestion. Hearts were removed from the Langendorff apparatus, by cutting below the atria, and the remaining ventricular tissue was rough-minced with scissors. The tissue was then placed in CIB supplemented with

insulin (100  $\mu$ U/mL), collagenase II (0.66 mg/mL; Worthington), protease XIV (0.033 mg/mL; Sigma-Aldrich), trypsin (0.033 mg/mL; Sigma-Aldrich), bovine serum albumin (BSA; 2 mg/mL; Sigma-Aldrich) and 0.7 mM  $\text{CaCl}_2$ , at 37  $^\circ\text{C}$  for 8 min, or until easy trituration was possible. Trituration, with a Pasteur pipette, was used to liberate the cardiomyocytes. The cardiomyocyte suspension was passed through a 400  $\mu\text{m}$  mesh, centrifuged (2 min at 300 rcf) and the ensuing supernatant discarded. The cardiomyocytes were allowed to settle in CIB supplemented with insulin (100  $\mu$ U/mL), BSA (2mg/mL) and  $\text{Ca}^{2+}$  (1.2 mM), at 37  $^\circ\text{C}$  for 10 min. Cardiomyocytes were then transferred to and re-suspended in 8 mL of Cardiac Myocyte Medium (CMM; 500:25:5:5 basal medium:fetal bovine serum:cardiac myocyte growth supplement:penicillin/streptomycin solution; ScienCell) for plating.

### *Primary Murine Cardiomyocyte Culture and Stable Isotope Labelling Assay*

Primary murine cardiomyocytes in CMM were plated, at a volume of 2 mL per well, onto 4 wells of a laminin coated 6-well tissue culture plate. They were then incubated for 2 hours at 37  $^\circ\text{C}$  and 5 %  $\text{CO}_2$ . The CMM, containing any unattached cells, was replaced with CMM supplemented with 0.2 mM L-carnitine (Trimethyl-d9, 98 %; Cambridge Isotope Laboratories) and either 0.1 % dimethyl sulfoxide (DMSO) (control), 5  $\mu\text{M}$  celecoxib in 0.1 % DMSO, 5  $\mu\text{M}$  rofecoxib in 0.1 % DMSO or 30 nM Etomoxir in 0.1 % DMSO. The cardiomyocytes were then incubated for 1 hour at 37  $^\circ\text{C}$  and 5 %  $\text{CO}_2$ , whilst the stable isotope labelling assay was performed: 50  $\mu\text{L}$  aliquots of media were taken, from each well at time 0, 1, 5, 10, 15, 30 and 60 min.

## **Metabolomic Protocols**

### *Methanol Crash*

The 50  $\mu$ L aliquots of media, derived from the stable isotope labelling assays, were immediately added to 200  $\mu$ L of cold methanol. The samples were vortex mixed and centrifuged (10 min at 15,000 rcf at 4 °C). The supernatant was then transferred to a new tube, dried down and stored at -80 °C for further analysis.

### *Non-Butylating Method of Preparation of Media Samples for LC-MS/MS Carnitine Assay*

This updated group protocol was developed by Dr James A. West, MRC HNR for the preparation of samples for the LC-MS/MS carnitine assay. Samples were reconstituted in 150  $\mu$ L of acetonitrile:water 1:1, vortex mixed, sonicated (10 min) and the supernatant was transferred to 1.2  $\mu$ m 96-well Filter Plates (Corning) over PlateOne 96-well Microplates with V bottoms (Starlab) for collection. The samples were centrifuged (10 min at 2000 rcf) to filter, the filter plate discarded and the collection plate sealed.

### *LC-MS/MS Carnitine Assay*

Please refer to In Vivo Experiments, LC-MS/MS Carnitine Assay.

### *Processing of Isotopically Labelled Metabolomic Data*

LC-MS/MS chromatograms were analysed using version 2.0 of Xcalibur (Thermo Scientific). For the LC-MS/MS data, the peaks were integrated individually. Where a carnitine species and its corresponding isotopically labelled compound were identified, the fractional incorporation of the label into the total pool, for that species, was calculated.

# *Statistical Analysis*

## **Univariate Analysis**

Univariate analysis was used to analyse relative concentrations of selected metabolites, obtained from metabolomic analyses, and relative target mRNA levels, obtained from RT-qPCR. Datasets were imported into Prism 6 (GraphPad) and processed, where appropriate, using the unpaired Student's t-test, Mann Whitney U-test, Ordinary one-way analysis of variance (ANOVA), Dunnett's multiple comparisons test, Pearson's r and linear regression.

### *Unpaired Student's t-Test*

Unpaired t-tests were used to compare the variable means of the IPNG COX-2<sup>-/-</sup> mice with their littermate controls. Unpaired t-tests make the assumption that the data are unmatched. The data conforms to this. Unpaired t-tests also assume that the data are sampled from populations following a normal distribution. This assumption is important with small sample sizes. Where results have been reported, the data passed the D'Agostino-Pearson omnibus normality test. In addition, Unpaired t-tests assume that the two populations have the same standard deviation (hence variance). Where results have been reported, the F test was used to confirm the equality of variance. A difference between the variable means was deemed statistically significant if  $P < 0.05$ . Significance was reported at four levels ( $P < 0.05$ ,  $P < 0.01$ ,  $P < 0.001$  and  $P < 0.0001$ ).

### *Mann-Whitney U-Test*

Mann-Whitney U-tests were used to compare the variable rank-sum of the IPNG COX-2<sup>-/-</sup> mice with their littermate controls, in cases where the data did not satisfy the criteria necessary for appropriate use of the unpaired t-test. The Mann-Whitney

U-tests make the assumptions that the data are unmatched, the errors are independent and the distribution of the populations follow the same shape. Where results have been reported, the data conforms to these. The Mann-Whitney U-test is a non-parametric test, therefore does not make the assumption that the data are sampled from populations following a given probability distribution. A difference between the variable rank-sums was deemed statistically significant if  $P < 0.05$ . Significance was reported at four levels ( $P < 0.05$ ,  $P < 0.01$ ,  $P < 0.001$  and  $P < 0.0001$ ).

### *Ordinary One-Way ANOVA*

Ordinary one-way ANOVA was used to compare the variable means of the different treatment groups (control, celecoxib and rofecoxib). ANOVA makes the assumptions that the data are unmatched and the errors are independent, characteristics which this data conforms to. ANOVA also assumes that the data are sampled from populations following a Gaussian distribution. This assumption is important with small sample sizes. Where results have been reported, the data passed either the D'Agostino-Pearson omnibus normality test (if  $n \geq 8$  per group) or the Shapiro-Wilk normality test (if  $n \geq 7$  per group). In addition, ANOVA assumes that all of the populations have the same standard deviation (hence variance). Where results have been reported, the Brown-Forsythe test and Bartlett's test were used to confirm the equality of variance. Differences among the means were deemed statistically significant if  $P < 0.05$ . Significance was reported at four levels ( $P < 0.05$ ,  $P < 0.01$ ,  $P < 0.001$  and  $P < 0.0001$ ).

### *Dunnett's Multiple Comparisons Test*

Significant one-way ANOVA results were followed up with Dunnett's multiple comparisons post-hoc test. Dunnett's test corrects for many-to-one type comparisons,

where a number of treatments (in this case celecoxib and rofecoxib) are compared to a single control. A difference between the control and treatment (either celecoxib or rofecoxib) mean was deemed statistically significant if the multiplicity adjusted  $P < 0.05$ . Significance was reported at four levels ( $P < 0.05$ ,  $P < 0.01$ ,  $P < 0.001$  and  $P < 0.0001$ ).

### *Pearson's r and Linear Regression*

Pearson's product moment correlation coefficient (Pearson's  $r$ ) was deemed statistically significant if the  $P < 0.05$ . Significance was reported at four levels ( $P < 0.05$ ,  $P < 0.01$ ,  $P < 0.001$  and  $P < 0.0001$ ). Linear regression was used to fit a line of best-fit to the data.

## **Multivariate Analysis**

Multivariate analysis was used to examine the metabolic profiles obtained from metabolomic techniques. Datasets were imported into SIMCA-P+ 12.0 (Umetrics) and processed using principal components analysis (PCA) and partial least squares discriminate analysis (PLS-DA). Models were validated using response permutation testing and ANOVA of cross-validated residuals (CV-ANOVA) [167].

Multivariate analysis assumes that only part of the data contains useful information, which is described in terms of latent variables - effectively the underlying trends in the data. These variables are extracted, by identifying correlation patterns within the data, until the amount of useful information recovered diminishes. Cross-validation is an out-of-sample model validation technique, which assesses the generalisability of a statistical analysis to an independent data-set and which is used to determine the point at which to stop this iterative process. PCA and PLS-DA are two methods used to infer latent variables (described below).

## *PCA and PLS-DA*

PCA is an unsupervised learning algorithm, and was used to visualise the dominant variation in the dataset. PLS-DA, which is a regression extension of PCA, is a supervised algorithm and was used to determine metabolic changes associated with pre-defined classifications. PCA models were assessed by examining the amount of explained variance described by the model ( $R^2$ ) while PLS-DA models were assessed using  $R^2$  and the predictive ability of the model ( $Q^2$ ).

## *Multivariate Model Validation*

Response permutation testing compares the diagnostic ( $R^2$  and  $Q^2$ ) statistics of a built classification model to those of  $n$  classification models in which sample labels are randomly permuted. It provides a reference distribution of the diagnostic statistics and therefore indicates the significance of the diagnostic statistics of the built model. Where reported,  $n = 20$  was used and the diagnostic statistics of the randomly permuted models did not exceed those of the built model. CV-ANOVA calculates the analysis of variance in the cross-validated predictive residuals. Its  $P$ -value is indicative of the statistical significance of the built model. The analysis was deemed statistically significant if the  $P < 0.05$ .

## ***Chapter 4: Hypotheses Generation***

## *Chapter Introduction*

The higher risk of HF, associated with the use of coxibs, is a recognised clinical phenomenon. However, the underlying mechanism has not yet been established [88, 89]. Moreover, it is unclear whether certain coxibs possess greater HF risk than others. For example, some evidence suggests that celecoxib may be associated with a lower HF risk than rofecoxib [5]. The reasons for this are also unclear. Whilst a number of studies have reported metabolic changes associated with coxib use, these analyses have either focused on prostanoid synthesis and related pathways, examined individual metabolites or explored metabolic changes in single-site samples (e.g. urine or blood) [4, 7-9, 156]. Little is therefore known about the wider systemic metabolic consequences of coxib treatment. Given that HF is intimately associated with metabolic remodelling, this information may hold the key to uncovering the processes by which the coxibs cause HF [10]. To address this issue, this study will employ a variety of metabolomic techniques, in a screening-capacity, to provide insight into the metabolic consequence of celecoxib and rofecoxib treatment, in the mouse. IL-1 $\beta$  (a pro-inflammatory cytokine) will be used to induce an inflammatory response, to better simulate the clinical scenario in which coxibs are used. Analyses will be performed on a range of tissues and biofluids, to capture systemic changes in metabolism. In so doing, this study will aim to:

**Generate hypotheses that can be tested, in mice, to provide insight into the mechanisms by which coxibs elevate the risk of HF**

## *Chapter Background*

### **Metabolomics for Hypothesis Generation**

Metabolomics is a powerful tool with which to investigate perturbations in biological systems [20]. The techniques employed are designed to interrogate metabolic networks, rather than individual pathways or enzymatic reactions [19].

One of the key advantages of metabolomics, compared to genomics, transcriptomics and proteomics, is that it captures information about the most down-stream indicators of biological activity [168]. This means that the effects of regulatory processes, which are intermediate between the genome, transcriptome, proteome and metabolome, are not lost, as they might be with other omics techniques. In addition, the metabolome rapidly remodels in response to genetic and environmental perturbations and this response is often amplified compared to changes in the other '-omes', engendering metabolomics with good sensitivity [20, 168]. However, these strengths are double-edged, as they predispose metabolomics to "biological noise," which can make the detection of biologically relevant changes more difficult [169].

Changes in metabolite concentrations are more pronounced than changes in metabolite flux (rate of turnover) when enzyme concentrations are altered [20, 170, 171]. However, metabolite concentration changes are not always easy to interpret. This is because the concentration of a metabolite depends on the difference between the rates of its production and consumption. Determining whether production, consumption or both are altered can prove difficult. Therefore the measurement of metabolite concentrations is not especially useful for testing mechanistic hypotheses, unless either the metabolites of interest are dead-end metabolites (only produced or only consumed) or the results are viewed in the context of additional information, such

as gene expression data. Instead, the measurement of metabolite concentrations is best used as a screening tool, to identify metabolic perturbations and generate hypotheses [19].

## **Targeted and Untargeted Metabolomics**

Metabolite concentrations can be measured using targeted and untargeted techniques. Untargeted techniques, such as NMR spectroscopy and open-profiling MS, measure all metabolites that are detectable, within a sample, with a chosen modality. Targeted techniques, for example closed-profiling MS such as conducted by a triple quadrupole MS, measure a sub-set of pre-determined metabolites [19]. Targeted metabolomic techniques are generally considered more sensitive, as the protocols used are optimised for the detection of specific metabolites. However, targeted techniques are inherently limited in their ability to identify unanticipated metabolic changes [172].

Whilst targeted techniques are usually considered hypothesis-driven and untargeted techniques usually considered hypothesis-generating, targeted techniques can also be employed in a hypothesis-generating capacity where little is known about a system [173, 174]. For example, certain metabolites are reflective of key metabolic pathway activities and targeted techniques that profile these add considerable depth to the metabolomic analysis. Ultimately, in hypothesis-generating work, it is important to strike a balance between the use of untargeted and targeted techniques, to ensure appropriate breadth and depth of analysis [174].

## **Selection of Metabolomic Techniques**

A combination of untargeted and targeted metabolomic techniques were chosen to address the aims of this study. The use of targeted techniques, in addition to

untargeted ones, was appropriate as, although little is known about the metabolic perturbations associated with coxib-induced HF, metabolomics has provided insight into HF and coxib treatment, separately. This work, which is reviewed in the background to this thesis, was used to help guide the selection of appropriate targeted metabolomic techniques. In addition, untargeted techniques were used to widen the scope of the analysis and capture perturbations in unexpected metabolic pathways.

### *LC-MS/MS Carnitine Assay*

Acylcarnitines can be used to follow FA oxidation [163]. FA oxidation is impaired in HF and this is reflected by perturbations in carnitine handling, which have been observed in human studies and animal models of HF, as described in Chapter 2 [13, 14, 16, 17, 127, 128, 132, 133]. Given the central role of impaired FA oxidation and carnitine handling in HF, these pathways represent good candidates for hypothesis-generating targeted analysis, in order to elucidate whether they also play a role in coxib-induced HF. The LC-MS/MS carnitine assay is a targeted-assay designed to quantify carnitine and acylcarnitine species, relative to known standards. In this assay, samples are extracted and the analytes separated by reversed-phase liquid chromatography (LC). LC employs a liquid mobile phase. In this assay, due to column selection, the most polar-analytes elute first. The LC system is coupled to a triple-quadrupole mass spectrometer, which ionises the eluted analytes by electrospray ionisation (ESI). The three quadrupoles then work in tandem to i) select specific ions of known mass, ii) fragment these ions via collision with an inert gas and iii) select specific product ions of these collisions. A discreet-dynode electron multiplier detects the precursors of product ions with an  $m/z$  of 85, using an MRM approach. These transitions correspond to the carnitine and acylcarnitine species of interest [163, 175].

## *LC-MS/MS Aqueous Metabolite Assay*

In addition to impairments in FA metabolism, perturbations in TCA cycle activity and amino acid metabolism have also been observed in HF, as described in Chapter 2 [13, 17, 123-128, 131-137, 139, 140, 145, 146]. Because it is possible that the mechanisms underlying coxib-induced HF are similar to those that cause other forms of HF, these pathways also represent good candidates for hypothesis-generating targeted analysis. The LC-MS/MS aqueous metabolite assay is a targeted-assay designed to quantify certain TCA cycle intermediates and amino acids (as well as selected nucleotides, oxidative-stress markers and other aqueous metabolites such as creatinine), relative to known standards. Like the carnitine assay, this assay employs reversed-phase chromatography and a UPLC system. Metabolites are separated according to a combination of polarity, hydrogen bonding capacity and  $\pi$ - $\pi$  interactions. This assay also uses a triple quadrupole mass spectrometer, ESI, discrete-dynode ion detection and an MRM approach. However, the carnitine and aqueous metabolite assays differ in terms of sample extraction protocol, reconstitution solvent, UPLC column, elution gradient and compound dependent MS parameters, as the two methods are optimised for compounds with distinct physicochemical properties [164].

## *GC-MS FAME Assay*

As described in Chapter 2, alterations in FA and lipid metabolism have been observed in HF [13, 14, 16, 17, 127-129, 132, 133, 147-149]. The GC-MS FAME assay is a targeted assay designed for the general profiling of lipid extracts. It provides useful insight into FA and lipid metabolism. In this assay, FAs are first derivatised to form FAMES. At this point, information regarding the origin of the FA (e.g. whether it is esterified or un-esterified) is lost. The different FAMES are then identified and quantified relative to known standards. FAMES are vaporised, then separated by gas

chromatography (GC). GC employs a gaseous mobile phase. In this assay, the most volatile FAMES elute first. The GC system is coupled to a single quadrupole mass spectrometer, which ionises the eluted FAMES by electron ionisation (EI). The single quadrupole guides these ions towards the detector. A conversion-dynode electron multiplier detects ions with an  $m/z$  of 50–650, representing a full spectral scan [162, 163].

### *One-Dimensional (1D) $^1\text{H}$ NMR Spectroscopy*

One dimensional  $^1\text{H}$  NMR spectroscopy is an inherently quantitative, untargeted technique [176]. It relies on the principle of nuclear spin, the total angular momentum of a nucleus [177]. Only nuclei which possess unpaired protons and/or neutrons have net spin. The hydrogen nuclei, which contains an unpaired proton, is an example and possesses a spin of  $\pm 1/2$  [178]. Because the hydrogen nuclei has net spin and a charge, it induces a small magnetic field perpendicular to the plane of its spin (Faraday's Law of Induction) [179]. Hydrogen nuclei can be imagined as small dipolar magnets. Normally the direction of their spin, hence magnetic field, is random. However, when placed in a strong external magnetic field, such as is used in NMR spectroscopy, the spins of hydrogen nuclei align in one of two energy states, parallel or antiparallel to the external field [180]. The parallel spin-state is lower in energy than the antiparallel spin-state and is therefore slightly more populated [181]. The extra hydrogen nuclei in the parallel spin-state creates a net magnetic field, aligned with the external field, and it is the behaviour of these nuclei that are followed in a 1D  $^1\text{H}$  NMR spectroscopy experiment. The small population difference engenders NMR spectroscopy with lower sensitivity than MS techniques. When a radiofrequency (RF) pulse, of electromagnetic (EM) radiation, is applied perpendicular to the external magnetic field, these hydrogen nuclei are deflected into a higher energy state. They

then precess back into alignment, in a process termed “relaxation,” re-emitting RF-EM radiation as they do so. This RF-EM radiation is then detected [182]. Hydrogens in different chemical environments experience different degrees of nuclear shielding, determined by the proximity of their electrons to their nuclei. Hydrogens bonded to more electronegative atoms experience less nuclear shielding. The degree of nuclear shielding determines the resonant frequency of the RF-EM absorption-re-emission process for each hydrogen [183]. The difference in resonant frequencies between hydrogens in a particular chemical environment and those in a standard, for example TSP or DSS, is termed the chemical shift (ppm) and it determines the position of each resonance on the NMR spectrum. Each resonance may or may not be split into multiple peaks. This multiplicity is determined by the number of hydrogens that are bonded to carbons adjacent to the carbon that the hydrogen under observation is bound. It gives rise to *the n+1 rule*: a particular resonance will be split into  $n+1$  peaks, where  $n$  is the number of hydrogens bonded to adjacent carbons. Molecules can be identified based on the number, chemical shifts and multiplicities of their resonances [184]. Whilst 1D  $^1\text{H}$  NMR spectroscopy is limited in its ability to resolve individual species in organic mixtures, due to signal overlap, it is well suited to identifying aqueous metabolites, provided their abundances exceed the limit of detection [185].

## *Chapter Methods*

Twenty-one mice were fed rofecoxib-containing, celecoxib-containing or control diets (n=7) for 3 weeks, then sacrificed. Four-hours before sacrifice IL-1 $\beta$  was injected to stimulate an acute inflammatory response. Various bio-fluids and tissues derived from these animals were analysed using a combination of NMR spectroscopy, GC-MS and LC-MS/MS, to explore the metabolic perturbations associated with coxib use.

The following methods (see chapter 3 for a detailed description of each) were used in this chapter:

- **Study 1**
- **Methanol/Chloroform/Water Metabolite Double Extraction**
- **Nuclear Magnetic Resonance (NMR) Spectroscopy**
- **Fatty Acid Methyl Ester (FAME) Derivatisation of the Organic Fraction, for Gas Chromatography Mass Spectrometry (GC-MS) Analysis**
- **GC-MS Analysis of Total FAMES**
- **Butylating Method of Sample Preparation for Liquid Chromatography – Mass Spectrometry/Mass Spectrometry (LC-MS/MS) Carnitine Assay**
- **LC-MS/MS Carnitine Assay**
- **LC-MS/MS Aqueous Metabolite Assay**
- **Processing of Metabolomic Data**
- **Ordinary One-Way ANOVA**
- **Dunnett's Multiple Comparisons Test**
- **PCA and PLS-DA**
- **Multivariate Model Validation**

## Chapter Results

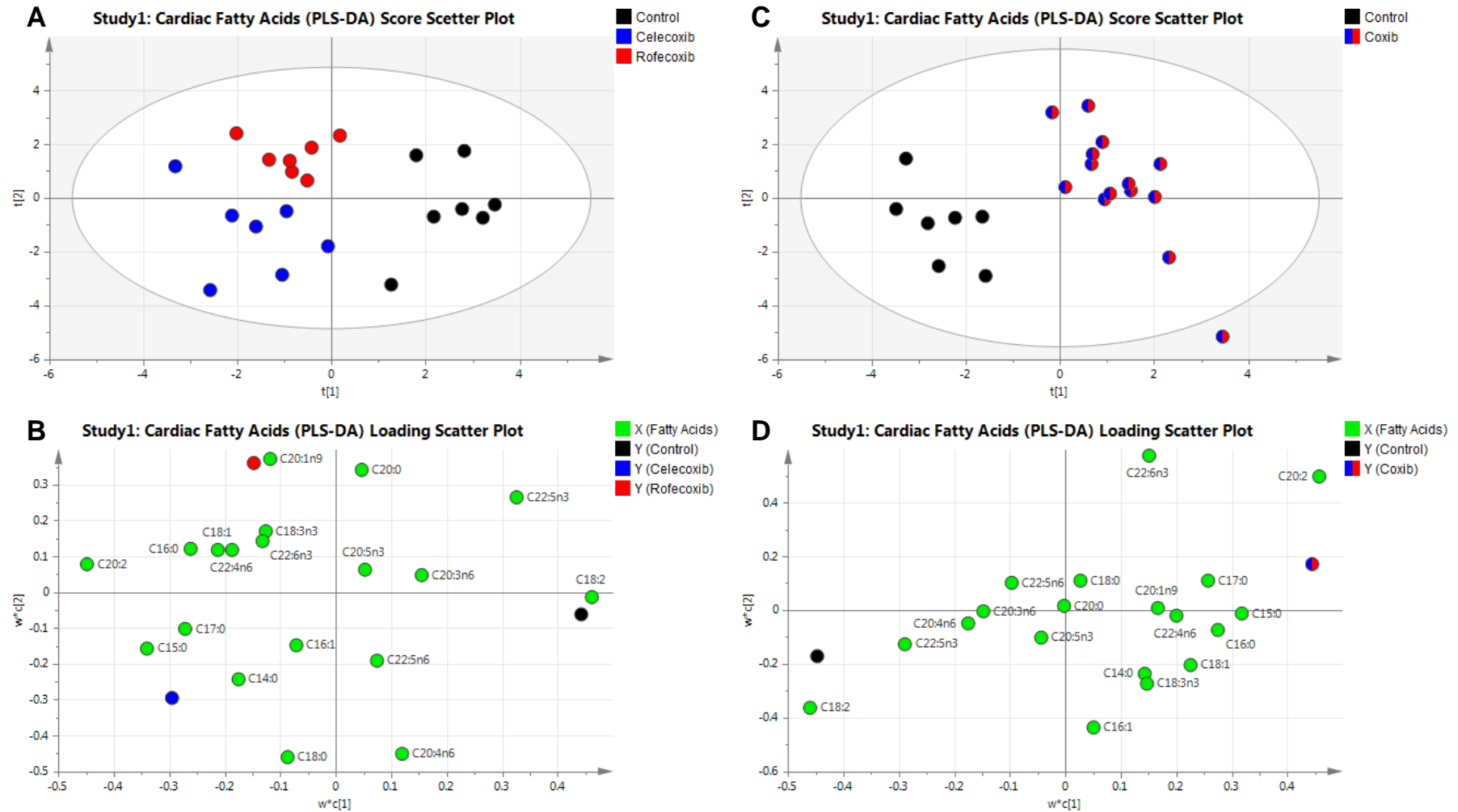
Mouse heart, aorta, skeletal muscle, kidney, liver and plasma samples were profiled using the GC-MS, LC-MS/MS and NMR spectroscopy assays described. Urine was profiled by NMR spectroscopy alone. No significant differences, in metabolite profiles, were observed between the treatment groups in the aorta and urine samples (data not shown). For the other tissues and plasma, only those multivariate analyses which yielded a statistically significant difference (CV-ANOVA < 0.05) are shown.

### Heart

#### GC-MS FAME Assay

Cardiac total- (esterified- plus free-) FAs were measured, using GC-MS. With multivariate analysis a PLS-DA model was built, which discriminated celecoxib treated, rofecoxib treated and control mice (3 latent variables from cross-validation;  $R^2X = 66.4\%$ ,  $R^2Y = 78.7\%$ ,  $Q^2 = 60.1\%$ ; CV-ANOVA = 0.0500) (*Figure 1 A*). A PLS-DA model was also built, when the two coxibs were grouped as a single class, which discriminated coxib-treated mice from controls (3 latent variables from cross-validation;  $R^2X = 66.9\%$ ,  $R^2Y = 96.7\%$ ,  $Q^2 = 89.1\%$ ; CV-ANOVA = 0.0001) (*Figure 1 C*). Generally, levels of saturated and monounsaturated total FAs were higher in the coxib treated mice, whilst levels of polyunsaturated total FAs were lower, compared to the control mice (*Figure 1 B and D*).

**Figure 1.**



Multivariate analysis (PLS-DA) of cardiac total-fatty acids, in mice treated with celecoxib or rofecoxib, for 3 weeks, compared to control, on an inflammatory background. (A) Scores plot showing the separation between celecoxib treated, rofecoxib treated and control mice; (B) Loadings plot, for the scores plot in A., showing the fatty acids responsible for the discrimination between groups; (C) Scores plot showing the separation between coxib treated and control mice; (D) Loadings plot, for the scores plot in C., showing the fatty acids responsible for the discrimination between groups. Measured by GC-MS. Data are individual samples,  $n = 7$  (A and B),  $n = 7$  and  $14$  (C and D).

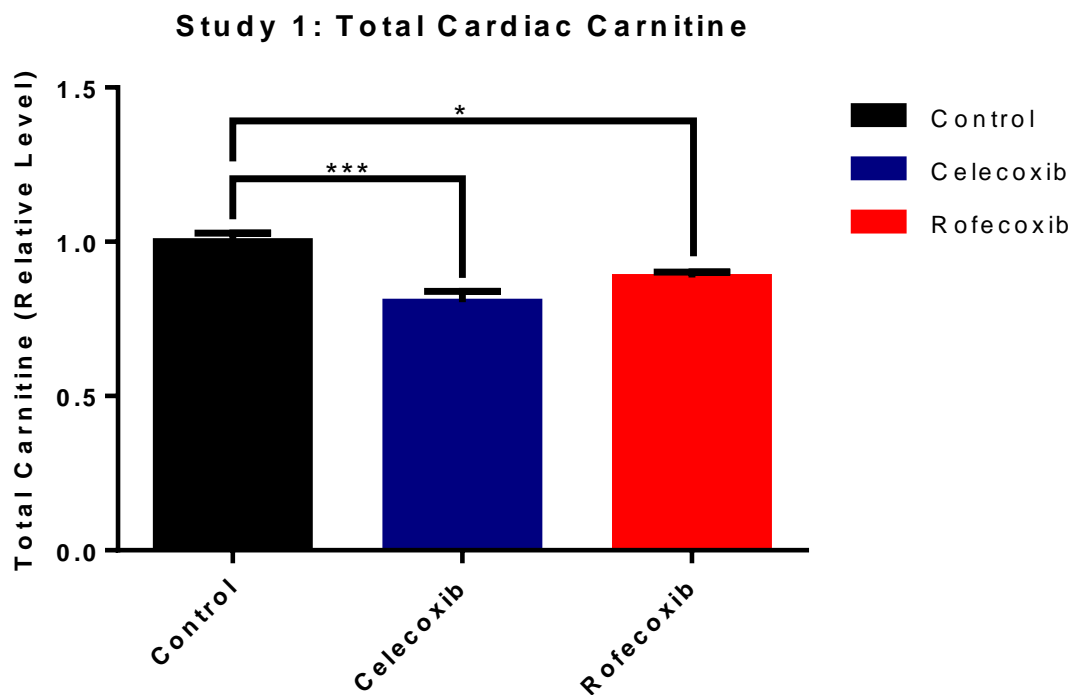
## *LC-MS/MS Carnitine Assay*

Cardiac carnitines were measured, using LC-MS/MS. A PLS-DA model was built, which discriminated celecoxib treated, rofecoxib treated and control mice (2 latent variables from cross-validation;  $R^2X = 66.4\%$ ,  $R^2Y = 49.7\%$ ,  $Q^2 = 24.5\%$ ; CV-ANOVA = 0.0057) (*Figure 2 A*). A PLS-DA model was also built, when the two coxibs were grouped as a single class, which discriminated coxib-treated mice from controls (2 latent variables from cross-validation;  $R^2X = 66.2\%$ ,  $R^2Y = 77.8\%$ ,  $Q^2 = 58.6\%$ ; CV-ANOVA = 0.0104) (*Figure 2 C*). Cardiac carnitines were lower in the coxib treated mice, compared to the control mice (*Figure 2 B and D*).



To confirm the findings of the multivariate analysis, carnitines were summed and the total cardiac carnitine concentrations were compared between the different groups, using univariate statistics. Ordinary One-Way ANOVA was performed and Dunnett's post-hoc test, was used to correct for multiple comparisons (*Figure 3*). Both celecoxib and rofecoxib treated mice exhibited significant lower concentrations of total cardiac carnitines of ~20% and ~12%, respectively, compared to the control mice (ANOVA = 0.0008; Dunnett's post-hoc test:  $P = 0.0004$  and  $P = 0.0270$  respectively).

**Figure 3.**



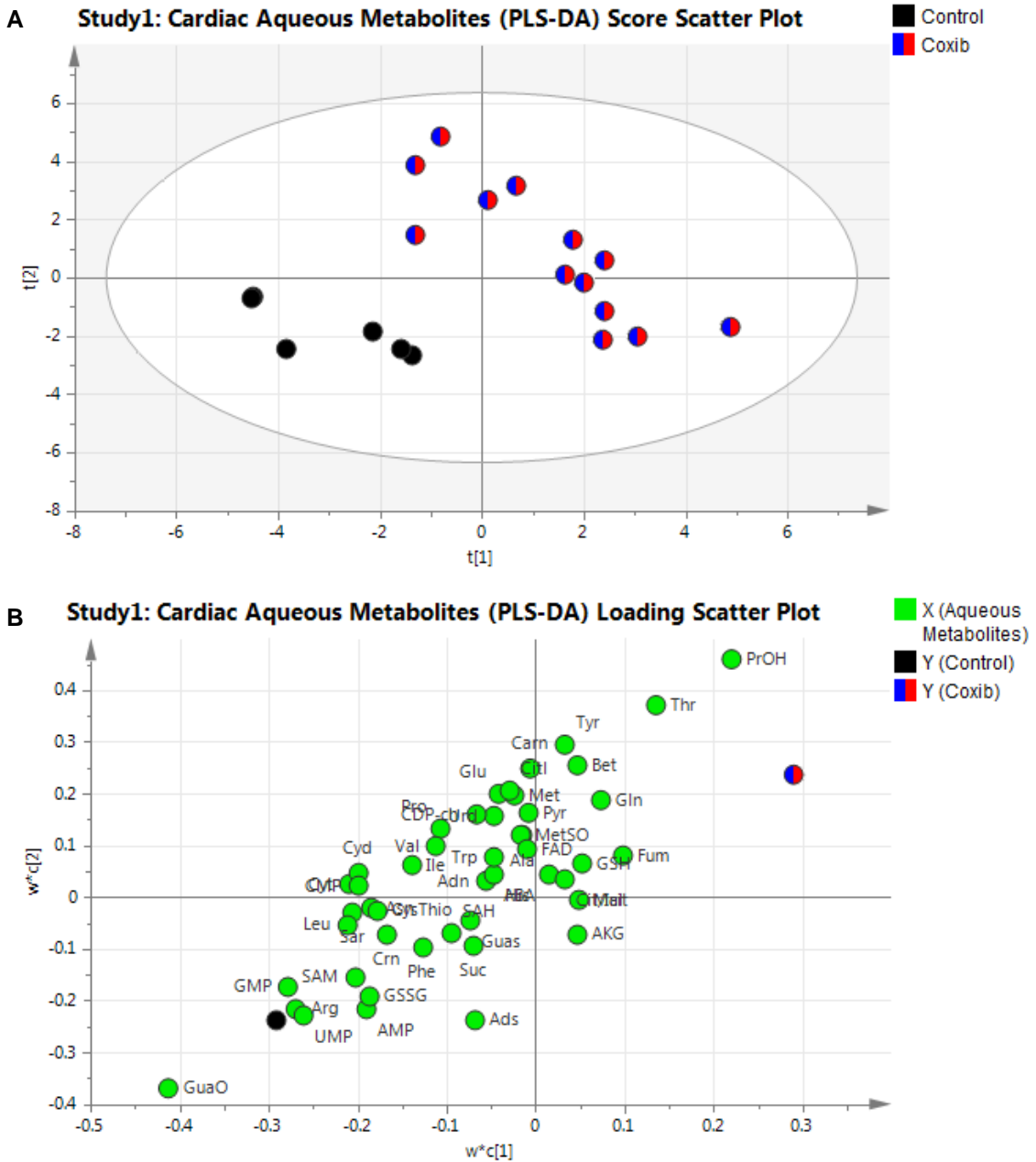
*Effect of 3 weeks of celecoxib and rofecoxib treatment on total cardiac carnitines, in mice, on an inflammatory background. Measured by LC-MS/MS. Data are mean  $\pm$  S.E.M for  $n = 6-7$ . (\* =  $P < 0.05$ , \*\*\* =  $P < 0.001$ ).*

### *LC-MS/MS Aqueous Metabolite Assay*

Selected cardiac aqueous metabolites were measured, using LC-MS/MS. A PLS-DA model was built, when the two coxibs were grouped as a single class, which discriminated coxib-treated mice from controls (2 latent variables from cross-

validation;  $R^2X = 33.4\%$ ,  $R^2Y = 90.4\%$ ,  $Q^2 = 61.9\%$ ; CV-ANOVA = 0.0061) (*Figure 4 A*). Notably, cardiac concentrations of hydroxyproline and threonine were higher in coxib treated mice, whilst concentrations of oxoguanine were lower, compared to the control mice (*Figure 4 B*).

**Figure 4.**



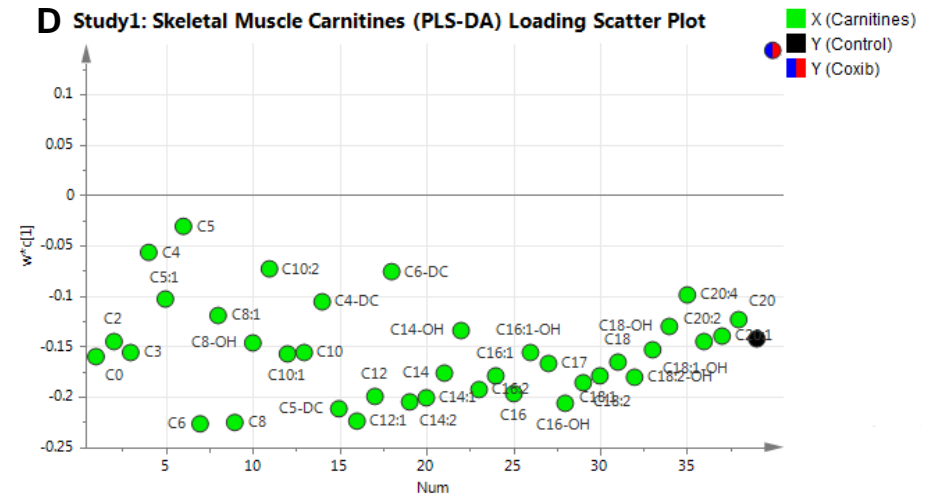
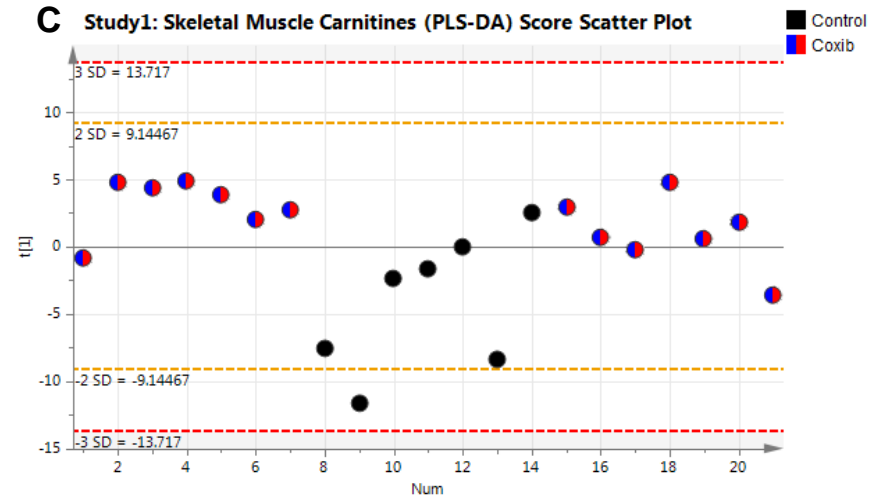
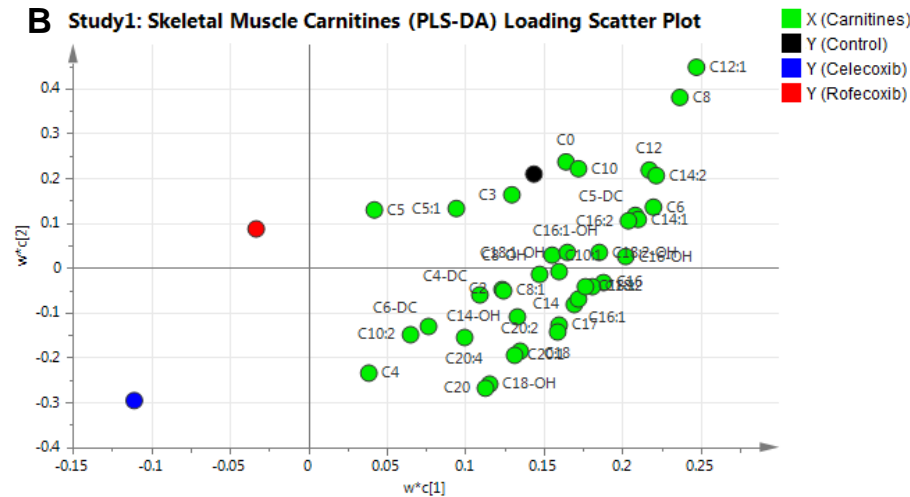
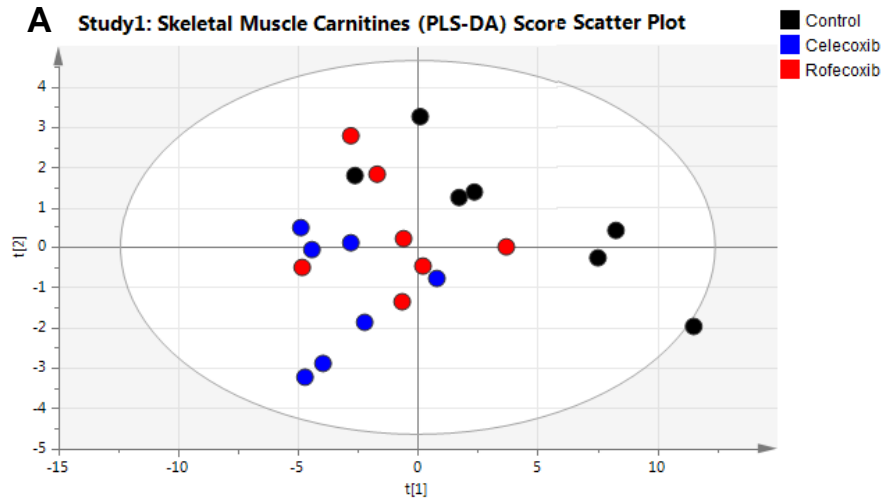
Multivariate analysis (PLS-DA) of cardiac aqueous metabolites, in mice treated with celecoxib or rofecoxib, for 3 weeks, compared to control, on an inflammatory background. (A) Scores plot showing the separation between coxib treated and control mice; (B) Loadings plot, for the scores plot in A., showing the aqueous metabolites responsible for the discrimination between groups. Measured by LC-MS/MS. Data are individual samples,  $n = 6$  and 13.

## Skeletal Muscle

### *LC-MS/MS Carnitine Assay*

Skeletal muscle carnitines were measured, using LC-MS/MS. A PLS-DA model was built, which discriminated celecoxib treated, rofecoxib treated and control mice (2 latent variables from cross-validation;  $R^2X = 68.0\%$ ,  $R^2Y = 36.9\%$ ,  $Q^2 = 17.7\%$ ; CV-ANOVA = 0.0448) (*Figure 5 A*). A PLS-DA model was also built, when the two coxibs were grouped as a single class, which discriminated coxib-treated mice from controls (1 latent variable from cross-validation;  $R^2X = 58.5\%$ ,  $R^2Y = 42.8\%$ ,  $Q^2 = 36.8\%$ ; CV-ANOVA = 0.0162) (*Figure 5 C*). Skeletal muscle carnitines were lower in coxib treated mice, compared to the control mice (*Figure 5 B and D*).

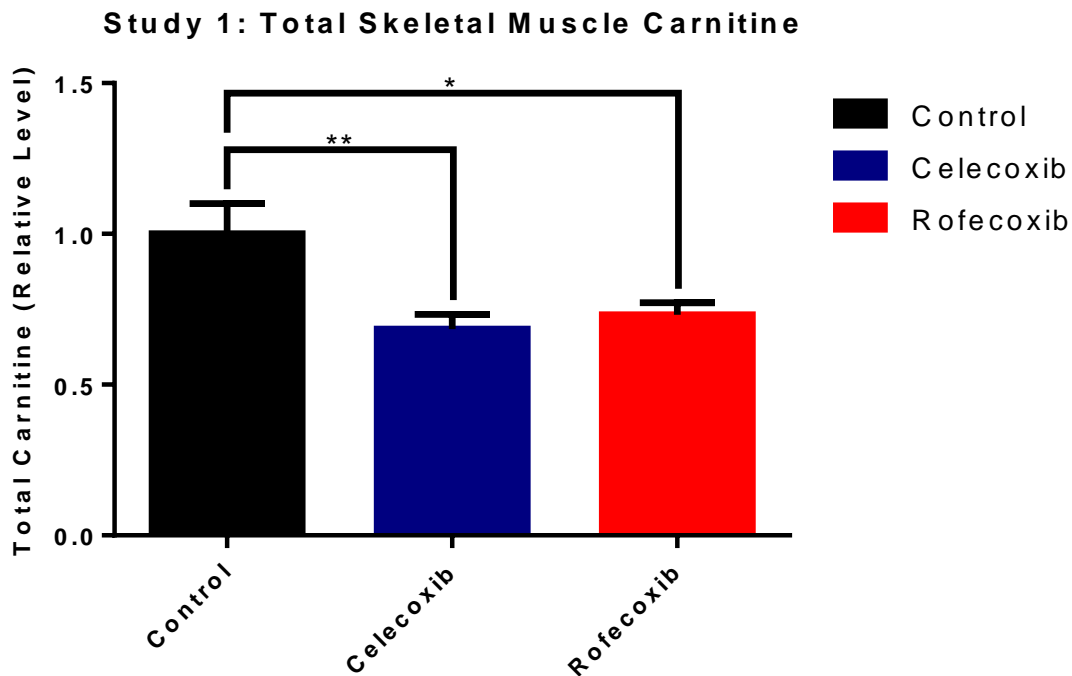
**Figure 5.**



Multivariate analysis (PLS-DA) of skeletal muscle carnitines, in mice treated with celecoxib or rofecoxib, for 3 weeks, compared to control, on an inflammatory background. (A) Scores plot showing the separation between celecoxib treated, rofecoxib treated and control mice; (B) Loadings plot, for the scores plot in A., showing the carnitines responsible for the discrimination between groups; (C) Scores plot showing the separation between coxib treated and control mice; (D) Loadings plot, for the scores plot in C., showing the carnitines responsible for the discrimination between groups. Measured by LC-MS/MS. Data are individual samples,  $n = 7$  (A and B),  $n = 7$  and  $14$  (C and D).

To confirm the findings of the multivariate analysis, differences in the total skeletal muscle carnitine concentrations were compared between the different groups, using univariate statistics (*Figure 6*). Both celecoxib and rofecoxib treated mice exhibited significantly lower concentrations of total skeletal muscle carnitines of ~32% and ~27%, respectively, compared to the control mice (ANOVA = 0.0091; Dunnett's post-hoc test:  $P = 0.0082$  and  $P = 0.0234$  respectively).

**Figure 6.**



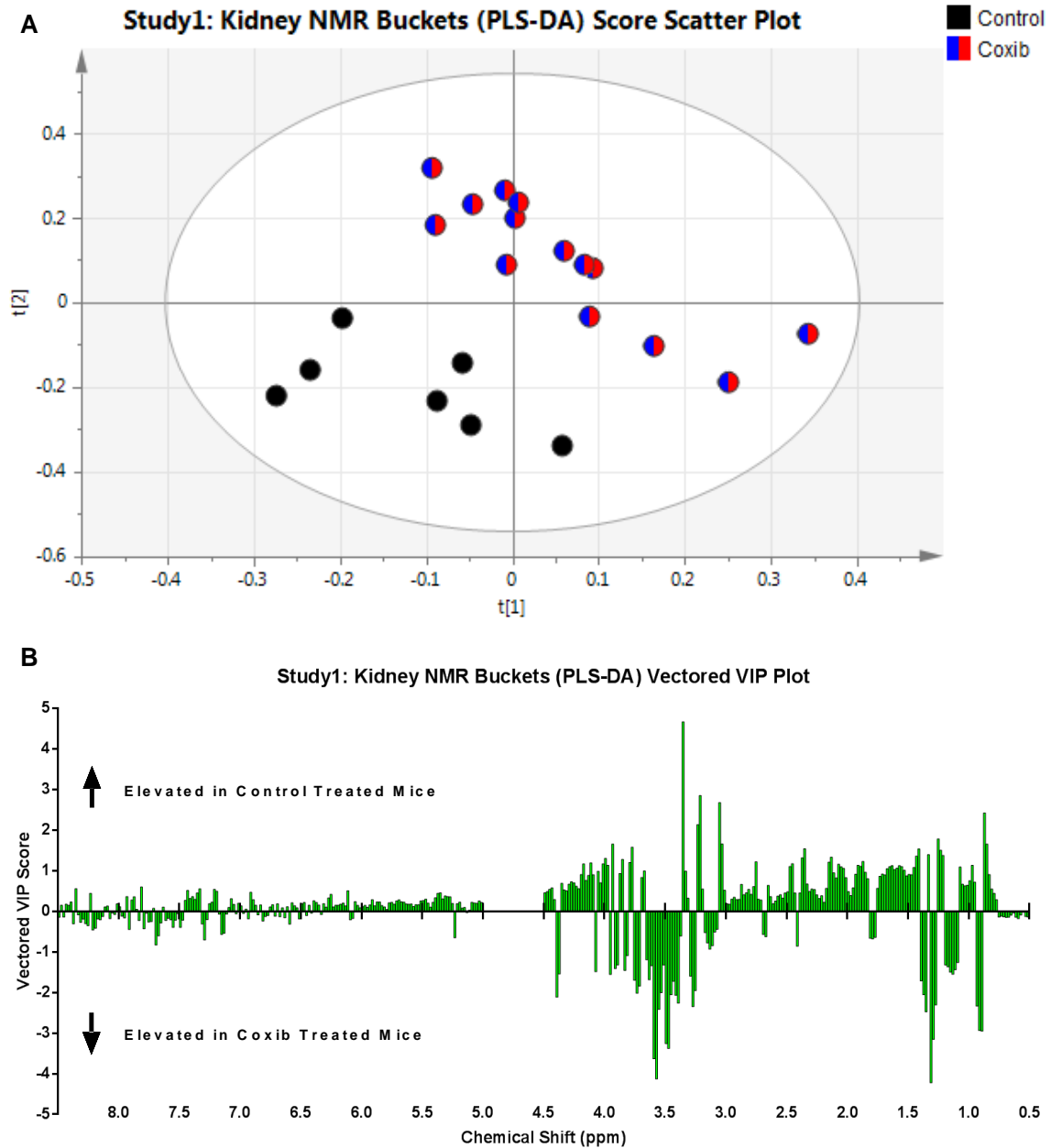
*Effect of 3 weeks of celecoxib and rofecoxib treatment on total skeletal muscle carnitines, in mice, on an inflammatory background. Measured by LC-MS/MS. Data are mean  $\pm$  S.E.M for  $n = 7$ . (\* =  $P < 0.05$ , \*\* =  $P < 0.01$ ).*

## Kidney

### *1D <sup>1</sup>H NMR Spectroscopy*

The aqueous fractions, of the kidney extracts, were analysed using 1D <sup>1</sup>H NMR spectroscopy. Spectra were bucketed. A PLS-DA model was built, when the two coxibs were grouped as a single class, which discriminated coxib-treated mice from controls (2 latent variables from cross-validation;  $R^2X = 72.8\%$ ,  $R^2Y = 89.0\%$ ,  $Q^2 = 85.0\%$ ; CV-ANOVA = 0.0011) (*Figure 7 A*). NMR spectroscopy buckets indicative of lactate (1.30-1.32 ppm) and myo-inositol (3.58-3.60 ppm) were higher in coxib treated mice, whilst those indicative of proline (3.34-3.36 ppm), choline/phosphocholine (3.20-3.22 ppm) and creatine (3.04-3.06 ppm) were lower, compared to the control mice (*Figure 7 B*).

Figure 7.

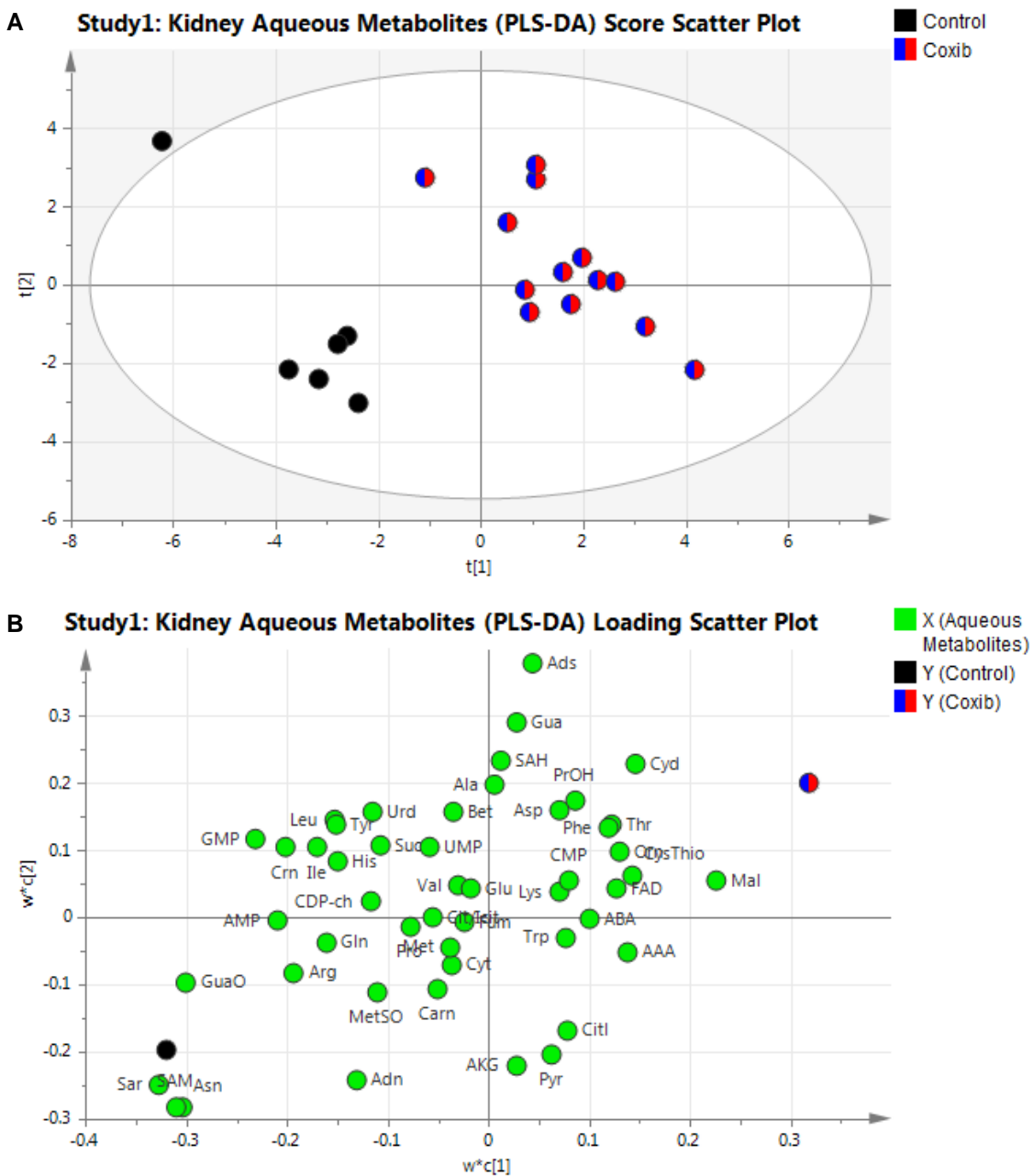


Multivariate analysis (PLS-DA) of kidney NMR spectroscopy buckets, in mice treated with celecoxib or rofecoxib, for 3 weeks, compared to control, on an inflammatory background. (A) Scores plot showing the separation between coxib treated and control mice; (B) Vectors Variable Importance in Projection (VIP) plot, for the scores plot in A., showing the most important variables over the model as a whole. Variables are arranged, as per an NMR spectroscopy spectrum, by ppm. The greater the magnitude of a VIP score, the greater the importance of that variable to the model. Positive vector VIP scores indicate that the variable is higher in the control group, whilst negative vector VIP scores indicate that the variable is higher in the coxib treated group. Measured by NMR spectroscopy. Data are individual samples,  $n = 7$  and  $14$ .

### *LC-MS/MS Aqueous Metabolite Assay*

Selected kidney aqueous metabolites were measured, using LC-MS/MS. A PLS-DA model was built, when the two coxibs were grouped as a single class, which discriminated coxib-treated mice from controls (3 latent variables from cross-validation;  $R^2X = 43.4\%$ ,  $R^2Y = 96.5\%$ ,  $Q^2 = 65.1\%$ ; CV-ANOVA = 0.0363) (*Figure 8 A*). Kidney concentrations of malate, adenosine and cytidine were higher in coxib treated mice, whilst concentrations of sarcosine, S-adenosylmethionine, asparagine and oxoguanine were lower, compared to the control mice (*Figure 8 B*).

**Figure 8.**



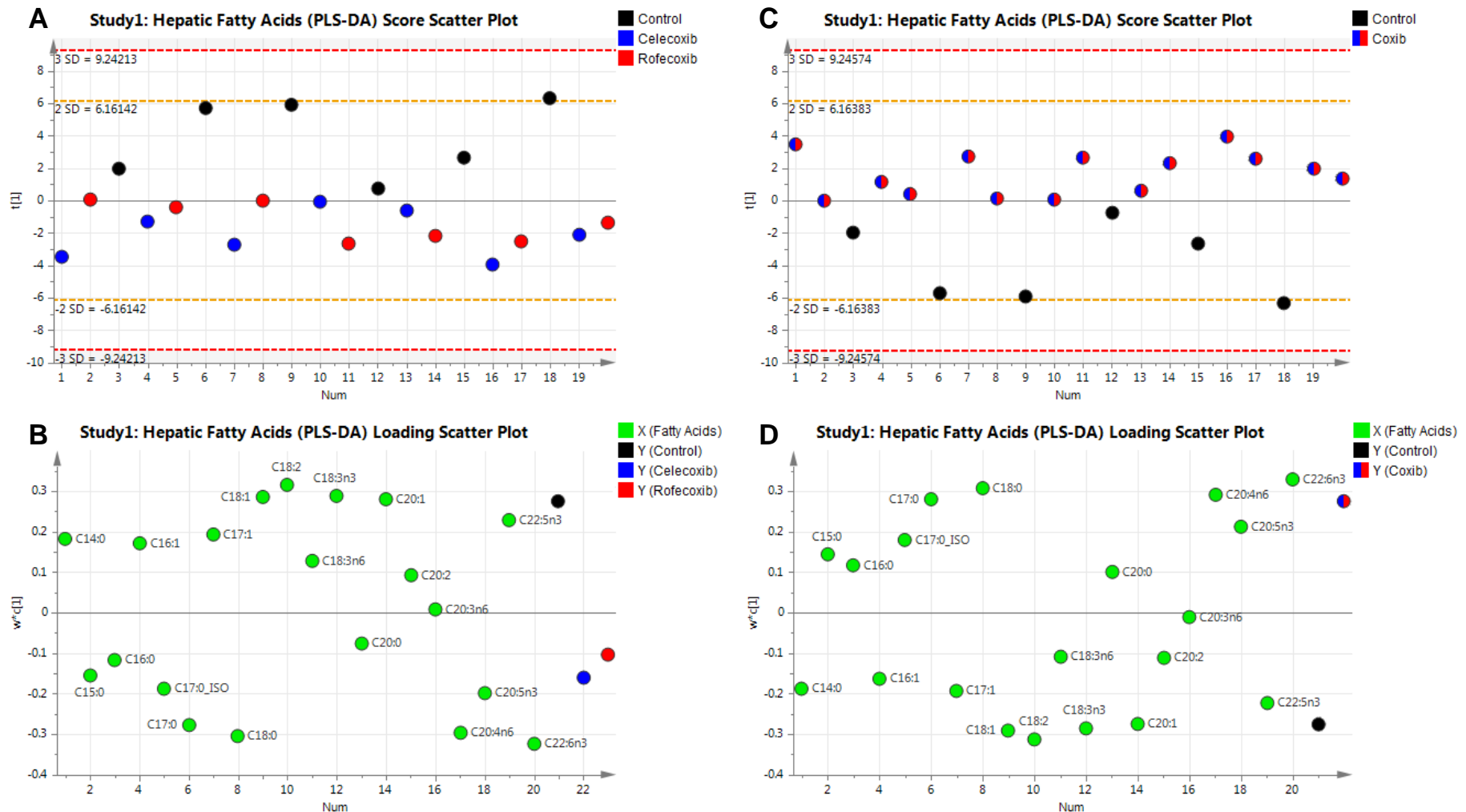
Multivariate analysis (PLS-DA) of kidney aqueous metabolites, in mice treated with celecoxib or rofecoxib, for 3 weeks, compared to control, on an inflammatory background. (A) Scores plot showing the separation between coxib treated and control mice; (B) Loadings plot, for the scores plot in A., showing the aqueous metabolites responsible for the discrimination between groups. Measured by LC-MS/MS. Data are individual samples,  $n = 6$  and 13.

## Liver

### GC-MS FAME ASSAY

Hepatic total-FAs were measured, using GC-MS. A PLS-DA model was built, which discriminated celecoxib treated, rofecoxib treated and control mice (1 latent variable from cross-validation;  $R^2X = 48.6\%$ ,  $R^2Y = 35.4\%$ ,  $Q^2 = 31.2\%$ ; CV-ANOVA = 0.0005) (*Figure 9 A*). A PLS-DA model was also built, when the two coxibs were grouped as a single class, which discriminated coxib-treated mice from controls (1 latent variable from cross-validation;  $R^2X = 48.7\%$ ,  $R^2Y = 71.6\%$ ,  $Q^2 = 67.0\%$ ; CV-ANOVA < 0.0001) (*Figure 9 C*). Generally, the total saturated FAs were higher in the coxib treated mice, compared to the control mice (*Figure 9 B and D*).

**Figure 9.**



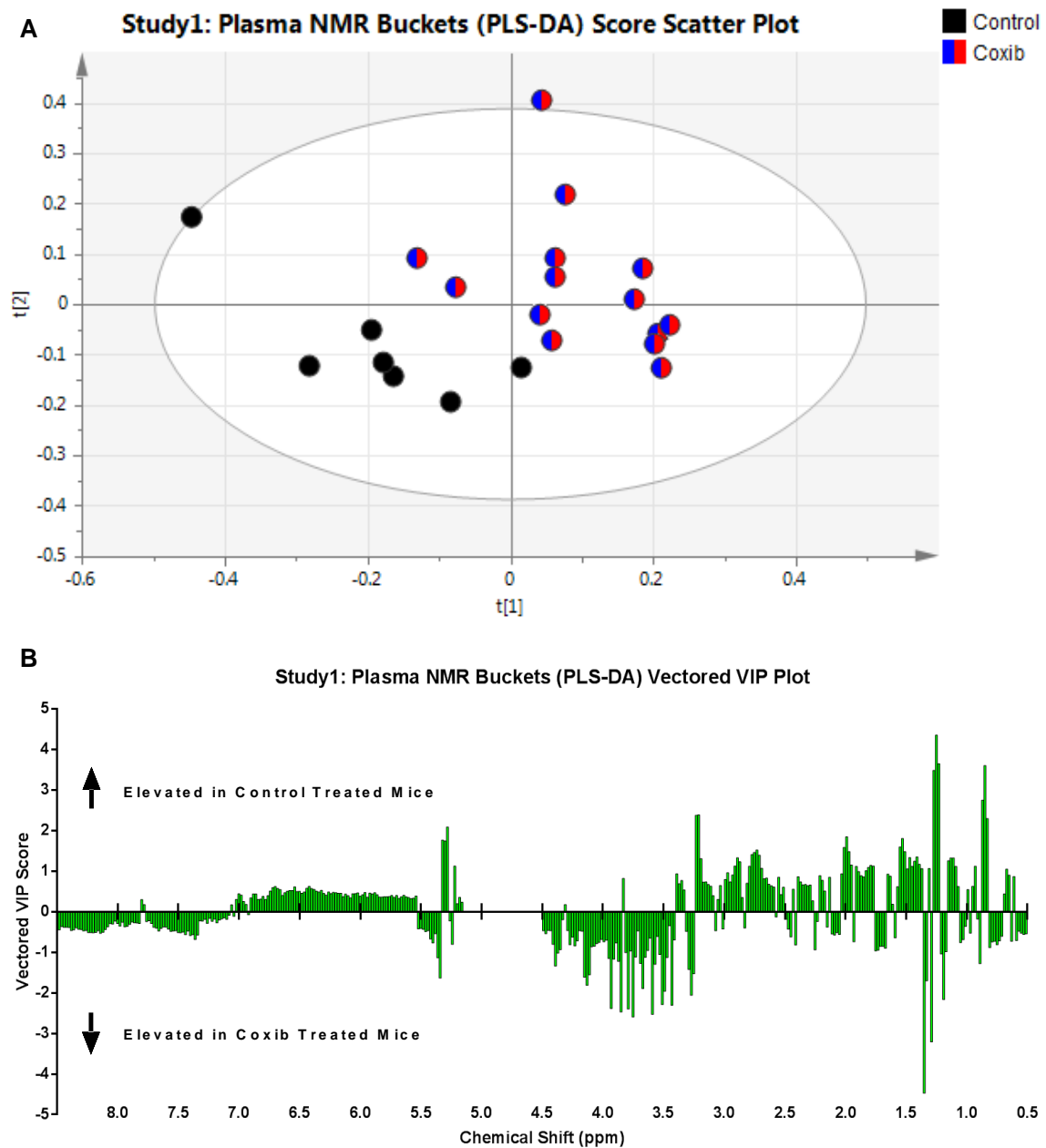
Multivariate analysis (PLS-DA) of hepatic total-fatty acids, in mice treated with celecoxib or rofecoxib, for 3 weeks, compared to control, on an inflammatory background. (A) Scores plot showing the separation between celecoxib treated, rofecoxib treated and control mice; (B) Loadings plot, for the score plot in A., showing the fatty acids responsible for the discrimination between groups; (C) Scores plot showing the separation between coxib treated and control mice; (D) Loadings plot, for the scores plot in C., showing the fatty acids responsible for the discrimination between groups. Measured by GC-MS. Data are individual samples,  $n = 6-7$  (A and B),  $n = 6$  and  $14$  (C and D).

## Plasma

### *1D <sup>1</sup>H NMR Spectroscopy*

The aqueous fractions of the plasma extracts were analysed using 1D <sup>1</sup>H NMR spectroscopy and spectra were bucketed. A PLS-DA model was built, when the two coxibs were grouped as a single class, which discriminated coxib-treated mice from controls (2 latent variables from cross-validation;  $R^2X = 52.8\%$ ,  $R^2Y = 74.8\%$ ,  $Q^2 = 62.2\%$ ; CV-ANOVA = 0.0022) (*Figure 10 A*). NMR spectroscopy buckets indicative of alkyl groups, including methylene (1.2-1.3 ppm) and methyl (0.8-0.9 ppm) groups, were lower in coxib treated mice compared to control mice (*Figure 10 B*). The identities of the lipid species that these represent were not established using an MS-based lipidomic approach, due to time constraints, as it was felt that the carnitine findings were the most promising line of further investigation.

Figure 10.



Multivariate analysis (PLS-DA) of plasma NMR spectroscopy buckets, in mice treated with celecoxib or rofecoxib, for 3 weeks, compared to control, on an inflammatory background. (A) Scores plot showing the separation between coxib treated and control mice; (B) VIP plot, for the scores plot in A., showing the most important variables over the model as a whole. Variables are arranged, as per an NMR spectroscopy spectrum, by ppm. The greater the magnitude of a VIP score, the greater the importance of that variable to the model. Positive vector VIP scores indicate that the variable is higher in the control group, whilst negative vector VIP scores indicate that the variable is higher in the coxib treated group. Measured by NMR spectroscopy. Data are individual samples,  $n = 7$  and  $14$ .

## *Chapter Discussion*

Metabolomic differences associated with coxib treatment were identified, using multivariate statistics, in the heart, skeletal muscle, kidney, liver and plasma, in the mouse. Both celecoxib and rofecoxib behaved similarly, in terms of the metabolic changes they induced, and no clear differences between the two were observed.

Notably, no differences were observed, between coxib treated mice and controls, in aortic metabolites. Coxib-mediated inhibition of prostacyclin synthesis, at the vascular endothelium, is key to the mechanistic explanation of the increased CV-risk seen with the coxibs, suggested by FitzGerald [3] It may, therefore, seem surprising that no metabolic changes were observed in this tissue. However, the exploratory assays used in this study were not designed to profile the prostanoids and the aorta is fairly metabolically inactive [186].

The aorta aside, only a single metabolite was consistently altered across all of the tissues. This metabolite, oxo-guanine, was significantly lower in tissues derived from coxib treated mice, compared to controls (data not shown for skeletal muscle and liver). To understand this observation, it is important to consider the context of these findings, namely that an acute inflammatory response was induced in these mice, with IL-1 $\beta$  injection, prior to sacrifice. Inflammation generates a range of reactive oxygen species, including the nitrosoperoxycarbonate anion. This anion is able to perform specific one-electron oxidation of DNA at guanine bases, generating oxo-guanine [187]. Therefore, in the coxib treated mice, where inflammation is pharmacologically suppressed, one would expect lower oxo-guanine concentrations, compared to controls, consistent with the findings of this study.

At a systemic level, the greatest differences, between coxib treated mice and controls, were observed in the heart and kidney. HF is intimately associated with both cardiac and renal dysfunction [188]. Given that the coxibs are associated with HF, it seems an unlikely coincidence that the most profound metabolic changes in coxib treated mice occurred in those organs most associated with HF.

The metabolite changes associated with coxib treatment, observed in the kidney, were limited to the aqueous fraction. These changes involved alterations in metabolites which play a role in renal energy metabolism, such as lactate, malate, and creatine, and metabolites which serve as organic osmolytes in the kidney, including myo-inositol and a number of the amino acids [189-191]. Whilst these observations are by no means definitive, they imply that coxib treatment might alter renal energy metabolism and osmoregulation, and it is plausible that this could reflect the increase in blood pressure observed with coxib treatment [1]. These observations certainly bring into focus those findings of Ahmetaj-Shala et al., discussed in the background to this thesis, who reported higher ADMA concentrations with coxib treatment and linked this to the kidney [4]. Further exploration of renal metabolism, and ADMA specifically, may therefore prove useful in understanding the link between the coxibs and HF.

On the other hand, metabolite changes in the heart presented a clearer picture, a picture consistent with findings in the other tissues and plasma. The integration of these results suggest that coxib treatment alters systemic carnitine and lipid metabolism.

## **Carnitine Metabolism**

The results of this study demonstrate that both cardiac and skeletal muscle carnitine concentrations are lower in mice treated with coxibs compared to controls. As

discussed in Chapter 2, HF is intimately associated with alterations in cardiac FA metabolism, which manifest as changes in cardiac carnitine concentrations. However, unlike the findings of this study, which demonstrate lower concentrations of most cardiac carnitine species, the literature primarily suggests lower cardiac concentrations and higher blood concentrations of long-chain acyl-carnitines are present in HF [13, 14, 16, 17, 127, 132]. Given that skeletal muscle carnitine concentrations are also affected in this study, a change not seen in HF, and neither tissues synthesise carnitine, it is conceivable that these changes reflect alterations in systemic carnitine handling, rather than cardiac FA metabolism [192, 193]. This suggests that the lower concentrations of cardiac carnitines, seen in this model, are not a consequence of HF development. This is supported by the results of functional analyses performed at the University of Pennsylvania, which demonstrate no evidence of HF in these mice. That being said, the higher concentration of cardiac hydroxyproline, in the coxib treated mice compared to controls, could be indicative of early structural remodelling preceding functional impairment [194].

It is possible that the lower concentrations of cardiac carnitines, observed in coxib treated mice, might predispose to HF, elevating its risk. In fact, in a mouse model of systemic carnitine deficiency, which also exhibits lower concentrations of cardiac carnitines, the mice possess normal cardiac function until they are challenged with additional CV risk factors [195]. This is in-line with the relationship, between coxibs and HF, described in the clinical literature [5, 6, 89]. Carnitine metabolism, therefore, represents a good candidate pathway for follow-up analysis.

## Lipid Metabolism

The results of this study also suggest that systemic lipid metabolism is altered in coxib treated mice, compared to controls. Cardiac, hepatic and plasma lipid compositions differ and renal choline and phosphocholine concentrations are altered. In the heart this is characterised by higher concentrations of saturated and monounsaturated total FAs and lower concentrations of polyunsaturated total FAs, whilst in the liver the saturated total FAs are higher in coxib treated mice compared to controls. In the plasma, NMR spectroscopy buckets (integral regions) indicative of lipid species are important in discriminating the coxib treated mice from controls. In addition, in the kidney, whilst there are no differences in total FA composition, renal concentrations of phosphocholine and choline, which are break-down products of structural and messenger lipids, are lower in coxib treated mice compared to controls.

In addition to their role as an energy substrate, lipids also serve structural and signalling functions [196]. Aberrant lipid metabolism is therefore well positioned to adversely affect cardiac function. Indeed, alterations in the composition of blood lipids and choline and phosphocholine concentrations have been reported in HF and dyslipidaemia is associated with HF [127-129, 147, 197].

The liver is central to lipid metabolism and is responsible for endogenous lipid synthesis [198, 199]. It is therefore plausible that the differences in cardiac and plasma lipid composition, and renal choline and phosphocholine concentrations, are caused by alternations in hepatic FA biosynthesis and lipogenesis. Hepatic lipid metabolism, therefore, represents another good candidate pathway for further exploration.

## *Chapter Conclusions and Future Directions*

The results of this study demonstrate that, in this mouse model of coxib treatment in inflammation, celecoxib and rofecoxib have profound effects on systemic metabolism. These effects are most pronounced in the heart and kidney, but also manifest as changes in skeletal muscle and hepatic metabolism.

Perhaps the clearest findings are those of altered carnitine metabolism, demonstrated by significant alterations in cardiac and skeletal muscle carnitine concentrations. Carnitine shuttles activated long-chain FAs across the inner mitochondrial membrane to the mitochondrial matrix, where they are oxidised by  $\beta$ -oxidation, and alterations in the concentrations of cardiac carnitines are a key feature of the metabolic remodelling seen in HF, as discussed in the background to this thesis [192, 200]. Therefore, it is pertinent to confirm these findings and test the following hypothesis:

**Celecoxib and rofecoxib treated mice exhibit lower concentrations of total cardiac carnitines than controls.**

Moreover, the results of this study present an initial view that celecoxib and rofecoxib behave similarly in terms of the metabolic alterations, measured in this study, which they induce. Therefore, these observations should also be confirmed and the following hypothesis tested:

**Celecoxib and rofecoxib alter murine carnitine metabolism to a similar extent.**

Moving forward, future work should also attempt to establish the mechanisms underlying these observations.

This study highlights the effects of coxib treatment on hepatic fatty acid and lipid metabolism. Fatty acid and lipid metabolism are intimately related to carnitine

metabolism and the three pathways exhibit considerable cross-talk and overlapping regulatory processes, for example regulation by peroxisome proliferator-activated receptor-alpha (PPAR- $\alpha$ ) [201]. Future work will therefore aim to explore hepatic metabolism and establish the role, if any, it plays in bringing about changes in the concentrations of cardiac carnitines.

In addition, this study highlights the effects of coxib treatment on renal metabolism. In light of recent evidence suggesting a role for ADMA in coxib induced adverse CV events, future work will also aim to explore ADMA and renal metabolism in the context of coxib-induced HF [4].

This study has a number of limitations, which will be addressed in future work. Firstly, IL-1 $\beta$  was used to induce an inflammatory response. Whilst it is true that this enables the simulation of the clinical scenario in which coxibs are used more accurately, it also introduces a confounding variable, as coxib, but not control treatment, suppresses the inflammatory response. Therefore, this experimental design models both the on-target consequences of coxib treatment and any off-target effects which may exist. It is therefore reasonable to assume that any off-target effects may, at least in part, be masked by the differences in inflammatory status between the groups. To address this concern, the reproducibility of the findings of this study will be explored in a non-inflammatory context. Secondly, this study does not address the time-course of the observations. Given that the risk of HF with coxibs may only present after several months, it is appropriate to confirm that these observations persist over time [1]. Therefore, future work will aim to establish whether the findings of this study also present in a longer-term study, more in-line with the time-course of HF risk reported with coxib treatment. Thirdly, this study fails to address the specific role of COX-2 inhibition, in causing the observations. This is because both celecoxib and rofecoxib

inhibit COX-1 to some extent, and both have been reported as having off-target effects [61, 202-209]. This will be addressed in future work, which will employ the genetic knock-out of COX-2, thereby avoiding the pharmacological promiscuity associated with celecoxib and rofecoxib.

Ultimately, despite the limitations described, this hypotheses generating study has achieved its aim: To generated hypotheses that can be tested, in mice, to provide insight into the mechanisms by which coxibs elevate the risk of HF. Further work will test these hypotheses, to provide additional insight into the mechanisms underlying the HF risk with which the coxibs are associated.

## ***Chapter 5: Coxibs and Carnitine Metabolism***

## *Chapter Introduction*

Carnitine is an amino acid derivative responsible for the shuttling of activated long chain FAs across the inner mitochondrial membrane to the mitochondrial matrix, where they are oxidised by  $\beta$ -oxidation [192]. Aberrant carnitine metabolism is a key feature of HF and the results of Chapter 4 suggest that murine carnitine metabolism may be altered by celecoxib and rofecoxib treatment [200]. Both celecoxib and rofecoxib increase the risk of HF, although celecoxib may carry less risk than rofecoxib [5]. Carnitine is therefore well positioned to act as a mechanistic bridge between coxibs and the HF risk associated with their use. Alternatively, alterations in carnitine metabolism could reflect early dysfunction, in coxib treated patients, and serve as a useful predictor of HF development. However, it is unclear whether the results observed in Chapter 4 are reproducible. This chapter attempts to address the question: Are the coxibs, celecoxib and rofecoxib, associated with lower concentrations of total cardiac carnitines in mice? This issue will be explored in a range of contexts, including: a non-inflammatory background, longer term treatment regimens and concomitant hypertension. These contexts will provide insight into the nature, time-course and predisposing factors of the carnitine results. The following hypothesis will be tested in these contexts:

**Celecoxib and rofecoxib treated mice exhibit lower concentrations of total cardiac carnitines than controls.**

In addition, a key aim of this study will be:

**To elucidate the mechanism by which celecoxib and rofecoxib exhibit lower concentrations of cardiac carnitines, in mice.**

This is important, as the insight it provides will help determine whether the lower concentrations of cardiac carnitines, seen with celecoxib and rofecoxib use, could serve as a mechanistic bridge between coxibs and HF or reflect early dysfunction.

Lastly, given that celecoxib may carry a lower risk of HF than rofecoxib, this study will attempt to address the question: Does celecoxib affect murine carnitine metabolism to a lesser extent than rofecoxib? This question will be considered both in terms of the concentrations of cardiac carnitines and features related to the underlying mechanism. The preliminary findings of Chapter 4 indicate that celecoxib and rofecoxib have a similar effect on cardiac carnitines. The following hypothesis will therefore be tested:

**Celecoxib and rofecoxib alter murine carnitine metabolism to a similar extent.**

These hypotheses were tested in wild type C57BL/B6 mice fed bespoke coxib-containing diets, designed to release 100 mg celecoxib/kg body weight per day or 50 mg rofecoxib/kg body weight per day, equivalent to low human doses of the drugs. IL-1 $\beta$  was not used in these experiments. Mice were treated for 3 weeks or 2 months with the coxibs. The IPNG COX-2<sup>-/-</sup> mouse, a model of genetic COX-2 deletion, was also used. Targeted metabolomic analyses and RT-qPCR were used to measure metabolite and transcriptional changes, to provide insight into the effect of celecoxib and rofecoxib treatment on murine carnitine metabolism.

## *Chapter Background*

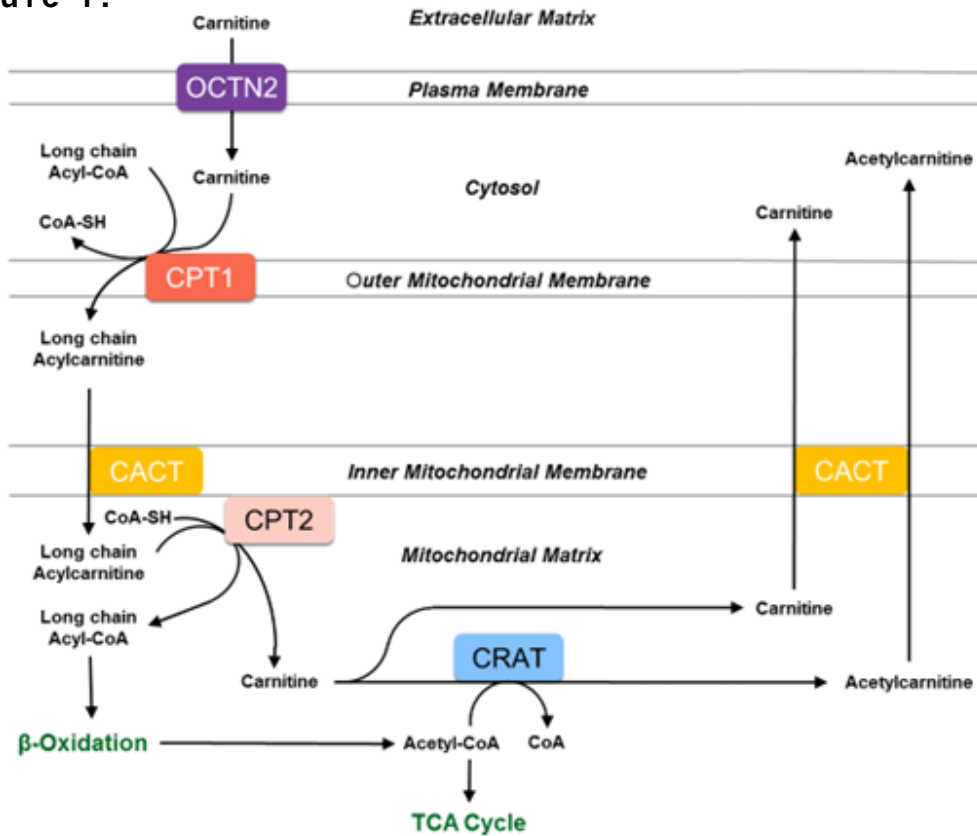
Carnitine is a branched-chain non-essential amino acid derivative and conditionally-essential nutrient that plays an essential role in the oxidation of long chain FAs [192, 210]. Carnitine also functions to buffer the free-coenzyme A (CoA):acyl-CoA ratio, by removing excess acyl-groups [210]. It therefore also indirectly participates in TCA cycle activity, branched chain amino acid metabolism and the detoxification of organic acids and xenobiotics [211]. In addition, carnitine may function as a free radical scavenger, act as a stabiliser of cell membranes and influence inflammation [212, 213]. Dysregulation of carnitine metabolism, therefore, has wide-ranging implications. Given the importance of FA oxidation to cardiac energy metabolism, aberrant carnitine metabolism is intimately linked to CV diseases, such as HF, though whether it is causal or merely consequential remains to be determined [211]. That being said, pharmacological manipulation of carnitine metabolism has yielded some success in the management of these conditions, suggesting that carnitine may be involved in their pathogenesises [214].

### **The Cardiac Carnitine Shuttle**

Carnitine shuttles long chain acyl-CoAs (activated long-chain FAs) across the inner mitochondrial membrane to the mitochondrial matrix, supplying substrate for  $\beta$ -oxidation which is the primary source of energy generation in the healthy heart [12, 138]. The components of the cardiac carnitine shuttle are summarised (*Figure 1*). NB: For the purposes of this thesis, the term “carnitine shuttle” will apply to those enzymes/transporters classically referred to as the carnitine shuttle (Carnitine palmitoyltransferase 1 (CPT1); Carnitine palmitoyltransferase 2 (CPT2); Carnitine-acylcarnitine translocase (CACT) and Carnitine O-acetyltransferase

(CRAT)) as well as the transporter responsible for cellular carnitine uptake, organic cation transporter 2 (OCTN2).

**Figure 1.**



*The carnitine shuttle. Carnitine is actively transported, across the plasma membrane, into the cell via OCTN2. It is then acylated by CPT1. CACT shuttles the acylcarnitine, across the inner mitochondrial membrane, into the mitochondrial matrix. CPT2 transfers the carnitine bound acyl-group to CoA-SH, regenerating carnitine. CRAT acetylates carnitine. CACT shuttles L- and acetyl- carnitine, across the inner mitochondrial membrane, into the cytosol. Abbreviations: Organic cation transporter 2 (OCTN2); Carnitine palmitoyltransferase 1 (CPT1); Carnitine palmitoyltransferase 2 (CPT2); Carnitine-acylcarnitine translocase (CACT); Carnitine O-acetyltransferase (CRAT); Tricarboxylic acid (TCA); Coenzyme A (CoA). Adapted from Flanagan et al. [192].*

OCTN2 is a high affinity, sodium-dependent, cell-membrane carnitine transporter as well as a sodium-independent organic cation transporter [215]. OCTN2 mediated carnitine transport is saturable [192]. In the heart OCTN2 is primarily expressed in the vessels and also the cardiomyocytes [216]. It is responsible for the cardiac extraction of carnitines, from the circulation, against a significant concentration gradient [192]. In humans, several OCTN2 polymorphisms exhibit less activity and these are associated

with HF. In addition, in various mouse models of cardiomyopathy, OCTN2 expression is less and in certain cases this correlates with cardiac dysfunction [217].

CPT1 isoform B (CPT1B) is an outer mitochondrial membrane-associated acyltransferase [218]. Whilst it does possess transmembrane domains, the active site is located on the cytosolic side [219]. CPT1B contributes the majority of total CPT1 activity in cardiomyocytes and catalyses the rate limiting step of FA  $\beta$ -oxidation: The conversion of long-chain acyl-CoAs to their respective long-chain acylcarnitines, through the transfer of acyl-groups from CoA to intracellular carnitine. Long-chain acylcarnitines cross the outer mitochondrial membrane via porin [220]. Malonyl-CoA, an intermediate of FA biosynthesis, is an inhibitor of CPT1 activity and therefore a key regulator of FA oxidation [138]. Animal studies have demonstrated that CPT1B deficiency aggravates models of cardiac hypertrophy, a precursor to HF [221].

CACT is an inner mitochondrial membrane translocase which facilitates the diffusion of acylcarnitine into the mitochondrial matrix, in 1:1 stoichiometric exchange for carnitine [222, 223]. It is also able to facilitate the export of acetylcarnitine from the mitochondria [192]. Human CACT deficiency is associated with a range of complications, including cardiomyopathies [224].

CPT2 is an acyltransferase associated with the luminal surface of the inner mitochondrial membrane [225]. It catalyses the regeneration of long-chain acyl-CoAs and carnitine, from CoA and mitochondrial matrix-imported long-chain acyl-carnitines, via acyl-group transfer [223]. These long-chain acyl-CoAs are then degraded, by  $\beta$ -oxidation, to yield acetyl-CoA units [226]. CPT2 deficiencies range from lethal-neonatal to mild-myopathic, and all but the mildest form are associated with cardiac dysfunction [227].

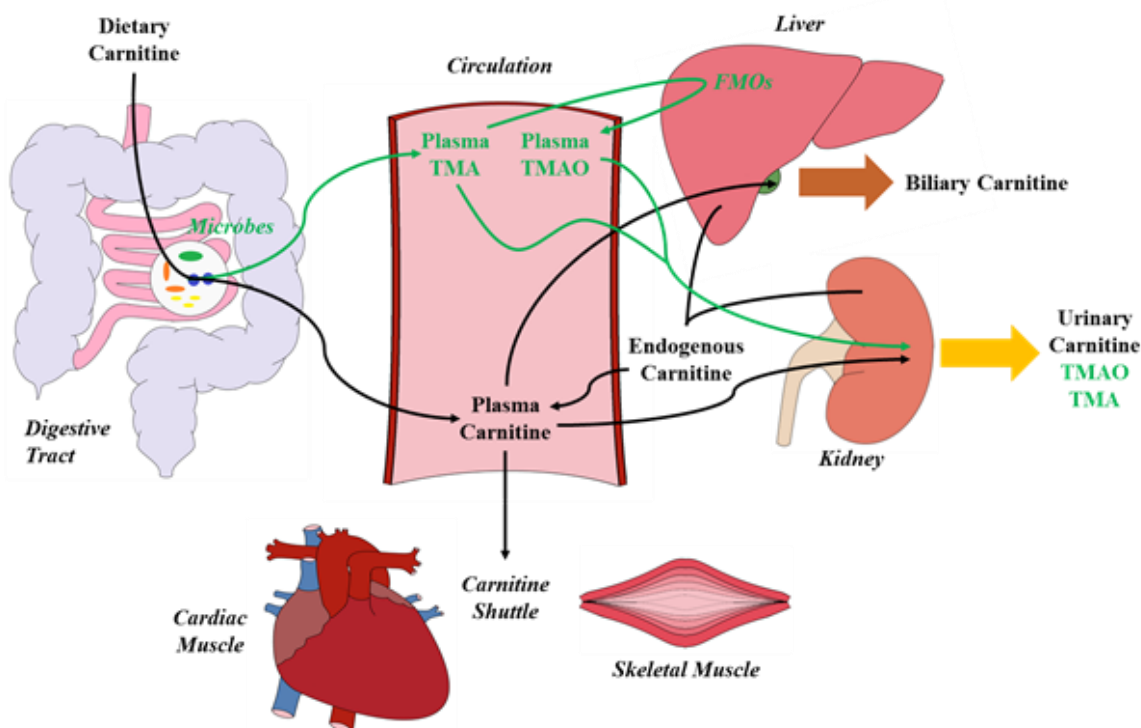
Mitochondrial CRAT is an acyltransferase localised to the mitochondrial matrix [228]. It catalyses the reversible conversion of carnitine and acetyl-CoA to acetylcarnitine and CoA [229]. The reversibility of this reaction enables carnitine to buffer acetyl-CoA [223]. Like malonyl-CoA, acetyl-CoA may also play a role in the regulation of FA oxidation. It serves as an acetyl-donor, enabling the post-translational acetylation and regulation of mitochondrial enzymes involved in  $\beta$ -oxidation [230].

The concerted action of these components ensures the delivery of FAs to their site of  $\beta$ -oxidation, enabling the heart to efficiently extract energy from their metabolism.

## **Systemic Carnitine Handling**

Cardiac muscle is unable to synthesise carnitine, as it does not express a critical enzyme in the synthetic pathway. It must therefore obtain carnitine from the circulation. The same is true of skeletal muscle [192]. Cardiac and skeletal muscle carnitine content therefore depends on carnitine shuttle activity, including tissue carnitine import and export, and systemic carnitine concentrations. Systemic carnitine concentrations are determined by the balance between systemic inputs and outputs. Microbiome-mediated carnitine metabolism, which affects carnitine bioavailability, adds an additional layer of complexity to systemic carnitine handling. These pathways are summarised (*Figure 2*).

**Figure 2.**



*Systemic carnitine handling. Systemic carnitine inputs include dietary absorption and endogenous synthesis by the liver and kidney. Systemic carnitine outputs include renal and biliary carnitine excretion. Cardiac and skeletal muscle uptake carnitine from the circulation. Intestinal microbes convert carnitine to TMA, which is oxidised by hepatic FMOs to form TMAO, reducing carnitine bioavailability. TMA and TMAO are excreted by the kidney. Abbreviations: Trimethylamine (TMA); Trimethylamine-N-oxide (TMAO); Flavin monooxygenases (FMOs).*

## ***Systemic Carnitine Inputs and Bioavailability***

In mammals carnitine is largely obtained from the diet (meats - especially red meat, poultry, fish and milk are the richest sources) [193]. For example, humans acquire 75% from the diet. Carnitine bioavailability is affected by dietary composition and is higher in individuals adapted to low carnitine diets [192]. This may be due to enhanced intestinal OCTN2 activity, which facilitates dietary carnitine uptake [231]. The microbiome also affects dietary carnitine bioavailability [232].

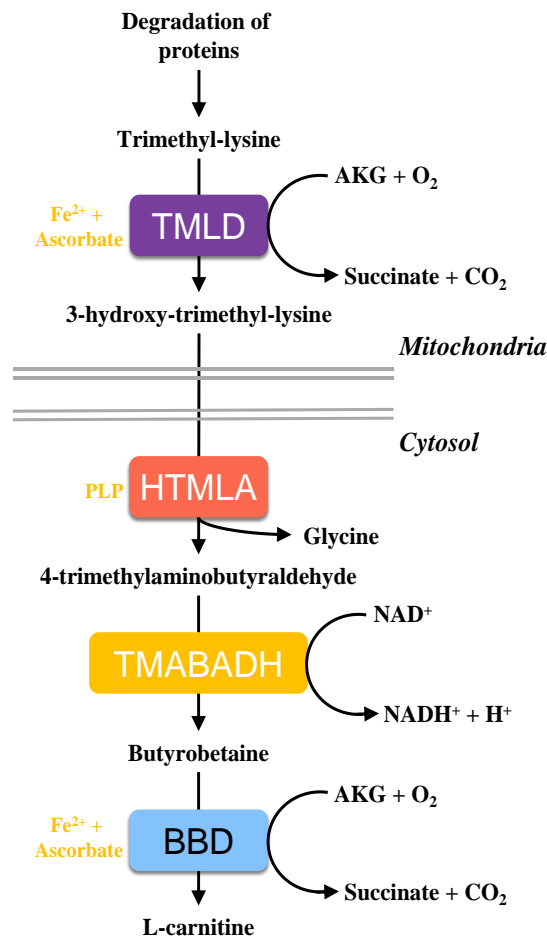
Microbes residing within the mammalian digestive tract are capable of metabolising carnitine, to yield trimethylamine (TMA). They are also able to synthesise TMA from dietary cholines and phosphatidylcholines, which are found in meat, poultry, fish, milk,

eggs, whole grains and legumes [233]. These microbes metabolise carnitine prior to its absorption, as well as unabsorbed carnitine, which reduces its bioavailability [232]. Once absorbed, TMA can be converted to trimethylamine-N-oxide (TMAO) by liver flavin monooxygenases (FMOs), especially FMO1 and FMO3 [234]. Both TMA and TMAO production is contingent on microbial activity and depends on dietary composition [232]. However, the microbes and intermediates involved in this process are not well characterised. Zhu et al. reported that a novel two-component Rieske-type oxygenase/reductase, possessed by certain microbes found in the human digestive tract, is necessary and sufficient to synthesise TMA from carnitine, *in vitro* [235]. That being said, recent evidence suggests that carnitine may first be metabolised to butyrobetaine, then to TMA. Given that butyrobetaine and TMA synthesis occur at anatomically distinct sites, the implication is that TMA synthesis may occur by the concerted action of several microbial species [236]. In actuality, it is likely that several different microbial-pathways contribute to TMA synthesis. Circulating TMA and TMAO are primarily excreted in the urine and, in fact, active tubular secretion of TMAO may occur [237]. Interestingly, TMAO has been implicated in CV disease and elevations in its plasma concentration are associated with poorer prognoses in chronic kidney disease [234, 237].

Carnitine not obtained from the diet is endogenously synthesised (*Figure 3*) [193]. In mammals, synthesis begins with trimethyl-lysine (TML). TML is generated by post-translational methylation of protein-bound lysine, using S-adenosylmethionine as the methyl- donor. Protein degradation releases free TML [238]. Free TML can then be hydroxylated, by TML deoxygenase (TMLD), to form 3-hydroxy-TML. This is converted to 4-trimethylaminobutyraldehyde, by 3-hydroxy-TML aldolase (HTMLA), then dehydrogenated, by 4-trimethylaminobutanal dehydrogenase (TMABADH), to

form 4-trimethylammoniobutanoate (butyrobetaine). Finally, butyrobetaine is hydroxylated, by butyrobetaine dioxygenase (BBD), to yield carnitine [193, 239].

**Figure 3.**



The mammalian pathway of carnitine synthesis. Carnitine is synthesised, from free trimethyl-lysine, by the sequential actions of TMLD, HTMLA, TMABADH and BBD. Abbreviations: Trimethyl-lysine deoxygenase (TMLD); 3-Hydroxy-trimethyl-lysine aldolase (HTMLA); 4-Trimethylaminobutanal dehydrogenase (TMABADH); Butyrobetaine dioxygenase (BBD); 4-Trimethylammoniobutanoate (butyrobetaine); Alpha-ketoglutarate (AKG); Oxidised nicotinamide adenine dinucleotide ( $NAD^+$ ); Reduced nicotinamide adenine dinucleotide ( $NADH^+$ ); Pyridoxal phosphate (PLP). Adapted from Vaz et al. [193].

In humans, carnitine is predominantly synthesised in the liver and kidneys, organs which possess all the enzymatic components of the synthetic pathway. Most other tissues, including cardiac and skeletal muscle, lack BBD activity and are unable to complete carnitine synthesis [192, 193]. Mice and certain other species lack significant renal BBD activity and in these animals the liver is probably the primary source of endogenous carnitine [193].

The rate of mammalian carnitine synthesis has largely been attributed to TML availability [193]. However, more recently, a PPAR- $\alpha$  dependent regulatory mechanism has also been established. Besides substrate availability, BBD activity is the rate-limiting step of carnitine synthesis [240]. The genes encoding BBD and TMABADH have been shown to contain functional peroxisome proliferator response elements (PPREs) within their regulatory regions and are direct targets of PPAR- $\alpha$  [241]. Expression of these genes is upregulated in response to fasting, in wild-type but not PPAR- $\alpha$  KO mice, and correlates with hepatic carnitine content [241-243]. Taken together, these findings demonstrate that PPAR- $\alpha$  has the capacity to regulate hepatic carnitine synthesis in mice. Whilst this regulatory mechanism has not yet been characterised in humans, there is undoubtedly precedent for its existence.

### *Systemic Carnitine Outputs*

Carnitine is not catabolised by mammals [244]. Instead it is mainly excreted in the urine as carnitine, acetylcarnitine and longer chain acyl-carnitines [240]. Acyl-carnitines are more readily excreted than carnitine [244]. However, the renal reabsorption of carnitines, mediated by tubular OCTN2, is efficient [239]. Under normal circumstances less than 10% of filtered carnitines are excreted. In fact, some estimates suggest that less than 2% are excreted [240]. This range may reflect the adaptive ability of the kidney, to modulate the urinary excretion of carnitines according to dietary carnitine intake [245].

Carnitines, especially acyl-carnitines, are also excreted in the bile [244, 246]. However, the contribution of this pathway, to total carnitine excretion, is variable in humans and its biological purpose is yet to be established [244].

## **Carnitines and Heart Failure**

As discussed in Chapter 2, HF, with which coxibs are associated, is intimately linked to impaired FA metabolism. This is reflected by perturbations in cardiac carnitine handling, which have been observed in human studies of HF [13, 14, 127, 128]. Animal models of HF support these observations [16, 17, 132, 133]. On balance, these findings demonstrate higher plasma concentrations and lower cardiac concentrations of long-chain acyl-carnitines, in HF.

## *Chapter Methods*

In Study 2, 21 mice were fed rofecoxib-containing, celecoxib-containing or control diets (n=7) for 3 weeks, then sacrificed. In Study 3, 30 mice were fed rofecoxib-containing, celecoxib-containing or control diets (n=10) for 8 weeks, to simulate longer-term coxib taking, then sacrificed. In Study 5, 19 mice were used (10 global COX-2<sup>-/-</sup> mice and 9 littermate controls) to simulate genetic COX-2 deletion (thereby avoiding any off-target effects of the coxibs), then sacrificed. Various bio-fluids and tissues derived from these animals were analysed using a combination of NMR spectroscopy, GC-MS, LC-MS/MS and RT-qPCR, to explore the effects of coxibs on carnitine synthesis and systemic carnitine metabolism.

The following methods (see chapter 3 for a detailed description of each) were used in this chapter:

- **Studies 2, 3 and 5**
- **Methanol/Chloroform/Water Metabolite Double Extraction**
- **Nuclear Magnetic Resonance (NMR) Spectroscopy**
- **Fatty Acid Methyl Ester (FAME) Derivatisation of the Organic Fraction, for Gas Chromatography Mass Spectrometry (GC-MS) Analysis**
- **GC-MS Analysis of Total FAMES**
- **Butylating Method of Sample Preparation for Liquid Chromatography – Mass Spectrometry/Mass Spectrometry (LC-MS/MS) Carnitine Assay**
- **Non-Butylating Method of Sample Preparation for LC-MS/MS Carnitine Assay**
- **LC-MS/MS Carnitine Assay**
- **Processing of Metabolomic Data**
- **RNA Isolation from Tissue**

- **Reverse Transcription**
- **Quantitative Real Time PCR**
- **Processing of RT-qPCR Data**
- **Ordinary One-Way ANOVA**
- **Dunnett's Multiple Comparisons Test**
- **PCA and PLS-DA**
- **Multivariate Model Validation**

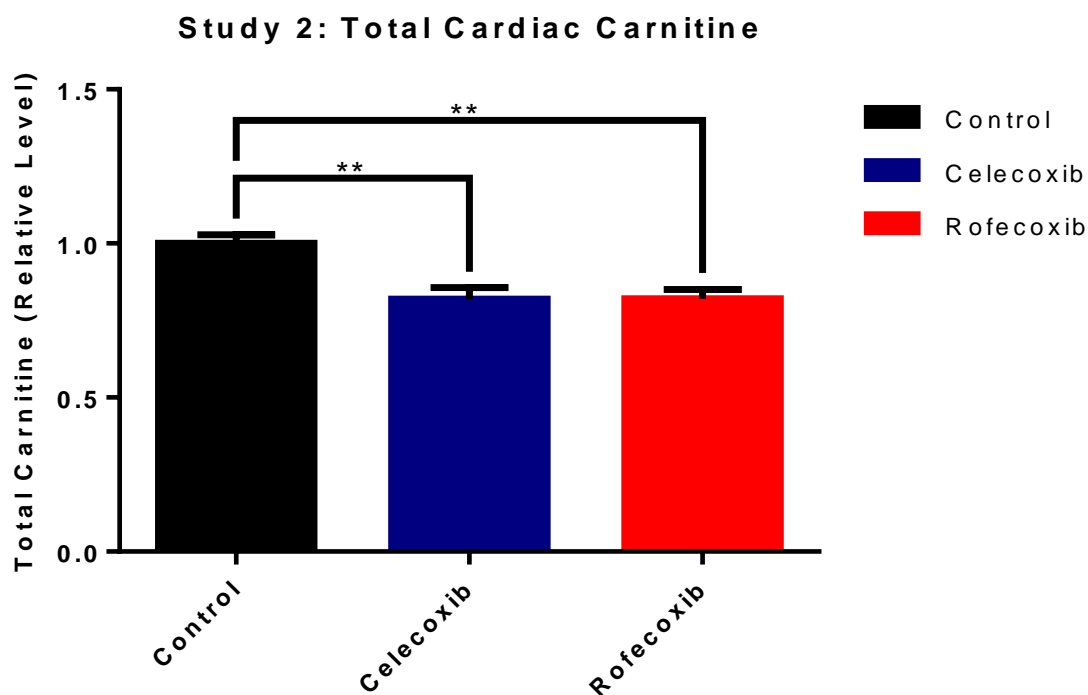
## Chapter Results

To follow up on the findings of Chapter 4, LC-MS/MS, GC-MS, NMR spectroscopy and RT-qPCR were used to investigate the effects of rofecoxib and celecoxib treatment and COX-2 KO on carnitine metabolism in mice not treated with IL-1 $\beta$ .

### Cardiac Carnitines

LC-MS/MS was used to profile cardiac carnitines in celecoxib and rofecoxib treated mice, not treated with IL-1 $\beta$  (Figure 4). Both celecoxib and rofecoxib treated mice exhibit significantly lower concentrations of total cardiac carnitines of ~18% compared to controls (ANOVA = 0.0010; Dunnett's post-hoc test:  $P = 0.0017$  and  $P = 0.0019$  respectively).

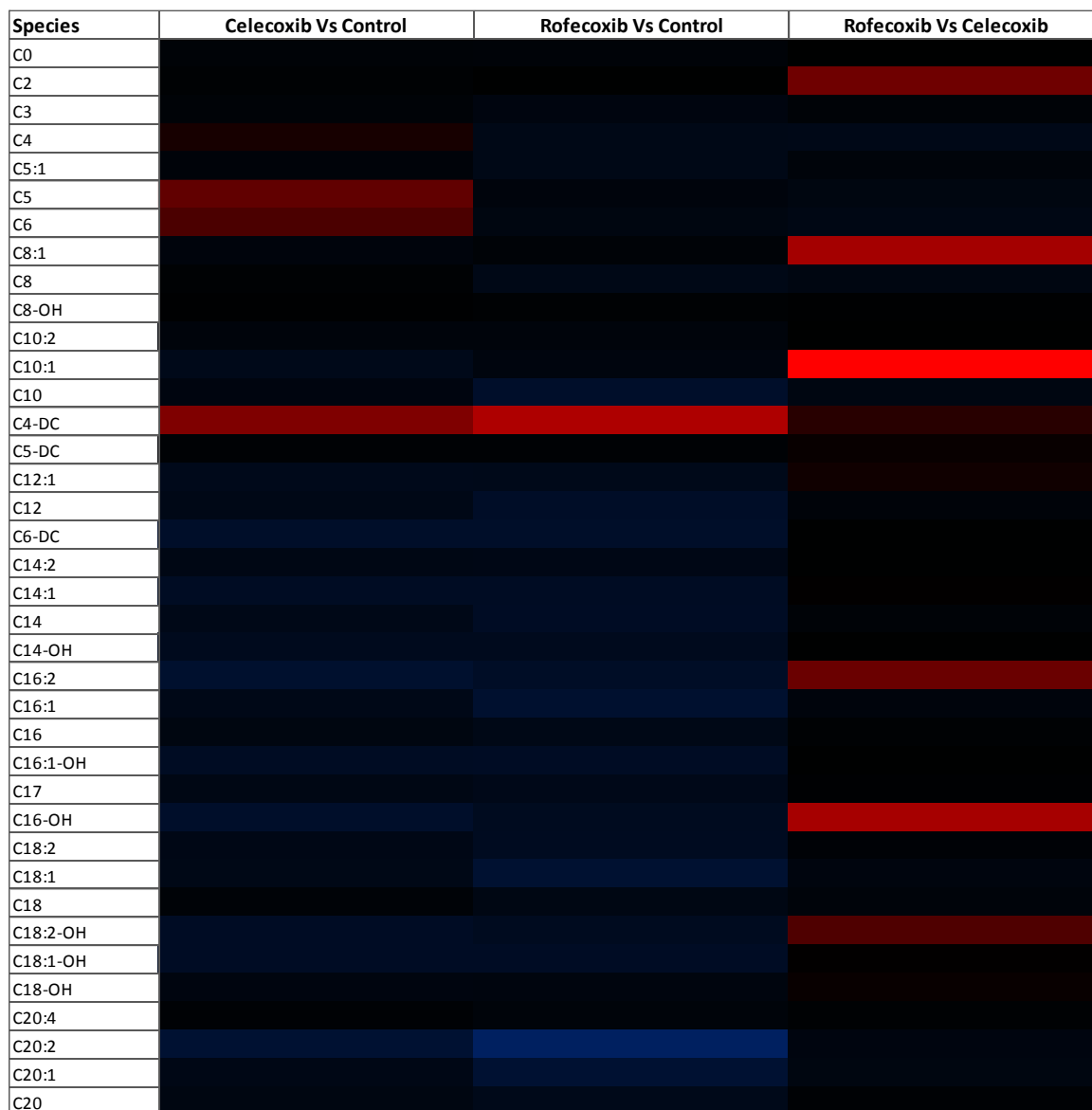
Figure 4.



Effect of 3 weeks of celecoxib and rofecoxib treatment on total cardiac carnitines in mice. Measured by LC-MS/MS. Data are mean  $\pm$  S.E.M for  $n = 7$ . (\*\* =  $P < 0.01$ ).

Differences in individual carnitine species, in the celecoxib and rofecoxib treated mice compared to controls, reflected the lower total carnitine concentrations (*Figure 5*). Of the 38 carnitine species measured, 34 were lower in celecoxib treated mice and 37 lower in rofecoxib treated mice, compared to controls. The few species which were higher in the drug treated mice, compared to controls, were not significantly so. No significant differences in cardiac carnitines were observed between the drug treated groups.

**Figure 5.**

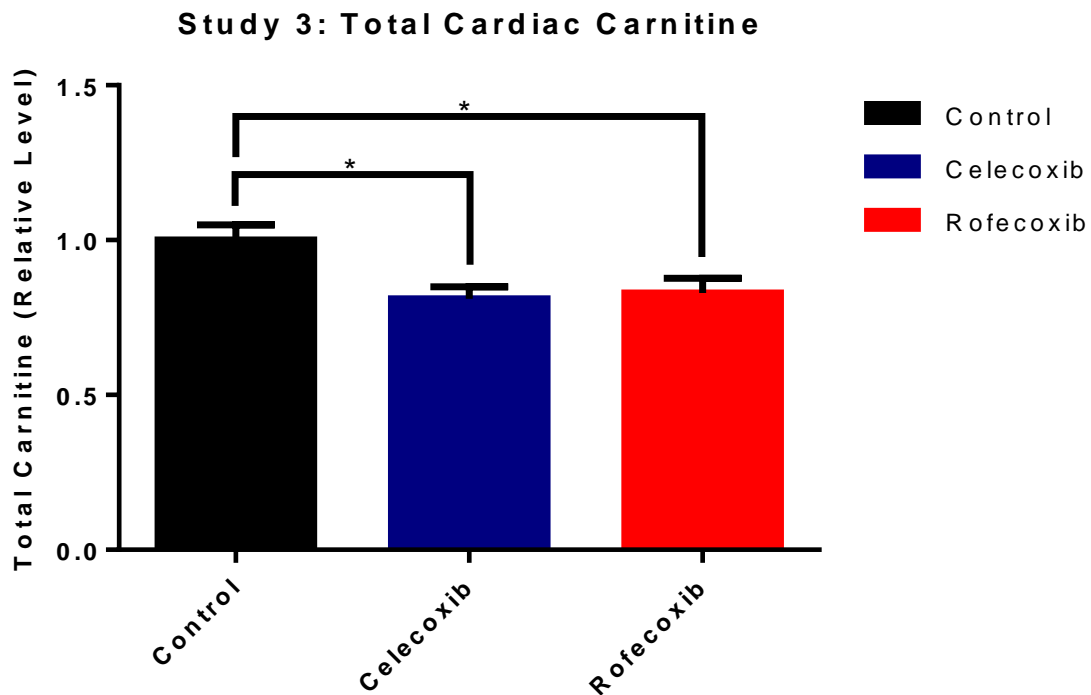


Heat-map demonstrating the effect of 3 weeks of celecoxib and rofecoxib treatment on concentrations of individual carnitine species in the heart, in mice. Measured by LC-MS/MS. Data are mean  $\pm$  S.E.M for  $n = 7$ . Blue = negative-fold change, black = no-fold change, red = positive-fold change, in relation to the first treatment group compared to the second treatment group named in each column heading.

The effect of longer-term celecoxib and rofecoxib treatment, on total cardiac carnitines, in mice not treated with IL-1 $\beta$ , was then examined (*Figure 6 A*). Lower concentrations of total cardiac carnitines were noted in the celecoxib and rofecoxib treated mice compared to controls, (ANOVA = 0.0118; Dunnett's post-hoc test:  $P = 0.0125$  and  $P =$

0.0245 respectively), with the difference being almost identical in magnitude to that observed with shorter-term coxib treatment.

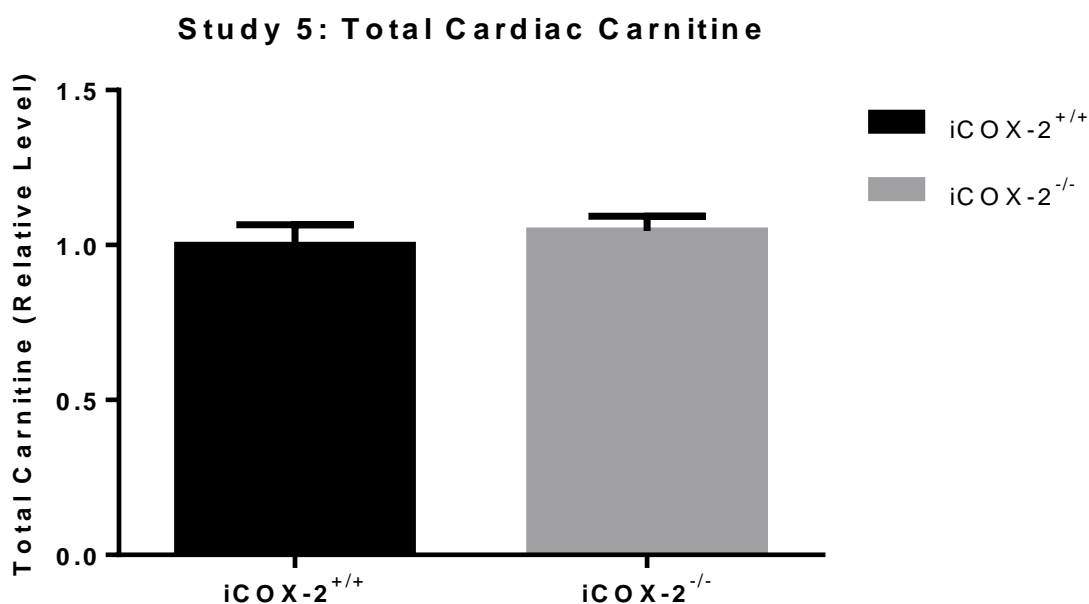
**Figure 6.**



*Effect of 2 months of celecoxib and rofecoxib treatment on total cardiac carnitines in mice. Measured by LC-MS/MS. Data are mean  $\pm$  S.E.M for  $n = 10$ . (\* =  $P < 0.05$ ).*

To establish whether the lower concentrations of total cardiac carnitines depend on the inhibition of COX-2 activity, the concentrations of cardiac carnitines were measured, using LC-MS/MS, in a model of COX-2 genetic deletion, the IPNG COX-2<sup>-/-</sup> mouse. This model is reviewed in detail in Chapter 7. The concentrations of cardiac carnitines were unchanged in the IPNG COX-2<sup>-/-</sup> mouse compared to COX-2<sup>+/+</sup> littermate controls (*Figure 7*), indicating that COX-2 KO (hence less COX-2 activity) is not associated with lower concentrations of cardiac carnitines and is therefore unlikely to underlie the effect observed with celecoxib and rofecoxib.

**Figure 7.**

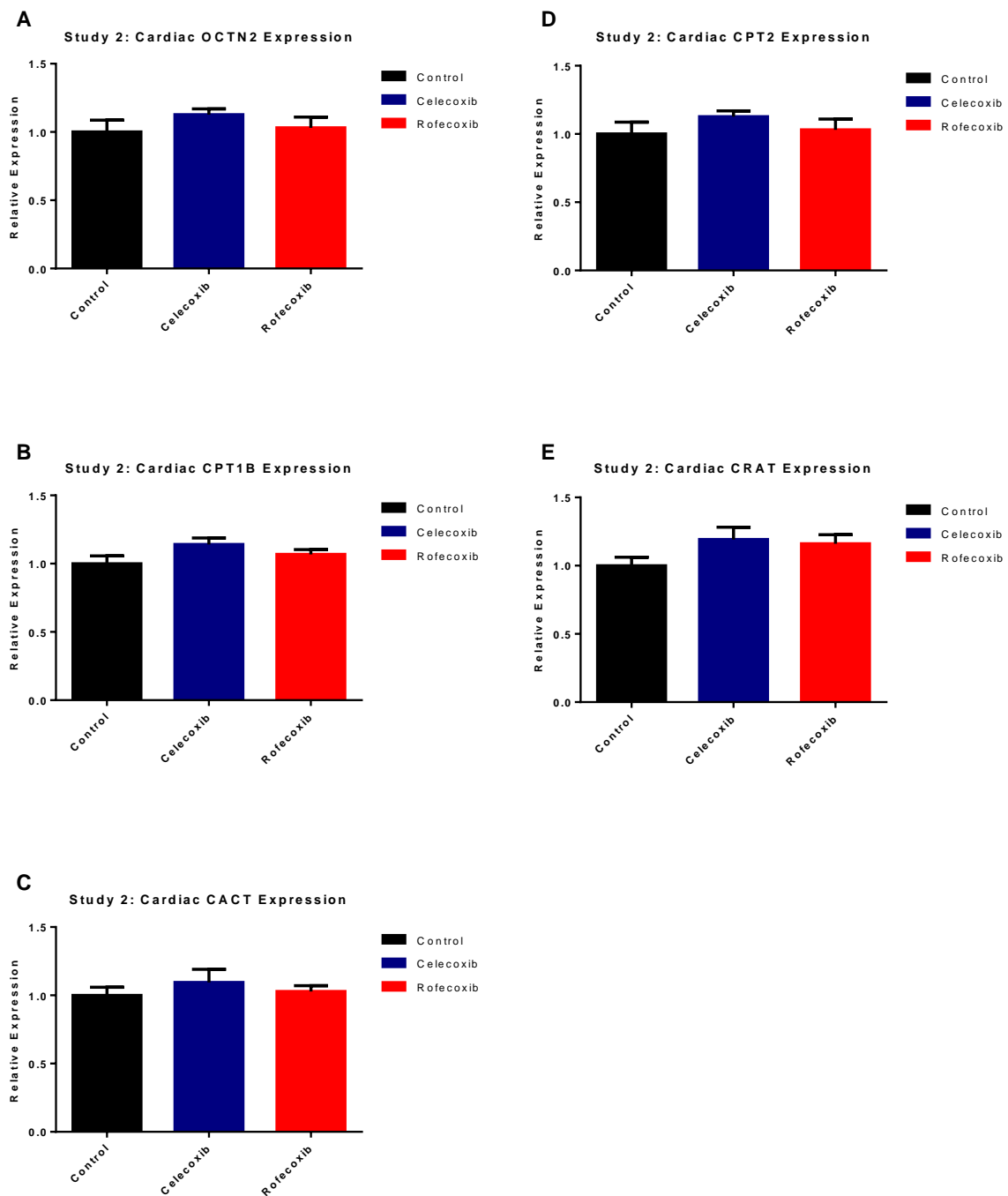


*Effect of post-natal COX-2 gene deletion on total cardiac carnitines, in mice. Measured by LC-MS/MS. Data are mean  $\pm$  S.E.M for n = 9 and 10. No significant changes were observed. Abbreviations: Inducible post-natal global cyclooxygenase-2 knock-out mouse (iCOX-2<sup>-/-</sup>); Inducible post-natal global cyclooxygenase-2 littermate control mouse (iCOX-2<sup>+/+</sup>).*

## The Cardiac Carnitine Shuttle

Given the lower concentrations of total cardiac carnitines observed in coxib treated mice compared to controls, in the absence of changes in the concentrations of plasma carnitines (data not shown), the cardiac carnitine uptake mechanism and shuttle were investigated in an attempt to rationalise these observations. To determine whether celecoxib and rofecoxib affected the expression of cardiac carnitine uptake and shuttle machinery, levels of mRNA transcripts, coding for OCTN2 (Figure 8 A), CPT1B (Figure 8 B), CACT (Figure 8 C), CPT2 (Figure 8 D) and CRAT (Figure 8 E) were measured using RT-qPCR. No significant differences, between coxib treated and control mice, were observed.

**Figure 8.**



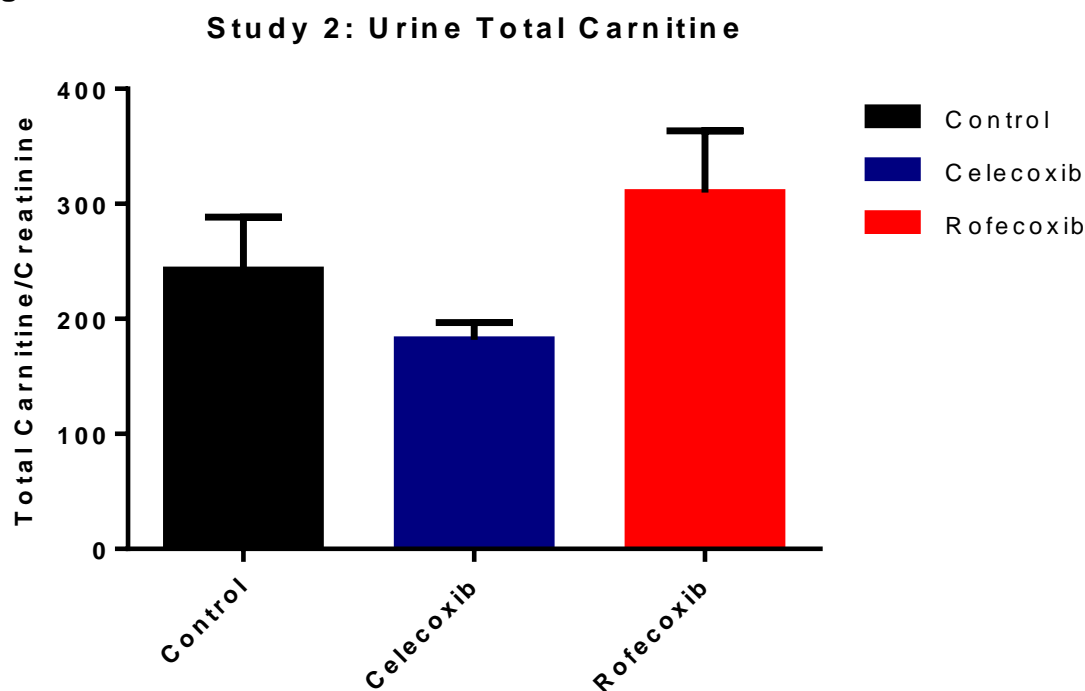
Effect of 3 weeks of celecoxib and rofecoxib treatment on expression levels of carnitine uptake and shuttle machinery, in mice. Effect of celecoxib and rofecoxib treatment on (A) OCTN2; (B) CPT1B; (C) CACT; (D) CPT2 and (E) CRAT expression levels. Measured by RT-qPCR. Data are mean  $\pm$  S.E.M for  $n = 7$ . No significant changes were observed. Abbreviations: Organic cation transporter 2 (OCTN2); Carnitine palmitoyltransferase 1 B (CPT1B); Carnitine palmitoyltransferase 2 (CPT2); Carnitine-acylcarnitine translocase (CACT); Carnitine O-acetyltransferase (CRAT).

To investigate whether celecoxib and rofecoxib directly inhibit carnitine shuttle activity, a pilot *in vitro* carnitine shuttle activity assay was developed. Celecoxib and rofecoxib did not affect carnitine shuttle activity in this assay (Please refer to Chapter 6 for details and results).

## **Renal Excretion of Carnitines**

The renal excretion of carnitines was examined as a possible cause of the lower concentrations of cardiac carnitines observed with coxib treatment. Total urinary carnitines were measured using LC-MS/MS. The data were normalised to urinary creatinine, measured by NMR spectroscopy, to account for differences in urine concentration. No significant differences in urinary total carnitines were observed between the coxib treated mice and controls (*Figure 9*). Urinary creatinine did not vary significantly between the groups (data not shown).

**Figure 9.**

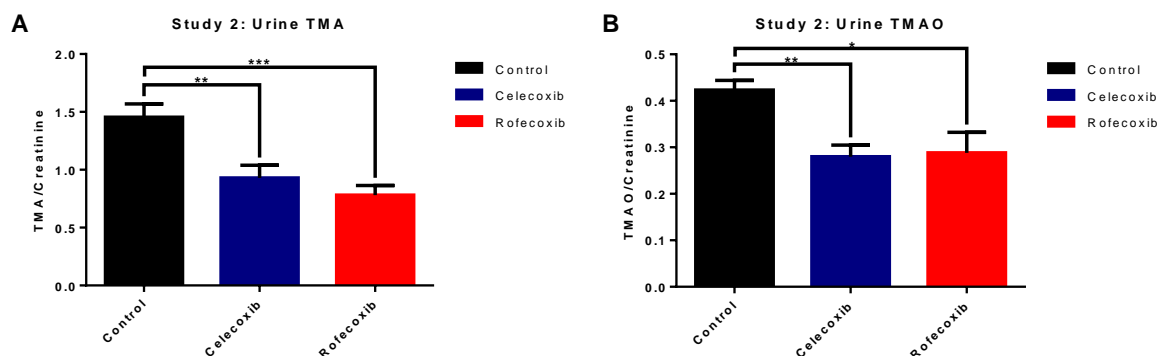


*Effect of 3 weeks of celecoxib and rofecoxib treatment on renal excretion of carnitines, in mice. Urine carnitines normalised to creatinine, measured by LC-MS/MS and NMR spectroscopy, respectively. Data are mean ± S.E.M for n = 8-10. No significant changes were observed.*

## **Microbiome-Mediated Carnitine Bioavailability**

Ingested carnitine can be converted to TMA, by microbes resident in the digestive tract, and thereafter to TMAO by hepatic FMOs. TMA and TMAO are primarily excreted by the kidney. To investigate whether the coxibs alter microbiome-mediated carnitine bioavailability, urinary TMA and TMAO were measured by LC-MS/MS. The data were normalised to urinary creatinine, measured by NMR spectroscopy, to account for differences in urine concentration. Urinary TMA (*Figure 10 A*) was significantly lower in both celecoxib and rofecoxib treated mice compared to controls (ANOVA = 0.0008; Dunnett's post-hoc test:  $P = 0.0042$  and  $P = 0.0007$  respectively) as was urinary TMAO (*Figure 10 B*) (ANOVA = 0.0052; Dunnett's post-hoc test:  $P = 0.0059$  and  $P = 0.0120$  respectively). Urinary creatinine did not vary significantly between the groups (data not shown).

**Figure 10.**

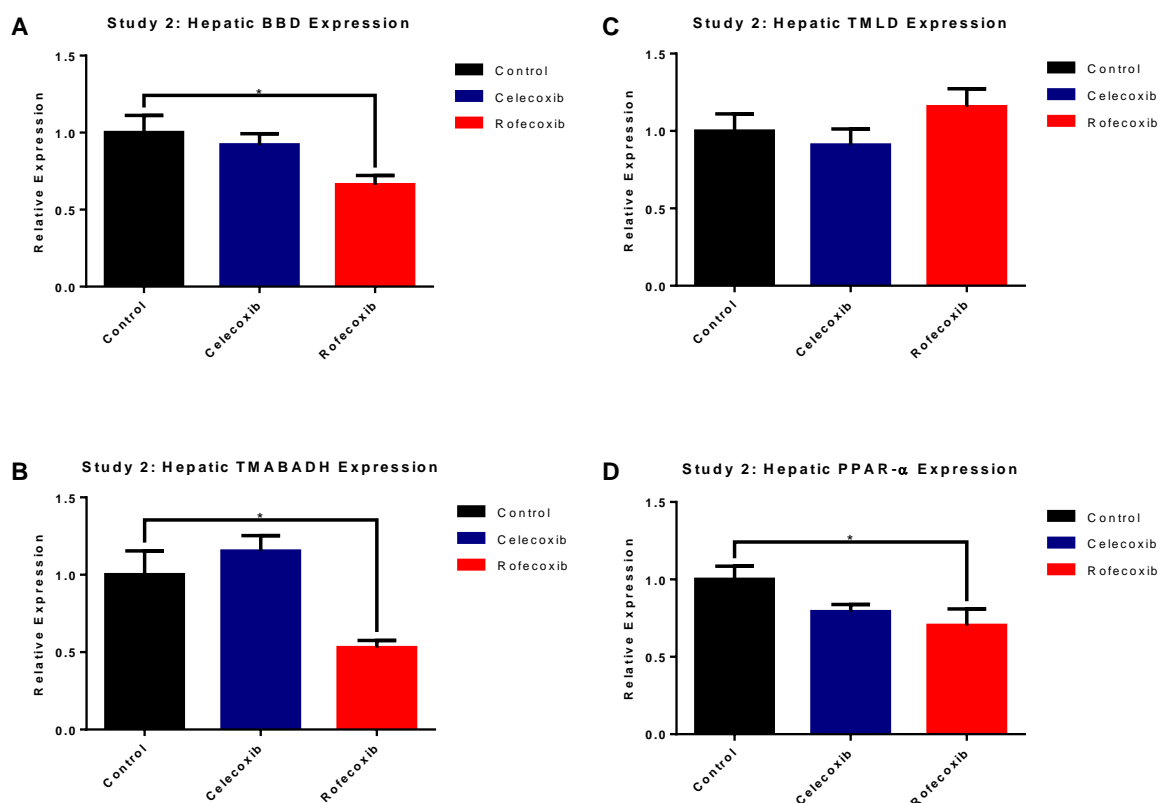


Effect of 3 weeks of celecoxib and rofecoxib treatment on microbiome-mediated carnitine bioavailability, in mice. Effect of celecoxib and rofecoxib treatment on urinary (A) TMA and (B) TMAO, measured by LC-MS/MS. Normalised to urinary creatinine, measured by NMR spectroscopy. Data are mean  $\pm$  S.E.M for  $n = 6-7$ . (\* =  $P < 0.05$ , \*\* =  $P < 0.01$ , \*\*\* =  $P < 0.001$ ). Abbreviations: Trimethylamine (TMA); Trimethylamine-N-oxide (TMAO).

## Hepatic Carnitine Synthesis

To establish whether the coxibs affect carnitine synthesis, levels of hepatic mRNA transcripts, encoding enzymes of carnitine synthesis, were measured using RT-qPCR. Expression of BBD (Figure 11 A), the rate limiting enzyme, was non-significantly lower in celecoxib treated mice and significantly lower in rofecoxib treated mice, compared to controls (ANOVA = 0.0289; Dunnett's post-hoc test:  $P = 0.7358$  and  $P = 0.0211$  respectively). Expression of TMABADH (Figure 11 B) was not lower in celecoxib treated mice, but was significantly lower in rofecoxib treated mice, compared to controls (ANOVA = 0.0026; Dunnett's post-hoc test:  $P = 0.5397$  and  $P = 0.0128$  respectively). TMLD expression (Figure 11 C) was unaffected. HTMLA has not yet been identified [247]. PPAR- $\alpha$ , which can regulate carnitine synthesis, was also examined. PPAR- $\alpha$  expression (Figure 11 D) was non-significantly lower in celecoxib treated mice and significantly lower in rofecoxib treated mice, compared to controls (ANOVA = 0.0581; Dunnett's post-hoc test:  $P = 0.2003$  and  $P = 0.0424$  respectively).

**Figure 11.**



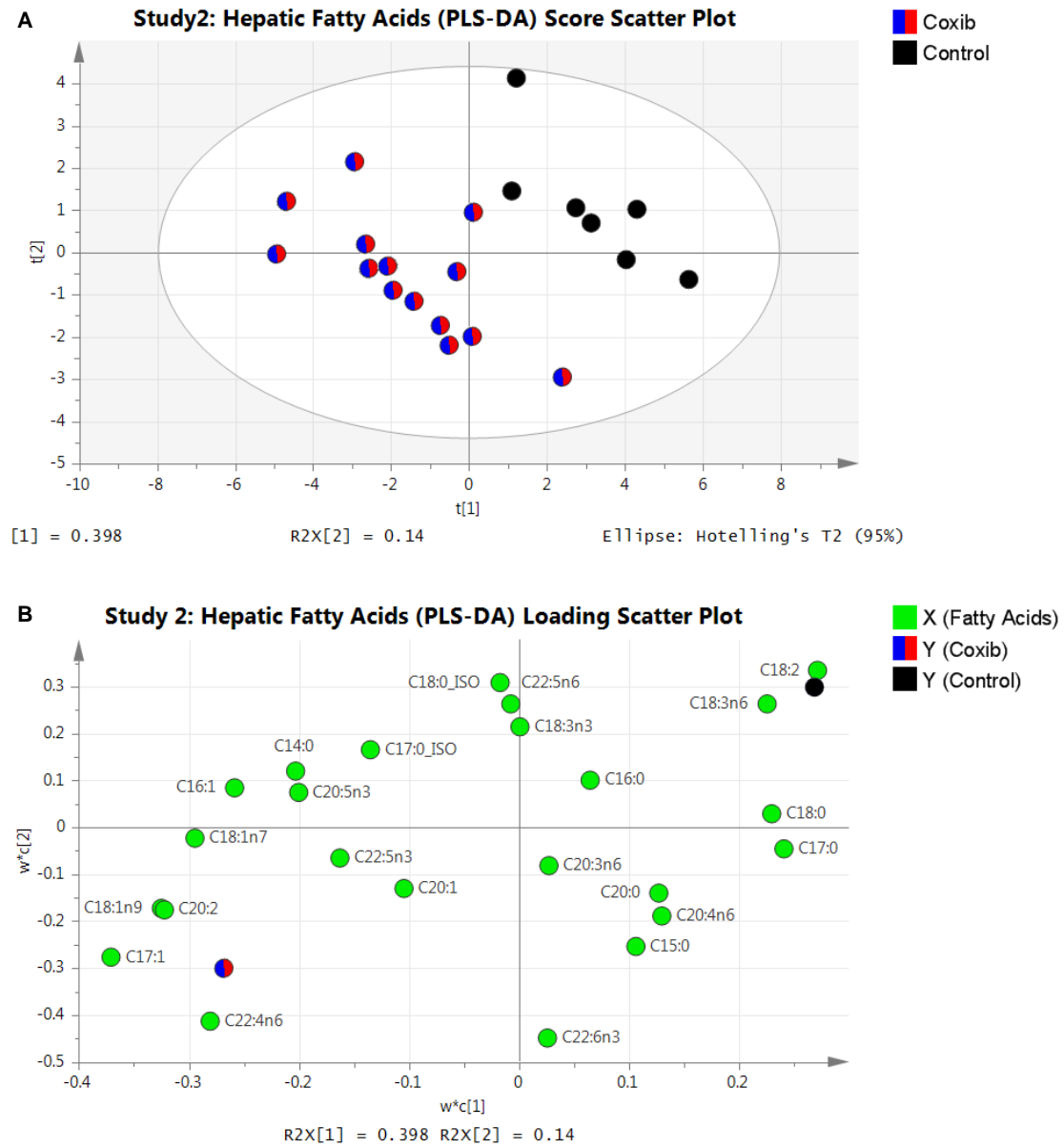
Effect of 3 weeks of celecoxib and rofecoxib treatment on expression levels of enzymes responsible for hepatic carnitine synthesis and their regulator, in mice. Effect of celecoxib and rofecoxib treatment on (A) BBD; (B) TMABADH; (C) TMLD and (D) PPAR- $\alpha$  expression levels. Measured by RT-qPCR. Data are mean  $\pm$  S.E.M for  $n = 6-10$ . (\* =  $P < 0.05$ ). Abbreviations: Butyrobetaine dioxygenase (BBD); 4-Trimethylaminobutanal dehydrogenase (TMABADH); Trimethyl-lysine deoxygenase (TMLD); Peroxisome proliferator-activated receptor- $\alpha$  (PPAR- $\alpha$ ).

## Hepatic Total-Fatty Acids

To investigate whether the differences in hepatic PPAR- $\alpha$  expression could be explained by alterations in FA signalling, hepatic total- (esterified- plus free-) FAs were measured, using GC-MS. With multivariate analysis a PLS-DA model was built, which clearly discriminated coxib-treated mice from controls (3 latent variables from cross-validation;  $R^2X = 63.3\%$ ,  $R^2Y = 93.7\%$ ,  $Q^2 = 76.7\%$ ; CV-ANOVA = 0.0020) (Figure 12 A). Concentrations of the most abundant hepatic polyunsaturated-FAs (PUFAs) measured: linoleic acid (C18:2), arachidonic acid (C20:4n6) and docosahexaenoic acid (22:6n3), were lower in coxib treated mice (Figure 12 B).

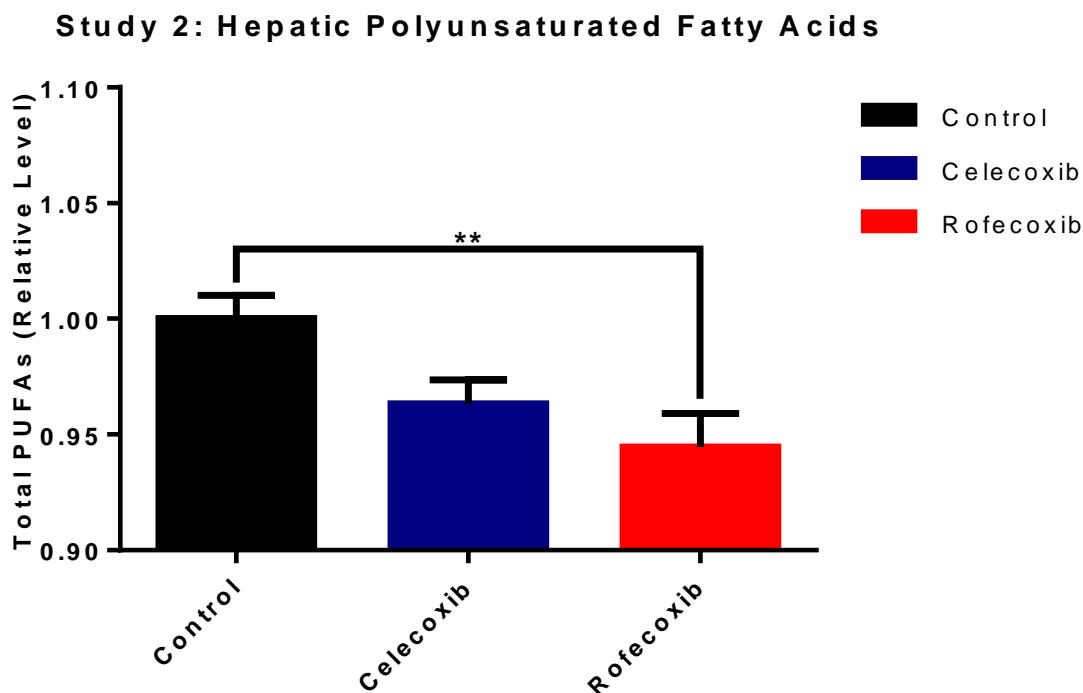
On the basis of the multivariate analysis, PUFAs were selected for univariate analysis. Hepatic PUFA concentrations were non-significantly lower (~4%) in celecoxib treated mice and significantly lower (~6%) in rofecoxib treated mice, compared to controls (ANOVA = 0.0120; Dunnett's post-hoc test:  $P = 0.0730$  and  $P = 0.0072$  respectively) (*Figure 13*).

**Figure 12.**



Multivariate analysis (PLS-DA) of hepatic total-fatty acids, in mice treated with celecoxib or rofecoxib, for 3 weeks, compared to controls. (A) Score plot showing the separation between coxib treated and control mice; (B) Loading plot, for the score plot in A., showing the fatty acids responsible for the discrimination between groups. Measured by GC-MS. Data are individual samples,  $n = 7$  and 14.

**Figure 13.**



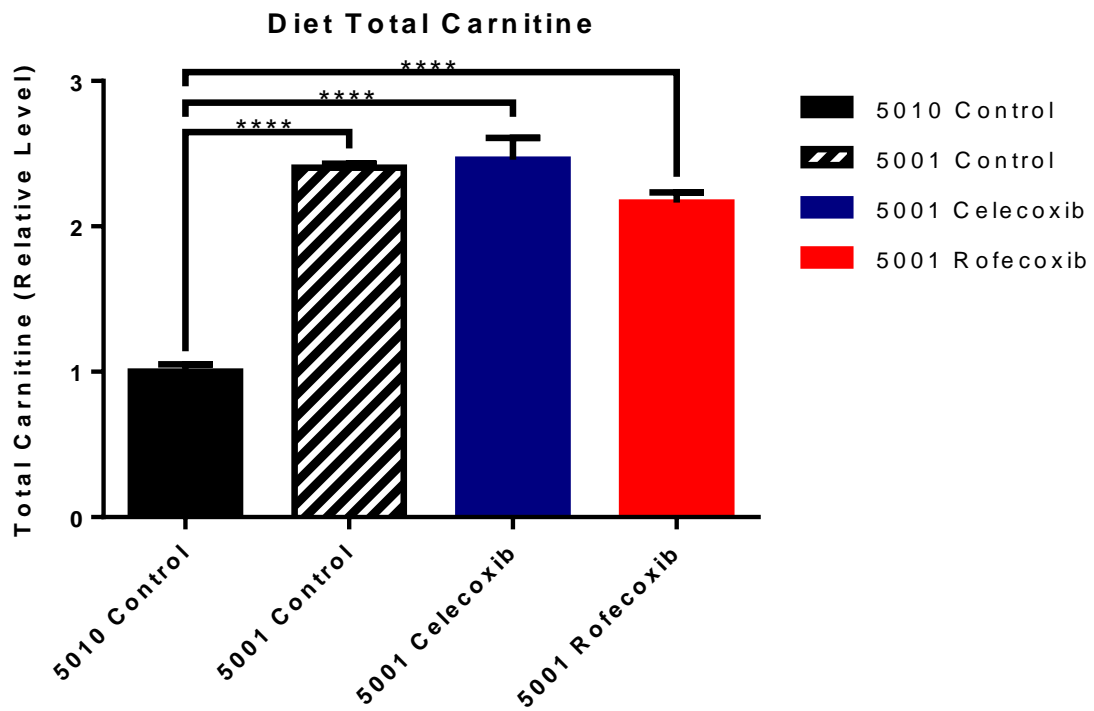
*Effect of 3 weeks of celecoxib and rofecoxib treatment on hepatic total-polyunsaturated-fatty acids, in mice. Measured by GC-MS. Data are mean  $\pm$  S.E.M for  $n = 7$ . (\*\* =  $P < 0.01$ ). Abbreviations: Polyunsaturated fatty acids (PUFAs).*

## **Addendum: Dietary Carnitines**

Following the completion of the experimental phase of this thesis, additional information, concerning a control-treatment diet mismatch, came to light. The animal facility at the University of Pennsylvania (USA), where all mouse studies were performed, incorrectly used Laboratory Autoclavable Rodent Diet 5010 (LabDiet) as the control diet, whilst incorporating celecoxib and rofecoxib into Laboratory Rodent Diet 5001 (LabDiet). Diet 5010 is claimed to be “similar to Laboratory Rodent Diet 5001 in nutrient composition and animal performance - same guaranteed analysis” (manufacturer’s diet information sheet). To determine what effect, if any, this mismatch may have had on carnitine metabolism in these studies, the dietary carnitines were measured by LC-MS/MS. The results of this analysis (*Figure 14*) demonstrated that

control diet 5010 contained less than half of the total carnitines found in control diet 5001, celecoxib containing diet 5001 and rofecoxib containing diet 5001 (ANOVA < 0.0001; Dunnett's post-hoc test:  $P < 0.0001$  for all).

**Figure 14.**



*A comparison of the total carnitines contained within Laboratory Autoclavable Rodent Diet 5010 and Laboratory Rodent Diet 5001. Measured by LC-MS/MS. Data are mean  $\pm$  S.E.M for  $n = 5$ . (\*\*\*\* =  $P < 0.0001$ ).*

## *Chapter Discussion*

### **Cardiac Carnitines**

Mice treated with celecoxib and rofecoxib for 3 weeks exhibited lower concentrations of total cardiac carnitines, which reflected lower concentrations of carnitine, acetyl-carnitine and most short- and long- chain acyl-carnitine species, compared to controls. The results were also reproduced in a 2-month study, suggesting they persist in the longer-term and are not transitory. This supports the hypothesis that celecoxib and rofecoxib treated mice exhibit lower concentrations of total cardiac carnitines than controls, with both drugs having a similar effect on murine metabolism.

These changes, in cardiac carnitines, present a different picture to those observed in human and animal models of HF, in which mainly long-chain acyl-carnitine concentrations are lower in the heart [13, 14, 16, 17, 127, 128, 132, 133]. In fact, these alterations, albeit less pronounced, are more akin to those seen in systemic carnitine deficiencies, such as primary carnitine deficiency (PCD). This suggests that, although coxib use is associated with a greater risk of HF, the lower concentrations of cardiac carnitines observed in coxib treated mice are not a consequence of its development. This is supported by the fact that the mice used in these studies display no evidence of HF.

PCD is caused by mutations in OCTN2, which impair tissue carnitine uptake and promote its urinary excretion, leading to lower concentrations of carnitines systemically, lower concentrations of cardiac carnitines and a higher risk of HF [192, 248]. Lower concentrations of cardiac carnitines have also been noted in a murine model of OCTN2 mutation, the juvenile visceral steatosis mouse [249]. Under normal conditions, heterozygous mice exhibit normal cardiac function, despite lower

concentrations of cardiac carnitines. However, they exhibit a greater risk of cardiac dysfunction compared to control mice in the presence of additional risk factors [195]. Unlike PCD and the mouse model of OCTN2 mutation, concentrations of blood carnitines are not altered in this chapter. That being said, the concentrations of blood carnitines do not necessarily reflect the concentrations of cardiac carnitines [250-252]. This is partly due to a substantial intracellular to extracellular carnitine gradient, partly because blood composition is dynamic and partly because venepuncture samples at a single time-point [253].

It is therefore conceivable that coxib treatment causes lower concentrations of cardiac carnitines, by altering systemic carnitine handling. Thereby predisposing to HF exacerbation, which is itself associated with lower concentrations of cardiac carnitines [200]. This is consistent with the relationship, between coxibs and HF, described in the literature [5, 6, 89].

Concentrations of cardiac carnitines are lower in coxib treated mice, compared to controls, both with and without IL-1 $\beta$  and to a similar extent. This suggests that an acute inflammatory background, with which COX-2 expression is intimately associated, does not affect cardiac carnitine concentrations. In addition, lower concentrations of cardiac carnitines are not observed in the IPNG COX-2<sup>-/-</sup> mouse, where COX-2 activity is suppressed due to KO. Taken together, these findings suggest that inhibition of COX-2 activity alone is not sufficient to bring about the lower concentrations of cardiac carnitines observed. Both celecoxib and rofecoxib inhibit COX-1, to some extent [61]. Therefore, one possibility is that the mechanism through which the coxibs cause lower concentrations of cardiac carnitines depends on the concerted inhibition of both COX-1 and COX-2. Alternatively, the effect could be mediated through an entirely off-target mechanism common to both.

## **The Cardiac Carnitine Shuttle**

Cardiac expression of carnitine shuttle components, including the carnitine importer OCTN2, were unaffected by coxib treatment. In contrast, alterations in cardiac CPT1, CPT2 and OCTN2 expression have been described in models of HF [16, 254, 255]. This adds weight to the argument that the coxib-mediated changes in cardiac carnitines are not a consequence of HF development. *In vitro* carnitine shuttle activity was also unaltered by coxib treatment. Furthermore, no differences were noted in cardiac concentrations of malonyl-CoA, the key regulator of carnitine shuttle activity [7]. It therefore seems unlikely that celecoxib and rofecoxib bring about lower concentrations of cardiac carnitines by impairing the expression or activity of components of the carnitine shuttle.

## **Renal Excretion of Carnitines**

Urinary concentrations of the carnitines were unaffected by coxib treatment. This indicates that the coxibs probably don't affect OCTN2-mediated renal reabsorption of carnitines. Renal OCTN2 expression would help confirm this, but was not examined due to a lack of available tissue for RT-qPCR. It should be noted that there was considerable inter-sample variability, which could have masked differences.

## **Microbiome-Mediated Carnitine Bioavailability**

Urinary concentrations of the microbe-dependent metabolites, TMA and TMAO, were significantly lower in coxib treated mice. This suggests that celecoxib and rofecoxib either reduce TMA-precursor availability or alter the composition of the digestive tract's microbial community [233]. Recent evidence supports the view that NSAIDs are capable of altering the intestinal microbiome. Liang et al. demonstrated that indomethacin alters the composition and diversity of intestinal microbes in mice, which

has a reciprocal effect on the pharmacokinetics and pharmacodynamics of indomethacin. This two-way relationship may explain some of the inter-individual variation seen in NSAID response and side-effect profile [256]. However, whilst it is interesting that celecoxib and rofecoxib appear to alter the microbiome, these observations are unlikely to underlie the lower concentrations of cardiac carnitines noted in coxib-treated mice.. This is because lower concentrations of urinary TMA and TMAO, as occurs with coxib treatment, implies less microbe-mediated degradation of dietary carnitine in the intestine. This would be expected to enhance carnitine bioavailability and systemic and cardiac carnitine concentrations [232]. Instead, coxib treatment is associated with lower concentrations of cardiac carnitines. Therefore, microbiome-mediated carnitine bioavailability does not appear to be an important factor in determining the lower concentrations of cardiac carnitines, noted in celecoxib and rofecoxib treated mice compared to controls.

## **Hepatic Carnitine Synthesis**

To determine whether the coxibs affect carnitine synthesis, hepatic expression of the enzymes responsible were measured in mice following 3 weeks of coxib treatment. Hepatic expression was examined, as the liver is the primary source of carnitine synthesis in the mouse [25]. Rofecoxib treatment is associated with significantly lower hepatic BBD and TMABADH, but not TMLD, expression. Celecoxib treatment is associated with lower hepatic BBD expression, but non-significantly. Because BBD activity is rate-limiting, these results are concomitant with impaired hepatic carnitine synthesis [35]. In addition, it has been demonstrated that pharmacological inhibition of BBD reduces the concentrations of cardiac carnitines in mice [257]. Therefore, it is biologically plausible that the lower concentrations of cardiac carnitines, detected with celecoxib and rofecoxib treatment, could be mediated through inhibition of BBD activity

and hepatic carnitine synthesis. In support of this, the hepatic expression of PPAR- $\alpha$  is also significantly down-regulated in rofecoxib treated mice and non-significantly down-regulated in celecoxib treated mice. BBD possesses a functional PPRE, and is under PPAR- $\alpha$  regulatory control [241]. This suggests that the coxibs may reduce hepatic PPAR- $\alpha$  expression and/or signalling, BBD expression, carnitine synthesis and ultimately the concentrations of cardiac carnitines.

One possible explanation for this, is that celecoxib and rofecoxib interfere with PPRE-mediated PPAR- $\alpha$  signalling. In support of this, celecoxib and rofecoxib have been shown to inhibit PPRE activity, by as much as 50%, in an intestinal epithelial cell line. The authors attributed this to the inhibition of COX-2-mediated PGI<sub>2</sub> synthesis [258]. However, hepatic COX-2 is not a major source of PGI<sub>2</sub> synthesis and the effect on cardiac carnitines is not recapitulated in the IPNG COX-2<sup>-/-</sup> mouse. Therefore, coxib-mediated inhibition of COX-2, PGI<sub>2</sub> synthesis and hepatic PPRE-mediate PPAR- $\alpha$  signalling is unlikely to fully explain the lower concentrations of cardiac carnitines noted in coxib treated mice compared to controls.

## **Hepatic Total-Fatty Acids**

PPAR- $\alpha$  activity can be regulated by free-FAs. Certain FAs have been shown to directly bind to and activate PPARs. These include the PUFAs: linoleic acid (C18:2),  $\alpha$ -linoleic acid (C18:3n3), arachidonic acid (C20:4n6) and docosahexaenoic acid (C22:6n3); and certain saturated-FAs including stearic acid (C18:0) and myristic acid (C14:0) [259]. PPAR activation can also regulate PPAR expression, via positive-feedback [260]. For example, the PPAR- $\alpha$  ligand, docosahexaenoic acid, upregulates PPAR- $\alpha$  expression [261].

Fascinatingly, total- (esterified- plus free-) concentrations of the most abundant of these FA ligands, linoleic acid, arachidonic acid, docosahexaenoic acid and stearic acid were all lower in coxib treated mice compared with controls. In addition, the sum of all hepatic total-PUFAs was also significantly lower. This suggests that coxib treatment reduces hepatic concentrations of these FAs and their lipid precursors, which would be expected to reduce the expression and activity of PPAR- $\alpha$  in the liver. This could then explain the lower hepatic BBD expression, the lower hepatic carnitine synthesis and, ultimately, the lower concentrations of cardiac carnitines.

How exactly the coxibs cause this alteration in hepatic FA composition is unclear, though the evidence suggests that it is a feature common to both celecoxib and rofecoxib treatment.

## **Addendum: Dietary Carnitines**

Owing to a mismatch of diets at the University of Pennsylvania animal facility, the diet into which the coxibs were incorporated (diet 5001) contained more than double the total carnitines of the control diet (diet 5010). This raises serious concerns regarding the validity of the findings presented in this chapter and necessitates replication of the affected experiments. Whilst there is no doubt that the affected experiments need to be replicated, there is reasonable evidence that the differences in dietary carnitines, between the coxib treated and control mice, does not underlie the differences in cardiac carnitines observed. Firstly, whilst the dietary carnitines were higher in the coxib treated mice, the cardiac carnitines were lower. These observations are at odds with the results of mouse carnitine supplementation experiments, which demonstrate that oral carnitine supplementation causes a relatively small increase in the concentrations of cardiac carnitines [262]. Secondly, even if the differences in dietary

and cardiac carnitines were in the same direction, carnitine supplementation experiments employ dose differences orders of magnitude greater than exists between diets 5001 and 5010, and observe smaller or no changes in cardiac and skeletal muscle carnitines [262-265]. Thirdly, it has been demonstrated that the rate of endogenous carnitine synthesis is unaffected by alterations in dietary carnitine intake [192]. Therefore, the alterations in hepatic carnitine synthesis are unlikely to be caused by the dietary carnitine differences. Finally, carnitine bioavailability varies according to long term dietary carnitine content, due to alterations in intestinal carnitine uptake. For example, a 70 kg adult who consumes 1 mg carnitine per day on a vegetarian diet typically absorbs 75% of it, whilst a 70 kg adult who consumes 23-135 mg carnitine per day on a standard diet absorbs 63% [240]. It is therefore conceivable that the amount of carnitine actually absorbed from the two diets is similar, despite their differences.

However, systemic carnitine concentrations do not solely depend on dietary carnitine intake and endogenous carnitine synthesis plays an important part. As discussed, carnitine synthesis can be regulated by FA-mediated PPAR- $\alpha$  signalling. Comparison of the manufacturer's diet information sheets reveals that coxib diet 5001 contains 26% less linoleic acid, the same amount of arachidonic acid and 29% less Omega-3 FAs than control diet 5010. It is therefore possible that the differences observed in hepatic carnitine synthesis may depend on the differences in dietary PUFA content and subsequent incorporation into hepatic lipids. Additionally, dietary nutrient intake also influences the gut microbiome composition, and hence TMA and TMAO synthesis [233].

In summary, the differences in dietary carnitines are unlikely to cause the lower concentrations of cardiac carnitines and urinary TMA and TMAO observed. However,

differences in dietary FA and nutrient composition, between diets 5001 and 5010, could certainly contribute.

## *Chapter Conclusions and Future Directions*

To first address the elephant in the room; it is difficult to draw meaningful conclusions from these results, regarding the aforementioned study hypotheses, due to the diet miss-match. This is because, contrary to the manufacturer's descriptions, diets 5001 and 5010 are not especially similar and exhibit key differences in carnitines and FAs, which confound the results. Nevertheless, other conclusions can be made. Firstly, the combinations of diet 5001 with celecoxib and rofecoxib, have similar effects on carnitine metabolism, hepatic PPAR- $\alpha$  signalling and PUFA concentrations, in mice. Therefore, if the lower concentrations of cardiac carnitines is a real effect associated with coxib treatment, rather than a dietary artefact, it is unlikely to explain the putative difference in HF risk observed in humans between celecoxib and rofecoxib and supports the view that they behave similarly. Secondly, the combination of a coxib with a high-carnitine low-PUFA diet causes lower concentrations of cardiac carnitines in mice. Whilst it remains unclear whether this effect is due to the drug, the diet or a combination, it highlights the potential importance of drug-diet interactions in the context of coxib induced HF. This is especially pertinent from a translational point of view as, in the real-world, patients taking these medications have varied diets. Finally, this drug-diet combination is also associated with lower PPAR- $\alpha$  expression and possibly signalling. PPAR- $\alpha$  is the master regulator of hepatic lipid metabolism [266]. This raises the possibility that this drug-diet combination might interact with pre-existing disorders associated with dysregulated lipid metabolism, such as non-alcoholic fatty liver disease, obesity, diabetes, hypertension, the metabolic syndrome

and coronary heart disease [267]. Ultimately, whilst this work is unsuitable to address the study hypotheses, it raises interesting and relevant concerns regarding the use of coxibs with certain diets.

The principal limitation of this work is the miss-match of diets, which resulted in the control mice being fed a different diet to the celecoxib and rofecoxib treated mice, thereby eliminating the utility of the control group. Therefore, the focus of future work should be to replicate the findings of this chapter in correctly controlled studies. This work was also limited by the fact that no functional read-outs were used. A clear functional effect would not be expected to manifest, with the relatively small differences in cardiac carnitines observed between the groups, unless the mice were stressed. The use of Doppler echocardiography, to measure CV dysfunction, in coxib-treated CV-compromised mice would address this. Finally, a rescue experiment of a similar design, employing carnitine supplementation or the use of a PPAR- $\alpha$  agonist, would help to confirm the proposed mechanism and its functional relevance.

## ***Chapter 6: Development of an In Vitro Carnitine Shuttle Activity Assay***

## Chapter Introduction

The carnitine shuttle is responsible for the shuttling of activated long chain FAs across the inner mitochondrial membrane to the mitochondrial matrix, where they are oxidised by  $\beta$ -oxidation [138]. Shuttle activity is a key regulator of fatty acid metabolism, which is an important energy source in oxidative skeletal and cardiac muscle [268]. Usually CPT1 activity controls carnitine shuttle activity (CSA), but under different physiological, pathological and pharmacological circumstances other shuttle components may become rate limiting [223, 257, 269, 270]. Current *in vitro* assays, used to measure CSA, are either not specific to the carnitine shuttle, not sensitive to rate limiting inhibition of all of its components or unable to provide a time-course of activity [271-273]. Recently, it has been demonstrated that acetylcarnitine is exported from primary skeletal muscle cells [274]. However, it is not known whether the extracellular acetylcarnitine produced reflects cellular carnitine uptake and shuttling, or whether it arises from cellular damage and loss of membrane integrity. Addressing this issue raises the possibility of using non-destructive extracellular sampling of acetylcarnitine to track CSA. This could overcome a number of the limitations associated with current CSA assays. This pilot study will attempt to address the question: Does extracellular acetylcarnitine reflect carnitine uptake and shuttling *in vitro* (i.e. does it represent a marker of CSA)? The following hypothesis will be tested:

**Cellular export of acetylcarnitine is reflective of cellular carnitine uptake and shuttling, *in vitro*.**

It has not yet been established if acetylcarnitine is exported in cultured primary cardiomyocytes. Given that carnitine shuttle gene defects manifest with cardiac abnormalities and cardiac carnitine metabolism is profoundly altered in diseases such as MI and HF, it is important to determine whether acetylcarnitine export could be used

as a measure of *cardiac* CSA [192]. This study will attempt to address the question: Do primary cardiomyocytes export acetylcarnitine extracellularly, *in vitro*? The following hypothesis will be tested:

**Primary cardiomyocytes export acetylcarnitine extracellularly, *in vitro*.**

In Chapter 5, celecoxib and rofecoxib treatments are noted to alter cardiac carnitine metabolism. It is unclear whether this may be, in part, mediated through direct effects on the carnitine shuttle and CSA. Elucidation of this will help resolve the relationship between the coxibs and cardiac carnitine metabolism and may provide insight into the adverse CV events with which the coxibs are associated. This study will attempt to address the question: Do the coxibs, celecoxib and rofecoxib, have direct effects on CSA? The following hypothesis will be tested:

**Celecoxib and rofecoxib do not have direct effects on CSA, *in vitro*.**

These hypotheses were tested in C2C12 murine skeletal muscle cells and primary murine cardiomyocytes (PMCs), derived from wild type C57BL/B6 mice, treated with celecoxib, rofecoxib or etomoxir (CPT1 inhibitor - positive control). Targeted metabolomic analysis was performed, to measure acetylcarnitine and its stable isotope d9-acetylcarnitine, in order to provide insight into the effect of celecoxib and rofecoxib treatment on carnitine shuttle activity.

## *Chapter Background*

Under normal conditions CPT1 activity, primarily under the control of malonyl-CoA, governs the rate of activity of the carnitine shuttle [270]. However, physiological, pathological and pharmacologic effects can disrupt this regulatory system, engendering other shuttle components with rate-limiting activity [223, 257, 269].

A recent hypothesis suggests that during low intensity endurance exercise skeletal muscle CPT1 is rate limiting, whilst at increased intensities intra-mitochondrial L-carnitine delivery to CPT1 by CACT becomes rate limiting. During endurance exercise, as intensity increases, acetyl-CoA accumulates. Acetyl-CoA is buffered by L-carnitine, as acetylcarnitine. This process reduces the total L-carnitine in skeletal muscle, which might be expected to reduce CPT1 flux. However, at lower endurance exercise intensities, this is compensated for by increased intra-mitochondrial L-carnitine, liberated from long chain acylcarnitine by CPT2 activity, delivered to CPT1 by CACT. At greater endurance exercise intensities, when L-carnitine falls to < 50% of the total carnitine pool, the delivery of intra-mitochondrial L-carnitine to CPT1 by CACT becomes rate limiting [223].

CSA is also dysregulated in certain disorders of fatty acid oxidation. In congenital CPT2 deficiency, if enzyme activity is < 25% of normal, CPT2 limits the activity of the carnitine shuttle [269]. Moreover, other more prevalent diseases, such as diabetes, MI and HF, are also associated with impairments in carnitine metabolism [138, 275, 276].

Targeted pharmacological inhibition of carnitine shuttle components, such as OCTN2, can also reduce CSA [257]. Given that alterations, in CSA, are found in a number of important diseases, an *in vitro* CSA assay represents an important investigative tool. Because physiological, pathological and pharmacological effects can modulate CSA

through different shuttle components, an assay that interrogates the entire shuttle is desirable. Methods currently used to assay CSA possess a number of limitations.

## **Limitations of Current *In Vitro* Carnitine Shuttle Activity Assays**

Methods currently used either to approximate or directly measure shuttle activity include specific enzyme and transporter assays, static metabolite measurements and metabolite-flux assays.

The spectrophotometric CPT1 assay is an example of a specific enzyme assay used to assess CSA. CPT1 activity is assayed by measuring the absorbance of thiol groups at 412 nm, indicative of CoA-SH release from palmitoyl-CoA [271]. Like other enzyme/transporter assays this CPT1 assay suffers from a number of limitations. As discussed, under certain conditions different carnitine shuttle components can become rate limiting [223, 257, 269]. Under these conditions an individual enzyme/transporter assay will not reflect shuttle activity. In addition, these assays are performed in cell lysates, not intact cells [271]. Thus, normal regulatory control, determined by intracellular concentrations of activators and inhibitors, may be lost.

The *in vitro* probe acylcarnitine assay is an example of a static metabolite measure. Cells are cultured in L-carnitine and palmitic acid. Concentrations of free- and acylcarnitines are then measured in the intracellular and extracellular extracts by mass spectrometry [272]. This assay is a useful tool for identifying enzyme defects. However it does not provide quantitative insight into the activity of the carnitine shuttle. This is because, like other static metabolite measures, the carnitines are measured at a single time-point.

Metabolite-flux assays provide additional insight. These assays track changes in metabolites, indicative of *in vitro* carnitine shuttle activity, using specific labels [277]. Metabolites are labelled by incorporating radio- or stable- isotopes into their chemical structure. Radioisotopes decay, emitting radiation, which can be measured [278]. Stable isotopes differ in mass, hence  $m/z$ , as they possess a different number of neutrons. This can be detected using mass spectrometry [277]. Thus, labelled and unlabelled metabolites can be distinguished. Therefore, when an appropriate labelled metabolite is introduced into the carnitine shuttle, its localisation and metabolism can be disentangled from that of its unlabelled counterpart already present. This allows changes in that metabolite to be tracked over time. Various radiolabelled carnitines have been employed to track OCTN2, CPT1, CPT2 and CACT activities *in vitro* [279-282]. However, these assays typically interrogate only a part of the shuttle. Radiolabelling has also been used to track the oxidation of long-chain fatty acids, which requires the carnitine shuttle and can therefore be used as a proxy for shuttle activity [283, 284]. Of note, fatty acid oxidation may be impaired by defects peripheral to the carnitine shuttle and is therefore not always a true reflection of shuttle activity. In addition, where possible, the use of stable isotopes is preferred as they neither emit radiation nor require additional safety precautions. Stable isotope labelling of long chain fatty acids has also been used to measure *in vitro* carnitine shuttle-dependent fatty acid oxidation rates [273]. Isotopically, like radiolabelled, fatty acid oxidation rates, only reflect CSA when shuttle activity is rate-limiting. If other components of the fatty acid oxidation machinery become rate-limiting, the approximation of CSA by fatty acid oxidation does not hold.

An ideal *in vitro* CSA assay would (1) be specific to the carnitine shuttle, (2) measure the rate of CSA, (3) be sensitive to rate-limiting inhibition of any shuttle component, (4) employ a stable isotope, rather than a radioisotope, labelling technique.

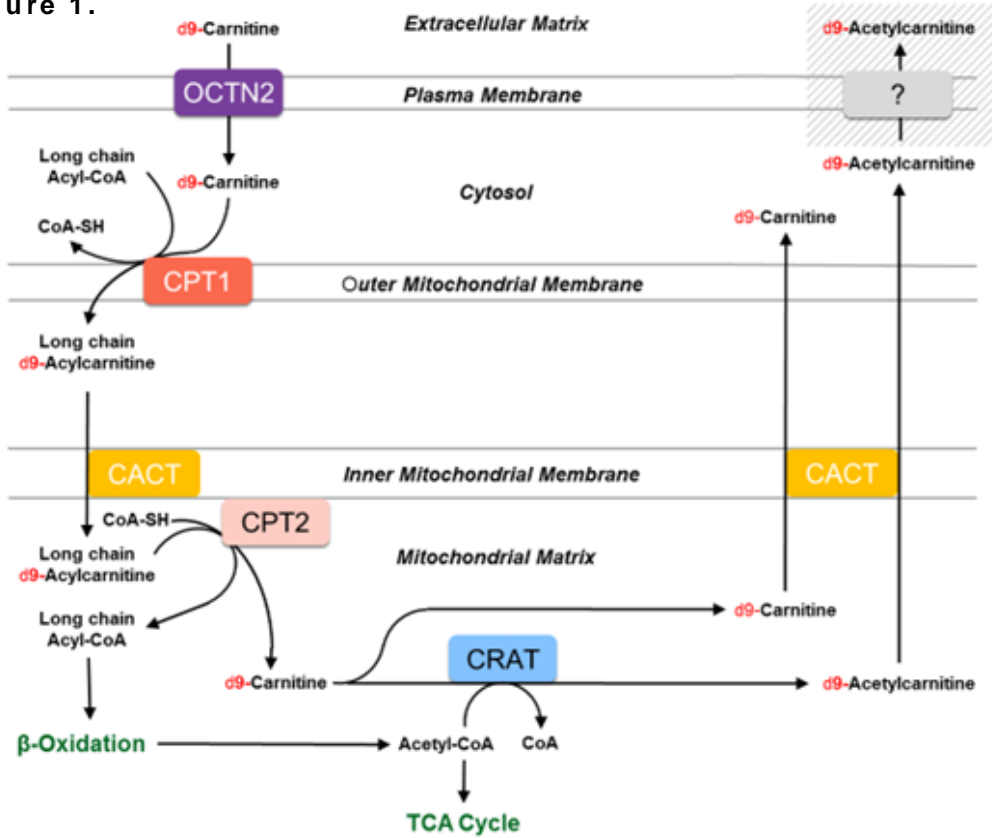
## **Theoretical Basis for an improved *In Vitro* Carnitine Shuttle Activity Assay**

To achieve specificity for the carnitine shuttle and sensitivity to rate-limiting inhibition of any of its components, the measurement of a detectable chemical modification to carnitine, indicative of the passage of carnitine through the entire shuttle, is required. Acetylation of carnitine, which can be detected by LC-MS/MS, requires the successive actions of OCTN2, CPT1, CACT, CPT2 and CRAT [192].

To calculate the rate of CSA *in vitro*, readings need to be taken over time. This precludes intracellular indicators, the measurement of which necessitate destruction of cellular integrity. Instead, the indicator must be transported from the cell cytosol to the extracellular environment (media). Nolan et al. observed the export of acetylcarnitine in cultured human primary skeletal muscle cells and Molstad et al. reported acetylcarnitine export in cultured Girardi human heart cells [274, 285].

Therefore, it is theoretically possible to culture cells in stable isotope labelled carnitine (d9-L-carnitine) and observe the accumulation of extracellular d9-acetylcarnitine, as a measure of overall CSA (*Figure 1*). This chapter will experimentally interrogate the d9-L-carnitine/d9-acetylcarnitine CSA assay, proposed here on a theoretical basis, in a bid to establish its utility as a measure of CSA.

Figure 1.



The  $d_9$ -L-carnitine/ $d_9$ -acetylcarnitine CSA assay. The stable isotope,  $d_9$ -L-carnitine, is added to cultured cells. The extracellular environment (media) is sampled over time. The accumulation of  $d_9$ -acetylcarnitine is measured, at each time point, by LC-MS/MS. From this, CSA is inferred. Abbreviations:  $d_9$ -L-Carnitine ( $d_9$ -Carnitine); Organic cation transporter 2 (OCTN2); Carnitine palmitoyltransferase 1 (CPT1); Carnitine palmitoyltransferase 2 (CPT2); Carnitine-acylcarnitine translocase (CACT); Carnitine O-acetyltransferase (CRAT); Tricarboxylic acid (TCA); Coenzyme A (CoA). Adapted from Flanagan et al. [192]

## *Chapter Methods*

C2C12 skeletal muscle cells were cultured (n=6) in the presence of isotopically labelled d9-L-carnitine, and the media analysed with LC-MS/MS, to determine whether this cell type exports acetyl-carnitine to the media and thus establish the feasibility of tracking carnitine shuttle activity via the d9-label. On the back of this work, primary murine cardiomyocytes were cultured in the presence of isotopically labelled d9-L-carnitine and celecoxib or rofecoxib (n=4), and the media analysed with LC-MS/MS, to determine whether this cell type exports acetyl-carnitine to the media and establish whether the coxibs alter carnitine shuttle activity.

The following methods (see chapter 3 for a detailed description of each) were used in this chapter:

- **C2C12 Culture**
- **C2C12 Stable Isotope Labelling Assay**
- **Primary Murine Cardiomyocyte Cell Isolation**
- **Primary Murine Cardiomyocyte Culture and Stable Isotope Labelling Assay**
- **Methanol Crash**
- **Non-Butylating Method of Preparation of Media Samples for LC-MS/MS Carnitine Assay**
- **LC-MS/MS Carnitine Assay**
- **Processing of Isotopically Labelled Metabolomic Data**
- **Pearson's r and Linear Regression**

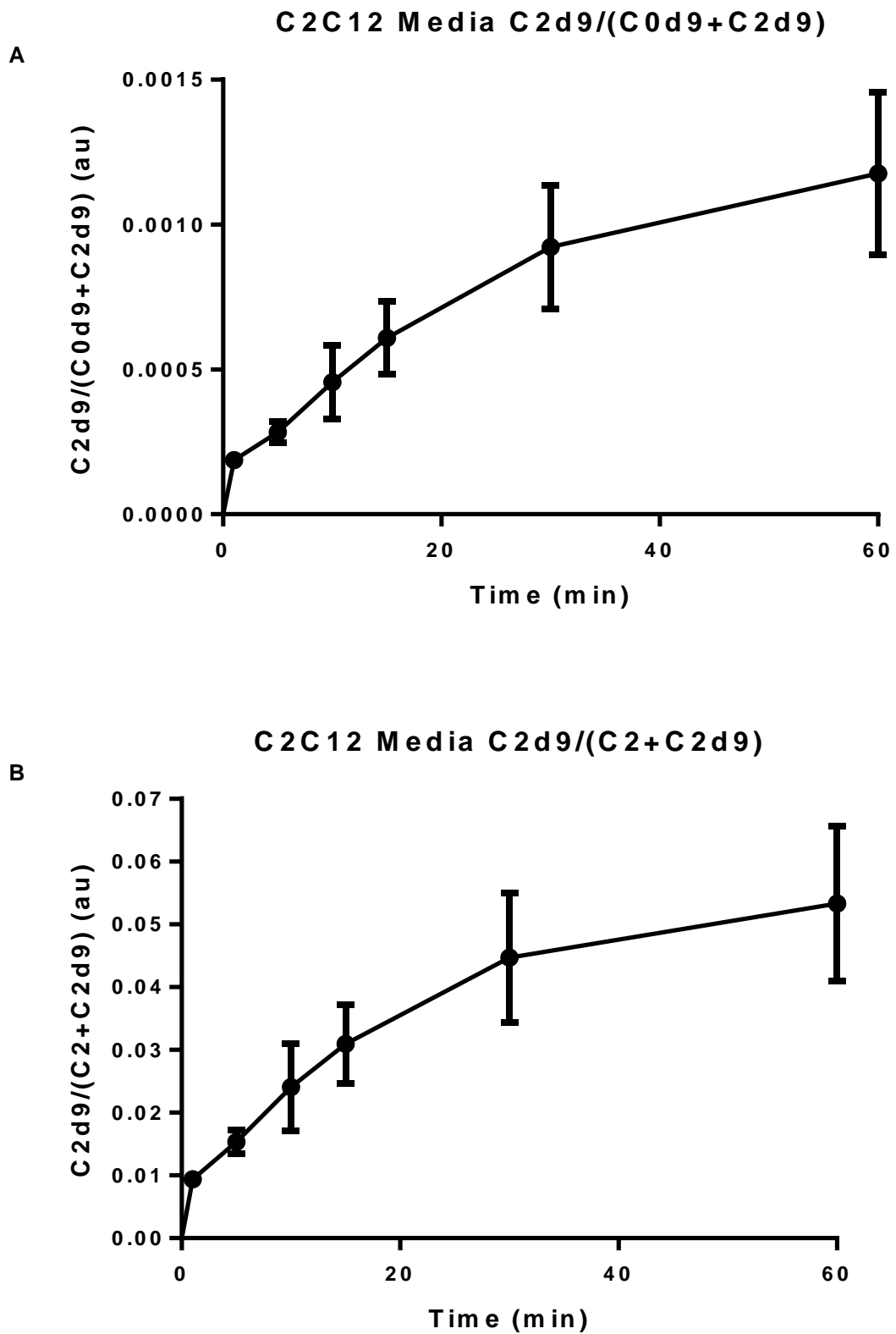
## *Chapter Results*

### **C2C12 Skeletal Muscle Cells**

The accumulation of d9-acetylcarnitine in the media of d9-L-carnitine treated C2C12 skeletal muscle cells was measured, using LC-MS/MS, to verify the d9-label flux anticipated in the d9-L-carnitine/d9-acetylcarnitine CSA assay (*Figure 1*). A cumulative increase, over time, in d9-acetylcarnitine was observed in the media of d9-L-carnitine treated C2C12 cells (*Figure 2 A and B*). Incorporation of the d9-label into other media acylcarnitine pools was also examined, but no appreciable accumulation was observed (data not shown).

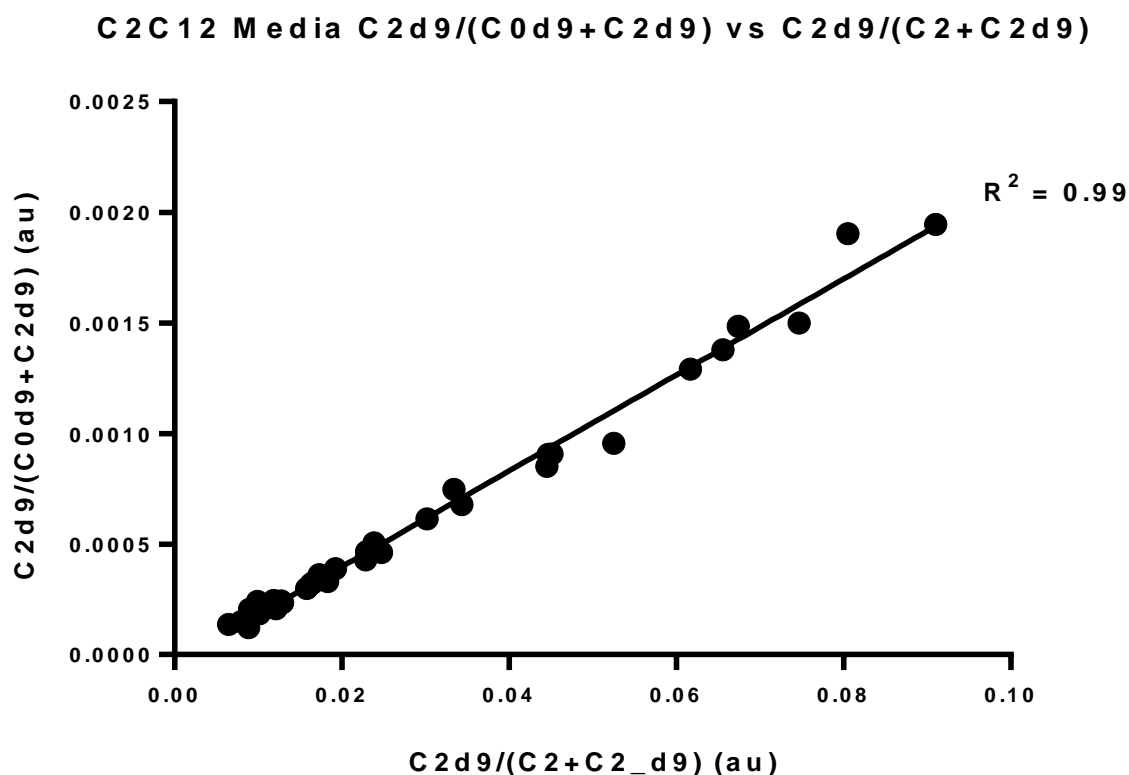
The fraction of d9-acetylcarnitine in the media, over either d9-L-carnitine plus d9-acetylcarnitine (*Figure 2 A*) or acetylcarnitine plus d9-acetylcarnitine (*Figure 2 B*) produced similarly shaped plots. The relationship between these two plots was determined by Pearson's product moment correlation coefficient. They exhibited a near perfect positive correlation (Pearson's  $r = 0.99$ , 95% CI = 0.99-1.00,  $P < 0.0001$ ) and linear regression (*Figure 3*).

Figure 2.



Accumulation of d9-acetylcarnitine in the media of d9-L-carnitine treated C2C12 skeletal muscle cells. Media C2d9 over (A) media C0d9 + C2d9 (B) media C2 + C2d9. Measured by LC-MS/MS. Data are mean  $\pm$  S.E.M for n = 6. Abbreviations: d9-L-Carnitine (C0d9); Acetylcarnitine (C2); d9-Acetylcarnitine (C2d9); C2C12 skeletal muscle cells (C2C12).

Figure 3.



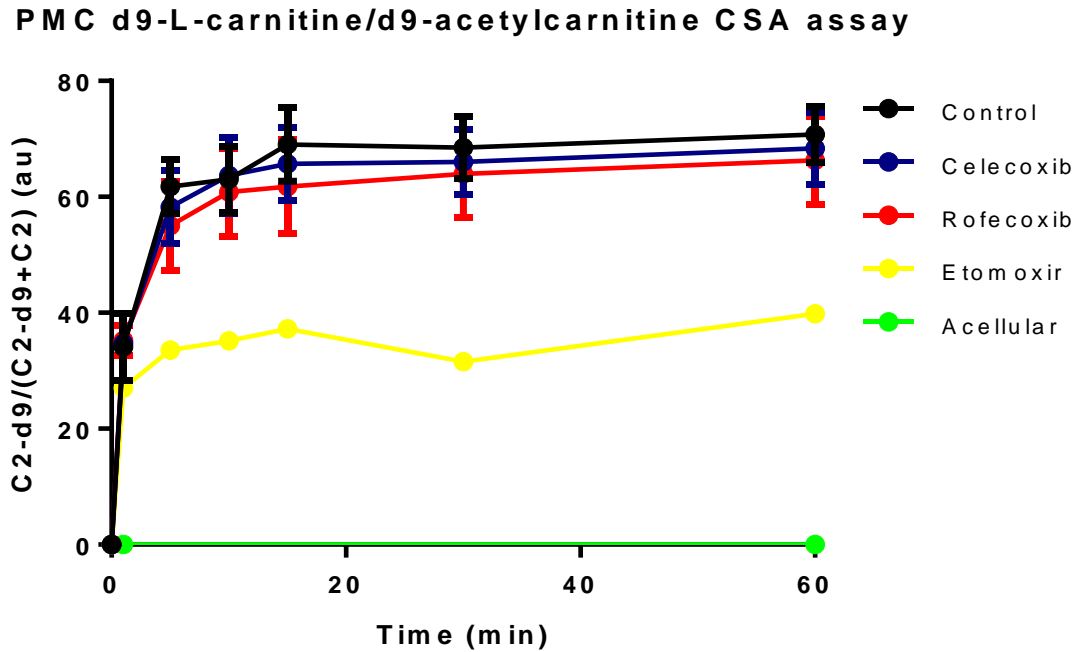
Linear regression of media d9-acetylcarnitine over media d9-L-Carnitine plus d9-acetylcarnitine versus media acetylcarnitine plus d9-acetylcarnitine. Measured by LC-MS/MS. Data are individual wells of cells,  $n = 36$ .  $R^2 = 0.99$ . Abbreviations: d9-L-Carnitine (C0d9); Acetylcarnitine (C2); d9-Acetylcarnitine (C2d9); C2C12 skeletal muscle cells (C2C12).

## Primary Murine Cardiomyocytes

The accumulation of d9-acetylcarnitine in the media of d9-L-carnitine treated PMCs was measured to confirm that the d9-label flux observed in C2C12 cells translated to this cell type and to demonstrate the utility of the d9-L-carnitine/d9-acetylcarnitine CSA assay. Five conditions were examined: PMCs alone, PMCs plus etomoxir treatment (positive control), PMCs plus celecoxib treatment, PMCs plus rofecoxib treatment and an acellular group. The acellular group was used to control for non-specific conversion of d9-L-carnitine to d9-acetylcarnitine. The acellular group exhibited no increase in d9-acetylcarnitine accumulation, the control, celecoxib and rofecoxib treated PMC

groups showed similar accumulation and the etomoxir treated PMC group exhibited decreased accumulation (*Figure 4*).

**Figure 4.**



Accumulation of d9-acetylcarnitine in the media of d9-L-carnitine treated primary murine cardiomyocytes. Media C2d9 over C2 + C2d9. Measured by LC-MS/MS. Data are mean  $\pm$  S.E.M for  $n = 4$  (control, celecoxib, rofecoxib),  $n = 3$  (acellular) and  $n = 1$  (etomoxir). Abbreviations: Acetylcarnitine (C2); d9-Acetylcarnitine (C2d9); Primary murine cardiomyocyte (PMC).

## *Chapter Discussion*

### **C2C12 Skeletal Muscle Cells**

The accumulation of d9-acetylcarnitine in the media of d9-L-carnitine treated C2C12 cells (*Figure 2*) serves as a proof of concept. It demonstrates that d9-acetylcarnitine accumulates in the media of this C2C12 cell system, which is in agreement with previous findings by Noland et al., who reported cellular export of acetylcarnitine in cultured human primary skeletal muscle cells [274]. This supports the theoretical basis of this assay (*Figure 1*) and indicates that media d9-acetyl carnitine may serve as a useful measure of CSA. However, in this experiment, appreciable accumulation of d9-labelled acylcarnitine species in the media was not observed (data not shown), whereas Noland et al. reported their cellular export [274]. This discrepancy may reflect differences in the duration of the two experiments and abundances of acetylcarnitine compared to acylcarnitine species. The present experiment recorded results after a 1 hour incubation with d9-L-carnitine, whereas Noland et al. measured the acylcarnitines following a 24 hour incubation with L-carnitine [274]. As the acylcarnitines are less abundant than acetylcarnitine, this experiment may have been too short for the acylcarnitines to accumulate in the media to detectable concentrations. This is supported by evidence demonstrating that the cellular export of carnitine species is largely dependent on their intracellular concentrations [286]. The results of this study support the hypothesis that cellular export of acetylcarnitine is reflective of cellular carnitine uptake and shuttling, in vitro.

The results of *Figure 2 A and B* both reflect flux through the carnitine shuttle. The results of *Figure 2 A* represent the cumulative synthesis of d9-acetylcarnitine from d9-L-carnitine and its export to the media. The results of *Figure 2 B* represent the

cumulative incorporation of the d9-label into the media acetylcarnitine pool. In reality they are a close, but differentially scaled, approximation of each other (*Figure 3*). This is because in this system, firstly, both d9-L-carnitine and unlabelled-acetylcarnitine are several orders of magnitude more abundant in the media than d9-acetylcarnitine. The d9-acetylcarnitine term in the denominator can therefore be ignored. Secondly, the amount of d9-L-carnitine converted to d9-acetylcarnitine is relatively small compared to the total d9-L-carnitine. The amount of unlabelled-acetylcarnitine is also fairly constant. The d9-L-carnitine and unlabelled-acetylcarnitine terms in the denominator are therefore effectively constant (termed here K and k, respectively).

$$\text{Equation of (Figure 2.A): } \frac{C_{2d9}}{C_{0d9} + C_{2d9}} \rightarrow \frac{C_{2d9}}{C_{0d9} + \cancel{C_{2d9}}} \rightarrow \frac{C_{2d9}}{C_{0d9}} \rightarrow \frac{C_{2d9}}{K}$$

$$\text{Equation of (Figure 2.B): } \frac{C_{2d9}}{C_2 + C_{2d9}} \rightarrow \frac{C_{2d9}}{C_2 + \cancel{C_{2d9}}} \rightarrow \frac{C_{2d9}}{C_2} \rightarrow \frac{C_{2d9}}{k}$$

In theory, *Figure 2 A and B* differ only by a scaling factor determined by the ratio of K to k. However, reporting the fraction of media d9-acetylcarnitine over unlabelled-acetylcarnitine has a key advantage. Unlike d9-L-carnitine, unlabelled-acetylcarnitine has almost identical physiochemical properties to d9-acetylcarnitine. This means that, when LC-MS/MS data are acquired, inter-sample instrument variability affects both compounds equally, avoiding the need for further normalisation [277].

## Primary Murine Cardiomyocytes

For the first time, cultured primary cardiomyocytes have been shown to export acetylcarnitine to the media (*Figure 4*), building on work done by Molstad et al. who demonstrated acetylcarnitine export in Girardi human heart cells [285]. In the acellular negative control experimental condition, no d9-L-carnitine is converted to

d9-acetylcarnitine. The positive control, etomoxir (a CPT1 inhibitor) is associated with less accumulation of d9-acetylcarnitine in the media. This appears to demonstrate the sensitivity of this assay to CPT1 inhibition, hence CSA. However, additional replicates of this observation are required. Neither of the coxibs significantly alter d9-acetylcarnitine accumulation compared to control. This suggests they do not have an effect on CSA; however positive controls of other shuttle components are required before it can be definitively concluded that this assay is sensitive to their inhibition.

After 15 minutes, further accumulation of d9-acetylcarnitine in the media practically ceases. Given that a large quantity of d9-L-carnitine remains, this suggests that either long-chain acyl-CoA becomes rate limiting, indicating depletion of its cytosolic pool, or the extracellular, cytosolic and intra-mitochondrial d9-acetylcarnitine pools are in exchange and have reached a state of equilibrium. Depletion of the long-chain acyl-CoA cytosolic pool is more likely. This is because, firstly, the transporter responsible for carnitine import, OCTN2, has a greater affinity for d9-L-carnitine than d9-acetylcarnitine [287]. Secondly, in this experiment, the concentration of d9-L-carnitine, in the media, was 25-fold greater than the maximum d9-acetylcarnitine concentration (data not shown). Therefore, d9-acetylcarnitine would be comprehensively outcompeted by d9-L-carnitine, rendering the plasma membrane relatively impermeable to d9-acetylcarnitine import and precluding equilibrium exchange between the extracellular and cytosolic d9-acetylcarnitine pools.

Rarely in metabolism are energy substrates discarded. This raises the intriguing possibility that the export of acetylcarnitine, by cardiomyocytes, may serve a useful biological function.

One possibility could be the maintenance of the intracellular L-carnitine pool. Even under steady state conditions, perfused rat hearts have been shown to synthesise more acetyl-CoA than can be metabolised through the TCA cycle [288]. Because the heart produces an excess of acetyl-CoA at steady state, transient-buffering by cytosolic L-carnitine, as occurs in skeletal muscle during endurance exercise, would terminally deplete the intracellular L-carnitine pool, inhibiting cardiac  $\beta$ -oxidation [223]. Instead, acetylcarnitine could be exported to the circulation and the loss of carnitine compensated for by enhanced L-carnitine uptake, thereby simultaneously preventing excess acetyl-CoA accumulation and maintaining the intracellular carnitine pool. This is plausible as the heart is excellent at extracting L-carnitine from the circulation [289]. Moreover, muscle contraction causes OCTN2 translocation to the plasma membrane of skeletal muscle cells, which enhances carnitine uptake [290]. A similar mechanism would enable the heart to titrate its carnitine uptake in response to workload hence excess acetylcarnitine production and export. It is therefore conceivable that the increase in plasma carnitine, noted in HF, may reflect some sort of signalling mechanism, rather than tissue leakage [210]. This could be determined using a combination of *in vivo* paired blood sampling from a peripheral arterial site and the coronary sinus, to show that plasma carnitine levels depend on some physiological parameter e.g. exercise intensity, and the measurement of intracellular enzyme concentrations in the media from these experiments, to exclude membrane leakage.

The exported acetylcarnitine may also serve a purpose as a signalling molecule. In support of this, Zhang et al. demonstrated that acetylcarnitine enhances insulin-dependent glucose uptake, through activation of adenosine monophosphate-activated protein kinase (AMPK) signalling, in a rat skeletal muscle cell line [291]. AMPK is a key energy sensor and regulates cellular and whole-body

energy metabolism [292]. The interaction with AMPK potentially positions acetylcarnitine as a modulator of these processes. Given its putative AMPK signalling capacity and role as a buffer of acetyl-CoA, acetylcarnitine would be well placed to signal acetyl-CoA status.

## *Chapter Conclusions and Future Directions*

The results of this chapter support the hypothesis that the cellular export of acetylcarnitine is reflective of cellular carnitine uptake and shuttling, *in vitro*. Furthermore it also appears to demonstrate that the d9-L-carnitine/d9-acetylcarnitine CSA assay is sensitive to CPT1 inhibition, although additional replicates of this observation are required. This serves as a useful proof of concept for this assay and paves the way for further development and refinement. In addition, this work supports the hypothesis that primary cardiomyocytes export acetylcarnitine extracellularly, *in vitro*. This raises the intriguing possibility that cardiac acetylcarnitine export may function in cellular energy homeostasis, signalling, or both. However, studies in the intact animal are needed to further address this. In addition, these results support the view that celecoxib and rofecoxib do not have direct effects on CSA, *in vitro*. This lends weight to the conclusions drawn in chapter 5, which suggest that these drugs may interfere with cardiac carnitine concentrations through an effect on hepatic carnitine synthesis.

This chapter has a number of limitations, which could be addressed in future studies. Firstly, the experiments underlying these studies used visual confirmation of cell viability and assumed equal plating of cells. Whilst these are reasonable, objective measures of cell viability and total protein, which could then be normalised for, would help reduce inter-group variability and improve the assay's sensitivity. Secondly, in the primary murine cardiomyocyte assay, only a single reading of d9-acetylcarnitine accumulation was made in the context of etomoxir treatment. Whilst accumulation clearly trended lower in this group than any of the replicates within any other group, additional experiments are required to confirm this. Thirdly, in the primary murine

cardiomyocyte assay, acetylcarnitine accumulation ceased after 15 minutes, probably indicative of exhaustion of the cytosolic long-chain acyl-CoA pool. To avoid this, cells could be supplemented with additional long-chain acyl-CoA. Thirdly, whilst the results indicate that the d9-L-carnitine/d9-acetylcarnitine CSA assay is sensitive to CPT1 inhibition, the inclusion of additional positive controls is required to demonstrate that the assay is sensitive to rate limiting inhibition of the other shuttle components. Finally, confirmation of the ability of this assay to measure CSA, using established CSA assays, would support the conclusions of this work.

## ***Chapter 7: Asymmetric Dimethylarginine and COX-2 Inhibition***

## *Chapter Introduction*

Methylarginines are endogenous inhibitors of NOS, enzymes which synthesise NO [293]. Methylarginine mediated inhibition of NO signalling, which has direct vascular and cardiac effects, has been implicated in HF [294]. In addition, the methylarginine ADMA has been proposed as a mechanistic bridge between COX-2 inhibition and the adverse CV events, such as HF, observed with the coxibs [4]. This hypothesis was based, in part, on findings of higher concentrations of blood ADMA in a mouse model of constitutive global COX-2 KO. However, some have questioned the validity of this mouse model, as it is compromised by severe developmental renal pathology [295]. To probe this mechanism further a reliable mouse model of COX-2 deletion is imperative where the adult effects of COX-2 inhibition can be dissected from the developmental problems associated with global COX-2 deletion. Such a mouse model would allow the simulation of the on-target effects of coxibs, in the adult human, whilst avoiding confounding intra-compound off-target variability. A second model, employing tamoxifen-inducible post-natal global COX-2 KO, circumvents the severe renal pathology seen with constitutive COX-2 KO and may be more reliable [296]. However, this model has been associated with transitory dilated cardiomyopathy (DCM) [297]. Whilst the transient DCM seen in this model was found to resolve functionally, genetically and histopathologically within a few weeks, it is unclear whether it has longer term pathological consequences on the heart [297]. This chapter will attempt to address the question: Does the IPNG COX-2<sup>-/-</sup> mouse exhibit long-term cardiac abnormalities, attributable to DCM? The following hypothesis will be tested:

**The IPNG COX-2<sup>-/-</sup> mouse does not exhibit long-term cardiac abnormalities, attributable to DCM.**

The ADMA-COX-2 hypothesis was also based on observations of higher concentrations of blood ADMA in short-term mouse and human studies of pharmacological COX-2 inhibition [4]. It is unclear whether these findings persist in the longer term. This is an important, clinically relevant, distinction as the adverse CV events observed with coxib use are almost exclusively reported in chronically dosed patients and manifest after a prolonged period of time [1, 88, 89]. This study will attempt to address the question: Does the long-term absence of COX-2 activity cause higher concentrations of ADMA or other methylarginines, in the mouse? The following hypothesis will be tested:

**The long-term absence of COX-2 activity, in the IPNG COX-2<sup>-/-</sup> mouse, is not associated with higher concentrations of ADMA or other methylarginines.**

These hypotheses were tested in the IPNG COX-2<sup>-/-</sup> mouse. COX-2<sup>-/-</sup> deletion was induced by 5 days of intraperitoneal 100 mg/kg/day tamoxifen, which is purported to cause transient DCM. The mice were sacrificed 2 months after study commencement, following over 7 weeks of COX-2 deletion. Targeted metabolomic analysis was performed, on heart and blood samples, to measure markers of cardiac dysfunction and the concentrations of the methylarginines.

# *Chapter Background*

## **Methylarginines**

### *Overview of Methylarginines*

ADMA, L-NMMA and symmetric dimethylarginine (SDMA) are endogenous methyl-derivatives of the amino acid L-arginine. They are formed by the successive actions of protein arginine methyltransferases (PRMTs) and proteolytic enzymes [293]. Protein-incorporated L-arginine can be methylated by PRMT-1, yielding L-NMMA. L-NMMA residues can then be methylated by PRMT-1 or PRMT-2 to yield ADMA or SDMA, respectively [293]. Proteolysis of methylarginine residue-containing proteins releases free-forms of the methylarginines into the cell cytosol [293]. They are exported into the circulation and taken up by other cells via system y<sup>+</sup>-carriers, members of the cationic amino acid transporter (CAT) family [298]. In humans methylarginines are excreted (< 20%), via the urine, and degraded (>80%), predominantly by dimethylarginine dimethylaminohydrolase 1 (DDAH1) [293, 299]. ADMA and L-NMMA, but not SDMA, directly inhibit NOS as they compete with L-arginine, the endogenous substrate, for access to its active site [293]. The degree of inhibition is determined by the substrate-inhibitor ratio and therefore by factors governing ADMA, L-NMMA and L-arginine availability [298]. SDMA may also impair NOS activity, as it competes with L-arginine for access to CAT, thereby reducing intracellular substrate availability [293, 300]. NOS catalyses the synthesis of NO and L-citrulline from L-arginine. Therefore, crucially, the methylarginines impair NO production. The NO/soluble guanylyl cyclase (sGC)/cyclic guanosine monophosphate (cGMP)/protein kinase G (PKG) signalling pathway promotes vasodilation, vascular proliferation and angiogenesis; reduces platelet aggregation and expression of cellular

adhesion molecules; and has direct effects on cardiomyocyte function [293, 298]. It is therefore unsurprising that the methylarginines have been implicated in a wide variety of diseases that can affect the CV system, including hypertension, peripheral and coronary artery disease, type II diabetes, chronic kidney disease, stroke, MI and HF [294, 301]. Of the methylarginines, ADMA has received the most scientific attention [293].

### *Methylarginines in the Context of Heart Failure*

A number of clinical studies have noted higher concentrations of ADMA, L-NMMA and SDMA in patients with HF. This may occur due to increased proteolysis, by autophagy and proteasome activity, during tissue remodelling and inflammation which are seen in HF [293]. Increases in the methylarginines correlate with greater dysfunction and predict major adverse CV events and mortality in HF patients [152, 153, 301-313]. For example, von Haehling et al. used LC-MS to measure ADMA concentrations in 113 patients with HF and 26 controls. They noted that patients with HF had, on average, a 15% greater concentration of blood ADMA compared to controls ( $P < 0.0001$ ). They also reported that ADMA concentrations were higher with increasing HF severity (defined by New York Heart Association (NYHA) functional class; ANOVA  $P < 0.0001$ ) and that HF of ischaemic origin and non-ischaemic origin did not differ in terms of blood ADMA concentrations [153]. Anderssohn et al. measured L-Arginine, ADMA and SDMA concentrations, using LC-MS, in 341 patients with HF. They noted significantly higher concentrations of blood ADMA ( $P < 0.001$ ) and SDMA ( $P < 0.001$ ), and lower concentrations of L-arginine ( $P < 0.01$ ), in patients with NYHA class III/IV compared to those with NYHA class I/II HF [304]. Hsu et al. measured blood concentrations of ADMA, using LC-MS, in 285 patients with HF of ischaemic origin. The authors noted that blood ADMA concentrations were positively correlated with NYHA functional class

( $P < 0.001$ ) and, using multivariate Cox regression analysis to adjust for confounding factors, demonstrated that ADMA was a significant independent risk factor for major adverse CV events [152]. Zairis et al. measured the blood ADMA concentrations, using LC-MS, of 651 consecutive patients admitted to hospital with acute decompensated HF, NYHA class III/IV. The authors stratified the patients into quartiles according to ADMA concentrations at presentation. They noted that, even after adjustment for confounding factors, patients belonging to the highest ADMA quartile were at greater risk of in-hospital mortality ( $P = 0.042$ ) and mortality at 31 days ( $P = 0.032$ ) and 1 year ( $P < 0.001$ ) compared to those in the lowest ADMA quartile [308]. These findings have been recapitulated in large and small animal models of HF [314, 315].

ADMA has also been directly linked to cardiac dysfunction and hypertension. For example, Achan et al. conducted a small, randomised, double-blind, placebo-controlled study into the effects of low-dose ADMA administration. They noted that ADMA caused lower heart rate ( $P < 0.001$ ), cardiac output ( $P < 0.001$ ) and the magnitude of the cardiac output adaptive-response to exercise ( $P < 0.05$ ), whilst also causing higher blood pressure ( $P < 0.005$ ) and systemic vascular resistance ( $P < 0.001$ ) [316]. Kielstein et al. also examined the effects of ADMA administration. The authors also demonstrated higher blood pressure in the AMDA treated group ( $P < 0.05$ ). In addition, they noted more sodium retention and renovascular resistance and less renal blood flow ( $P < 0.05$  for all three) [317]. Animal studies support these findings [318].

It has been postulated that methylarginine mediated inhibition of NO-signalling may exacerbate HF directly and indirectly [293]. NO plays a direct role in cardiac signalling and adaptation to stress and methylarginine mediated inhibition of NO synthesis impairs this. Post MI, NO/sGC/cGMP/PKG signalling modulates cardiac contractility

and remodelling and NO mediated s-nitrosylation of L-type  $\text{Ca}^{2+}$  channels and ryanodine receptors preserves cardiac ion balance. NO mediated s-nitrosylation also regulates GPCR signalling and phosphodiesterase type 5 (PDE5) stability, which protect against HF progression. Methylarginines may also promote superoxide production by uncoupling NOS, leading to free radical damage and promoting HF [293]. In addition, methylarginine-mediated impairment of NO synthesis indirectly promotes the exacerbation of HF by increasing several risk factors, including hypertension, atherosclerosis, coronary disease, renal dysfunction and diabetes [293].

However, whilst methylarginines are higher in HF, they have also been reported to be higher in numerous other CV diseases and non-CV diseases [294]. In addition, in the general population, who are at low-risk of CV disease, ADMA is a better predictor of total mortality than CV risk [319, 320]. Methylarginine accumulation is therefore a fairly non-specific marker of disease. Consequently, a consensus has not been reached regarding whether methylarginine accumulation can actually cause or exacerbate HF [293].

### *Methylarginines and Non-Steroidal Anti-Inflammatory Drug Use*

In the last couple of years, a hypothesis associating the CV events seen with NSAIDs and the methylarginines has been proposed. Ahmetaj-Shala et al. suggest that ADMA and L-NMMA serve as a biomarker and mechanistic link between COX-2 inhibition in the kidney and the adverse CV events associated with NSAIDs [4]. Their hypothesis is based on both animal studies and clinical observations. Transcriptome analysis of tissues from a constitutive global COX-2<sup>-/-</sup> mouse model demonstrated only a single gene change in the heart and aorta, but alterations in 1018 genes by >1.5 fold in the kidney medulla [4]. Ahmetaj-Shala et al. therefore applied a focused gene pathway

analysis, examining transcripts involved in blood pressure control, vascular tone and vascular hormones. This directed them towards ADMA and L-NMMA metabolism and, subsequently, they found a higher ADMA:L-arginine ratio (~12-fold,  $P = 0.03$ ) and the L-NMMA:L-arginine ratio (~17-fold,  $P = 0.03$ ), but not the SDMA:L-arginine ratio, in the blood of constitutive global COX-2<sup>-/-</sup> mice, compared to their COX-2<sup>+/+</sup> littermate controls [4]. However, the constitutive global COX-2<sup>-/-</sup> mouse model has been criticised because COX-2 is required for normal nephrogenesis [3]. Ahmetaj-Shala et al. next examined the effect of short-term pharmacological inhibition of COX-2. Firstly, they administered 100 mg/kg/day parecoxib – the pro-drug of valdecoxib, in drinking water for 4 days to wild-type (WT) mice. They reported a higher ADMA:L-arginine ratio (~3-fold,  $P = 0.009$ ) and L-NMMA:L-arginine ratio (~3-fold,  $P = 0.006$ ) in the blood of the parecoxib treated animals compared to controls. These differences were abolished in the presence of a high-salt diet [4]. It should be noted that a single oral dose of 5 mg/kg valdecoxib effectively attenuates pain in the mouse, suggesting that 100 mg/kg/day parecoxib may be excessive and could cause biologically relevant COX-1 inhibition [321]. Secondly, the authors conducted a small clinical study, where they administered healthy human volunteers either 200 mg celecoxib twice a day or 500 mg naproxen twice a day, for 1 week. They noted higher blood concentrations of ADMA (~1.2-fold,  $P = 0.05$ /~1.25-fold,  $P < 0.01$ ) and creatinine (~1.55/~1.5), but not L-NMMA and SDMA, in both the celecoxib/naproxen treated groups, respectively, compared to controls. This was a much smaller fold-change than they observed in mice [4]. The authors did not report L-arginine concentrations in this clinical study. This is surprising, as they themselves demonstrated that L-arginine supplementation reverses the vascular dysfunction seen in constitutive global COX-2<sup>-/-</sup> mice, highlighting the biological relevance of the relative concentrations of methylarginines and L-arginine

[4]. The higher levels of ADMA, observed in these studies, are consistent with the observation that NSAIDs increase systolic blood pressure (BP) [322]. However, neither of these studies were longer than 1 week in duration, which makes extrapolating their findings to long-term BP regulation difficult.

In support of the ADMA-COX-2 hypothesis, Kruszelnicka et al. reported that ADMA concentrations were higher in patients with RA and that higher ADMA correlated with atherosclerosis [323]. These patients were all taking NSAIDs [324]. In addition, some were prescribed proton pump inhibitors (PPIs) to protect against NSAID associated adverse GI events. PPIs have been shown to inhibit DDAH1, hence ADMA degradation. Kruszelnicka et al. proposed that in those patients with RA taking both NSAIDs and PPIs, ADMA accumulation may be greater [323].

However, another possibility is that concentrations of ADMA reflect levels of systemic inflammation [325]. This is biologically plausible as inflammation is associated with proteolysis and autophagy, which release ADMA in its free-form [293]. This is also supported by clinical data. For example, Sandoo et al. reported that, in 201 patients with RA, blood ADMA concentrations were associated with the mean inflammatory burden over the preceding 6 years, as calculated by C-reactive protein (CRP) measurements every 3 months [326]. On this basis one might anticipate that, in the case of diseases or insults with a significant inflammatory component, the NSAIDs may actually reduce blood ADMA concentrations. Recent evidence in smokers supports this. Smoking promotes an inflammatory environment, enhancing vascular and systemic inflammatory signalling through COX-2 [327-329]. In a randomised, double-blind, cross-over study, in 28 smokers, Vlachopoulos et al. reported that smoking a single cigarette causes an increase in blood ADMA, which is prevented by treatment with aspirin or celecoxib 3 hours before [329]. This evidence seems at-odds

with that presented by Ahmetaj-Shala et al. However it should be noted that their findings, regarding the effect of COX-2 inhibitors on ADMA concentrations, are based on observations in healthy volunteers and wild-type animals, without inflammatory burden [4]. It is therefore conceivable that, in the context of disease and inflammation, the anti-inflammatory (possibly ADMA-lowering) effects of NSAIDs may outweigh the apparent ADMA increasing effects detected in the absence of inflammation, observed by Ahmetaj-Shala et al. This calls into question the biological relevance of Ahmetaj-Shala et al.'s hypothesis.

## **Global COX-2<sup>-/-</sup> Mouse Models**

### *Constitutive Global COX-2<sup>-/-</sup> Mouse*

The constitutive global COX-2<sup>-/-</sup> mouse, used by Ahmetaj-Shala et al., was first published in 1995 by Morham et al. at a time when COX-2 was considered simply a mediator of inflammation [295]. The authors used a combination of restriction enzymes, the  $\lambda$ -bacteriophage vector and homologous recombination to generate an E14TG2a mouse embryonic stem cell (ESC) line in which the COX-2 gene was disrupted [295]. This mutant cell line was then injected into a C57BL/B6 mouse blastocyst. The resultant chimeric mouse was mated with a C57BL/B6 mouse, yielding heterozygous F1 progeny. These were interbred and homozygous mutant F2 mice were selected from their offspring. [295]. The authors reported that these constitutive global COX-2<sup>-/-</sup> mice exhibited glomerular sclerosis and tubulointerstitial injury at 16 weeks, but not at 3 days. In the mouse, the kidney continues to develop for a number of weeks after birth. These findings, which are concomitant with post-natal developmental arrest at the subcapsular nephrogenic zone, likely reflect a reduced number of overworked nephrons [295]. COX-2 has since been shown to be constitutively expressed in the developing mouse kidney, further indicating that it plays

a role in nephrogenesis [35, 330]. Moreover, pre-natal exposure of mice to a COX-2 inhibitor has been shown to produce similar results [3, 331]. Lastly, higher levels of ADMA are associated with glomerular sclerosis and tubulointerstitial injury [332, 333].

### *IPNG COX-2<sup>-/-</sup> Mouse*

The IPNG COX-2<sup>-/-</sup> mouse was developed by the FitzGerald group [159]. It was designed to overcome the limitations associated with constitutive COX-2 KO, to better simulate pharmacological inhibition of COX-2 in the adult human [159]. The FitzGerald group employed a Cre-Lox recombination strategy. Briefly, they used a combination of restriction enzymes, electroporation, and homologous recombination to generate a floxed ESC line. These cells possess LoxP sites at introns 5 and 8 of the COX-2 gene [159]. The floxed-COX-2 ESC line was injected into a C57BL/B6 mouse blastocyst. The resultant adult mouse was mated with a C57BL/B6 mouse and the F1 generation interbred. Homozygous floxed-COX-2 mice were selected and crossed with homozygous Cre-ER mice. Their F1 generation was interbred. Mice in the F2 generation, homozygous for both floxed-Cox-2 and Cre-ER, were selected. These mice exhibit inducible global COX-2 genetic deletion. This is because they express a Cre-recombinase-oestrogen receptor fusion protein that is tamoxifen inducible [159]. Cre-recombinase cuts at LoxP sites. When the Cre-ER fusion protein is induced by tamoxifen, the Cre-recombinase domain cuts at the LoxP sites in introns 5 and 8 of the COX-2 gene, deleting exons 6 to 8 and disrupting the gene [334]. It is therefore possible to induce the global COX-2 knock-out post-natally in the mouse, after the kidneys have fully developed. This avoids the developmental kidney pathology seen in the constitutive global COX-2<sup>-/-</sup> mouse [296]. However, it has been suggested that this mechanism of post-natal COX-2 knock-out causes cardiac toxicity [335]. Koitabashi et al. noted that, tamoxifen-induced nuclear translocation of the Cre-ER

fusion protein can cause severe transitory DCM in mice, accompanied by significant alterations in cardiac function, expression of genes governing cardiac energy metabolism and stress response. These effects were manifest three days after completing a 7-day course of oral 80 mg/kg/day tamoxifen and resolved after a further 18 days. No longer-term observations were made [297]. Despite the transitory nature of this cardiac insult, Ahmetaj Shala et al. concluded that the IPNG COX-2<sup>-/-</sup> mouse is a compromised system [4]. Despite this potential limitation, I believe that overall the IPNG COX-2<sup>-/-</sup> mouse represents a less confounded system in which to investigate the proposed link between inhibition of COX-2 in the kidney and ADMA, and is the primary focus of this chapter.

## *Chapter Methods*

In Study 5, 20 mice (11 inducible post-natal global COX-2<sup>-/-</sup> mice and 9 littermate controls) were sacrificed and their tissues and bio-fluids analysed using NMR spectroscopy and LC-MS/MS, to determine whether COX-2 deletion alters methylarginine metabolism and cardiac metabolic function. In Study 6, 20 mice (13 inducible post-natal global COX-2<sup>-/-</sup> mice and 10 littermate controls) were treated with angiotensin II for 4 weeks then sacrificed. Their tissues and bio-fluids were analysed using NMR spectroscopy and LC-MS/MS, to determine what impact blood pressure dysregulation has on methylarginine metabolism and cardiac metabolic function, in the context of COX-2 deletion.

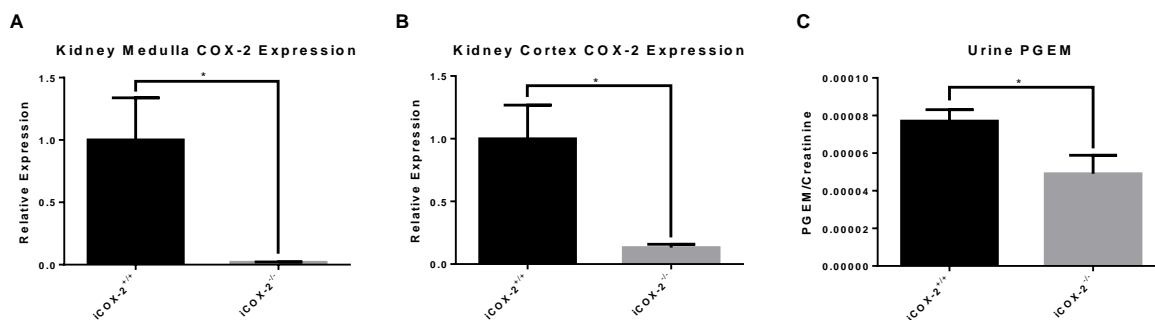
The following methods (see chapter 3 for a detailed description of each) were used in this chapter:

- **Studies 5 and 6**
- **Methanol/Chloroform/Water Metabolite Double Extraction**
- **Nuclear Magnetic Resonance (NMR) Spectroscopy**
- **Non-Butylating Method of Sample Preparation for LC-MS/MS Carnitine Assay**
- **LC-MS/MS Carnitine Assay**
- **LC-MS/MS Aqueous Metabolite Assay**
- **Processing of Metabolomic Data**
- **Unpaired t-Test**
- **Mann-Whitney U-Test**
- **PCA and PLS-DA**
- **Multivariate Model Validation**

## Chapter Results

Evidence that the IPNG COX-2<sup>-/-</sup> mice used in this study exhibit COX-2 gene deletion was provided by Dr Emanuela Ricciotti, of the University of Pennsylvania (Figure 1).

Figure 1.



COX-2 expression and urinary PGEM concentrations in IPNG COX-2<sup>-/-</sup> mice compared to littermate control mice. COX-2 expression in (A) kidney medulla and (B) kidney cortex, measured by RT-qPCR. (C) Urinary PGEM concentration, measured by LC-MS/MS. Data are mean  $\pm$  S.E.M for  $n = 4-6$ . (\* =  $P < 0.05$ ). Abbreviations: Cyclooxygenase-2 (COX-2); Prostaglandin E<sub>2</sub> Metabolite (PGEM); Inducible post-natal global COX-2 knock-out mice (iCOX-2<sup>-/-</sup>); Inducible post-natal global cyclooxygenase-2 littermate control mouse (iCOX-2<sup>+/+</sup>).

Kidney COX-2 expression and the urinary metabolite of PGE<sub>2</sub> (PGEM) are significantly lower in IPNG COX-2<sup>-/-</sup> mice compared to littermate control mice.

### IPNG COX-2<sup>-/-</sup> Mouse Cardiac Metabolism

To examine whether the mouse model used in this experiment exhibits unresolved alterations in cardiac metabolism, caused by prior severe transient DCM, cardiac metabolites were profiled in the cardiac tissue of IPNG COX-2<sup>-/-</sup> and COX<sup>+/+</sup> control mice, using LC-MS/MS, GC-MS and NMR spectroscopy. Metabolites involved in cardiac energy metabolism as well as other small molecule markers of cardiac dysfunction, associated with DCM, were examined

#### *Substrates of Cardiac Energy Metabolism*

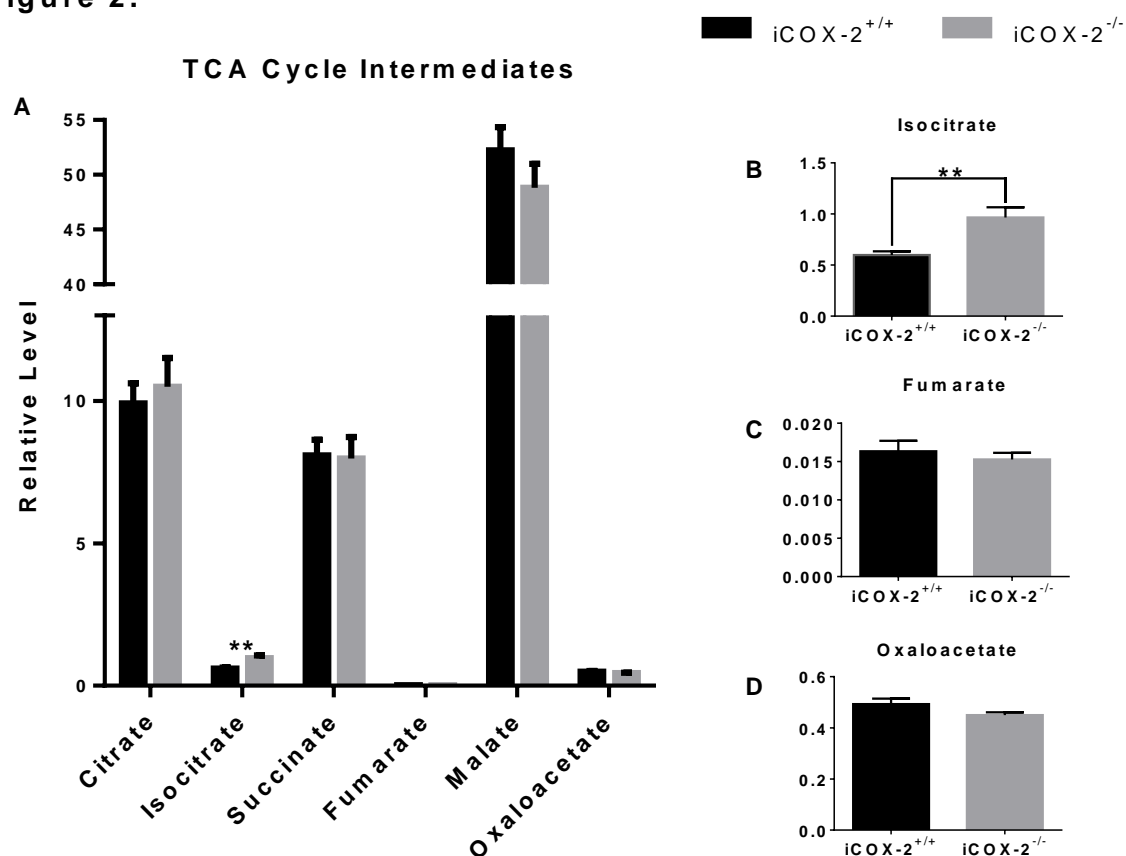
The heart preferentially metabolises FAs, though is metabolically omnivorous. Given the result of chapter 5 in which no significant differences were observed in cardiac

carnitine concentrations (which are indicative of FA metabolism) between IPNG COX-2<sup>-/-</sup> mice and COX-2<sup>+/+</sup> controls, other cardiac energy substrates were examined.

The heart is capable of deriving energy from glycolysis. Given that the lactate dehydrogenase (LDH) reaction is at near-equilibrium, heart lactate represents a useful way of sampling pyruvate concentrations and hence total cardiac glycolytic activity [336]. In addition, circulating lactate can be taken up by the heart and used as a fuel [337]. Therefore, heart lactate concentrations were measured using NMR spectroscopy. No differences in heart lactate were found between IPNG COX-2<sup>-/-</sup> and COX-2<sup>+/+</sup> control mice (data not shown).

The TCA cycle is at the centre of energy metabolism. Six TCA cycle intermediates (citrate, isocitrate, succinate, fumarate, malate and oxaloacetate) were measured with LC-MS/MS (*Figure 2*). Isocitrate was found to be higher in the hearts of IPNG COX-2<sup>-/-</sup> compared to COX-2<sup>+/+</sup> control mice (1.5-fold greater,  $P = 0.0015$ ). No differences were observed in the other five TCA cycle intermediates. Succinate and fumarate were also measured using NMR spectroscopy (data not shown) and the results confirmed the LC-MS/MS data.

**Figure 2.**

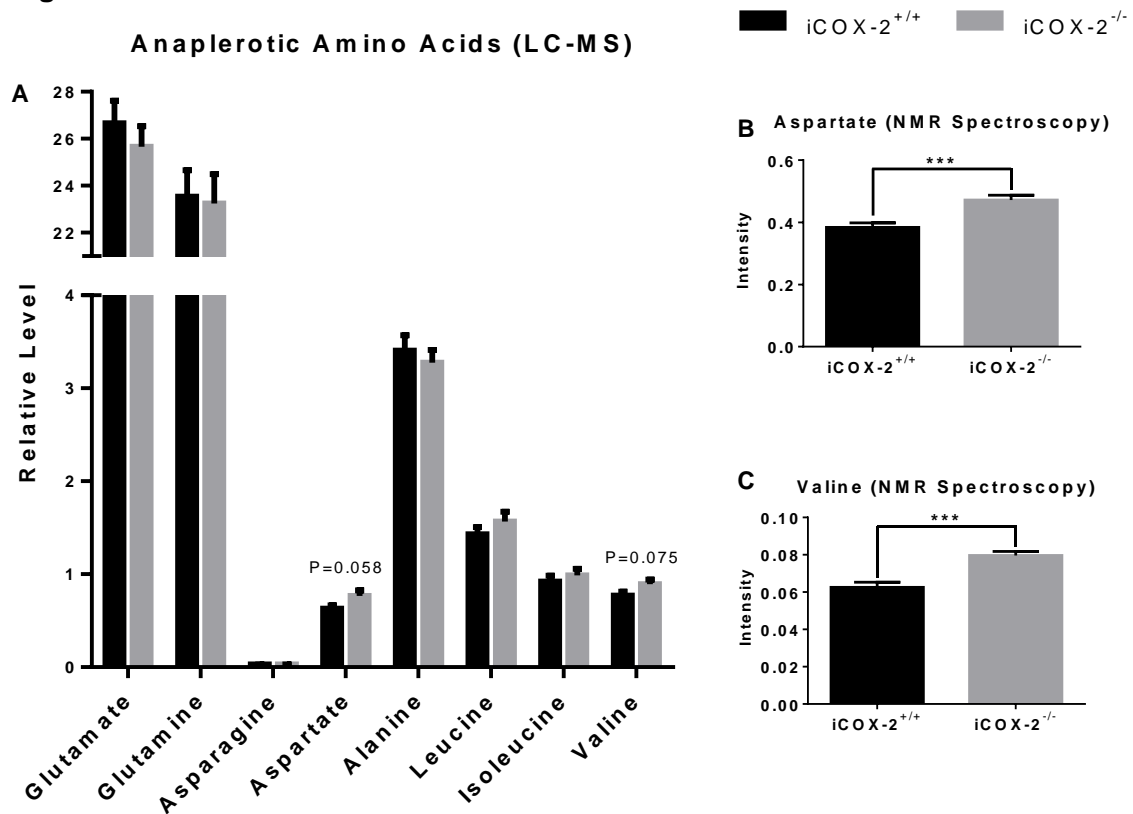


Effect of post-natal COX-2 gene deletion on concentrations of TCA cycle intermediates in the heart, in mice. Effect of post-natal COX-2 gene deletion on (A) Citrate, Isocitrate, Succinate, Fumarate, Malate and Oxaloacetate; (B) Isocitrate (expanded); (C) Fumarate (expanded) and (D) Oxaloacetate (expanded). Measured by LC-MS/MS. Data are mean  $\pm$  S.E.M for  $n = 9-10$ . (\*\* =  $P < 0.01$ ). Abbreviations: Tricarboxylic acid (TCA); Inducible post-natal global cyclooxygenase-2 knock-out mouse (iCOX-2<sup>-/-</sup>); Inducible post-natal global cyclooxygenase-2 littermate control mouse (iCOX-2<sup>+/+</sup>).

A range of anaplerotic substrates can replenish cardiac TCA cycle intermediates. Given the relatively higher levels of isocitrate in the IPNG COX-2<sup>-/-</sup> mice, in the absence of changes in FA and lactate metabolism, a number of anaplerotic substrates were investigated, in an attempt to rationalise this observation. Cardiac concentrations of the ketone body,  $\beta$ -hydroxybutyrate, were measured by LC-MS/MS. No significant differences were observed between IPNG COX-2<sup>-/-</sup> and COX-2<sup>+/+</sup> control mice (data not shown). A panel of eight anaplerotic amino acids, including the BCAAs, were measured using LC-MS/MS [338]. Five of these were also measured using NMR spectroscopy. Valine, for example, was analysed using both LC-MS/MS (precursor

m/z = 118.1, product m/z = 78.2, RT = 1.35 min on a C18 pentafluoropheny column, normalised to  $^{13}\text{C}^{15}\text{N}$  glutamic acid) and NMR spectroscopy (integration of the doublet at 1.03 ppm, normalised to TSP). The LC-MS/MS results indicated that, whilst not significantly different, aspartate and valine concentrations were higher in the hearts of IPNG COX-2<sup>-/-</sup> compare to COX-2<sup>+/+</sup> control mice (Figure 3 A). These findings were confirmed and extended by analysis of the NMR spectroscopy results (Figure 3 B and C), which demonstrated significantly higher levels of both aspartate and valine (1.2-fold higher,  $P = 0.0008$  and 1.3-fold higher,  $P = 0.0001$ , respectively). No differences were observed in the other anaplerotic amino acids.

**Figure 3.**



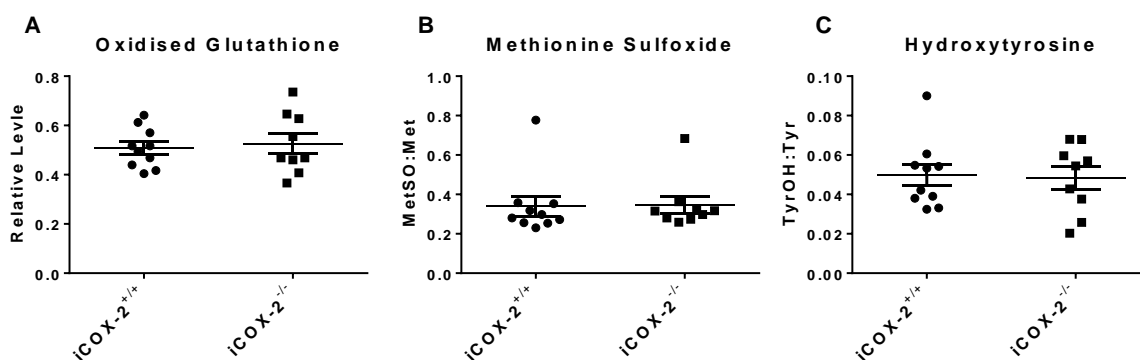
Effect of post-natal COX-2 gene deletion on concentrations of selected anaplerotic amino acids in the heart in mice. Effect of post-natal COX-2 gene deletion on (A) Glutamate, Glutamine, Asparagine, Aspartate, Alanine, Leucine, Isoleucine and Valine measured by LC-MS/MS; (B) Aspartate and (C) Valine measured by NMR spectroscopy. Data are mean  $\pm$  S.E.M for  $n = 9-10$ . (\*\*\*) =  $P < 0.001$ . Abbreviations: Inducible post-natal global cyclooxygenase-2 knock-out mouse (iCOX-2<sup>-/-</sup>); Inducible post-natal global cyclooxygenase-2 littermate control mouse (iCOX-2<sup>+/+</sup>).

Multivariate analysis was used to determine whether the changes observed in isocitrate, aspartate and valine were part of a global effect on cardiac energy metabolism. To do this, these metabolites were considered alongside the other cardiac energy substrates measured in this chapter. A PLS-DA model could not be built to discriminate IPNG COX-2<sup>-/-</sup> mice from COX-2<sup>+/+</sup> controls (data not shown).

### *Small Molecule Markers of Cardiac Dysfunction*

Cardiac dysfunction is often associated with increased oxidative stress, which has been reported in DCMs [339, 340]. Oxidised glutathione (GSSG), methionine sulfoxide (MetSO) and hydroxytyrosine (TyrOH) have previously been identified as markers of oxidative stress [341-343]. GSSG and the ratios of MetSO to methionine (Met) and TyrOH to tyrosine (Tyr) were measured by LC-MS/MS. No significant differences were noted in GSSG or the MetSO:Met and TyrOH:Tyr ratios in the hearts of IPNG COX-2<sup>-/-</sup> compared to COX-2<sup>+/+</sup> control mice (*Figure 4 A-C*).

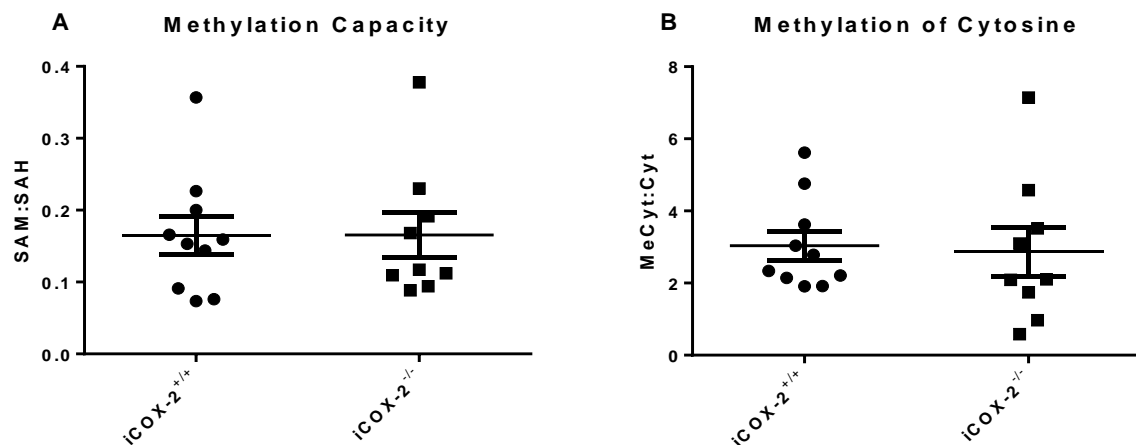
**Figure 4.**



*Effect of post-natal COX-2 gene deletion on concentrations of selected markers of oxidative stress in the heart, in mice. Effect of post-natal COX-2 gene deletion on (A) Oxidised Glutathione (B) Methionine Sulfoxide:Methionine ratio and (C) Hydroxytyrosine:Tyrosine ratio, measured by LC-MS/MS. Data are mean ± S.E.M for n = 9-10. No significant changes were observed. Abbreviations: Inducible post-natal global cyclooxygenase-2 knock-out mouse (iCOX-2<sup>-/-</sup>); Inducible post-natal global cyclooxygenase-2 littermate control mouse (iCOX-2<sup>+/+</sup>).*

Models of DCM have also been associated with aberrant DNA methylation in the heart [344]. Of the four DNA bases cytosine (Cyt) and adenine can be methylated, yielding methylcytosine (MeCyt) and methyladenine. The methyltransferases responsible for DNA methylation use S-adenosylmethionine (SAM) as a substrate and produce S-adenosylhomocysteine (SAH). The SAM:SAH ratio has been used as a measure of methylation capacity [345]. The SAM:SAH and MeCyt:Cyt ratios were measured by LC-MS/MS. No significant differences were noted in either the SAM:SAH or MeCyt:Cyt ratios, in the hearts of IPNG COX-2<sup>-/-</sup> compared to COX-2<sup>+/+</sup> control mice (*Figure 5 A and B*).

**Figure 5.**

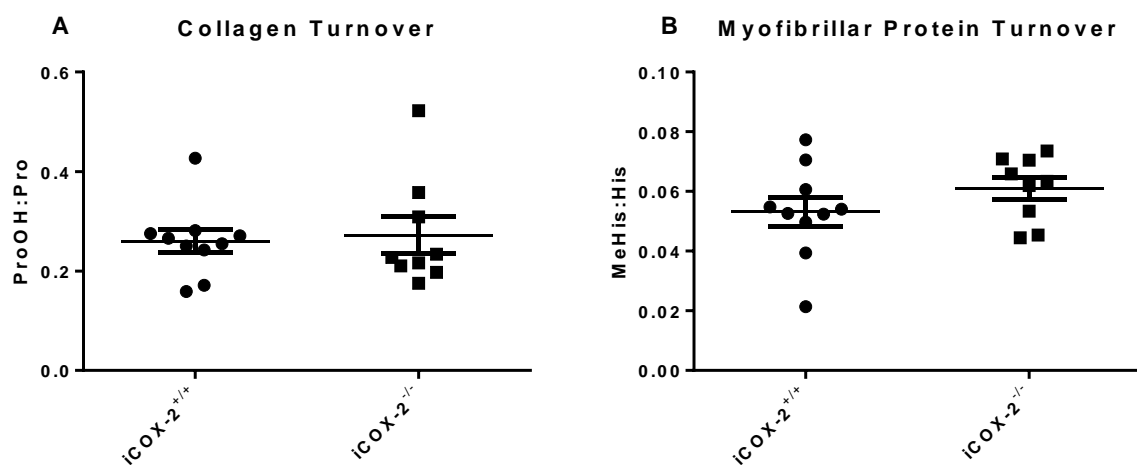


*Effect of post-natal COX-2 gene deletion on concentrations of selected markers of DNA methylation in the heart, in mice. Effect of post-natal COX-2 gene deletion on (A) S-Adenosylmethionine:S-Adenosylhomocysteine ratio and (B) 5-Methylcytosine:Cytosine ratio, measured by LC-MS/MS. Data are mean  $\pm$  S.E.M for n = 9-10. No significant changes were observed. Abbreviations: S-Adenosylmethionine (SAM); S-Adenosylhomocysteine (SAH); 5-Methylcytosine (MeCyt); Cytosine (Cyt); Inducible post-natal global cyclooxygenase-2 knock-out mouse (iCOX-2<sup>-/-</sup>); Inducible post-natal global cyclooxygenase-2 littermate control mouse (iCOX-2<sup>+/+</sup>).*

DCM is associated with cardiac structural remodelling. This includes degradation of the collagen scaffold and increased fibrosis, resulting in collagen turnover [346]. It may also be associated with the degradation of myofibrillar proteins [172]. When proline (Pro) is incorporated into collagen it is post-translationally modified, forming hydroxyproline (ProOH). Similarly, histidine (His) incorporated into myofibrillar proteins

can be post-translationally modified to form methylhistidine (MeHis) [194]. The free ProOH:Pro and MeHis:His ratios therefore serve as useful markers of collagen and myofibrillar protein turnover, respectively. The free ProOH:Pro and MeHis:His ratios were measured by LC-MS/MS. No significant differences were noted in either the free ProOH:Pro or MeHis:His ratios, in the hearts of IPNG COX-2<sup>-/-</sup> compared to COX-2<sup>+/+</sup> control mice (*Figure 6 A and B*).

**Figure 6.**



*Effect of post-natal COX-2 gene deletion on concentrations of selected markers of collagen and myofibrillar protein turnover in the heart, in mice. Effect of post-natal COX-2 gene deletion on (A) Hydroxyproline:Proline ratio and (B) Methylhistidine:Histidine ratio, measured by LC-MS/MS. Data are mean ± S.E.M for n = 9-10. No significant changes were observed. Abbreviations: Hydroxyproline (ProOH); Proline (Pro); Methylhistidine (MeHis); Histidine (His); Inducible post-natal global cyclooxygenase-2 knock-out mouse (iCOX-2<sup>-/-</sup>); Inducible post-natal global cyclooxygenase-2 littermate control mouse (iCOX-2<sup>+/+</sup>).*

## IPNG COX-2<sup>-/-</sup> Mouse Methylarginine Metabolism

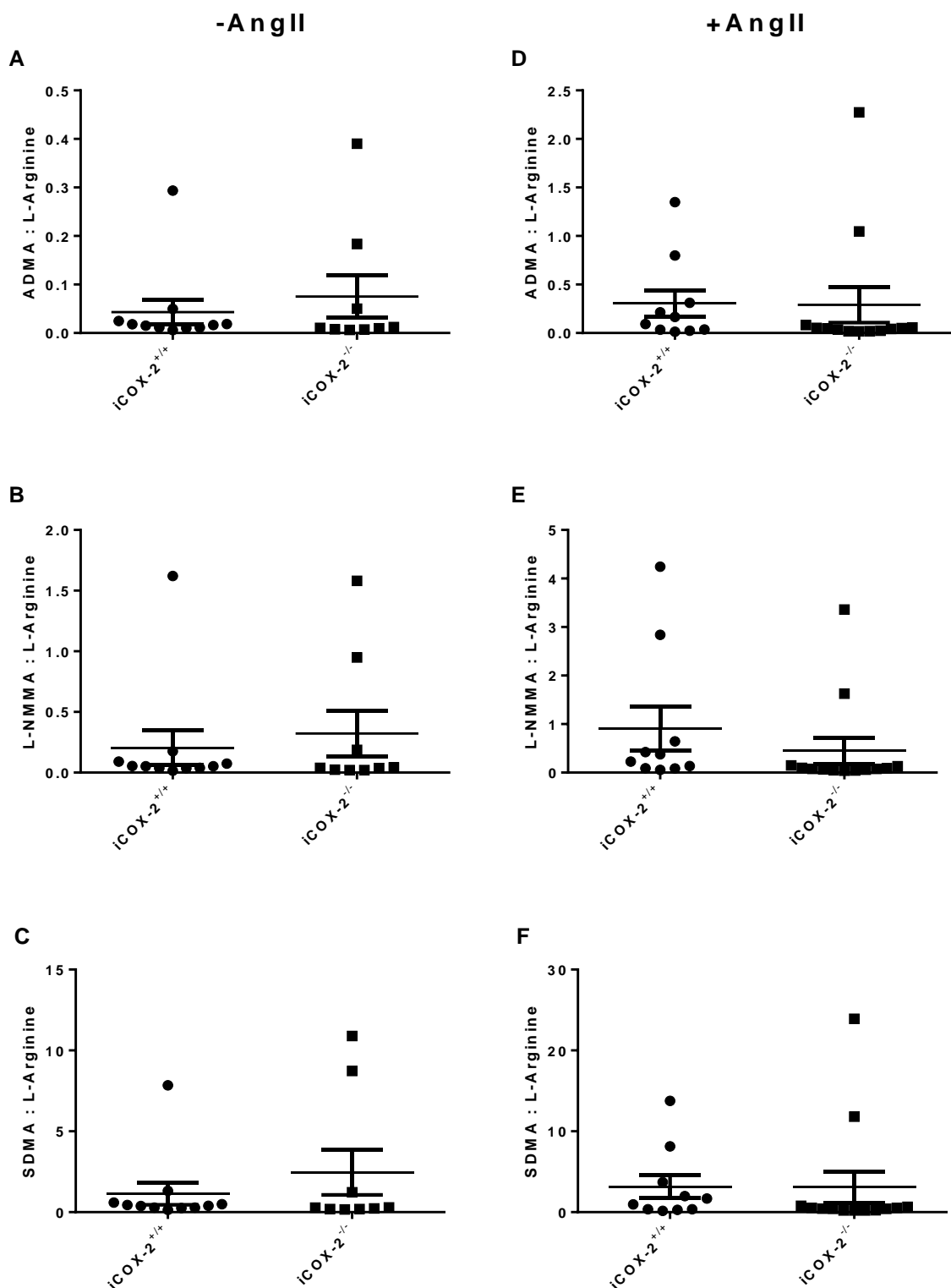
### *Arginine and Methylarginines in the Blood*

To address the validity of the higher blood ADMA:L-arginine and L-NMMA:L-arginine ratios, reported by Ahmetaj-Shala et al. in the constitutive global COX-2<sup>-/-</sup> mouse, an attempt to recapitulate these findings in the IPNG COX-2<sup>-/-</sup> mouse was made. Blood concentrations of L-arginine, ADMA, L-NMMA and SDMA were measured using LC-MS/MS. No differences were observed in the blood ADMA:L-arginine, L-NMMA:L-

arginine and SDMA:L-arginine ratios in the IPNG COX-2<sup>-/-</sup> mouse compared to COX-2<sup>+/+</sup> littermate controls (*Figure 7 A-C*). These findings are at odds with those reported in the constitutive global COX-2<sup>-/-</sup> mouse [4]. The methylarginines have been directly linked to hypertension. In addition, differences between parecoxib treated and control mice, with respect to blood ADMA:L-arginine and L-NMMA:L-arginine ratios, were abolished by dietary induced hypertension, with the control group then also exhibiting high ratios [4]. Furthermore, in cases where there is inappropriate activation of the renin angiotensin system, COX-2 has been shown to modulate the undesirable effects of angiotensin II [31]. Therefore, the effects of angiotensin II induced hypertension, on blood ADMA:L-arginine, L-NMMA:L-arginine and SDMA:L-arginine ratios, in the IPNG COX-2<sup>-/-</sup> mouse were examined. No differences were observed in the blood ADMA:L-arginine, L-NMMA:L-arginine and SDMA:L-arginine ratios in the IPNG COX-2<sup>-/-</sup> mouse compared to COX-2<sup>+/+</sup> controls (*Figure 7 D-F*). As anticipated, blood ADMA:L-arginine, L-NMMA:L-arginine and SDMA:L-arginine ratios were higher in the presence of angiotensin II infusion for all groups, though only higher ADMA:L-arginine and L-NMMA:L-arginine ratios in the COX-2<sup>+/+</sup> control mice reached statistical significance (7.9- and 5.7-fold greater, respectively,  $P = 0.0062$  for both; data not shown).

It was not possible to build a PLS-DA model, to discriminate the seven outliers from the other observations in Figure 7 (either together or separately as +/- angiotensin II groups) and therefore, besides the outlying methylarginine:arginine ratios, no other differences were observed and no explanations forthcoming.

**Figure 7.**

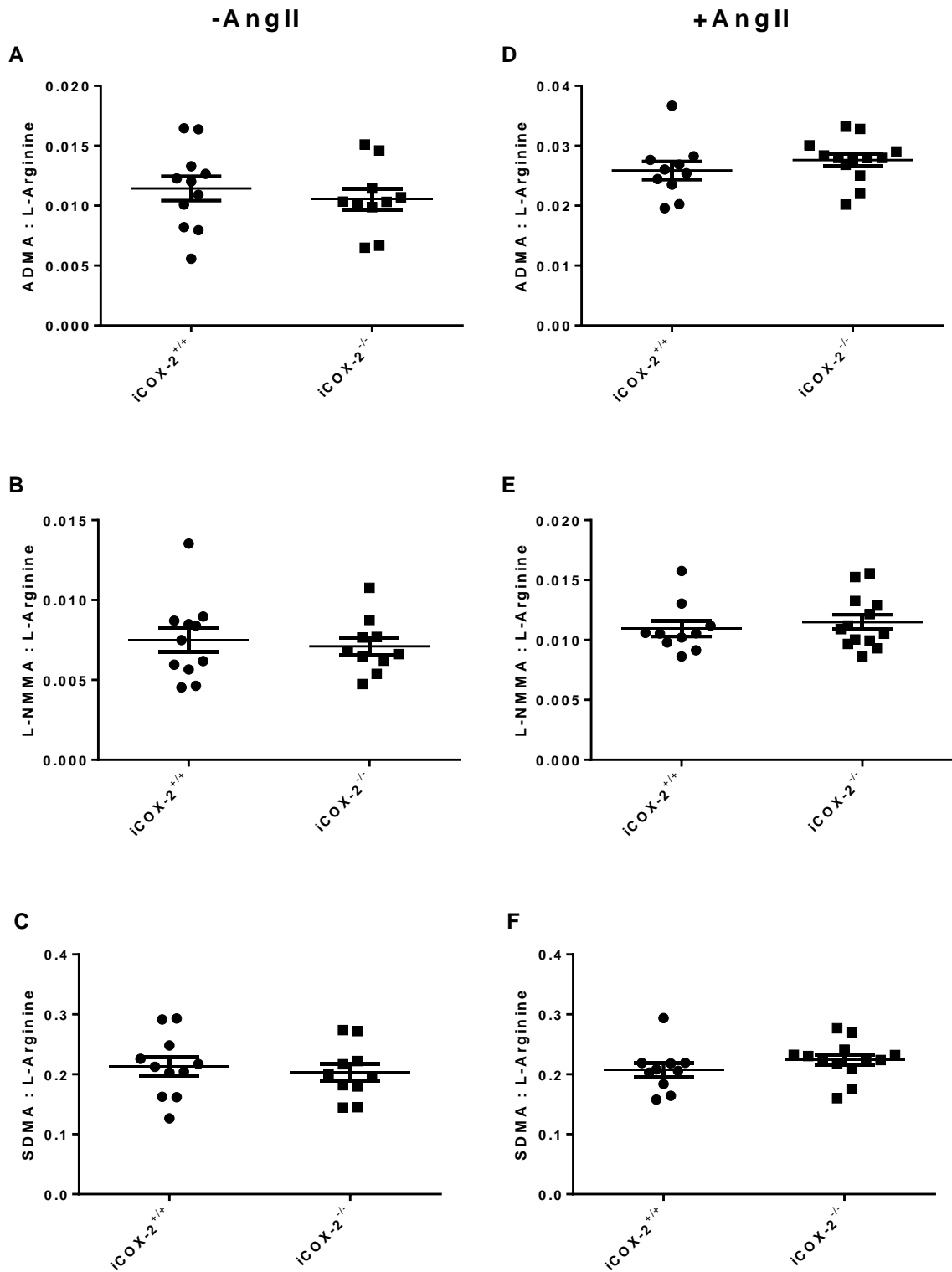


Effect of post-natal COX-2 gene deletion and AngII infusion on blood methylarginines to L-arginine ratios in mice. Effect of post-natal COX-2 gene deletion on (A) ADMA:L-Arginine; (B) L-NMMA:L-Arginine and (C) SDMA:L-Arginine. Effect of post-natal COX-2 gene deletion and AngII infusion on (D) ADMA:L-Arginine; (E) L-NMMA:L-Arginine and (F) SDMA:L-Arginine. Measured by LC-MS/MS. Data are mean  $\pm$  S.E.M for (A-C)  $n = 9-11$ , (D-F)  $n = 10-13$ . No significant changes were observed. Abbreviations: Asymmetric dimethylarginine (ADMA); Monomethyl-L-arginine (L-NMMA); Symmetric dimethylarginine (SDMA); Angiotensin II (AngII); Inducible post-natal global cyclooxygenase-2 knock-out mouse (*iCOX-2<sup>-/-</sup>*); Inducible post-natal global cyclooxygenase-2 littermate control mouse (*iCOX-2<sup>+/+</sup>*).

## *Arginine and Methylarginines in the Kidney*

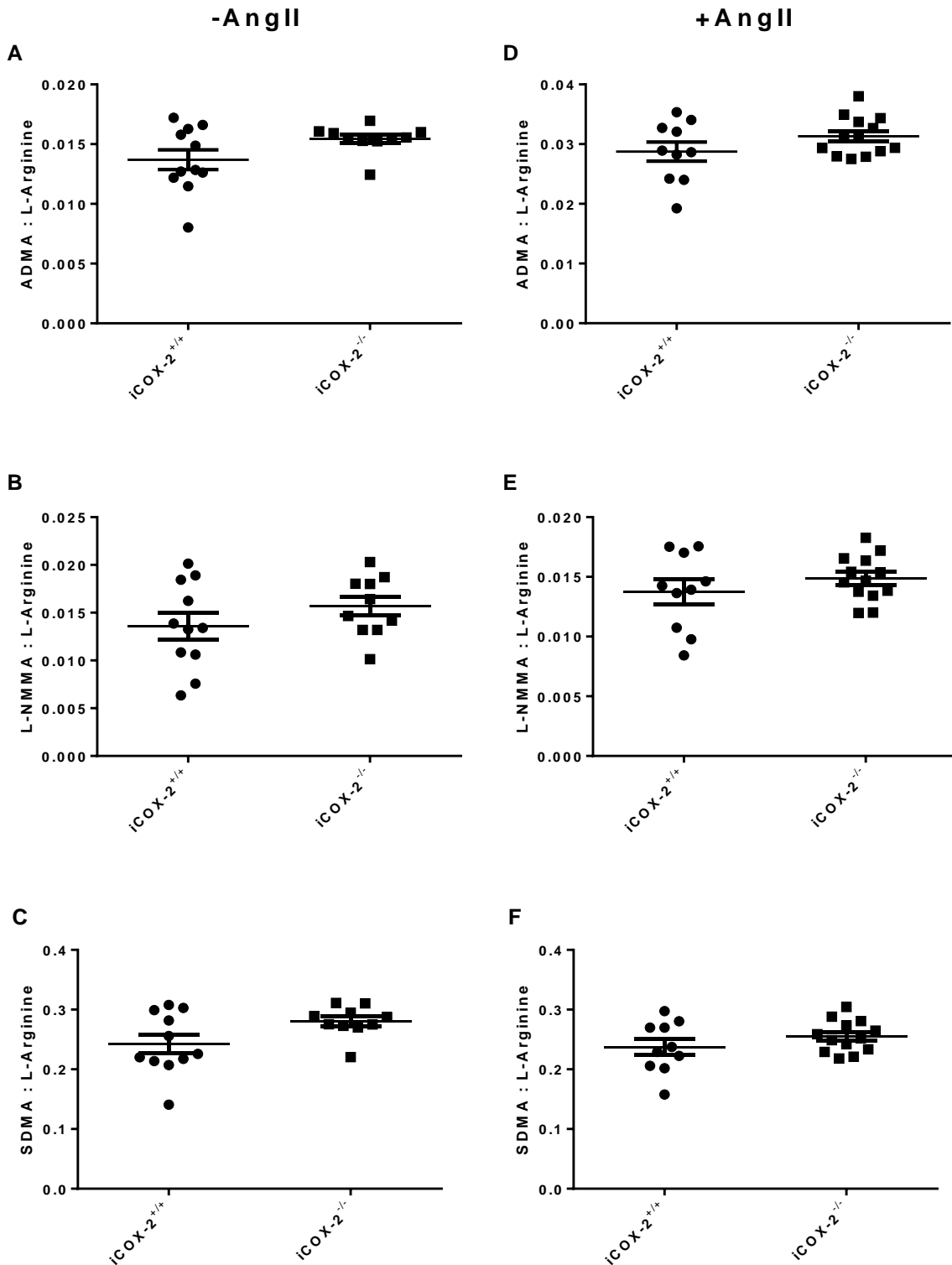
Methylarginine:L-arginine ratios were measured, by LC-MS/MS, in the kidney of the IPNG COX-2<sup>-/-</sup> mouse, to confirm the results found in the blood. The kidney medulla and cortex were analysed separately given the differences in COX-2 expression and regulation, including by angiotensin II, found in these tissues [31]. No differences were observed in ADMA:L-arginine, L-NMMA:L-arginine and SDMA:L-arginine ratios in the kidney medulla (*Figure 8*) or cortex (*Figure 9*) of the IPNG COX-2<sup>-/-</sup> mouse compared to COX-2<sup>+/+</sup> controls, with or without angiotensin II infusion. Like the blood results, kidney medulla ADMA:L-arginine and L-NMMA:L-arginine ratios were significantly higher in the presence of angiotensin II infusion in both IPNG COX-2<sup>-/-</sup> mice (2.6- and 1.6-fold greater,  $P < 0.0001$  for both; data not shown) and COX-2<sup>+/+</sup> control mice (2.3-fold greater,  $P < 0.0001$  and 1.4-fold greater,  $P = 0.0011$  respectively; data not shown). The SDMA:L-arginine ratio was unchanged. In the kidney cortex, only the ADMA:L-arginine ratio was significantly higher with angiotensin II infusion, in the IPNG COX-2<sup>-/-</sup> and COX-2<sup>+/+</sup> control mice (2.0- and 2.1-fold greater respectively,  $P < 0.0001$  for both; data not shown). These findings support and extend those noted in the blood of the IPNG COX-2<sup>-/-</sup> mouse.

**Figure 8.**



Effect of post-natal COX-2 gene deletion and AngII infusion on kidney medulla methylarginines to L-arginine ratios, in mice. Effect of post-natal COX-2 gene deletion on (A) ADMA:L-Arginine; (B) L-NMMA:L-Arginine and (C) SDMA:L-Arginine. Effect of post-natal COX-2 gene deletion and AngII infusion on (D) ADMA:L-Arginine; (E) L-NMMA:L-Arginine and (F) SDMA:L-Arginine. Measured by LC-MS/MS. Data are mean  $\pm$  S.E.M for (A-C)  $n = 10-11$ , (D-F)  $n = 10-13$ . No significant changes were observed. Abbreviations: Asymmetric dimethylarginine (ADMA); Monomethyl-L-arginine (L-NMMA); Symmetric dimethylarginine (SDMA); Angiotensin II (AngII); Inducible post-natal global cyclooxygenase-2 knock-out mouse (*iCOX-2<sup>-/-</sup>*); Inducible post-natal global cyclooxygenase-2 littermate control mouse (*iCOX-2<sup>+/+</sup>*).

Figure 9.



Effect of post-natal COX-2 gene deletion and AngII infusion on kidney cortex methylarginines to L-arginine ratios, in mice. Effect of post-natal COX-2 gene deletion on (A) ADMA:L-Arginine; (B) L-NMMA:L-Arginine and (C) SDMA:L-Arginine. Effect of post-natal COX-2 gene deletion and AngII infusion on (D) ADMA:L-Arginine; (E) L-NMMA:L-Arginine and (F) SDMA:L-Arginine. Measured by LC-MS/MS. Data are mean  $\pm$  S.E.M for (A-C)  $n = 10-11$ , (D-F)  $n = 10-13$ . No significant changes were observed. Abbreviations: Asymmetric dimethylarginine (ADMA); Monomethyl-L-arginine (L-NMMA); Symmetric dimethylarginine (SDMA); Angiotensin II (AngII); Inducible post-natal global cyclooxygenase-2 knock-out mouse (iCOX-2<sup>-/-</sup>); Inducible post-natal global cyclooxygenase-2 littermate control mouse (iCOX-2<sup>+/+</sup>).

## *Chapter Discussion*

### **IPNG COX-2<sup>-/-</sup> Mouse Cardiac Metabolism**

The IPNG COX-2<sup>-/-</sup> mouse, designed to simulate pharmacological inhibition of COX-2 in the adult human, exhibits effective suppression of the formation of prostaglandins, both systemically and by stimulated peritoneal macrophages, as well as their major urinary metabolites, indicative of COX-2 deletion [158]. COX-2 deletion was observed in the IPNG COX-2<sup>-/-</sup> mice used in this study (*Figure 1*). However, the IPNG COX-2<sup>-/-</sup> mouse has been criticised on the basis that other models of genetic deletion, employing tamoxifen-induced Cre-LoxP recombination, have been associated with severe transitory DCM, involving significant perturbations in cardiac energy metabolism and stress response [297, 335]. The findings of this study support the view that there is no evidence of longer term detrimental alterations to cardiac metabolism, caused by tamoxifen-induced Cre-LoxP recombination, in the IPNG COX-2<sup>-/-</sup> mouse.

In the present study, no evidence of perturbations in energy metabolism, that might indicate persistent aberrant cardiac metabolism, were observed in the hearts of IPNG COX-2<sup>-/-</sup> mice. That is not to say that changes in cardiac energy metabolites were not observed. As reported in Chapter 5, FA metabolism, which is the primary source of energy generation in the healthy heart, was unaffected. In addition, no changes were noted in lactate metabolism, suggesting unaltered glycolysis. Of the six TCA cycle intermediates measured, only isocitrate was altered - 1.5 fold higher (*Figure 3 A*). Whilst no differences were observed in the ketone body  $\beta$ -hydroxybutyrate, the potentially anaplerotic amino acids aspartate and valine were 1.2- and 1.3-fold higher, respectively (*Figure 4 A and B*). Six other anaplerotic amino acids were unaffected (*Figure 4 A*). These findings reflect relatively small changes, in a few isolated

metabolites, that play a relatively minor role in cardiac energy generation. This is supported by the results of the multivariate analysis, which demonstrates that these changes are not part of a global effect on cardiac energy metabolism. Furthermore, if we applied a stringent Bonferonni correction to the data the number of changes would be further reduced. This is in stark contrast to what might be expected if these mice exhibited persistent cardiac dysfunction as a consequence of tamoxifen-induced Cre-LoxP recombination. Three days after cessation of tamoxifen treatment, Koitabashi et al. noted significantly lower expression of PPAR $\alpha$  and its coactivator peroxisome proliferator-activated receptor gamma coactivator 1- $\alpha$  (PGC1 $\alpha$ ) in mice expressing Cre-ER [297]. The PPAR $\alpha$ -PGC1 $\alpha$  axis is the master regulator of cardiac energy metabolism and controls both FA and glucose metabolism [347, 348]. Dysregulation of this axis causes profound alterations in cardiac metabolism, structure and function [349, 350]. Such alterations in cardiac energy metabolism were not evident in the IPNG COX-2<sup>-/-</sup> mice of this study, which were subject to tamoxifen-induced Cre-LoxP recombination, when compared to the floxed COX-2<sup>+/+</sup> littermate controls, in which tamoxifen was administered but Cre-LoxP recombination did not occur.

In support of the finding related to cardiac energy metabolism, this study demonstrates no changes in the concentrations of small-molecule markers of cardiac dysfunction associated with DCM. Markers of cardiac oxidative stress (*Figure 4*), aberrant DNA methylation (*Figure 5*) and structural remodelling (*Figure 6*), processes which have all been observed in DCM, are unaltered in the IPNG COX-2<sup>-/-</sup> mouse [172, 339, 340, 344, 346]. Moreover, the transient DCM associated with tamoxifen-induced Cre-LoxP recombination, noted by Koitabashi et al., exhibited mononuclear infiltration indicative of myocarditis [297]. This is also associated with oxidative stress and structural remodelling [351, 352]. Therefore, 7-weeks post-tamoxifen, the heart of the IPNG

COX-2<sup>-/-</sup> mouse does not exhibit changes in small molecule markers indicative of long-term consequences of DCM.

Together, this evidence suggests that the severe transitory DCM noted by Koitabashi et al., three days after tamoxifen-induced Cre-LoxP recombination, is fully resolved and has no long-term consequences after 7 weeks. This is in agreement with functional, transcriptional and histological resolution noted 18 days after tamoxifen treatment [297]. Ultimately, this argues against the criticisms levelled at the IPNG COX-2<sup>-/-</sup> mouse by Ahmetaj Shala et al. [4].

### **IPNG COX-2<sup>-/-</sup> Mouse Methylarginine Metabolism**

Ahmetaj Shala et al. observed higher concentrations of blood ADMA, using a constitutive COX-2<sup>-/-</sup> mouse model, which they attributed to the homeostatic role of COX-2 in the adult kidney [4]. However, this model is confounded by severe renal pathology, caused by impaired nephrogenesis due to the function of COX-2 in the development of the kidney [295]. This study demonstrates that a more robust model of COX-2 deletion - the IPNG COX-2<sup>-/-</sup> mouse, which isn't accompanied by renal pathology, is not associated with higher concentrations of ADMA or other methylarginines.

Blood (*Figure 7*), kidney medulla (*Figure 8*) and kidney cortex (*Figure 9*) ratios of ADMA, L-NMMA and SDMA to L-arginine were unchanged in IPNG COX-2<sup>-/-</sup> compared to COX-2<sup>+/+</sup> littermate control mice. This is in direct opposition to the results observed in the constitutive COX-2<sup>-/-</sup> mouse. This may reflect the absence of renal pathology in the IPNG COX-2<sup>-/-</sup> mouse. In support of this assertion, higher ADMA concentrations are detected in, and reflect the severity of, chronic kidney disease (CKD) [353-355]. CKD also shares features, glomerular sclerosis and tubulointerstitial

injury, with the developmental renal pathology observed in the constitutive COX-2<sup>-/-</sup> mouse [356]. However Ahmetaj Shala et al. also noted far more modest increases in concentrations of blood ADMA in wild type mice, following short-term high-dose parecoxib administration, and healthy human volunteers, following short term therapeutic doses of celecoxib and naproxen [4]. These results differ from those observed in the IPNG COX-2<sup>-/-</sup> mouse. This may be due to a time-dependent effect which manifests in the short term, but not in the longer term. Both the mouse-parecoxib and human-celecoxib/naproxen studies were less than 1 week in duration, whilst the present study involved around 2 months of COX-2 deletion. One possibility could be the transient reduction in urinary sodium excretion detected with COX-2 inhibition [357, 358]. This might temporarily exacerbate the blood pressure elevating effects of these drugs, reflected by an increase in ADMA [293]. The relatively small increases in blood ADMA, observed by Ahmetaj Shala et al., following pharmacological inhibition of COX-2 in wild type mice and healthy human volunteers, may actually be of little clinical relevance. This is because in clinical practice COX-2 inhibitors are not given to healthy volunteers, but to those patients with inflammatory diseases, and recent evidence indicates that ADMA concentrations may reflect inflammatory burden [326]. If correct, any small increases in ADMA, caused by COX-2 inhibition in the absence of inflammation, would be more than offset by the anti-inflammatory effects of COX-2 inhibition in an inflammatory context.

This chapter also reports a greater blood (*Figure 7*), kidney medulla (*Figure 8*) and kidney cortex (*Figure 9*) ADMA to L-arginine ratio in IPNG COX-2<sup>-/-</sup> and COX-2<sup>+/+</sup> mice with angiotensin II induced hypertension, compared to those without. This is entirely anticipated, as ADMA concentrations are higher in hypertension [293].

These results support the view that long-term genetic COX-2 inhibition does not affect methylarginine metabolism in the absence of inflammation in the adult mouse. This opposes the conclusions drawn by Ahmetaj Shala et al., who made use of what I believe is an inappropriate genetic model of COX-2 deletion, confounded by severe developmental kidney pathology. Whilst this work does not support the position of ADMA as a mechanistic link between COX-2 inhibition and adverse CV events, it is entirely consistent with the hypothesis that ADMA concentrations reflect long-term inflammatory burden.

## *Chapter Conclusions and Future Directions*

The results of this chapter support the hypothesis that the IPNG COX-2<sup>-/-</sup> mouse does not exhibit long-term cardiac abnormalities, attributable to DCM. It therefore appears not to be compromised, in the long-term, by the early transient DCM noted by Koitabashi et al. This supports the argument that the IPNG COX-2<sup>-/-</sup> mouse is a more reliable system, in which to simulate pharmacological COX-2 inhibition in the adult human, than the constitutive COX-2<sup>-/-</sup> mouse. The results also support the hypothesis that the long-term absence of COX-2 activity, in the IPNG COX-2<sup>-/-</sup> mouse, does not cause higher concentrations of ADMA or other methylarginines. This is in disagreement with the conclusions drawn by Ahmetaj Shala et al., who may have used an inappropriate model of COX-2 deletion. Furthermore, it suggests that the higher concentrations of blood ADMA, seen in short-term studies examining pharmacological inhibition of COX-2 in wild-type mice and healthy humans, may have been over-extrapolated. Ultimately, these results are consistent with, though do not provide additional evidence for, the ADMA-inflammatory burden hypothesis.

This chapter has a number of limitations, which could be addressed in future studies. Firstly, the IPNG COX-2<sup>-/-</sup> mice were all sacrificed 2 months after study commencement, just over 7 weeks after the final tamoxifen dose. The results at this time-point were taken to be representative of 'long-term,' outcomes. Intermediate and later time-points would provide greater granularity regarding the conclusions drawn and help to confirm the results. Secondly, outcomes were defined on the basis of metabolomic analyses alone. Whilst metabolomics has proven sensitive in detecting alterations in cardiac health, physiological measures of cardiac function would lend additional support. Echocardiography would be particularly insightful. Thirdly, this

chapter does not examine the effects of long-term pharmacological inhibition of COX-2. Whilst this experiment was actually performed, and corroborated the findings of the IPNG COX-2<sup>-/-</sup> mouse study, it suffered from the same diet-mismatch described in Chapter 5, so was withdrawn from this chapter. A replicate of this experiment, using the correct diets, would help here. Finally, this work was not designed to address the relationship between ADMA concentrations and long-term inflammatory burden. Therefore, whilst it refutes the ADMA-COX-2 hypothesis, it does not explicitly support the ADMA-inflammatory burden hypothesis *per se*. Measurement of blood ADMA, with/without pharmacological inhibition of COX-2, in a mouse model of rheumatoid arthritis would provide the necessary insight for this.

## ***Chapter 8: Thesis Conclusions***

## *Thesis Themes*

This chapter consolidates the findings of the previous chapters into themes and considers these themes in terms of the primary research questions of the thesis, which are:

**What are the metabolomic consequences of coxib treatment, in the mouse?**

**Do celecoxib and rofecoxib cause similar metabolic changes?**

**Are perturbations in pathways, as opposed to isolated metabolites, evident?**

**Is there an evidence-base linking these pathways to HF?**

**What are the underlying mechanisms, driving these pathway differences?**

The results of chapters 4 and 5 indicate that the celecoxib and rofecoxib treatment regimens used in these studies, which are confounded by the control diet miss-match previously described, are associated with significantly lower cardiac carnitine concentrations. It is not possible from these results to conclude that either the coxibs or the diet underlie the lower cardiac carnitine concentrations observed. However, these results highlight the importance of diet in the context of coxib treatment and HF. In fact, they raise the possibility that manipulation of dietary composition could be leveraged to abrogate the dysregulation of carnitine handling and cardiac fatty acid metabolism observed in coxib-induced and other forms of HF [13, 14, 127, 128]. What's more, these findings suggest that dietary fatty acid composition may actually have a greater effect on cardiac carnitine concentrations than dietary carnitine content. This, at least, warrants further investigation as it may prove a more effective way of manipulating endogenous carnitine synthesis and cardiac carnitine concentrations than carnitine loading, which has been used with only limited success [262-265]. In the context of the primary research questions, these studies successfully identify

perturbations in a pathway linked to HF, carnitine metabolism, and provide insight into its mechanism. Moreover, the results indicate that celecoxib and rofecoxib treatment exhibit similar metabolomic effects, in the mouse. However, the diet miss-match means that these differences cannot be attributed to coxib treatment alone and the first of the three primary research questions cannot be addressed at this time.

The results of chapter 6 suggest that primary murine cardiomyocytes export acetyl-carnitine. This is the first demonstration of acetyl-carnitine export in cultured primary cardiomyocytes. Moreover, the results also indicate that neither celecoxib nor rofecoxib alter carnitine uptake, shuttling and export, *in vitro*. This suggests that the lower concentrations of cardiac carnitines, seen in chapter 4 and 5, are unlikely to be caused by altered cardiac carnitine shuttle activity. In the context of the primary research questions, the results of this study help to narrow-down the possible mechanistic explanations of the lower concentrations of cardiac carnitines observed in chapters 4 and 5 and provide further evidence that celecoxib and rofecoxib behave similarly in terms of their metabolic effects.

The results of chapter 7 contradict those presented as evidence for the ADMA hypothesis, by Ahmetaj-Shala et al. [4] and demonstrate that genetic COX-2 inhibition, induced postnatally in the mouse, alters neither plasma nor renal ADMA concentrations. Instead, the results align more closely with the inflammatory burden hypothesis, proposed by Sandoo et al. [326] and indicate that ADMA may actually reflect long term inflammatory burden. This suggests that ADMA is unlikely to serve as a mechanistic bridge between the coxibs, COX-2 inhibition and the adverse CV events with which they are associated. This provides context for understanding the mechanism by which the coxibs increase the risk of HF.

## *Thesis Limitations and Future Directions*

In addition to the limitations described at the end of each chapter, a number of limitations are pertinent to the entirety of this work and concern the study scope, design, instrumentation and analysis. Future work is proposed to address these limitations.

The scope of this investigation was purposefully limited to two compounds, celecoxib and rofecoxib, for practical reasons. Future work could build on this to include other NSAIDs. Naproxen would be the most appropriate next choice, as it has the best CV safety profile [88]. Similarly, to ensure that the gap in the knowledge was appropriately addressed within the time-frame of this thesis, the experiments were focused on characterising the metabolomic consequence of coxib use. Given more time, functional measures, such as echocardiography, could be used to objectively measure physiological parameters indicative of cardiac function, which would provide greater mechanistic insight into the effects of coxib treatment. Furthermore, future work should aim to confirm the key findings of this work in the human, to validate their generalisability and clinical relevance.

General modifications, to the design of the different studies, would also help address a number of limitations. Metabolomic techniques measure the most downstream indicators of biological activity. These indicators are affected by a range of biological processes and turn-over rapidly. Metabolomic measures are therefore subject to biological variability and noise, which limits their reproducibility [169]. Additional experimental replicates would help mitigate this risk. Moreover, a greater sample size would help reduce the impact of biological variation and increase the power of the studies to detect small metabolic changes.

The metabolomic techniques, employed over the course of this work, are also subject to certain limitations. The MS methods make use of internal standards, of known mass and retention time, for the assignment of compounds. The more internal standards used in an assay, the lower the risk of inappropriately assigning compounds detected in the assay. Therefore, inclusion of additional standards in these methods is experimentally desirable and would enhance compound assignment in future work. However, it should be noted that there is a cost associated with the use of additional standards. NMR spectroscopy is less sensitive than MS. This can, to a degree, be compensated for by preparation of additional tissue/bio-fluids for analysis. However, in the mouse, there is not always a sufficient quantity of tissue, especially of the aorta, to do this. To address this, a larger model organism, such as the rat, could be used in future work.

Whilst sample preparation was carried out without knowledge of the group origin of the sample, data analysis was not expressly blinded. Whilst every effort was made to avoid bias, and samples were treated equally, a formal blinding process would ensure the absence of unintended bias. Future work would therefore benefit from formal blinding.

## *Thesis Concluding Remarks*

Ultimately, the nature of the mechanisms underlying the higher risk of HF, seen with the coxibs, remain elusive. However, a new class of anti-inflammatory drugs currently under development, the COX-inhibiting NO donators (CINODs), may present a better side-effect safety profile [34]. The CINODs are at the intersection of prostanoid and NO biology. Interestingly, this mirrors the debate between the Fitzgerald and ADMA hypotheses, both proposed to explain the coxib-associated adverse CV events and

discussed in this thesis. CINODs are fusions of traditional NSAIDs with NO donating moieties and combat the adverse gastric and vascular effects of the NSAIDs with the protective effects engendered by NO donation [359]. However, even when the CINODs enter the market, there will remain considerable scope for coxib use given their exceptional anti-inflammatory properties. Even more-so if their CV risk can be tempered. Ultimately, this could be as straightforward as dietary modification, to maintain cardiac carnitine concentrations, which may present a simpler approach to the NO-donator fusion paradigm currently being evaluated [360].

# References

1. Bresalier, R.S., et al., *Cardiovascular events associated with rofecoxib in a colorectal adenoma chemoprevention trial*. N Engl J Med, 2005. **352**(11): p. 1092-102.
2. Graham, D.J., et al., *Risk of acute myocardial infarction and sudden cardiac death in patients treated with cyclo-oxygenase 2 selective and non-selective non-steroidal anti-inflammatory drugs: nested case-control study*. Lancet, 2005. **365**(9458): p. 475-81.
3. FitzGerald, G.A. and C. Patrono *The Coxibs, Selective Inhibitors of Cyclooxygenase-2*. New England Journal of Medicine, 2001. **345**(6): p. 433-442.
4. Ahmetaj-Shala, B., et al., *Evidence that links loss of cyclooxygenase-2 with increased asymmetric dimethylarginine: novel explanation of cardiovascular side effects associated with anti-inflammatory drugs*. Circulation, 2015. **131**(7): p. 633-42.
5. Ungprasert, P., N. Srivali, and C. Thongprayoon, *Nonsteroidal Anti-inflammatory Drugs and Risk of Incident Heart Failure: A Systematic Review and Meta-analysis of Observational Studies*. Clin Cardiol, 2015.
6. Ungprasert, P., N. Srivali, and W. Kittanamongkolchai, *Non-steroidal anti-inflammatory drugs and risk of heart failure exacerbation: A systematic review and meta-analysis*. Eur J Intern Med, 2015. **26**(9): p. 685-90.
7. Liu, J.-Y., et al., *Metabolic profiling of murine plasma reveals an unexpected biomarker in rofecoxib-mediated cardiovascular events*. Proceedings of the National Academy of Sciences, 2010. **107**(39): p. 17017-17022.
8. Um, S.Y., et al., *Pattern recognition analysis for the prediction of adverse effects by nonsteroidal anti-inflammatory drugs using <sup>1</sup>H NMR-based metabolomics in rats*. Anal Chem, 2009. **81**(12): p. 4734-41.
9. Ho, V.W., et al., *A low carbohydrate, high protein diet combined with celecoxib markedly reduces metastasis*. Carcinogenesis, 2014. **35**(10): p. 2291-9.
10. Hill, B.G. and P.C. Schulze, *Insights into metabolic remodeling of the hypertrophic and failing myocardium*. Circ Heart Fail, 2014. **7**(6): p. 874-6.
11. Kolwicz, S.C., Jr., S. Airhart, and R. Tian, *Ketones Step to the Plate: A Game Changer for Metabolic Remodeling in Heart Failure?* Circulation, 2016.
12. Doenst, T., T.D. Nguyen, and E.D. Abel, *Cardiac metabolism in heart failure: implications beyond ATP production*. Circ Res, 2013. **113**(6): p. 709-24.
13. Bedi, K.C., Jr., et al., *Evidence for Intramyocardial Disruption of Lipid Metabolism and Increased Myocardial Ketone Utilization in Advanced Human Heart Failure*. Circulation, 2016. **133**(8): p. 706-16.
14. Ahmad, T., et al., *Prognostic Implications of Long-Chain Acylcarnitines in Heart Failure and Reversibility With Mechanical Circulatory Support*. J Am Coll Cardiol, 2016. **67**(3): p. 291-9.
15. Cohn, J.N., R. Ferrari, and N. Sharpe, *Cardiac remodeling—concepts and clinical implications: a consensus paper from an international forum on cardiac remodeling*. Journal of the American College of Cardiology, 2000. **35**(3): p. 569-582.
16. Omori, Y., et al., *L-Carnitine prevents the development of ventricular fibrosis and heart failure with preserved ejection fraction in hypertensive heart disease*. J Hypertens, 2012. **30**(9): p. 1834-44.
17. Sansbury, B.E., et al., *Metabolomic analysis of pressure-overloaded and infarcted mouse hearts*. Circ Heart Fail, 2014. **7**(4): p. 634-42.
18. Chen, Y., et al., *A metabolomic study of rats with doxorubicin-induced cardiomyopathy and Shengmai injection treatment*. PLoS One, 2015. **10**(5): p. e0125209.
19. Griffin, J.L., et al., *Metabolomics as a tool for cardiac research*. Nat Rev Cardiol, 2011. **8**(11): p. 630-43.
20. Dunn, W.B., et al., *Systems level studies of mammalian metabolomes: the roles of mass spectrometry and nuclear magnetic resonance spectroscopy*. Chem Soc Rev, 2011. **40**(1): p. 387-426.
21. Cheng, Y., et al., *Principles of regulatory information conservation between mouse and human*. Nature, 2014. **515**(7527): p. 371-375.
22. Yue, F., et al., *A comparative encyclopedia of DNA elements in the mouse genome*. Nature, 2014. **515**(7527): p. 355-364.
23. Stergachis, A.B., et al., *Conservation of trans-acting circuitry during mammalian regulatory evolution*. Nature, 2014. **515**(7527): p. 365-370.
24. Cairns, J.A., *The coxibs and traditional nonsteroidal anti-inflammatory drugs: A current perspective on cardiovascular risks*. Canadian Journal of Cardiology, 2007. **23**(2): p. 125-131.
25. Knights, K.M., A.A. Mangoni, and J.O. Miners, *Defining the COX inhibitor selectivity of NSAIDs: implications for understanding toxicity*. Expert Rev Clin Pharmacol, 2010. **3**(6): p. 769-76.
26. Ricciotti, E. and G.A. FitzGerald, *Prostaglandins and inflammation*. Arterioscler Thromb Vasc Biol, 2011. **31**(5): p. 986-1000.
27. Yasojima, K., et al., *Distribution of cyclooxygenase-1 and cyclooxygenase-2 mRNAs and proteins in human brain and peripheral organs*. Brain Res, 1999. **830**(2): p. 226-36.
28. Lee, S.H., et al., *Selective expression of mitogen-inducible cyclooxygenase in macrophages stimulated with lipopolysaccharide*. J Biol Chem, 1992. **267**(36): p. 25934-8.
29. Kniss, D.A., *Cyclooxygenases in reproductive medicine and biology*. J Soc Gynecol Investig, 1999. **6**(6): p. 285-92.

30. Kirkby, N.S., et al., *Systematic study of constitutive cyclooxygenase-2 expression: Role of NF-kappaB and NFAT transcriptional pathways*. Proc Natl Acad Sci U S A, 2016. **113**(2): p. 434-9.
31. Green, T., et al., *The Complex Interplay between COX-2 and Angiotensin II in Regulating Kidney Function*. Curr Opin Nephrol Hypertens, 2012. **21**(1): p. 7-14.
32. Yuan, C., et al., *Partnering between monomers of cyclooxygenase-2 homodimers*. Proceedings of the National Academy of Sciences, 2006. **103**(16): p. 6142-6147.
33. Rouzer, C.A. and L.J. Marnett, *Cyclooxygenases: structural and functional insights*. J Lipid Res, 2009. **50** Suppl: p. S29-34.
34. Meek, I.L., M. van de Laar, and H.E. Vonkeman, *Non-Steroidal Anti-Inflammatory Drugs: An Overview of Cardiovascular Risks*. 2010: Pharmaceuticals (Basel). 2010 Jul;3(7):2146-62. doi:10.3390/ph3072146.
35. Zarghi, A. and S. Arfaei, *Selective COX-2 Inhibitors: A Review of Their Structure-Activity Relationships*. Iran J Pharm Res, 2011. **10**(4): p. 655-83.
36. Reddy, S.T. and H.R. Herschman, *Transcellular prostaglandin production following mast cell activation is mediated by proximal secretory phospholipase A2 and distal prostaglandin synthase 1*. J Biol Chem, 1996. **271**(1): p. 186-91.
37. Dubois, R.N., et al., *Cyclooxygenase in biology and disease*. The FASEB Journal, 1998. **12**(12): p. 1063-1073.
38. O'Banion, M.K., *Cyclooxygenase-2: molecular biology, pharmacology, and neurobiology*. Crit Rev Neurobiol, 1999. **13**(1): p. 45-82.
39. Marnett, L.J., *Prostaglandin synthase-mediated metabolism of carcinogens and a potential role for peroxy radicals as reactive intermediates*. Environ Health Perspect, 1990. **88**: p. 5-12.
40. Smyth, E.M., et al., *Prostanoids in health and disease*. J Lipid Res, 2009. **50** Suppl: p. S423-8.
41. Caughey, G.E., et al., *Roles of cyclooxygenase (COX)-1 and COX-2 in prostanoid production by human endothelial cells: selective up-regulation of prostacyclin synthesis by COX-2*. J Immunol, 2001. **167**(5): p. 2831-8.
42. Feletou, M., P.M. Vanhoutte, and T.J. Verbeuren, *The thromboxane/endoperoxide receptor (TP): the common villain*. J Cardiovasc Pharmacol, 2010. **55**(4): p. 317-32.
43. Nakahata, N., *Thromboxane A2: physiology/pathophysiology, cellular signal transduction and pharmacology*. Pharmacol Ther, 2008. **118**(1): p. 18-35.
44. Midgett, C., et al., *PROSTACYCLIN RECEPTOR REGULATION --- FROM TRANSCRIPTION TO TRAFFICKING*. Curr Mol Med, 2011. **11**(7): p. 517-28.
45. Kang, K.H., et al., *PGF2 alpha causes bronchoconstriction and pulmonary vasoconstriction via thromboxane receptors in rat lung*. Korean J Intern Med, 1996. **11**(1): p. 74-81.
46. Breyer, M.D. and R.M. Breyer, *G protein-coupled prostanoid receptors and the kidney*. Annu Rev Physiol, 2001. **63**: p. 579-605.
47. Basu, S., *Novel cyclooxygenase-catalyzed bioactive prostaglandin F2alpha from physiology to new principles in inflammation*. Med Res Rev, 2007. **27**(4): p. 435-68.
48. Sarashina, H., et al., *Opposing immunomodulatory roles of prostaglandin D2 during the progression of skin inflammation*. J Immunol, 2014. **192**(1): p. 459-65.
49. Kalinski, P., *Regulation of immune responses by prostaglandin E2*. J Immunol, 2012. **188**(1): p. 21-8.
50. Nasrallah, R., R. Hassouneh, and R.L. Hebert, *PGE2, Kidney Disease, and Cardiovascular Risk: Beyond Hypertension and Diabetes*. J Am Soc Nephrol, 2016. **27**(3): p. 666-76.
51. Boor, P., *EP4: a new piece in the fibrotic puzzle*. Kidney Int, 2012. **82**(2): p. 132-5.
52. Alfranca, A., et al., *Prostanoid signal transduction and gene expression in the endothelium: Role in cardiovascular diseases*. Cardiovascular Research, 2006. **70**(3): p. 446-456.
53. Maroon, J.C., J.W. Bost, and A. Maroon, *Natural anti-inflammatory agents for pain relief*. Surg Neurol Int, 2010. **1**.
54. Vane, J.R., *Inhibition of prostaglandin synthesis as a mechanism of action for aspirin-like drugs*. Nat New Biol, 1971. **231**(25): p. 232-5.
55. Seaver, B. and J.R. Smith, *Inhibition of COX isoforms by nutraceuticals*. J Herb Pharmacother, 2004. **4**(2): p. 11-8.
56. Viladomiu, M., et al., *Preventive and prophylactic mechanisms of action of pomegranate bioactive constituents*. Evid Based Complement Alternat Med, 2013. **2013**: p. 789764.
57. Rao, P. and E.E. Knaus, *Evolution of nonsteroidal anti-inflammatory drugs (NSAIDs): cyclooxygenase (COX) inhibition and beyond*. J Pharm Pharm Sci, 2008. **11**(2): p. 81s-110s.
58. Mackowiak, P.A., *Brief history of antipyretic therapy*. Clin Infect Dis, 2000. **31** Suppl 5: p. S154-6.
59. Vane, J.R. and R.M. Botting, *The mechanism of action of aspirin*. Thromb Res, 2003. **110**(5-6): p. 255-8.
60. Rowlinson, S.W., et al., *Spatial requirements for 15-(R)-hydroxy-5Z,8Z,11Z,13E-eicosatetraenoic acid synthesis within the cyclooxygenase active site of murine COX-2. Why acetylated COX-1 does not synthesize 15-(R)-hete*. J Biol Chem, 2000. **275**(9): p. 6586-91.
61. Peterson, K., et al., *Drug Class Reviews, in Drug Class Review: Nonsteroidal Antiinflammatory Drugs (NSAIDs): Final Update 4 Report*. 2010, Oregon Health & Science University: Portland (OR).
62. Warner, T.D., S. Nylander, and C. Whatling, *Anti-platelet therapy: cyclo-oxygenase inhibition and the use of aspirin with particular regard to dual anti-platelet therapy*. Br J Clin Pharmacol, 2011. **72**(4): p. 619-33.

63. Deleon, D., et al., *THE EFFECT OF ADDING CLOPIDOGREL OR WARFARIN TO THE GOLD STANDARD, ASPIRIN, ON THE RATE OF REPEAT CORONARY ANGIOGRAPHY AND EARLY SAPHENOUS VEIN GRAFT FAILURE*. Journal of the American College of Cardiology, 2015. **65**(10\_S).
64. Awtry, E.H. and J. Loscalzo, *Aspirin*. Circulation, 2000. **101**(10): p. 1206-18.
65. Toruner, M., *Aspirin and gastrointestinal toxicity*. Anadolu Kardiyol Derg, 2007. **7 Suppl 2**: p. 27-30.
66. Dhikav, V., et al., *Non-steroidal drug-induced gastrointestinal toxicity: mechanisms and management*. J Indian Acad Clin Med, 2003. **4**(4): p. 315-322.
67. Cryer, B. and M. Feldman, *Effects of very low dose daily, long-term aspirin therapy on gastric, duodenal, and rectal prostaglandin levels and on mucosal injury in healthy humans*. Gastroenterology, 1999. **117**(1): p. 17-25.
68. Martin, L.-A., *Silylation of Non-Steroidal Anti-Inflammatory Drugs*. AnalytiX. **10**.
69. Praticò, D. and J.-M. Dogné, *Selective Cyclooxygenase-2 Inhibitors Development in Cardiovascular Medicine*. Circulation, 2005. **112**(7): p. 1073-1079.
70. Nielsen, O.H., et al., *Systematic review: coxibs, non-steroidal anti-inflammatory drugs or no cyclooxygenase inhibitors in gastroenterological high-risk patients?* Alimentary Pharmacology & Therapeutics, 2006. **23**(1): p. 27-33.
71. Trummelitz, G., J. van Ryn, and T.D. Warner, *The molecular and biological basis for COX-2 selectivity, in COX-2 inhibitors*. 2004, Springer. p. 41-65.
72. Hawkey, C.J., *COX-2 inhibitors*. The Lancet, 1999. **353**(9149): p. 307-314.
73. Jacobsen, R.B. and B.B. Phillips, *Reducing Clinically Significant Gastrointestinal Toxicity Associated with Nonsteroidal Antiinflammatory Drugs*. Annals of Pharmacotherapy, 2004. **38**(9): p. 1469-1481.
74. Emery, P., et al., *Celecoxib versus diclofenac in long-term management of rheumatoid arthritis: randomised double-blind comparison*. Lancet, 1999. **354**(9196): p. 2106-11.
75. Simon, L.S., et al., *Anti-inflammatory and upper gastrointestinal effects of celecoxib in rheumatoid arthritis: a randomized controlled trial*. Jama, 1999. **282**(20): p. 1921-8.
76. Goldstein, J.L., et al., *Reduced incidence of gastroduodenal ulcers with celecoxib, a novel cyclooxygenase-2 inhibitor, compared to naproxen in patients with arthritis*. Am J Gastroenterol, 2001. **96**(4): p. 1019-27.
77. Bombardier, C., et al., *Comparison of upper gastrointestinal toxicity of rofecoxib and naproxen in patients with rheumatoid arthritis*. VIGOR Study Group. N Engl J Med, 2000. **343**(21): p. 1520-8, 2 p following 1528.
78. Laine, L., et al., *A randomized trial comparing the effect of rofecoxib, a cyclooxygenase 2-specific inhibitor, with that of ibuprofen on the gastroduodenal mucosa of patients with osteoarthritis*. Rofecoxib Osteoarthritis Endoscopy Study Group. Gastroenterology, 1999. **117**(4): p. 776-83.
79. Kivitz, A., et al., *Randomized placebo-controlled trial comparing efficacy and safety of valdecoxib with naproxen in patients with osteoarthritis*. J Fam Pract, 2002. **51**(6): p. 530-7.
80. Sikes, D.H., et al., *Incidence of gastroduodenal ulcers associated with valdecoxib compared with that of ibuprofen and diclofenac in patients with osteoarthritis*. Eur J Gastroenterol Hepatol, 2002. **14**(10): p. 1101-11.
81. Cryer, B., *The role of cyclooxygenase selective inhibitors in the gastrointestinal tract*. Current Gastroenterology Reports, 2003. **5**(6): p. 453-458.
82. Silverstein, F.E., et al., *Gastrointestinal toxicity with celecoxib vs nonsteroidal anti-inflammatory drugs for osteoarthritis and rheumatoid arthritis: the CLASS study: A randomized controlled trial*. Celecoxib Long-term Arthritis Safety Study. Jama, 2000. **284**(10): p. 1247-55.
83. Michaels, D. and M. Jones, *Doubt is their product*. Scientific American, 2005(292): p. 96-101.
84. Karha, J. and E.J. Topol, *The sad story of Vioxx, and what we should learn from it*. Cleve Clin J Med, 2004. **71**(12): p. 933-4, 936, 938-9.
85. Solomon, D.H., et al., *NONsteroidal anti-inflammatory drug use and acute myocardial infarction*. Archives of Internal Medicine, 2002. **162**(10): p. 1099-1104.
86. Qureshi, Z.P., et al., *Market withdrawal of new molecular entities approved in the United States from 1980 to 2009*. Pharmacoepidemiol Drug Saf, 2011. **20**(7): p. 772-7.
87. Geusens, P. and W. Lems, *Efficacy and tolerability of lumiracoxib, a highly selective cyclo-oxygenase-2 (COX2) inhibitor, in the management of pain and osteoarthritis*. Ther Clin Risk Manag, 2008. **4**(2): p. 337-44.
88. Kearney, P.M., et al., *Do selective cyclo-oxygenase-2 inhibitors and traditional non-steroidal anti-inflammatory drugs increase the risk of atherothrombosis? Meta-analysis of randomised trials*. Bmj, 2006. **332**(7553): p. 1302-8.
89. Coxib and traditional NSAID Trialists' (CNT) Collaboration, *Vascular and upper gastrointestinal effects of non-steroidal anti-inflammatory drugs: meta-analyses of individual participant data from randomised trials*. The Lancet, 2013. **382**(9894): p. 769-779.
90. Altman, D.G. and J.M. Bland, *How to obtain the P value from a confidence interval*. BMJ, 2011. **343**.
91. Patrono, C., *Cardiovascular Effects of Nonsteroidal Anti-inflammatory Drugs*. Curr Cardiol Rep, 2016. **18**(3): p. 25.
92. *Collaborative meta-analysis of randomised trials of antiplatelet therapy for prevention of death, myocardial infarction, and stroke in high risk patients*. BMJ, 2002. **324**(7329): p. 71-86.
93. Baigent, C., et al., *Aspirin in the primary and secondary prevention of vascular disease: collaborative meta-analysis of individual participant data from randomised trials*. Lancet, 2009. **373**(9678): p. 1849-60.

94. Lee, M., et al., *Risk-benefit profile of warfarin versus aspirin in patients with heart failure and sinus rhythm: a meta-analysis*. *Circ Heart Fail*, 2013. **6**(2): p. 287-92.
95. Hopper, I., M. Skiba, and H. Krum, *Updated meta-analysis on antithrombotic therapy in patients with heart failure and sinus rhythm*. *Eur J Heart Fail*, 2013. **15**(1): p. 69-78.
96. Bermingham, M., et al., *Aspirin use in heart failure: is low-dose therapy associated with mortality and morbidity benefits in a large community population?* *Circ Heart Fail*, 2014. **7**(2): p. 243-50.
97. Cleland, J.G. and S. Parsons, *Aspirin for heart failure: theory- or evidence-based?* *Circ Heart Fail*, 2014. **7**(2): p. 237-8.
98. Cleland, J.G., et al., *The Warfarin/Aspirin Study in Heart failure (WASH): a randomized trial comparing antithrombotic strategies for patients with heart failure*. *Am Heart J*, 2004. **148**(1): p. 157-64.
99. Massie, B.M., et al., *The Warfarin and Antiplatelet Therapy in Heart Failure trial (WATCH): rationale, design, and baseline patient characteristics*. *J Card Fail*, 2004. **10**(2): p. 101-12.
100. McGettigan, P. and D. Henry, *Use of Non-Steroidal Anti-Inflammatory Drugs That Elevate Cardiovascular Risk: An Examination of Sales and Essential Medicines Lists in Low-, Middle-, and High-Income Countries*. *PLoS Med*, 2013. **10**(2).
101. Garcia Rodriguez, L.A., S. Tacconelli, and P. Patrignani, *Role of dose potency in the prediction of risk of myocardial infarction associated with nonsteroidal anti-inflammatory drugs in the general population*. *J Am Coll Cardiol*, 2008. **52**(20): p. 1628-36.
102. Tegeder, I. and G. Geisslinger, *Cardiovascular risk with cyclooxygenase inhibitors: general problem with substance specific differences?* *Naunyn Schmiedebergs Arch Pharmacol*, 2006. **373**(1): p. 1-17.
103. Grosser, T., Y. Yu, and G.A. Fitzgerald, *Emotion recollected in tranquility: lessons learned from the COX-2 saga*. *Annu Rev Med*, 2010. **61**: p. 17-33.
104. Gislason, G.H., et al., *Increased mortality and cardiovascular morbidity associated with use of nonsteroidal anti-inflammatory drugs in chronic heart failure*. *Arch Intern Med*, 2009. **169**(2): p. 141-9.
105. Timmers, L., et al., *Cyclooxygenase-2 inhibition increases mortality, enhances left ventricular remodeling, and impairs systolic function after myocardial infarction in the pig*. *Circulation*, 2007. **115**(3): p. 326-32.
106. Campolo, J., et al., *Blood glutathione as independent marker of lipid peroxidation in heart failure*. *International Journal of Cardiology*. **117**(1): p. 45-50.
107. Jacobshagen, C., et al., *Celecoxib modulates hypertrophic signalling and prevents load-induced cardiac dysfunction*. *Eur J Heart Fail*, 2008. **10**(4): p. 334-42.
108. Lloyd, S.M., et al., *Abstract A65: An integromics approach identifies immune escape as a potential mechanism for prostate cancer disparities*. *Cancer Epidemiology Biomarkers & Prevention*, 2016. **25**(3 Supplement): p. A65.
109. Daviss, B., *Growing pains for metabolomics: the newest 'omic science is producing results--and more data than researchers know what to do with*. *The Scientist*, 2005. **19**(8): p. 25-29.
110. McDunn, J.E., et al., *Metabolomic signatures of aggressive prostate cancer*. *Prostate*, 2013. **73**(14): p. 1547-60.
111. Farmakis, D., et al., *The medical and socioeconomic burden of heart failure: A comparative delineation with cancer*. *International Journal of Cardiology*, 2016. **203**: p. 279-281.
112. Francis, G.S., R. Cogswell, and T. Thenappan, *The Heterogeneity of Heart Failure Will Enhanced Phenotyping Be Necessary for Future Clinical Trial Success?\**. *Journal of the American College of Cardiology*, 2014. **64**(17): p. 1775-1776.
113. "Heart Failure", in *Gale Encyclopedia of Medicine (2008)*. Retrieved 7th May 2016 from <http://medical-dictionary.thefreedictionary.com/heart+failure>.
114. Cheng, R.K., et al., *Outcomes in patients with heart failure with preserved, borderline, and reduced ejection fraction in the Medicare population*. *Am Heart J*, 2014. **168**(5): p. 721-30.
115. De Keulenaer, G.W. and D.L. Brutsaert, *Systolic and diastolic heart failure are overlapping phenotypes within the heart failure spectrum*. *Circulation*, 2011. **123**(18): p. 1996-2004; discussion 2005.
116. Solomon, S.D., et al., *Influence of ejection fraction on cardiovascular outcomes in a broad spectrum of heart failure patients*. *Circulation*, 2005. **112**(24): p. 3738-44.
117. Borlaug, B.A. and M.M. Redfield, *Diastolic and systolic heart failure are distinct phenotypes within the heart failure spectrum*. *Circulation*, 2011. **123**(18): p. 2006-13; discussion 2014.
118. Gaasch, W.H., et al., *Distribution of Left Ventricular Ejection Fraction in Patients With Ischemic and Hypertensive Heart Disease and Chronic Heart Failure*. *The American Journal of Cardiology*, 2009. **104**(10): p. 1413-1415.
119. Dunlay, S.M., et al., *Hospitalizations After Heart Failure Diagnosis: A Community Perspective*. *J Am Coll Cardiol*, 2009. **54**(18): p. 1695-702.
120. Fonarow, G.C., et al., *Organized Program to Initiate Lifesaving Treatment in Hospitalized Patients with Heart Failure (OPTIMIZE-HF): rationale and design*. *Am Heart J*, 2004. **148**(1): p. 43-51.
121. Sciarretta, S. and J. Sadoshima, *New insights into the molecular phenotype of eccentric hypertrophy*. *J Mol Cell Cardiol*, 2010. **49**(2): p. 153-6.
122. Aubert, G., et al., *The Failing Heart Relies on Ketone Bodies as a Fuel*. *Circulation*, 2016. **133**(8): p. 698-705.
123. Du, Z., et al., *<sup>1</sup>H-NMR-based metabolic analysis of human serum reveals novel markers of myocardial energy expenditure in heart failure patients*. *PLoS One*, 2014. **9**(2): p. e88102.

124. Dunn, W.B., et al., *Serum metabolomics reveals many novel metabolic markers of heart failure, including pseudouridine and 2-oxoglutarate*. *Metabolomics*, 2007. **3**(4): p. 413-426.
125. Deidda, M., et al., *Metabolomic approach to profile functional and metabolic changes in heart failure*. *J Transl Med*, 2015. **13**: p. 297.
126. Tenori, L., et al., *Metabolomic fingerprint of heart failure in humans: a nuclear magnetic resonance spectroscopy analysis*. *Int J Cardiol*, 2013. **168**(4): p. e113-5.
127. Cheng, M.L., et al., *Metabolic disturbances identified in plasma are associated with outcomes in patients with heart failure: diagnostic and prognostic value of metabolomics*. *J Am Coll Cardiol*, 2015. **65**(15): p. 1509-20.
128. Zordoky, B.N., et al., *Metabolomic fingerprint of heart failure with preserved ejection fraction*. *PLoS One*, 2015. **10**(5): p. e0124844.
129. Wang, J., et al., *Metabolomic identification of diagnostic plasma biomarkers in humans with chronic heart failure*. *Mol Biosyst*, 2013. **9**(11): p. 2618-26.
130. Turer, A.T., et al., *Metabolomic profiling reveals distinct patterns of myocardial substrate use in humans with coronary artery disease or left ventricular dysfunction during surgical ischemia/reperfusion*. *Circulation*, 2009. **119**(13): p. 1736-46.
131. Yang, D., et al., *Urinary Metabolomic Profiling Reveals the Effect of Shenfu Decoction on Chronic Heart Failure in Rats*. *Molecules*, 2015. **20**(7): p. 11915-29.
132. Shibayama, J., et al., *Metabolic remodeling in moderate synchronous versus dyssynchronous pacing-induced heart failure: integrated metabolomics and proteomics study*. *PLoS One*, 2015. **10**(3): p. e0118974.
133. Lai, L., et al., *Energy metabolic reprogramming in the hypertrophied and early stage failing heart: a multisystems approach*. *Circ Heart Fail*, 2014. **7**(6): p. 1022-31.
134. Guo, N., et al., *Metabonomic study of chronic heart failure and effects of Chinese herbal decoction in rats*. *J Chromatogr A*, 2014. **1362**: p. 89-101.
135. Qiu, Q., et al., *Plasma metabonomics study on Chinese medicine syndrome evolution of heart failure rats caused by LAD ligation*. *BMC Complement Altern Med*, 2014. **14**: p. 232.
136. Maekawa, K., et al., *Global metabolomic analysis of heart tissue in a hamster model for dilated cardiomyopathy*. *J Mol Cell Cardiol*, 2013. **59**: p. 76-85.
137. De Souza, A.I., et al., *Proteomic and metabolomic analysis of atrial profibrillatory remodelling in congestive heart failure*. *J Mol Cell Cardiol*, 2010. **49**(5): p. 851-63.
138. Schooneman, M.G., et al., *Acylcarnitines: Reflecting or Inflicting Insulin Resistance?* *Diabetes*, 2013. **62**(1): p. 1-8.
139. Davili, Z., et al., *Succinate dehydrogenase deficiency associated with dilated cardiomyopathy and ventricular noncompaction*. *Eur J Pediatr*, 2007. **166**(8): p. 867-70.
140. Lussey-Lepoutre, C., et al., *Loss of succinate dehydrogenase activity results in dependency on pyruvate carboxylation for cellular anabolism*. *Nat Commun*, 2015. **6**.
141. Kang, S.M., et al., *(1)H nuclear magnetic resonance based metabolic urinary profiling of patients with ischemic heart failure*. *Clin Biochem*, 2011. **44**(4): p. 293-9.
142. Chung, J.H., et al., *Urinary ketone is associated with the heart failure severity*. *Clin Biochem*, 2012. **45**(18): p. 1697-9.
143. Lommi, J., et al., *Blood ketone bodies in congestive heart failure*. *J Am Coll Cardiol*, 1996. **28**(3): p. 665-72.
144. Funada, J., et al., *Substrate utilization by the failing human heart by direct quantification using arterio-venous blood sampling*. *PLoS One*, 2009. **4**(10): p. e7533.
145. Wang, T.J. and D.K. Gupta, *Metabolite profiles in heart failure: looking for unique signatures in a heterogeneous syndrome*. *J Am Coll Cardiol*, 2015. **65**(15): p. 1521-4.
146. Burg, M.B. and J.D. Ferraris, *Intracellular Organic Osmolytes: Function and*. *J Biol Chem*, 2008. **283**(12): p. 7309-13.
147. van Meer, G., D.R. Voelker, and G.W. Feigenson, *Membrane lipids: where they are and how they behave*. *Nat Rev Mol Cell Biol*, 2008. **9**(2): p. 112-24.
148. Karliner, J.S. and J.H. Brown, *Lipid signalling in cardiovascular pathophysiology*. *Cardiovasc Res*, 2009. **82**(2): p. 171-4.
149. Wymann, M.P. and R. Schneider, *Lipid signalling in disease*. *Nat Rev Mol Cell Biol*, 2008. **9**(2): p. 162-176.
150. Gupta, R.C., J.T. Goad, and W.L. Kadel, *Carbofuran-induced alterations (in vivo) in high-energy phosphates, creatine kinase (CK) and CK isoenzymes*. *Archives of toxicology*, 1991. **65**(4): p. 304-310.
151. Rule, A.D., et al., *Using serum creatinine to estimate glomerular filtration rate: accuracy in good health and in chronic kidney disease*. *Annals of internal medicine*, 2004. **141**(12): p. 929-937.
152. Hsu, C.P., et al., *Asymmetric dimethylarginine predicts clinical outcomes in ischemic chronic heart failure*. *Atherosclerosis*, 2012. **225**(2): p. 504-10.
153. von Haehling, S., et al., *Elevated levels of asymmetric dimethylarginine in chronic heart failure: a pathophysiologic link between oxygen radical load and impaired vasodilator capacity and the therapeutic effect of allopurinol*. *Clin Pharmacol Ther*, 2010. **88**(4): p. 506-12.
154. Meana, C., et al., *Correlation between endogenous polyamines in human cardiac tissues and clinical parameters in patients with heart failure*. *J Cell Mol Med*, 2016. **20**(2): p. 302-12.

155. Yang, J., et al., *Quantitative Profiling Method for Oxylipin Metabolome by Liquid Chromatography Electrospray Ionization Tandem Mass Spectrometry*. *Anal Chem*, 2009. **81**(19): p. 8085-93.
156. Attur, M., et al., *Activation of diverse eicosanoid pathways in osteoarthritic cartilage: a lipidomic and genomic analysis*. *Bull NYU Hosp Jt Dis*, 2012. **70**(2): p. 99-108.
157. Daugherty, A. and L. Cassis, *Chronic angiotensin II infusion promotes atherogenesis in low density lipoprotein receptor -/- mice*. *Ann N Y Acad Sci*, 1999. **892**: p. 108-18.
158. Yu, Z., et al., *Disruption of the 5-lipoxygenase pathway attenuates atherogenesis consequent to COX-2 deletion in mice*. *Proc Natl Acad Sci U S A*, 2012. **109**(17): p. 6727-32.
159. Wang, D., et al., *Cardiomyocyte cyclooxygenase-2 influences cardiac rhythm and function*. *Proc Natl Acad Sci U S A*, 2009. **106**(18): p. 7548-52.
160. Hayashi, S. and A.P. McMahon, *Efficient recombination in diverse tissues by a tamoxifen-inducible form of Cre: a tool for temporally regulated gene activation/inactivation in the mouse*. *Dev Biol*, 2002. **244**(2): p. 305-18.
161. Le Belle, J.E., et al., *A comparison of cell and tissue extraction techniques using high-resolution 1H-NMR spectroscopy*. *NMR Biomed*, 2002. **15**(1): p. 37-44.
162. Morrison, W.R. and L.M. Smith, *PREPARATION OF FATTY ACID METHYL ESTERS AND DIMETHYLACETALS FROM LIPIDS WITH BORON FLUORIDE--METHANOL*. *J Lipid Res*, 1964. **5**: p. 600-8.
163. Roberts, L.D., et al., *Methods for performing lipidomics in white adipose tissue*. *Methods Enzymol*, 2014. **538**: p. 211-31.
164. Ament, Z., et al., *PPAR-pan activation induces hepatic oxidative stress and lipidomic remodelling*. *Free Radic Biol Med*, 2016. **95**: p. 357-68.
165. Ashmore, T., et al., *Nitrate enhances skeletal muscle fatty acid oxidation via a nitric oxide-cGMP-PPAR-mediated mechanism*. *BMC Biol*, 2015. **13**: p. 110.
166. Kerr, J.P., et al., *Detyrosinated microtubules modulate mechanotransduction in heart and skeletal muscle*. *Nat Commun*, 2015. **6**.
167. Eiden, M., et al., *Mechanistic insights revealed by lipid profiling in monogenic insulin resistance syndromes*. *Genome medicine*, 2015. **7**(1): p. 1.
168. Horgan, R.P. and L.C. Kenny, *'Omic' technologies: genomics, transcriptomics, proteomics and metabolomics*. *The Obstetrician & Gynaecologist*, 2011. **13**(3): p. 189-195.
169. Mark, R.V., *Metabolomics of aquatic organisms: the new &#145;omics&#146;; on the block*. *Marine Ecology Progress Series*, 2007. **332**: p. 301-306.
170. Raamsdonk, L.M., et al., *A functional genomics strategy that uses metabolome data to reveal the phenotype of silent mutations*. *Nat Biotechnol*, 2001. **19**(1): p. 45-50.
171. Ishii, N., et al., *Multiple high-throughput analyses monitor the response of E. coli to perturbations*. *Science*, 2007. **316**(5824): p. 593-7.
172. West, J.A., et al., *A targeted metabolomics assay for cardiac metabolism and demonstration using a mouse model of dilated cardiomyopathy*. *Metabolomics*, 2016. **12**(3): p. 1-18.
173. Clarke, C.J. and J.N. Haselden, *Metabolic profiling as a tool for understanding mechanisms of toxicity*. *Toxicol Pathol*, 2008. **36**(1): p. 140-7.
174. Quanbeck, S.M., et al., *Metabolomics as a Hypothesis-Generating Functional Genomics Tool for the Annotation of Arabidopsis thaliana Genes of "Unknown Function"*. *Front Plant Sci*, 2012. **3**: p. 15.
175. Ho, C.S., et al., *Electrospray Ionisation Mass Spectrometry: Principles and Clinical Applications*. *The Clinical Biochemist Reviews*, 2003. **24**(1): p. 3-12.
176. Da Silva, L., et al., *High-Resolution Quantitative Metabolome Analysis of Urine by Automated Flow Injection NMR*. *Analytical Chemistry*, 2013. **85**(12): p. 5801-5809.
177. Spiess, H.W., *Rotation of Molecules and Nuclear Spin Relaxation*, in *Dynamic NMR Spectroscopy*. 1978, Springer Berlin Heidelberg: Berlin, Heidelberg. p. 55-214.
178. Price, B.H., *Martin A. Goldstein, MD*. *Essentials of Neuroimaging for Clinical Practice*, 2008: p. 21.
179. Westbrook, C., *MRI at a glance*. 2015: John Wiley & Sons.
180. Khan, F.M. and J.P. Gibbons, *Khan's the physics of radiation therapy*. 2014: Lippincott Williams & Wilkins.
181. Ghoshal, S., *Fundamentals of bioanalytical techniques and instrumentation*. 2009: PHI Learning Pvt. Ltd.
182. Hore, P.J., *Nuclear magnetic resonance*. 2015: Oxford University Press, USA.
183. Emsley, J.W., J. Feeney, and L.H. Sutcliffe, *High resolution nuclear magnetic resonance spectroscopy*. Vol. 2. 2013: Elsevier.
184. Günther, H., *NMR Spectroscopy: Basic Principles, Concepts and Applications in Chemistry, 3rd Edition*. Nov 2013. 734.
185. Willker, W. and D. Leibfritz, *Assignment of mono-and polyunsaturated fatty acids in lipids of tissues and body fluids*. *Magnetic resonance in chemistry*, 1998. **36**(S79): p. S84.
186. Huusko, T., *Genetic and Molecular Background of Ascending Aortic Aneurysms*, in *University of Oulu, Faculty of Medicine, Institute of Clinical Medicine, Department of Internal Medicine*. 2013, University of Oulu: Oulu : University of Oulu, 2013.
187. Cadet, J., T. Douki, and J.-L. Ravanat, *One-electron oxidation of DNA and inflammation processes*. *Nat Chem Biol*, 2006. **2**(7): p. 348-349.

188. Udani, S.M. and J.L. Koyner, *The Effects of Heart Failure on Renal Function*. *Cardiology clinics*, 2010. **28**(3): p. 453-465.
189. Baverel, G., M. Bonnard, and M. Pellet, *Lactate and pyruvate metabolism in isolated human kidney tubules*. *FEBS letters*, 1979. **101**(2): p. 282-286.
190. Nakanishi, T., R.J. Turner, and M.B. Burg, *Osmoregulatory changes in myo-inositol transport by renal cells*. *Proc Natl Acad Sci U S A*, 1989. **86**(15): p. 6002-6.
191. Khan, S.H., et al., *Naturally occurring organic osmolytes: from cell physiology to disease prevention*. *IUBMB Life*, 2010. **62**(12): p. 891-5.
192. Flanagan, J.L., et al., *Role of carnitine in disease*. *Nutr Metab (Lond)*, 2010. **7**: p. 30.
193. Vaz, F.M. and R.J. Wanders, *Carnitine biosynthesis in mammals*. *Biochem J*, 2002. **361**(Pt 3): p. 417-29.
194. Holm, L. and M. Kjaer, *Measuring protein breakdown in individual proteins in vivo*. *Curr Opin Clin Nutr Metab Care*, 2010. **13**(5): p. 526-31.
195. Takahashi, R., et al., *Pressure overload-induced cardiomyopathy in heterozygous carrier mice of carnitine transporter gene mutation*. *Hypertension*, 2007. **50**(3): p. 497-502.
196. Schmitt, F., et al., *A plural role for lipids in motor neuron diseases: energy, signaling and structure*. *Frontiers in Cellular Neuroscience*, 2014. **8**: p. 25.
197. Velagaleti, R., C. Sims, and J. Gaziano, *DYSLIPIDEMIA TREATMENT AND HEART FAILURE RISK*. *Journal of the American College of Cardiology*, 2013. **61**(10\_S).
198. Papackova, Z. and M. Cahova, *Fatty acid signaling: the new function of intracellular lipases*. *Int J Mol Sci*, 2015. **16**(2): p. 3831-55.
199. Galli, C. and P. Risé, *Origin of fatty acids in the body: endogenous synthesis versus dietary intakes*. *European journal of lipid science and technology*, 2006. **108**(6): p. 521-525.
200. Regitz, V., A.L. Shug, and E. Fleck, *Defective myocardial carnitine metabolism in congestive heart failure secondary to dilated cardiomyopathy and to coronary, hypertensive and valvular heart diseases*. *Am J Cardiol*, 1990. **65**(11): p. 755-60.
201. Contreras, A.V., N. Torres, and A.R. Tovar, *PPAR-alpha as a key nutritional and environmental sensor for metabolic adaptation*. *Adv Nutr*, 2013. **4**(4): p. 439-52.
202. Reddy, L.R. and E.J. Corey, *Facile air oxidation of the conjugate base of rofecoxib (Vioxx™), a possible contributor to chronic human toxicity*. *Tetrahedron Letters*, 2005. **46**(6): p. 927-929.
203. Oitate, M., et al., *Mechanism for Covalent Binding of Rofecoxib to Elastin of Rat Aorta*. *Journal of Pharmacology and Experimental Therapeutics*, 2007. **320**(3): p. 1195-1203.
204. Miyajima, A., et al., *Disruption of elastic lamellae in aorta and dysfunction of vaso-regulation by rofecoxib in rats*. *J Toxicol Sci*, 2013. **38**(5): p. 719-29.
205. Griffoni, C., et al., *Selective inhibition of prostacyclin synthase activity by rofecoxib*. *J Cell Mol Med*, 2007. **11**(2): p. 327-38.
206. Steffel, J., et al., *Celecoxib Decreases Endothelial Tissue Factor Expression Through Inhibition of c-Jun Terminal NH2 Kinase Phosphorylation*. *Circulation*, 2005. **111**(13): p. 1685-1689.
207. Klein, T., et al., *Celecoxib dilates guinea-pig coronaries and rat aortic rings and amplifies NO/cGMP signaling by PDE5 inhibition*. *Cardiovasc Res*, 2007. **75**(2): p. 390-7.
208. Frolov, R.V., I.G. Berim, and S. Singh, *Inhibition of Delayed Rectifier Potassium Channels and Induction of Arrhythmia: A NOVEL EFFECT OF CELECOXIB AND THE MECHANISM UNDERLYING IT*. *Journal of Biological Chemistry*, 2008. **283**(3): p. 1518-1524.
209. Shapiro, M.S., *An ion channel hypothesis to explain divergent cardiovascular safety of cyclooxygenase-2 inhibitors: the answer to a hotly debated puzzle?* *Mol Pharmacol*, 2009. **76**(5): p. 942-5.
210. Hoppel, C., *The role of carnitine in normal and altered fatty acid metabolism*. *Am J Kidney Dis*, 2003. **41**(4 Suppl 4): p. S4-12.
211. Marcovina, S.M., et al., *Translating the basic knowledge of mitochondrial functions to metabolic therapy: role of L-carnitine*. *Transl Res*, 2013. **161**(2): p. 73-84.
212. Tousoulis, D., M. Charakida, and C. Stefanadis, *Inflammation and endothelial dysfunction as therapeutic targets in patients with heart failure*. *Int J Cardiol*, 2005. **100**(3): p. 347-53.
213. Ueland, T., et al., *Disturbed carnitine regulation in chronic heart failure--increased plasma levels of palmitoyl-carnitine are associated with poor prognosis*. *Int J Cardiol*, 2013. **167**(5): p. 1892-9.
214. Dinicolantonio, J.J., et al., *L-carnitine for the treatment of acute myocardial infarction*. *Rev Cardiovasc Med*, 2014. **15**(1): p. 52-62.
215. Frigeni, M., et al., *Wide tolerance to amino acids substitutions in the OCTN1 ergothioneine transporter*. *Biochim Biophys Acta*, 2016. **1860**(6): p. 1334-42.
216. Grube, M., et al., *Uptake of cardiovascular drugs into the human heart: expression, regulation, and function of the carnitine transporter OCTN2 (SLC22A5)*. *Circulation*, 2006. **113**(8): p. 1114-22.
217. Grube, M., et al., *Selective regulation of cardiac organic cation transporter novel type 2 (OCTN2) in dilated cardiomyopathy*. *Am J Pathol*, 2011. **178**(6): p. 2547-59.
218. Lane, M.D., et al., *Regulation of food intake and energy expenditure by hypothalamic malonyl-CoA*. *Int J Obes (Lond)*, 2008. **32 Suppl 4**: p. S49-54.
219. van der Leij, F.R., et al., *Genomics of the human carnitine acyltransferase genes*. *Mol Genet Metab*, 2000. **71**(1-2): p. 139-53.
220. Kerner, J. and C. Hoppel, *Fatty acid import into mitochondria*. *Biochim Biophys Acta*, 2000. **1486**(1): p. 1-17.

221. He, L., et al., *Carnitine palmitoyltransferase-1b deficiency aggravates pressure overload-induced cardiac hypertrophy caused by lipotoxicity*. *Circulation*, 2012. **126**(14): p. 1705-16.
222. Pande, S.V., *A mitochondrial carnitine acylcarnitine translocase system*. *Proceedings of the National Academy of Sciences of the United States of America*, 1975. **72**(3): p. 883-887.
223. Stephens, F.B. and S.D. Galloway, *Carnitine and fat oxidation*. *Nestle Nutr Inst Workshop Ser*, 2013. **76**: p. 13-23.
224. Rubio-Gozalbo, M.E., et al., *Carnitine-acylcarnitine translocase deficiency, clinical, biochemical and genetic aspects*. *Mol Aspects Med*, 2004. **25**(5-6): p. 521-32.
225. Rufer, A.C., et al., *Carnitine palmitoyltransferase 2: analysis of membrane association and complex structure with a substrate analog*. *FEBS Lett*, 2007. **581**(17): p. 3247-52.
226. Houten, S.M. and R.J.A. Wanders, *A general introduction to the biochemistry of mitochondrial fatty acid  $\beta$ -oxidation*. *Journal of Inherited Metabolic Disease*, 2010. **33**(5): p. 469-477.
227. Vavlukis, M., et al., *Rhabdomyolysis and Cardiomyopathy in a 20-Year-Old Patient with CPT II Deficiency*. *Case Rep Genet*, 2014. **2014**: p. 496410.
228. Kienesberger, K., et al., *L-carnitine and PPAR $\alpha$ -agonist fenofibrate are involved in the regulation of Carnitine Acetyltransferase (CrAT) mRNA levels in murine liver cells*. *BMC Genomics*, 2014. **15**: p. 514.
229. Cordente, A.G., et al., *Redesign of carnitine acetyltransferase specificity by protein engineering*. *J Biol Chem*, 2004. **279**(32): p. 33899-908.
230. Abo Alrob, O. and G.D. Lopaschuk, *Role of CoA and acetyl-CoA in regulating cardiac fatty acid and glucose oxidation*. *Biochem Soc Trans*, 2014. **42**(4): p. 1043-51.
231. Kato, Y., et al., *Organic cation/carnitine transporter OCTN2 (Slc22a5) is responsible for carnitine transport across apical membranes of small intestinal epithelial cells in mouse*. *Mol Pharmacol*, 2006. **70**(3): p. 829-37.
232. Koeth, R.A., et al., *Intestinal microbiota metabolism of L-carnitine, a nutrient in red meat, promotes atherosclerosis*. *Nature medicine*, 2013. **19**(5): p. 576-585.
233. Tang, W.H.W. and S.L. Hazen, *The contributory role of gut microbiota in cardiovascular disease*. *The Journal of Clinical Investigation*, 2014. **124**(10): p. 4204-4211.
234. Mendelsohn, A.R. and J.W. Larrick, *Dietary modification of the microbiome affects risk for cardiovascular disease*. *Rejuvenation Res*, 2013. **16**(3): p. 241-4.
235. Zhu, Y., et al., *Carnitine metabolism to trimethylamine by an unusual Rieske-type oxygenase from human microbiota*. *Proc Natl Acad Sci U S A*, 2014. **111**(11): p. 4268-73.
236. Koeth, R.A., et al., *gamma-Butyrobetaine is a proatherogenic intermediate in gut microbial metabolism of L-carnitine to TMAO*. *Cell Metab*, 2014. **20**(5): p. 799-812.
237. Tang, W.H., et al., *Gut microbiota-dependent trimethylamine N-oxide (TMAO) pathway contributes to both development of renal insufficiency and mortality risk in chronic kidney disease*. *Circ Res*, 2015. **116**(3): p. 448-55.
238. van Vlies, N., et al., *Submitochondrial localization of 6-N-trimethyllysine dioxygenase - implications for carnitine biosynthesis*. *Febs j*, 2007. **274**(22): p. 5845-51.
239. Sharma, S. and S.M. Black, *CARNITINE HOMEOSTASIS, MITOCHONDRIAL FUNCTION, AND CARDIOVASCULAR DISEASE*. *Drug discovery today*. Disease mechanisms, 2009. **6**(1-4): p. e31-e39.
240. Osorio, J.H., *Supplementation with carnitine for weight loss: a biochemical approach*. Vol. 42. 2011.
241. Ringseis, R., G. Wen, and K. Eder, *Regulation of Genes Involved in Carnitine Homeostasis by PPAR $\alpha$  across Different Species (Rat, Mouse, Pig, Cattle, Chicken, and Human)*. *PPAR Research*, 2012. **2012**: p. 11.
242. van Vlies, N., et al., *PPAR  $\alpha$ -activation results in enhanced carnitine biosynthesis and OCTN2-mediated hepatic carnitine accumulation*. *Biochim Biophys Acta*, 2007. **1767**(9): p. 1134-42.
243. Koch, A., et al., *PPAR  $\alpha$  mediates transcriptional upregulation of novel organic cation transporters-2 and -3 and enzymes involved in hepatic carnitine synthesis*. *Exp Biol Med (Maywood)*, 2008. **233**(3): p. 356-65.
244. Rebouche, C.J. and H. Seim, *Carnitine metabolism and its regulation in microorganisms and mammals*. *Annu Rev Nutr*, 1998. **18**: p. 39-61.
245. Spiekerkoetter, U., et al., *Current issues regarding treatment of mitochondrial fatty acid oxidation disorders*. *J Inherit Metab Dis*, 2010. **33**(5): p. 555-61.
246. Zhao, D., et al., *Identification of the plasma metabolomics as early diagnostic markers between biliary atresia and neonatal hepatitis syndrome*. *PLoS One*, 2014. **9**(1): p. e85694.
247. Shekhawat, P.S., et al., *Enzymes involved in L-carnitine biosynthesis are expressed by small intestinal enterocytes in mice: Implications for gut health*. *Journal of Crohn's & colitis*, 2013. **7**(6): p. e197-e205.
248. Fu, L., M. Huang, and S. Chen, *Primary Carnitine Deficiency and Cardiomyopathy*. *Korean Circulation Journal*, 2013. **43**(12): p. 785-792.
249. Kuwajima, M., et al., *Cardiomegaly in the juvenile visceral steatosis (JVS) mouse is reduced with acute elevation of heart short-chain acyl-carnitine level after L-carnitine injection*. *FEBS Lett*, 1999. **443**(3): p. 261-6.
250. Sole, M.J. and K.N. Jeejeebhoy, *Conditioned nutritional requirements and the pathogenesis and treatment of myocardial failure*. *Curr Opin Clin Nutr Metab Care*, 2000. **3**(6): p. 417-24.
251. Siliprandi, N., et al., *Transport and function of L-carnitine and L-propionylcarnitine: relevance to some cardiomyopathies and cardiac ischemia*. *Z Kardiol*, 1987. **76 Suppl 5**: p. 34-40.

252. Narin, F., et al., *Carnitine levels in patients with chronic rheumatic heart disease*. Clin Biochem, 1997. **30**(8): p. 643-5.
253. Soukoulis, V., et al., *Micronutrient deficiencies an unmet need in heart failure*. J Am Coll Cardiol, 2009. **54**(18): p. 1660-73.
254. Cordero-Reyes, A.M., et al., *Freshly isolated mitochondria from failing human hearts exhibit preserved respiratory function*. J Mol Cell Cardiol, 2014. **68**: p. 98-105.
255. Sankaralingam, S. and G.D. Lopaschuk, *Cardiac energy metabolic alterations in pressure overload–induced left and right heart failure (2013 Grover Conference Series)*. Pulmonary Circulation, 2015. **5**(1): p. 15-28.
256. Liang, X., et al., *Bidirectional interactions between indomethacin and the murine intestinal microbiota*. 2015. **4**: p. e08973.
257. Liepinsh, E., et al., *Inhibition of L-carnitine biosynthesis and transport by methyl-gamma-butyrobetaine decreases fatty acid oxidation and protects against myocardial infarction*. Br J Pharmacol, 2015. **172**(5): p. 1319-32.
258. Shao, J., H. Sheng, and R.N. DuBois, *Peroxisome proliferator-activated receptors modulate K-Ras-mediated transformation of intestinal epithelial cells*. Cancer Res, 2002. **62**(11): p. 3282-8.
259. Varga, T., Z. Czimmerer, and L. Nagy, *PPARs are a unique set of fatty acid regulated transcription factors controlling both lipid metabolism and inflammation()*. Biochimica et Biophysica Acta, 2011. **1812**(8): p. 1007-1022.
260. Treacy, M.P. and T.P. Hurst, *The case for intraocular delivery of PPAR agonists in the treatment of diabetic retinopathy*. BMC Ophthalmol, 2012. **12**: p. 46.
261. van Schothorst, E.M., et al., *Induction of lipid oxidation by polyunsaturated fatty acids of marine origin in small intestine of mice fed a high-fat diet*. BMC Genomics, 2009. **10**: p. 110-110.
262. Costell, M. and S. Grisolia, *Effect of carnitine feeding on the levels of heart and skeletal muscle carnitine of elderly mice*. FEBS Lett, 1993. **315**(1): p. 43-6.
263. Rebouche, C.J., *Kinetics, pharmacokinetics, and regulation of L-carnitine and acetyl-L-carnitine metabolism*. Ann N Y Acad Sci, 2004. **1033**: p. 30-41.
264. Barnett, C., et al., *Effect of L-carnitine supplementation on muscle and blood carnitine content and lactate accumulation during high-intensity sprint cycling*. Int J Sport Nutr, 1994. **4**(3): p. 280-8.
265. Vukovich, M.D., D.L. Costill, and W.J. Fink, *Carnitine supplementation: effect on muscle carnitine and glycogen content during exercise*. Med Sci Sports Exerc, 1994. **26**(9): p. 1122-9.
266. Rakhshandehroo, M., et al., *Peroxisome Proliferator-Activated Receptor Alpha Target Genes*. PPAR Research, 2010. **2010**: p. 612089.
267. Fabbri, E., S. Sullivan, and S. Klein, *Obesity and Nonalcoholic Fatty Liver Disease: Biochemical, Metabolic and Clinical Implications*. Hepatology (Baltimore, Md.), 2010. **51**(2): p. 679-689.
268. Foster, D.W., *Malonyl-CoA: the regulator of fatty acid synthesis and oxidation*. The Journal of Clinical Investigation, 2012. **122**(6): p. 1958-1959.
269. Demaugre, F., et al., *Infantile form of carnitine palmitoyltransferase II deficiency with hepatomuscular symptoms and sudden death. Physiopathological approach to carnitine palmitoyltransferase II deficiencies*. J Clin Invest, 1991. **87**(3): p. 859-64.
270. Zammit, V.A., *Carnitine palmitoyltransferase 1: central to cell function*. IUBMB Life, 2008. **60**(5): p. 347-54.
271. Linher-Melville, K., et al., *Establishing a relationship between prolactin and altered fatty acid  $\beta$ -Oxidation via carnitine palmitoyl transferase 1 in breast cancer cells*. BMC Cancer, 2011. **11**: p. 56.
272. Purevsuren, J., et al., *Intracellular in vitro probe acylcarnitine assay for identifying deficiencies of carnitine transporter and carnitine palmitoyltransferase-1*. Anal Bioanal Chem, 2013. **405**(4): p. 1345-51.
273. O'Donnell, J.M., et al., *Coupling of mitochondrial fatty acid uptake to oxidative flux in the intact heart*. Biophys J, 2002. **82**(1 Pt 1): p. 11-8.
274. Noland, R.C., et al., *Carnitine Insufficiency Caused by Aging and Overnutrition Compromises Mitochondrial Performance and Metabolic Control*. The Journal of Biological Chemistry, 2009. **284**(34): p. 22840-22852.
275. van Bilsen, M., et al., *Metabolic remodelling of the failing heart: the cardiac burn-out syndrome?* Cardiovascular Research, 2004. **61**(2): p. 218-226.
276. Dodd, M.S., et al., *Impaired in vivo mitochondrial Krebs cycle activity after myocardial infarction assessed using hyperpolarized magnetic resonance spectroscopy*. Circ Cardiovasc Imaging, 2014. **7**(6): p. 895-904.
277. Chokkathukalam, A., *Stable isotope-labeling studies in metabolomics: new insights into structure and dynamics of metabolic networks*. 2014. **6**(4): p. 511-24.
278. Nassar, A.E.F., S.M. Bjorge, and D.Y. Lee, *On-Line Liquid Chromatography-Accurate Radioisotope Counting Coupled with a Radioactivity Detector and Mass Spectrometer for Metabolite Identification in Drug Discovery and Development*. Analytical Chemistry, 2003. **75**(4): p. 785-790.
279. Tyni, T., et al., *Mitochondrial Fatty Acid [bgr]-Oxidation in the Retinal Pigment Epithelium*. Pediatr Res, 2002. **52**(4): p. 595-600.
280. L, I.J., et al., *Functional analysis of mutant human carnitine acylcarnitine translocases in yeast*. Biochem Biophys Res Commun, 2001. **280**(3): p. 700-6.
281. Wanders, R.J.A., et al., *The enzymology of mitochondrial fatty acid beta-oxidation and its application to follow-up analysis of positive neonatal screening results*. J Inherit Metab Dis, 2010. **33**(5): p. 479-94.

282. Zierz, S. and A.G. Engel, *Different sites of inhibition of carnitine palmitoyltransferase by malonyl-CoA, and by acetyl-CoA and CoA, in human skeletal muscle*. *Biochem J*, 1987. **245**(1): p. 205-9.
283. Manning, N.J., et al., *A comparison of [9,10-3H]palmitic and [9,10-3H]myristic acids for the detection of defects of fatty acid oxidation in intact cultured fibroblasts*. *J Inherit Metab Dis*, 1990. **13**(1): p. 58-68.
284. Olpin, S.E., et al., *Improved detection of long-chain fatty acid oxidation defects in intact cells using [9,10-3H]oleic acid*. *J Inherit Metab Dis*, 1997. **20**(3): p. 415-9.
285. Molstad, P., *The efflux of L-carnitine from cells in culture (CCL 27)*. *Biochim Biophys Acta*, 1980. **597**(1): p. 166-73.
286. Pochini, L., F. Oppedisano, and C. Indiveri, *Reconstitution into liposomes and functional characterization of the carnitine transporter from renal cell plasma membrane*. *Biochim Biophys Acta*, 2004. **1661**(1): p. 78-86.
287. Kobayashi, D., et al., *Transport of carnitine and acetylcarnitine by carnitine/organic cation transporter (OCTN) 2 and OCTN3 into epididymal spermatozoa*. *Reproduction*, 2007. **134**(5): p. 651-8.
288. Li, Q., et al., *Multiple mass isotopomer tracing of acetyl-CoA metabolism in Langendorff-perfused rat hearts: channeling of acetyl-CoA from pyruvate dehydrogenase to carnitine acetyltransferase*. *J Biol Chem*, 2015. **290**(13): p. 8121-32.
289. Martin, M.A., et al., *Myocardial carnitine and carnitine palmitoyltransferase deficiencies in patients with severe heart failure*. *Biochim Biophys Acta*, 2000. **1502**(3): p. 330-6.
290. Furuichi, Y., et al., *Muscle contraction increases carnitine uptake via translocation of OCTN2*. *Biochem Biophys Res Commun*, 2012. **418**(4): p. 774-9.
291. Zhang, Z., et al., *Acetyl-L-carnitine inhibits TNF-alpha-induced insulin resistance via AMPK pathway in rat skeletal muscle cells*. *FEBS Lett*, 2009. **583**(2): p. 470-4.
292. Hardie, D.G., F.A. Ross, and S.A. Hawley, *AMPK: a nutrient and energy sensor that maintains energy homeostasis*. *Nat Rev Mol Cell Biol*, 2012. **13**(4): p. 251-62.
293. Liu, X., et al., *Effect of asymmetric dimethylarginine (ADMA) on heart failure development*. *Nitric Oxide*, 2016.
294. Kasapkara, C.S., et al., *Asymmetric dimethylarginine (ADMA) and L-arginine levels in children with glycogen storage disease type I*. *J Pediatr Endocrinol Metab*, 2013. **26**(5-6): p. 427-31.
295. Morham, S.G., et al., *Prostaglandin synthase 2 gene disruption causes severe renal pathology in the mouse*. *Cell*, 1995. **83**(3): p. 473-82.
296. Ishikawa, T.O. and H.R. Herschman, *Conditional knockout mouse for tissue-specific disruption of the cyclooxygenase-2 (Cox-2) gene*. *Genesis*, 2006. **44**(3): p. 143-9.
297. Koitabashi, N., et al., *Avoidance of transient cardiomyopathy in cardiomyocyte-targeted tamoxifen-induced MerCreMer gene deletion models*. *Circ Res*, 2009. **105**(1): p. 12-5.
298. Visser, M., et al., *The role of asymmetric dimethylarginine and arginine in the failing heart and its vasculature*. *Eur J Heart Fail*, 2010. **12**(12): p. 1274-81.
299. Hu, X., et al., *Dimethylarginine dimethylaminohydrolase-1 is the critical enzyme for degrading the cardiovascular risk factor asymmetrical dimethylarginine*. *Arterioscler Thromb Vasc Biol*, 2011. **31**(7): p. 1540-6.
300. Closs, E.I., et al., *Interference of L-arginine analogues with L-arginine transport mediated by the y+ carrier hCAT-2B*. *Nitric Oxide*, 1997. **1**(1): p. 65-73.
301. Ivanova, M., et al., *HPLC determination of plasma dimethylarginines: method validation and preliminary clinical application*. *Clin Chim Acta*, 2010. **411**(21-22): p. 1632-6.
302. Pilz, S., et al., *Associations of methylarginines and homoarginine with diastolic dysfunction and cardiovascular risk factors in patients with preserved left ventricular ejection fraction*. *J Card Fail*, 2014. **20**(12): p. 923-30.
303. Kohashi, K., et al., *Effects of eicosapentaenoic acid on the levels of inflammatory markers, cardiac function and long-term prognosis in chronic heart failure patients with dyslipidemia*. *J Atheroscler Thromb*, 2014. **21**(7): p. 712-29.
304. Anderssohn, M., et al., *The L-Arginine-asymmetric dimethylarginine ratio is an independent predictor of mortality in dilated cardiomyopathy*. *J Card Fail*, 2012. **18**(12): p. 904-11.
305. Napora, M., et al., *Relationship between serum asymmetric dimethylarginine and left ventricular structure and function in patients with endstage renal disease treated with hemodialysis*. *Pol Arch Med Wewn*, 2012. **122**(5): p. 226-34.
306. Tutarel, O., et al., *Asymmetrical dimethylarginine--more sensitive than NT-proBNP to diagnose heart failure in adults with congenital heart disease*. *PLoS One*, 2012. **7**(3): p. e33795.
307. Shao, Z., et al., *Pulmonary hypertension associated with advanced systolic heart failure: dysregulated arginine metabolism and importance of compensatory dimethylarginine dimethylaminohydrolase-1*. *J Am Coll Cardiol*, 2012. **59**(13): p. 1150-8.
308. Zairis, M.N., et al., *Plasma asymmetric dimethylarginine and mortality in patients with acute decompensation of chronic heart failure*. *Heart*, 2012. **98**(11): p. 860-4.
309. Seljeflot, I., et al., *The L-arginine-asymmetric dimethylarginine ratio is strongly related to the severity of chronic heart failure. No effects of exercise training*. *J Card Fail*, 2011. **17**(2): p. 135-42.
310. Tang, W.H., et al., *Differential effects of arginine methylation on diastolic dysfunction and disease progression in patients with chronic systolic heart failure*. *Eur Heart J*, 2008. **29**(20): p. 2506-13.
311. Duckelmann, C., et al., *Asymmetric dimethylarginine enhances cardiovascular risk prediction in patients with chronic heart failure*. *Arterioscler Thromb Vasc Biol*, 2007. **27**(9): p. 2037-42.

312. Usui, M., et al., *Increased endogenous nitric oxide synthase inhibitor in patients with congestive heart failure*. Life Sci, 1998. **62**(26): p. 2425-30.
313. Saitoh, M., et al., *High plasma level of asymmetric dimethylarginine in patients with acutely exacerbated congestive heart failure: role in reduction of plasma nitric oxide level*. Heart Vessels, 2003. **18**(4): p. 177-82.
314. Ohnishi, M., et al., *Endothelin stimulates an endogenous nitric oxide synthase inhibitor, asymmetric dimethylarginine, in experimental heart failure*. Clin Sci (Lond), 2002. **103 Suppl 48**: p. 241s-244s.
315. Feng, Q., et al., *Elevation of an endogenous inhibitor of nitric oxide synthesis in experimental congestive heart failure*. Cardiovasc Res, 1998. **37**(3): p. 667-75.
316. Achan, V., et al., *Asymmetric dimethylarginine causes hypertension and cardiac dysfunction in humans and is actively metabolized by dimethylarginine dimethylaminohydrolase*. Arterioscler Thromb Vasc Biol, 2003. **23**(8): p. 1455-9.
317. Kielstein, J.T., et al., *Cardiovascular effects of systemic nitric oxide synthase inhibition with asymmetrical dimethylarginine in humans*. Circulation, 2004. **109**(2): p. 172-7.
318. Richir, M.C., et al., *Low arginine/asymmetric dimethylarginine ratio deteriorates systemic hemodynamics and organ blood flow in a rat model*. Crit Care Med, 2009. **37**(6): p. 2010-7.
319. Maier, L.S., et al., *Hotline update of clinical trials and registries presented at the German Cardiac Society meeting 2008. (PEPCAD, LokalTax, INH, German ablation registry, German device registry, DES.DE registry, DHR, Reality, SWEETHEART registry, ADMA, GERSHWIN)*. Clin Res Cardiol, 2008. **97**(6): p. 356-63.
320. Boger, R.H., et al., *Plasma asymmetric dimethylarginine and incidence of cardiovascular disease and death in the community*. Circulation, 2009. **119**(12): p. 1592-600.
321. Guo, C.X., et al., *An effective dose of valdecoxib in experimental mouse models of pain*. Methods Find Exp Clin Pharmacol, 2007. **29**(6): p. 383-8.
322. Aljadhey, H., et al., *Comparative effects of non-steroidal anti-inflammatory drugs (NSAIDs) on blood pressure in patients with hypertension*. BMC Cardiovasc Disord, 2012. **12**: p. 93.
323. Kruszelnicka, O., E. Wieczorek-Surdacka, and A. Surdacki, *Letter by Kruszelnicka et al regarding article, "evidence that links loss of cyclooxygenase-2 with increased asymmetric dimethylarginine: novel explanation of cardiovascular side effects associated with anti-inflammatory drugs"*. Circulation, 2015. **132**(17): p. e212.
324. Ahmetaj-Shala, B., et al., *Reply to letter regarding article, "evidence that links loss of cyclooxygenase-2 with increased asymmetric dimethylarginine: novel explanation of cardiovascular side effects associated with anti-inflammatory drugs"*. Circulation, 2015. **132**(17): p. e213-4.
325. Wloch, A., et al., *Asymmetric dimethylarginine reflects cumulative inflammatory burden in rheumatoid arthritis. A novel mechanism of excessive cardiovascular morbidity?* Rheumatology (Oxford), 2015. **54**(7): p. 1135-6.
326. Sandoo, A., et al., *Cumulative inflammation associates with asymmetric dimethylarginine in rheumatoid arthritis: a 6 year follow-up study*. Rheumatology (Oxford), 2015. **54**(7): p. 1145-52.
327. Messner, B. and D. Bernhard, *Smoking and cardiovascular disease: mechanisms of endothelial dysfunction and early atherogenesis*. Arterioscler Thromb Vasc Biol, 2014. **34**(3): p. 509-15.
328. Perlstein, T.S. and R.T. Lee, *Smoking, metalloproteinases, and vascular disease*. Arterioscler Thromb Vasc Biol, 2006. **26**(2): p. 250-6.
329. Vlachopoulos, C., et al., *Arterial stiffening and systemic endothelial activation induced by smoking: The role of COX-1 and COX-2*. Int J Cardiol, 2015. **189**: p. 293-8.
330. Patrignani, P., et al., *New insights into COX-2 biology and inhibition*. Brain Res Brain Res Rev, 2005. **48**(2): p. 352-9.
331. Komhoff, M., et al., *Cyclooxygenase-2-selective inhibitors impair glomerulogenesis and renal cortical development*. Kidney Int, 2000. **57**(2): p. 414-22.
332. Fujimi-Hayashida, A., et al., *Association of asymmetric dimethylarginine with severity of kidney injury and decline in kidney function in IgA nephropathy*. Am J Nephrol, 2011. **33**(1): p. 1-6.
333. Ueda, S., et al., *Involvement of asymmetric dimethylarginine (ADMA) in glomerular capillary loss and sclerosis in a rat model of chronic kidney disease (CKD)*. Life Sci, 2009. **84**(23-24): p. 853-6.
334. Vardeh, D., *COX2 in CNS neural cells mediates mechanical inflammatory pain hypersensitivity in mice*. 2009. **119**(2): p. 287-94.
335. Papanicolaou, K.N., et al., *Preserved heart function and maintained response to cardiac stresses in a genetic model of cardiomyocyte-targeted deficiency of cyclooxygenase-2*. J Mol Cell Cardiol, 2010. **49**(2): p. 196-209.
336. Rogatzki, M.J., et al., *Lactate is always the end product of glycolysis*. Front Neurosci, 2015. **9**.
337. Chatham, J.C., *Lactate – the forgotten fuel!* J Physiol, 2002. **542**(Pt 2): p. 333.
338. Drake, K.J., et al., *Amino Acids as Metabolic Substrates during Cardiac Ischemia*. Exp Biol Med (Maywood), 2012. **237**(12).
339. Lynch, T.L.t., et al., *Oxidative Stress in Dilated Cardiomyopathy Caused by MYBPC3 Mutation*. Oxid Med Cell Longev, 2015. **2015**: p. 424751.
340. Yucel, D., et al., *Increased oxidative stress in dilated cardiomyopathic heart failure*. Clin Chem, 1998. **44**(1): p. 148-54.
341. Kadiiska, M.B., et al., *Biomarkers of Oxidative Stress Study V: Ozone exposure of rats and its effect on lipids, proteins and DNA in plasma and urine*. Free Radic Biol Med, 2013. **0**: p. 408-15.

342. Galasko, D., *Biomarkers of oxidative damage and inflammation in Alzheimer's disease*. 2010. **4**(1): p. 27-36.
343. Drazic, A., et al., *Methionine oxidation activates a transcription factor in response to oxidative stress*. Proc Natl Acad Sci U S A, 2013. **110**(23): p. 9493-8.
344. Haas, J., et al., *Alterations in cardiac DNA methylation in human dilated cardiomyopathy*. EMBO Mol Med, 2013. **5**(3): p. 413-29.
345. Caudill, M.A., et al., *Intracellular S-adenosylhomocysteine concentrations predict global DNA hypomethylation in tissues of methyl-deficient cystathionine beta-synthase heterozygous mice*. J Nutr, 2001. **131**(11): p. 2811-8.
346. Lopez, B., A. Gonzalez, and J. Diez, *Circulating biomarkers of collagen metabolism in cardiac diseases*. Circulation, 2010. **121**(14): p. 1645-54.
347. Finck, B.N. and D.P. Kelly, *Peroxisome proliferator-activated receptor gamma coactivator-1 (PGC-1) regulatory cascade in cardiac physiology and disease*. Circulation, 2007. **115**(19): p. 2540-8.
348. Duncan, J.G. and B.N. Finck, *The PPARalpha-PGC-1alpha Axis Controls Cardiac Energy Metabolism in Healthy and Diseased Myocardium*. PPAR Res, 2008. **2008**: p. 253817.
349. Loichot, C., et al., *Deletion of peroxisome proliferator-activated receptor-alpha induces an alteration of cardiac functions*. Am J Physiol Heart Circ Physiol, 2006. **291**(1): p. H161-6.
350. Finck, B.N., et al., *The cardiac phenotype induced by PPARalpha overexpression mimics that caused by diabetes mellitus*. J Clin Invest, 2002. **109**(1): p. 121-30.
351. Tada, Y. and J. Suzuki, *Oxidative stress and myocarditis*. Curr Pharm Des, 2016. **22**(4): p. 450-71.
352. Gonzalez, A., et al., *New targets to treat the structural remodeling of the myocardium*. J Am Coll Cardiol, 2011. **58**(18): p. 1833-43.
353. Reddy, Y.S., et al., *Nitric oxide status in patients with chronic kidney disease*. Indian J Nephrol, 2015. **25**(5): p. 287-91.
354. Kielstein, J.T., et al., *Marked increase of asymmetric dimethylarginine in patients with incipient primary chronic renal disease*. J Am Soc Nephrol, 2002. **13**(1): p. 170-6.
355. Schmidt, R.J. and C. Baylis, *Total nitric oxide production is low in patients with chronic renal disease*. Kidney Int, 2000. **58**(3): p. 1261-6.
356. Fogo, A.B., *Mechanisms of progression of chronic kidney disease*. Pediatr Nephrol, 2007. **22**(12): p. 2011-22.
357. Whelton, A., et al., *Effects of celecoxib and naproxen on renal function in the elderly*. Arch Intern Med, 2000. **160**(10): p. 1465-70.
358. Gajraj, N.M., *COX-2 inhibitors celecoxib and parecoxib: valuable options for postoperative pain management*. Curr Top Med Chem, 2007. **7**(3): p. 235-49.
359. Keeble, J.E. and P.K. Moore, *Pharmacology and potential therapeutic applications of nitric oxide-releasing non-steroidal anti-inflammatory and related nitric oxide-donating drugs*. British Journal of Pharmacology, 2002. **137**(3): p. 295-310.
360. Velazquez, C., et al., *Synthesis and biological evaluation of 3,4-diphenyl-1,2,5-oxadiazole-2-oxides and 3,4-diphenyl-1,2,5-oxadiazoles as potential hybrid COX-2 inhibitor/nitric oxide donor agents*. Bioorg Med Chem, 2005. **13**(8): p. 2749-57.